



**European Space Agency
Agence spatiale européenne**

**directorate of technical and operational support
ground systems engineering department
mission support office
mission analysis section**

RO-ESC-RP-5500

**ROSETTA: CONSOLIDATED REPORT ON
MISSION ANALYSIS
CHURYUMOV-GERASIMENKO 2004
*(Issue 5, Rev. 0)***

by

J. Rodríguez Canabal

J. M. Sánchez Pérez

Arturo Yáñez Otero

August, 2003

European Space Operations Centre


Robert-Bosch-Str. 5


D - 64293 Darmstadt

ROSETTA: CONSOLIDATED REPORT ON MISSION ANALYSIS
First Edition (Issue **5**, Rev. 0), 2003

ESA/ESOC, 64293 Darmstadt, Germany, August, 2003

Document Approval

Prepared by	Address Code	Signature	Date
J.M. Sánchez Pérez	ESA/TOS/GMA		

Approved by	Address Code	Signature	Date
J.RodríguezCanabal	ESA/TOS/GMA		

Change Record

Date	Issue	Rev.	Page/Para. affected	Description	Approval authority

Distribution List

Project :

C. Berner
J. van Casteren
G. Coupe
J. Ellwood
Ph. Kletzkine
D. Koschny
J. Salvignol
R. Schulz
G. Schwehm

ESOC :

MAS

V. Companys
P. Ferri
J. Fertig
W. Frank
J.F. Kaufeler
M. Lauer
E. Montagnon
T. Morley
R. Münch
J. Schoenmaekers
A. Smith
J. Wardill
M. Warhaut

Table of Content

1. PURPOSE.....	1
2. REFERENCES.....	2
2.1 Applicable Documents	2
2.2 Reference Documents	2
3. MISSION REQUIREMENTS AND CONSTRAINTS	4
3.1 General Description	4
3.2 Scientific Requirements	4
3.2.1 Comet Characterisation	5
3.2.2 Asteroids Characterisation	6
3.3 Launcher Requirements	6
3.4 Spacecraft Requirements.....	7
3.5 Ground Station and Radio Tracking System.....	8
4. MISSION OVERVIEW	9
4.1 Mission Baseline Description	9
4.1.1 Rosetta Baseline Mission	9
4.2 Launcher Description.....	15
4.2.1 Launch Procedure.....	16
4.2.2 Launcher Performances and Launch Dates.....	16
4.3 Spacecraft Description	17
4.4 Mission Operation Phases.....	18
5. LAUNCH WITH ARIANE 5	21
5.1 Injection with Coast Arc	21
5.1.1 Sequence of Events	22
5.1.2 Eclipses	22
5.1.3 Ground Station Coverage.....	24
5.1.4 Injection Errors.....	26
5.2 General Launch Window	27
5.3 Daily Launch Window	33
5.4 Non-Optimal Ariane 5 Flight Program Launch	33
5.5 Maximum Spacecraft Mass and Launch Window	33
5.6 Cost of Delayed Launch.....	34
6. INTERPLANETARY TRAJECTORY	37
6.1 Detailed Mission Description	38
6.1.1 Numerical Trajectory Data.....	38
6.1.2 Geometrical Data	39
6.1.3 Ground Station Coverage.....	69
6.1.4 Early Orbit Determination and First Correction Manoeuvre	85
6.1.5 Interplanetary Navigation.....	92
7. ASTEROID FLY-BY POSSIBILITIES	102
7.1 Extra Delta-V Assessment	102
7.2 Effect to Interplanetary Trajectory.....	105
7.2.1 Asteroid fly-by in phase from 2 nd Earth to 3 rd Earth swing-by.....	105
7.2.2 Asteroid fly-by in phase from 3 rd Earth swing-by to comet.....	110
8. NEAR COMET OPERATIONS	114
8.1 Comet Model.....	114
8.2 Range of Comet Models.....	116
8.3 Near Comet Drift Phase	118
8.4 Far Approach Trajectory.....	124

8.5	Close Approach Trajectory	130
8.6	Transition to Global Mapping.....	133
8.7	Global Mapping Phase	140
8.8	Close Observation Phase.....	149
8.9	SSP Delivery	160
8.10	Relay Phase	172
8.11	Extended Monitoring Phase	178
9.	PROPELLANT BUDGET	179
10.	ABBREVIATIONS	180
11.	APPENDIX A. DETAILED TRAJECTORY	182

List of Figures

Figure 3-1: Rosetta Ground Station Network.	8
Figure 4-1: Ecliptic Projection of the Rosetta Trajectory (Launch 26/02/2004 – Only DSM 1.1).	13
Figure 4-2: Ecliptic Projection of the Rosetta Trajectory (Launch 07/03/2004 – DSM 1.1 and DSM1.2)	14
Figure 4-3: Ecliptic Projection of the Rosetta Trajectory (Launch 17/03/2004 – Only DSM 1.2).	15
Figure 5-1: Rosetta Launch in January 2003 with Coast Arc.	21
Figure 5-2: Eclipse Arc during Coast Arc.....	23
Figure 5-3: Launch Network. Ground Station Coverage during Coast Arc.....	25
Figure 5-4: Launch Network. Elevation from Ground Stations during Coast Arc.	25
Figure 5-5: Launch Network. Range from Ground Stations during Coast Arc.	26
Figure 5-6: Total trajectory ΔV as function of the Launch Day.	28
Figure 5-7: Variation of mass after Rendezvous Manoeuvre as function of the Launch Day..	28
Figure 5-8: ΔV of first arc manoeuvres as a function of Launch Date.	29
Figure 5-9: Right Ascension of Earth departure hyperbolic velocity (osculating at injection).	29
Figure 5-10: Pericentre height of first Earth swing-by as a function of Launch Date.	30
Figure 5-11: Pericentre height of second Earth swing-by as a function of Launch Date.	30
Figure 5-12: Impact vectors on B-plane of first Earth swing-by.	31
Figure 5-13: Impact vectors on B-plane of Mars swing-by.	31
Figure 5-14: Impact vectors on B-plane of second Earth swing-by.	32
Figure 5-15: Impact vectors on B-plane of third Earth swing-by.	32
Figure 5-16: Total trajectory ΔV for delayed launch.	35
Figure 5-17: Right Ascension of Earth departure hyperbolic velocity (osculating at injection).	36
Figure 6-1: Evolution of spacecraft distance to Sun and Earth 39	39
Figure 6-2: Evolution of Spacecraft communication angles..... 40	40
Figure 6-3: Evolution of spacecraft declination..... 41	41
Figure 6-4: Phase from Launch to Earth. Ecliptic projection of the trajectory 42	42
Figure 6-5: Phase from Launch to Earth. Spacecraft distance to Sun and Earth 42	42
Figure 6-6: Phase from Launch to Earth. Spacecraft declination 43	43
Figure 6-7: Phase from Launch to Earth. Spacecraft communication angle..... 43	43
Figure 6-8: Phase from Launch to Earth. Angle Earth-S/C-Sun during LEOP. 44	44
Figure 6-9: Phase from Launch to Earth. Angle S/C-Earth-Sun during LEOP. 44	44
Figure 6-10: Phase First Earth swing-by. Trajectory relative to the Earth. 45	45

Figure 6-11: Phase First Earth swing-by. Spacecraft communication angle.	46
Figure 6-12: Phase First Earth swing-by. Eclipse condition.	46
Figure 6-13: Phase from Earth to Mars. Ecliptic projection of the trajectory	47
Figure 6-14: Phase from Earth to Mars. Spacecraft distance to Sun and Earth.....	48
Figure 6-15: Phase from Earth to Mars. Spacecraft declination.....	48
Figure 6-16: Phase from Earth to Mars. Spacecraft communication angle	49
Figure 6-17: Phase Swing-by Mars. Spacecraft trajectory XY projection relative to Mars.....	51
Figure 6-18: Phase Swing-by Mars. Spacecraft trajectory XZ projection relative to Mars.....	51
Figure 6-19: Phase Swing-by Mars. Spacecraft distances to Mars, Phobos and Deimos.....	52
Figure 6-20: Phase Swing-by Mars. Illumination angles to Phobos and Deimos.....	52
Figure 6-21: Phase Swing-by Mars. Spacecraft communication angles.....	53
Figure 6-22: Phase Swing-by Mars. Communication black-out due to spacecraft occultation by Mars.....	53
Figure 6-23: Phase from Mars to Earth. Ecliptic projection of the trajectory.....	54
Figure 6-24: Phase from Mars to Earth. Spacecraft distance to Sun and Earth.....	55
Figure 6-25: Phase from Mars to Earth. Spacecraft declination.....	55
Figure 6-26: Phase from Mars to Earth. Spacecraft communication angle	56
Figure 6-27: Phase Second Earth swing-by. Trajectory relative to the Earth.....	57
Figure 6-28: Phase Second Earth swing-by. Spacecraft communication angle.....	57
Figure 6-29: Phase Second Earth swing-by. Eclipse condition.....	58
Figure 6-30: Phase from Earth to Earth. Ecliptic projection of the trajectory.....	59
Figure 6-31: Phase from Earth to Earth. Spacecraft distance to Sun and Earth.....	59
Figure 6-32: Phase from Earth to Earth. Evolution of spacecraft declination.....	60
Figure 6-33: Phase from Earth to Earth. Communication angles.....	60
Figure 6-34: Phase Third Earth swing-by. Trajectory relative to the Earth.....	61
Figure 6-35: Phase Third Earth swing-by. Spacecraft communication angle.....	62
Figure 6-36: Phase Third Earth swing-by. Eclipse condition.....	62
Figure 6-37: Phase from Earth to 67P/C-G. Ecliptic projection of the trajectory.....	63
Figure 6-38: Phase from Earth to 67P/C-G. Out ecliptic projection of the trajectory.....	64
Figure 6-39: Phase from Earth to 67P/C-G. Spacecraft distance to Sun and Earth.....	64
Figure 6-40: Phase from Earth to 67P/C-G. Evolution of spacecraft declination.....	65
Figure 6-41: Phase from Earth to 67P/C-G. Communication angles.....	65
Figure 6-42: Phase from 67P/C-G RDV to Perihelion. Ecliptic projection of the trajectory... ..	66
Figure 6-43: Phase from 67P/C-G RDV to Perihelion. Out ecliptic projection of the trajectory.....	67
Figure 6-44: Phase from 67P/C-G RDV to Perihelion. Spacecraft distance to Sun and Earth.....	67

Figure 6-45: Phase from 67P/C-G RDV to Perihelion. Evolution of spacecraft declination. .. 68
Figure 6-46: Phase from 67P/C-G RDV to Perihelion. Communication angles..... 68
Figure 6-47: Phase from Launch to Earth. Beginning and End of Visibility Interval from New Norcia during the Day versus Calendar Date. 71
Figure 6-48: Phase from Launch to Earth. Beginning and End of Visibility Interval from Kourou during the Day versus Calendar Date..... 71
Figure 6-49: Phase from Launch to Earth. Visibility Duration for the two Ground Stations versus Calendar Date. 72
Figure 6-50: Phase from Earth to Mars. Beginning and End of Visibility Interval from New Norcia during the Day versus Calendar Date. 72
Figure 6-51: Phase from Earth to Mars. Beginning and End of Visibility Interval from Kourou during the Day versus Calendar Date. 73
Figure 6-52: Phase from Earth to Mars. Visibility Duration for the two Ground Stations versus Calendar Date. 73
Figure 6-53: Phase from Mars to Earth. Beginning and End of Visibility Interval from New Norcia during the Day versus Calendar Date. 74
Figure 6-54: Phase from Mars to Earth. Beginning and End of Visibility Interval from Kourou during the Day versus Calendar Date. 74
Figure 6-55: Phase from Mars to Earth. Visibility Duration for the two Ground Stations versus Calendar Date. 75
Figure 6-56: Phase from Earth to Earth. Beginning and End of Visibility Interval from New Norcia during the Day versus Calendar Date. 75
Figure 6-57: Phase from Earth to Earth. Beginning and End of Visibility Interval from Kourou during the Day versus Calendar Date. 76
Figure 6-58: Phase from Earth to Earth. Visibility Duration for the two Ground Stations versus Calendar Date. 76
Figure 6-59: Phase from Earth to DSM 4. Beginning and End of Visibility Interval from New Norcia during the Day versus Calendar Date. 77
Figure 6-60: Phase from Earth to DSM 4. Beginning and End of Visibility Interval from Kourou during the Day versus Calendar Date..... 77
Figure 6-61: Phase from Earth to DSM 4. Visibility Duration for the two Ground Stations versus Calendar Date. 78
Figure 6-62: Phase from DSM 4 to 67P/C-G. Beginning and End of Visibility Interval from New Norcia during the Day versus Calendar Date..... 78
Figure 6-63: Phase from DSM 4 to 67P/C-G. Beginning and End of Visibility Interval from Kourou during the Day versus Calendar Date..... 79
Figure 6-64: Phase from DSM 4 to 67P/C-G. Visibility Duration for the two Ground Stations versus Calendar Date. 79
Figure 6-65: Phase 67P/C-G to Perihelion. Beginning and End of Visibility Interval from New Norcia during the Day versus Calendar Date. 80
Figure 6-66: Phase 67P/C-G to Perihelion. Beginning and End of Visibility Interval from Kourou during the Day versus Calendar Date..... 80

Figure 6-67: Phase 67P/C-G to Perihelion. Visibility Duration for the two Ground Stations versus Calendar Date.	81
Figure 6-68: Phase Launch to Perihelion. Beginning and End of Visibility Interval from New Norcia during the Day versus Calendar Date.	82
Figure 6-69: Phase Launch to Perihelion. Beginning and End of Visibility Interval from Kourou during the Day versus Calendar Date.	82
Figure 6-70: Phase Launch to Perihelion. Beginning and End of Visibility Interval from Cebreros during the Day versus Calendar Date.	83
Figure 6-71: Phase Launch to Perihelion. Visibility Duration from New Norcia and Kourou versus Calendar Date.	83
Figure 6-72: Phase Launch to Perihelion. Visibility Duration from New Norcia and Cebreros versus Calendar Date.	84
Figure 6-73: Evolution with time of pointing dispersion from Kourou at first pass.	85
Figure 6-74: Evolution with time of range-rate dispersion relative to Kourou at first pass.	86
Figure 6-75: Early Orbit Trajectory. Equatorial projection.	87
Figure 6-76: Early Orbit Trajectory. Distance to Earth and Moon.	87
Figure 6-77: Early Orbit Trajectory. Range Rate Measurements from Kourou and New Norcia.	88
Figure 6-78: Early Orbit Trajectory. Orbit Determination Position Error.	89
Figure 6-79: Early Orbit Trajectory. Velocity Error.	89
Figure 6-80: Dispersion 1- σ ellipses at 1 st Earth pericentre target plane.	94
Figure 6-81: Dispersion 1- σ ellipses at Mars pericentre target plane.	96
Figure 6-82: Dispersion 1- σ ellipses at Mars pericentre target plane.	96
Figure 6-83: Dispersion 1- σ ellipses at 2 nd Earth pericentre target plane.	98
Figure 6-84: Dispersion 1- σ ellipses at 3 rd Earth pericentre target plane.	99
Figure 6-85: Dispersion 1- σ ellipses at 3 rd Earth pericentre target plane.	100
Figure 7-1: Distances to the Sun during phase EAR2-EAR3.	106
Figure 7-2: Distances to the Earth during phase EAR2-EAR3.	107
Figure 7-3: Equatorial declination during phase EAR2-EAR3.	107
Figure 7-4: Angle Spacecraft-Earth-Sun during phase EAR2-EAR3.	108
Figure 7-5: Angle Earth-Spacecraft-Sun during phase EAR2-EAR3.	109
Figure 7-6: Ecliptic XY projection of the trajectory of phase EAR2-EAR3.	109
Figure 7-7: Ecliptic XZ projection of the trajectory of phase EAR2-EAR3.	109
Figure 7-8: Distances to the Sun during phase EAR3-Comet.	110
Figure 7-9: Distances to the Earth during phase EAR3-Comet.	111
Figure 7-10: Equatorial declination during phase EAR3-Comet.	111
Figure 7-11: Angle Spacecraft-Earth-Sun during phase EAR3-Comet.	112
Figure 7-12: Angle Earth-Spacecraft-Sun during phase EAR3-Comet.	112

Figure 7-13: Ecliptic XY projection of the trajectory of phase EAR3-Comet.	113
Figure 7-14: Ecliptic XZ projection of the trajectory of phase EAR3-Comet.....	113
Figure 8-1: Model of Comet shape	115
Figure 8-2: Evolution of the Distances from the Earth and the Sun to the Rosetta S/C.....	121
Figure 8-3: NCD Strategy	122
Figure 8-4: Numerical Trajectory (RST Frame).....	123
Figure 8-5: S/C Auxiliary Parameters during Near Comet Drift.....	124
Figure 8-6: FAT Strategy	126
Figure 8-7: FAT Numerical Trajectory (RST Frame)	127
Figure 8-8: S/C Auxiliary Parameters during Far Approach Trajectory.	128
Figure 8-9 Estimation of spacecraft relative state with respect to comet	129
Figure 8-10: CAT Strategy.....	131
Figure 8-11: CAT Numerical Trajectory (RST Frame).....	132
Figure 8-12: S/C auxiliary parameters during Close Approach Trajectory.....	133
Figure 8-13: TGM Strategy.....	135
Figure 8-14: TGM Numerical Trajectory (RST Frame).....	136
Figure 8-15: S/C Auxiliary Parameters during Transition to Global Mapping phase.	137
Figure 8-16: Comet Kinematics Estimation Errors during Transition to Global Mapping. ...	138
Figure 8-17: Landmark Position Estimation Errors during Transition to Global Mapping....	139
Figure 8-18: Gravitational Field Estimation Errors during Transition to Global Mapping....	140
Figure 8-19: Global Mapping Orbital Plane Selection	141
Figure 8-20: GMP Numerical Trajectory (RST Frame)	143
Figure 8-21: S/C Auxiliary Parameters during Global Mapping phase.....	144
Figure 8-22: Comet Kinematics Estimation Errors during Global Mapping.....	145
Figure 8-23: Landmark Position Estimation Errors during Global Mapping.	146
Figure 8-24: Gravitational Field Estimation Errors during Global Mapping.	147
Figure 8-25: Mapped Surface of the Comet after 4 days.....	148
Figure 8-26: Mapped Surface of the Comet at end of GMP.....	149
Figure 8-27: COP Strategy.....	152
Figure 8-28: COP Numerical Trajectory (RST Frame)	153
Figure 8-29: S/C Auxiliary Parameters during Close Observation Phase.	154
Figure 8-30: Comet Kinematics Estimation Errors during Close Observation Phase.	155
Figure 8-31: Landmark Position Estimation Errors during Close Observation Phase.....	156
Figure 8-32: Gravitational Field Estimation Errors during Close Observation Phase.....	157
Figure 8-33: Gravitational Field Estimation Errors during Close Observation Phase.....	158
Figure 8-34: Nadir Observation and Field of View of NAC camera.....	159

Figure 8-35: SPD optimisation variables.....	164
Figure 8-36: SPD Strategy	164
Figure 8-37: S/C Trajectory during SSP Operations. In RST Frame.....	165
Figure 8-38: Detail of S/C and Probe Trajectories in Principal Frame	166
Figure 8-39: Detail of S/C and Probe Trajectories in RST Frame.....	167
Figure 8-40: S/C Auxiliary Parameters during Surface Probe Delivery Phase.	168
Figure 8-41: Spacecraft position with respect to jets during Surface Probe Delivery Phase. .	169
Figure 8-42: S/C Position and Velocity Errors during Surface Probe Delivery Phase.....	170
Figure 8-43: Probe Position and Velocity Errors during Surface Probe Delivery Phase.	171
Figure 8-44: Ellipse of Dispersion at the Probe Landing for a Typical Case.....	172
Figure 8-45: SPR Strategy.....	174
Figure 8-46: SPR Numerical Trajectory (RST Frame).....	175
Figure 8-47: S/C Auxiliary Parameters during Relay Phase.....	176
Figure 8-48: Lander – Spacecraft parameters.....	177

List of Tables

Table 4-1: Parameters for February-March 2004 Mission to Churyumov-Gerasimenko.....	12
Table 4-2: Rosetta Telecommunication Subsystem.....	18
Table 4-3: Parameters of the Operation Phases of the Rosetta Mission.....	20
Table 5-1: Eclipses during Launch Phase (UTC for 26/02/2004).	23
Table 5-2: Ground Station Visibility during Launch Phase (elapsed time from ignition).	24
Table 5-3: Ariane 5 dispersion matrix for injection in escape orbit.....	26
Table 5-4: Launch hour as function of launch date, and escape right ascension.....	34
Table 6-1: Major events of the Rosetta mission	38
Table 6-2: Orbital and Physical properties of Mars Satellites.....	50
Table 6-3: Duration of visibility gaps and overlaps (Min. elevation: 10 deg).....	84
Table 6-4: Ariane 5 Injection Accuracy for Rosetta Escape Mission with Coast Arc	86
Table 6-5: Statistical Results of Manoeuvre for Correction of Injection Errors	91
Table 6-6: Statistics of required ΔV for trajectory guidance of arc from launch to Earth.	91
Table 6-7: Statistics of required perigee altitude change of 1 st Earth swing-by for trajectory guidance.....	92
Table 6-8: Statistics of the Mid-Course Correction Manoeuvres up to 1 st Earth swing-by.....	93
Table 6-9: Position dispersion errors at pericentre 1 st Earth swing-by.....	94
Table 6-10: Statistics of the Mid-Course Correction Manoeuvres from Earth to Mars	95
Table 6-11: Position dispersion errors at pericentre of Mars swing-by.....	95
Table 6-12: Statistics of the Mid-Course Correction Manoeuvres from Mars to Earth	97
Table 6-13: Position dispersion errors at pericentre of 2 nd Earth swing-by.....	97
Table 6-14: Statistics of the Mid-Course Correction Manoeuvres from 2 nd Earth to 3 rd Earth swing-by.....	98
Table 6-15: Position dispersion errors at pericentre of 3 rd Earth swing-by	99
Table 6-16: Statistics of the Mid-Course Correction Manoeuvres from 3 rd Earth swing-by to comet.....	100
Table 6-17: Accumulated ΔV statistics of the trim correction manoeuvres	101
Table 7-1: Single asteroid fly-by missions.....	103
Table 7-2: Fly-by parameters of asteroid candidates.....	104
Table 7-3: Double asteroid fly-by missions. Additional delta-V required.	104
Table 4: Asteroid fly-by opportunities as a function of available ΔV	105
Table 8-1: Initial Estimation errors of Comet Kinematics.....	119
Table 8-2: Distances S/C-Sun and S/C-Earth from Rendezvous Manoeuvre to Perihelion. ..	121
Table 9-1: Propellant Budget.....	179

PAGE INTENTIONALLY LEFT BLANK

1. PURPOSE

The Rosetta Consolidated Report on Mission Analysis summarizes the current status of the Rosetta Mission Analysis tasks performed by ESOC/TOS/GMA, and presents relevant mission data for the continuation of the Project.

After the failure of the Ariane 5 ECA in December 2002, a joint Arianespace - ESA commission was established to review the status of the Ariane 5 P1+ to be used for the launch of Rosetta. The recommendations of this commission forced to stop the launch of the original Rosetta mission with launch in January 2003 and rendezvous with 46P/Wirtanen in November 2011.

Possible alternative missions were presented to the Rosetta Science Working Team on Feb. 2003. In the resolution unanimously approved by the SWT, one of the recommendations is to prepare for a mission to be launched in February-March 2004 by an Ariane 5 P1+ using a delayed ignition of the upper stage. This alternative mission will rendezvous comet 67P/Churyumov-Gerasimenko in 2014.

The most important mission aspects treated in this document are:

- Parametric analysis.
- Mission baseline description.
- Launch with Ariane 5 and launch window.
- Interplanetary trajectory and derived auxiliary calculations
- Launcher injection correction and Interplanetary navigation
- Asteroid fly-by possibilities
- Near comet operations.
- Delta-V budget.

2. REFERENCES

2.1 *Applicable Documents*

AD 1. RO-EST-RS-2001. ROSETTA System Requirements Specifications.

2.2 *Reference Documents*

- RD 1.** Ariane 5 User's Manual.
- RD 2.** P. Claudel, J-P. Duluot. AE/DI/E/LM/ No.292/96. Ariane 5 Feasibility Mission Analysis. Trajectory and Performance Study. Rosetta Escape Mission in Single Launch Configuration.
- RD 3.** J. Breton. DC/P/ST No. 98 554. Rev. 0. Synthesis of the Performance Data Provided to ESA for the Rosetta Mission. October 1998.
- RD 4.** J. Breton. DC/P/ST No. 98 554. Rev. 2. Synthesis of the Performance Data Provided to ESA for the Rosetta Mission. November 1998.
- RD 5.** E. González-Laguna. Rosetta Launch with Ariane 5. MAS Working Paper No. 375. November 1995.
- RD 6.** E. González-Laguna. Rosetta: Baseline Trajectory Description. MAS Working Paper No. 388. July 1996.
- RD 7.** Rosetta Mission Implementation Plan, RO-ESC-PL-5100, Draft 1, June 1997.
- RD 8.** M. Belló Mora, Near Comet Orbit Planning and Navigation Tool, Final Report, Jan. 1997, ESA CR (P) 4106
- RD 9.** M. Belló Mora, Study on Delivery and Navigation of Active Probes, Final Report, ESA-ESOC, March 1998, ESA CR (P)
- RD 10.** V.V. Ivashkin, Comet Gas, Dust and Jet Models, GMVSA 2059/96, Final Report, March 1996.
- RD 11.** Rosetta Lander Mission Analysis Working Group. Final Report, Draft 0, Sep. 1998, RO-ESC-RP-5003.
- RD 12.** Arianespace Industrial Directorate. Preliminary Mission Analysis - Trajectory and Performance Study Rosetta. Ariane 5/P1+ Escape Mission - Single Launch Configuration. Oct, 2001. A5-DAMP-TRAJ-ROSETTA.
- RD 13.** J. Rodríguez Canabal J.M. Sánchez Pérez J.L. Pellón Bailón A. Yáñez. Rosetta: Consolidated Report on Mission Analysis. RO-ESC-RP-5500 Issue 4, Rev 0. June 2002.
- RD 14.** J.L. Pellón Bailón, J. Rodríguez Canabal, J.M. Sánchez Pérez, Rosetta Launch Window. MAS Working Paper No. 436. January 2002.

- RD 15.** J.M. Sánchez Pérez, J. Rodríguez Canabal, Rosetta Consolidated Report on Mission Analysis. Churyumov-Gerasimenko 2004. Feb. 2003, Issue 1.
- RD 16.** J.M.Sánchez-Pérez, J.Rodríguez-Canabal, Rosetta: Missions to 67P/Churyumov-Gerasimenko including fly-by of 2 asteroids. MAO Working Paper 457, April 2003.
- RD 17.** Arianespace Industrial Directorate. Preliminary Mission Analysis - Trajectory and Performance Study Rosetta (Churyumov-Gerasimenko). Ariane 5G+ Escape Mission - Single Launch Configuration. July 2003. A5-DAMP-TRAJ-ROSETTA2.

3. MISSION REQUIREMENTS AND CONSTRAINTS

3.1 General Description

To support investigations of the Solar System origin and evolution, an in-situ analysis of minor bodies in the Solar System is mandatory. Previous space missions have recently increased the amount of data available on asteroids and comets. Comet Halley was flown-by by the probes Giotto, Vega, Sagigake, and Susei in 1986. In July 1992, during its extended mission, Giotto had a close encounter with comet Grigg-Skjellerup. Also Galileo has flown-by the asteroids Gaspra and Ida before starting the tour around the Jupiter moons. More recently the mission NEAR had rendezvous with asteroid Eros, having an en route encounter with asteroid Mathilde. Together with spacecraft based observations of minor celestial bodies, observation campaigns have been carried out by telescopes (either space or ground telescopes) at almost all wavelengths (visible, infrared, ultraviolet, microwave, radio). From this wealth of new information, it seems apparent that asteroids and comets constitute an almost continuous set of progressively less evolved objects, reflecting the radial gradient in the crowd of planetesimals during the formation of the Solar System. A better understanding of the relationship between asteroids, comets and planetesimals will help the scientific community to reconstitute the first stages of the formation of our Solar System.

As far as it is known, comets are in a low evolution level, which likely converts them in a potential source of information on the early components and evolution of the Solar System.

The study of unaltered cometary samples has become an important objective because of its high content of volatiles and organic material. The former CNSR (Comet Nucleus Sample Return) mission aimed to return to the Earth a sample of a cometary nucleus. The probe would rendezvous the comet, land, take a piece of cometary material, and return it to the Earth for analysis. The present Rosetta mission will analyse *in situ* the cometary nucleus, by remote sensing instruments and a Surface Science Package (Lander). The scientific instruments of the lander will perform measurements on the comet surface and transmit the results to the comet orbiting probe. This strategy allows minimal perturbation of the nucleus, and microgravity environment. The last part of the mission, up to perihelion will allow to observe the evolution of the cometary activity as the nucleus get closer to the Sun.

The mission will provide information about the comet kinematics, mass properties, density, composition, structure, superficial layers, volatile components, and gas and dust emissions.

3.2 Scientific Requirements

After the decision on the target comet change, Rosetta will study the nucleus of comet 67P/Churyumov-Gerasimenko and in its way to the comet, it will obtain scientific data from asteroids one or two asteroids (TBD). The probe will remain almost 15 months near 67P/Churyumov-Gerasimenko until the comet perihelion. A complex strategy will allow first

remote observation, secondly comet characterization, later a lander deployment for *in situ* analysis, and at last study of the cometary activity.

The Rosetta Science Team has defined the prime scientific objective as:

- Study the origin of comets, the relationship between cometary and interstellar material, and the implications for the origin of the Solar System.

The following measures should lead to the fulfilment of above main objective.

- Nucleus global characterisation, dynamic properties determination, surface morphology, and composition.
- Chemical, mineralogical, and isotopic compositions of volatiles and refractories in the nucleus.
- The physical properties and interrelation of volatiles and refractories in the nucleus.
- The study of the development of cometary activity and the processes in the surface layer of the nucleus and the inner coma (dust-gas interaction).
- The global characterization of the asteroids, determination of their dynamic properties, surface morphology, and composition.

For the successful completion of the scientific mission, the following general scientific requirements have been imposed on the mission design, spacecraft, and mission operation:

- *During the prime mission from 3.25 AU through perihelion passage high resolution mapping of the nucleus (more than 80 % of the surface) should be possible.*
- *The instrument line of sight shall be independently selectable to any point of the comet.*
- *Rosetta shall extensively fly over dust and gas jets to collect a satisfactory amount of material in the dust collectors.*
- *The Rosetta orbiter in principle shall be able to reach any position around the nucleus at any given time.*

3.2.1 Comet Characterisation

The characterization of the comet will start with the determination of the global parameters defining the nucleus: ephemerides, parameters related with its gravitational field (mass and density), state of rotation and shape. The information about all this parameters will be acquired by processing the images provided by the on board cameras.

The improvement in the knowledge of the comet ephemerides will be achieved by combining on board measurements (relative position of the spacecraft w.r.t. the comet) and on-ground measurements (relative position of the spacecraft w.r.t. the Earth).

The shape of the comet will be reconstructed on ground using the images taken at different times. The global mapping phase is the most important from the point of view of the comet model reconstitution. Once the comet shape has been determined, the accelerations acting on the spacecraft will provide information about the comet density.

The images will also provide information about the orientation evolution with the time and this information will be used to determine both the rotation period of the comet and the orientation of the spin axis.

All this information can be collected during the spacecraft approximation and orbit around the comet and will provide clues concerning vertical gradients, and hence the relationship between the outer layers and the underlying material.

After the probe landing, additional information will be available to reach a deeper characterization of comet properties such as materials composition and nucleus activity. The analysis of the volatile materials of the active areas will provide more detailed information about the constituents of the cometary nucleus. The surface can be monitored during a large fraction of the activity cycle, which should bring to light clues concerning to the compositional heterogeneity of active regions. A study of the development of cometary activity and processes in the surface layer can be performed.

After the end of the activities related to the surface package science, the spacecraft will spend at least 200 days in the vicinity of the comet until perihelion passage. During this period the gas and dust of the inner coma can be analysed from the onset to the peak activity.

3.2.2 Asteroids Characterisation

During the fly-by of an asteroid, the on board cameras will provide images of it. Combining these images with the on-ground measurements, the ephemerides of the asteroid shall be improved. In addition to the ephemerides, a global characterization of the asteroid will be carried out, determining its dynamic properties, surface morphology and composition.

3.3 *Launcher Requirements*

The Rosetta spacecraft will use a dedicated Ariane 5 launcher. To ensure the required performance, spacecraft wet mass of 3064 kg, and escape velocity of 3.545 km/s with declination of -2° , the launch procedure must include a delayed ignition of the Ariane 5 upper stage, EPS.

The launch will take place in a very short launch window of about 20 days on February-March 2004. The mass of the spacecraft delivered in orbit around the comet depends on the day of launch. The injection conditions do not depend on the launch day allowing the use of only one Ariane 5 flight program.

Rosetta requires a launch involving a delayed ignition of the upper stage (EPS). Analysis performed by ESA and by Arianespace show very good agreement on the launcher performance for the delayed ignition of the EPS stage, and no major technical problem associated with this flight procedure. Flight software including delayed EPS ignition and re-ignition is qualified and has been demonstrated on Ariane 503 flight. From Ariane 517 onwards the EPS will have full re-ignition capability and a ballistic phase capability of up to 6 hours.

Arianespace has provided to ESA a summary of the Ariane 5 performances for the Rosetta mission.

3.4 Spacecraft Requirements

General mission requirements formulated in the document RO-EST-RS-2001 that are related to Mission Analysis are listed here. Within parenthesis is given the reference in that document.

The following ones are related to the general spacecraft configuration:

- The wet mass of the spacecraft will be < 2900 kg. (GERE-20). Updated to 3064 kg.
- The on-board propulsion system will have a minimum capability of 2200 m/s. (GERE-23). Updated to 2130 m/s.
- The power will be provided by means of both solar cell array and batteries. (POWR-1)
- The spacecraft will autonomously and without the need for batteries re-acquire sun pointing of the solar arrays upon detection of potential loss of solar power. (MISS-12)
- The spacecraft shall accommodate the Surface Science Package - Rosetta Lander. (GERE-3)

Spacecraft requirements related to different mission phases are:

- The spacecraft will support a mission with Earth and Mars gravity assists, with a minimum distance to the Sun of 0.9 AU, a maximum distance of 5.25 AU, and a maximum distance to the Earth of 6.2 AU. (MISS-2)
- The spacecraft shall operate autonomously throughout the aphelion cruise up to the rendezvous manoeuvre during 29 months. (MISS-10)
- The spacecraft shall support deep space manoeuvres and the rendezvous manoeuvre at a maximum distance to the Sun of 4.4 AU. (MISS-11)

- The spacecraft shall support full science operation at a distance not less than 3.25 AU from the Sun. (MISS-20)
- The spacecraft propulsion subsystem shall support a post launch orbit manoeuvre to correct for injection errors, and to ensure a launch window of at least 10 days and a daily launch window of 20 minutes. (MISS-5)
- The propulsion system shall provide the capability to perform major orbit manoeuvres with a minimum thrust level of 40 N. (PROP-15)
- The propulsion system shall be capable of performing orbit corrections with a resolution of 1 mm/s. (MISS-23)
- Optimisation of data down linking during the Near Comet Operation phase will impose continuous HGA pointing to the Earth, except in very specific cases (lander delivery). (MISS-26)
- Near comet orbits shall be planned to avoid collision with the comet in case of failures on the spacecraft or in ground operations. (MISS-47)

3.5 Ground Station and Radio Tracking System

The Ground Station Network for Rosetta is composed of New Norcia (34 m dish) and Kourou (15 m dish). The NASA Deep Space Network will be used as back-up (See Figure 3-1). New Norcia will be used during the whole mission operations and Kourou for near Earth operations.

ROSETTA Ground Station Network

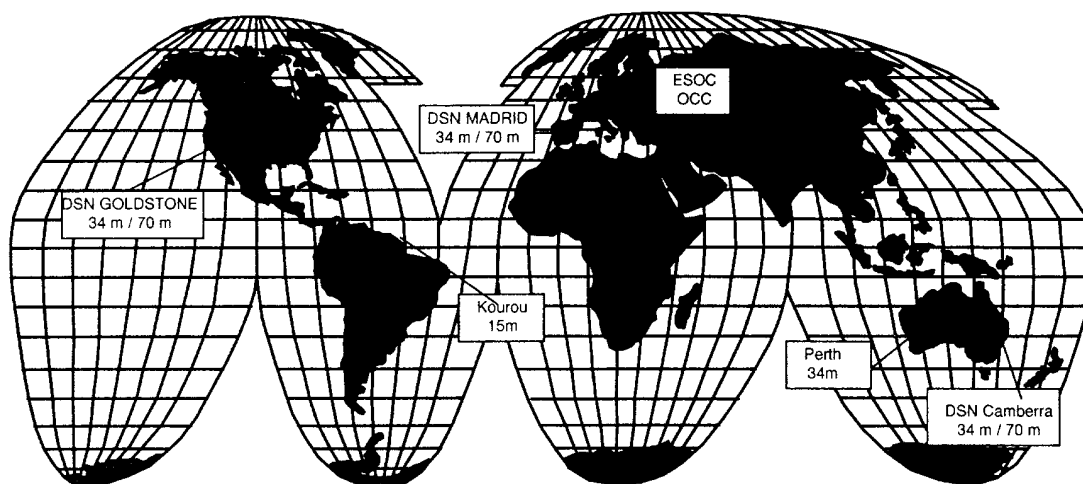


Figure 3-1: Rosetta Ground Station Network.

4. MISSION OVERVIEW

4.1 Mission Baseline Description

The current baseline for the Rosetta mission is to rendezvous comet 67P/Churyumov-Gerasimenko in May 2014. To achieve this objective the probe follows a tour of planets composed of one swing-by in Mars, and a three Earth swing-by. Figure 4-1 shows an ecliptic projection of the Rosetta baseline mission.

The results presented in this chapter have been obtained using numerical propagation including all relevant orbital perturbations, such as third body gravitational attractions and solar radiation pressure. An average specific impulse of 290 s is assumed for the trajectory manoeuvres with the 10 N thrusters. No manoeuvres are needed at or near the fly-by of planets Mars and Earth. The complete trajectory requires the implementation of four or five deterministic manoeuvres. Depending on the launch day, the first Delta-V Gravity Assist, ΔV_{GA} , Earth-Earth arc includes one manoeuvre at the perihelion or one manoeuvre at the aphelion or both manoeuvres at perihelion and aphelion. One deep space manoeuvre is needed in the interplanetary arc from the Earth to Mars, one more in the second Earth-Earth arc and the last manoeuvre is performed at a distance of 4.4 AU from the Sun in the way from the Earth to the comet, before entering the aphelion hibernation.

4.1.1 Rosetta Baseline Mission

The mission can be decomposed in the following phases (data for the phases after the Commissioning Phase is given for the nominal Rosetta launch date on 26, February, 2004.):

Launch: Ariane 5 will place the spacecraft in an escape orbit characterised by an excess velocity of 3.545 km/s and an asymptote declination of -2.0° . To achieve these escape conditions, and given the expected mass of Rosetta, the Ariane 5 flight will include a delayed ignition of the upper stage, EPS. Possible injection errors due to the launcher will be corrected by the own on board propulsion system of the spacecraft.

Commissioning: After spacecraft separation from Ariane 5, the Rosetta spacecraft acquires its three axes stabilized Sun pointing attitude and deploys the solar arrays autonomously. Ground Control establishes communications with the spacecraft, and checks on-board equipment, spacecraft functions, instruments and payload. Trajectory correction is commanded if needed. This phase ends after three months.

Arc Earth-Earth: A period of 370 days is required from launch to Earth return. During this arc an interplanetary deep space manoeuvre (DSM) of about 173 m/s is performed.

Earth swing-by I: (2 March 2005) The perigee altitude is about 4290 km.

Arc Earth-Mars: approximately 730 days are required for the more than one revolution around the Sun travel from the Earth to Mars. There is a solar conjunction during this arc for a period of almost one month in April of 2006. A deep space manoeuvre of about 65 m/s near perihelion after a complete revolution around the Sun is performed.

Mars Swing-by: (27 February 2007). About 5-6 months before Mars arrival the spacecraft will be activated to prepare the Mars swing-by. The minimum altitude with respect to the Martian surface is 200 km (value selected to ensure a safe swing-by). During the swing-by a communications black-out of approximately 14 minutes is expected due to occultation of the spacecraft by Mars. Furthermore the spacecraft is expected to be in eclipse for about 24 minutes.

Arc Mars-Earth: interplanetary phase of 260 days, no intermediate trajectory manoeuvre is performed.

Earth swing-by II: (15 November 2007). The perigee altitude is about 13890 km.

Arc Earth-Earth: Cruise phase of 727 days with spacecraft hibernation and deep space manoeuvre of about 129 m/s. A solar conjunction will take place January 2009, together with another two conjunctions of the Earth-S/C-Sun angle (Sun-Earth conjunction as seen from the spacecraft).

Earth swing-by III: (11 November 2009). The perigee altitude is about 300 km.

Arc Earth III-DSM: Long cruise phase of 546 days with the spacecraft hibernated.

Deep Space Manoeuvre: (10 May 2011). The manoeuvre is carried out at 4.4 AU from the Sun and the required ΔV is 533 m/s

Arc DSM-Churyumov-Gerasimenko: Aphelion cruise phase of 1108 days with the spacecraft hibernated.

Churyumov-Gerasimenko orbit matching manoeuvre: (23 May 2014). The spacecraft reaches the comet at a distance of 4.0 AU from the Sun. The mission duration up to rendezvous is 10.2 years, which is exactly 3739 days. All the comet approach and operation phase will follow a complex strategy that will be treated in chapter 8 – ‘Near Comet Operations’. In this section the orbit-matching manoeuvre is simplified as a single braking manoeuvre at the time of closest approach to the nucleus. This is a major manoeuvre of about 774 m/s. With a more complex strategy some extra ΔV will be required, therefore the figure given here is a lower limit of the size of the orbit-matching manoeuvre.

Near Comet operation: It includes a drift phase, the comet nucleus detection and approach, the comet mapping and close observation, the delivery of the Rosetta Lander and the extended monitoring of the nucleus till the end of the mission, nominally at perihelion, around 445 days after rendezvous with the comet. (August 2015). The complete duration of the mission from launch to the perihelion of the comet is 11.5 years, which is about 4184 days.

Some complementary information can be found in section 4.4.

Table 4-1 shows the variations of mission parameters over a 21-days launch period. Selected days are the beginning, middle and end of the window and the ± 5 days with respect to the middle launch day.

Event	Parameter	OPEN	MID -5	MID	MID +5	CLOSE
<i>Launch</i>	date	2004/02/26	2004/03/02	2004/03/07	2004/03/12	2004/03/17
	V_{inf} (Km/s)	3.545	3.545	3.545	3.545	3.545
	δ (°)	-2.0	-2.0	-2.0	-2.0	-2.0
<i>DSM 1.1</i>	date	2004/05/25	2004/05/25	2004/05/29	2004/05/29	
	days	89	84	83	78	
	r_E (AU)	0.28	0.26	0.25	0.23	
	r_S (AU)	0.89	0.89	0.89	0.90	
	ΔV (m/s)	173.5	158.8	87.7	22.2	0
	α_S (°)	85.5	87.3	89.1	87.1	
	α_E (°)	162.1	159.8	158.5	157.1	
<i>DSM 1.2</i>	date			2004/11/29	2004/11/30	2004/11/15
	days			267	263	243
	r_E (AU)			0.30	0.29	0.35
	r_S (AU)			1.11	1.10	1.10
	ΔV (m/s)	0	0	82.0	161.1	200.7
	α_S (°)			88.3	89.8	96.0
	α_E (°)			29.9	30.7	33.2
<i>Earth 1 swing-by</i>	date	2005/03/02	2005/03/06	2005/03/06	2005/03/06	2005/03/08
	days	370	369	364	359	356
	h_p (Km)	4287	2586	2266	1993	1239
	V_{inf} (Km/s)	3.904	3.878	3.879	3.880	3.888
<i>DSM 2</i>	date	2006/10/21	2006/10/20	2006/10/20	2006/10/20	2006/10/20
	days	968	962	957	952	947
	r_E (AU)	1.89	1.88	1.88	1.88	1.88
	r_S (AU)	1.00	0.99	0.99	0.99	0.99
	ΔV (m/s)	64.3	66.3	65.5	67.8	68.0
	α_S (°)	85.8	88.3	87.7	85.6	90.4
	α_E (°)	67.5	69.6	68.9	66.8	71.6
<i>Mars swing-by</i>	date	2007/02/27	2007/02/28	2007/02/28	2007/03/01	2007/03/01
	days	1097	1093	1088	1084	1079
	r_E (AU)	2.10	2.09	2.09	2.09	2.09
	r_S (AU)	1.44	1.44	1.44	1.44	1.44
	h_p (Km)	200	200	200	200	200
	V_{inf} (Km/s)	8.772	8.757	8.758	8.754	8.755

Event	Parameter	OPEN	MID -5	MID	MID +5	CLOSE
<i>Earth 2 swing-by</i>	date	2007/11/15	2007/11/15	2007/11/15	2007/11/16	2007/11/16
	days	1358	1353	1348	1344	1339
	h_p (Km)	13893	14127	14138	14233	14180
	V_{inf} (Km/s)	9.331	9.329	9.330	9.328	9.336
<i>DSM 3</i>	date	2009/03/15	2009/03/15	2009/03/14	2009/03/15	2009/03/15
	days	1844	1839	1833	1829	1824
	r_E (AU)	2.89	2.90	2.91	2.90	2.90
	r_S (AU)	2.20	2.21	2.21	2.21	2.208
	ΔV (m/s)	129.4	126.2	125.3	125.7	124.6
	α_S ($^\circ$)	94.7	93.5	93.8	93.8	92.5
	α_E ($^\circ$)	78.2	77.3	77.7	77.7	76.4
<i>Earth 3 swing-by</i>	date	2009/11/11	2009/11/11	2009/11/11	2009/11/11	2009/11/11
	days	2085	2080	2075	2070	2065
	h_p (Km)	300	300	300	300	300
	V_{inf} (Km/s)	9.983	9.966	9.963	9.961	9.965
<i>DSM 4</i>	date	2011/05/10	2011/05/10	2011/05/10	2011/05/10	2011/05/10
	days	2630	2625	2620	2615	2610
	r_E (AU)	3.40	3.40	3.40	3.40	3.40
	r_S (AU)	4.40	4.40	4.40	4.40	4.40
	ΔV (m/s)	532.6	511.9	513.7	509.1	501.3
	α_S ($^\circ$)	96.6	95.9	96.0	95.9	95.4
	α_E ($^\circ$)	94.8	94.1	94.2	94.1	93.6
<i>Churyumov-Gerasimenko rendezvous</i>	date	2014/05/23	2014/05/23	2014/05/23	2014/05/23	2014/05/23
	days	3739	3734	3729	3724	3719
	r_E (AU)	3.31	3.31	3.31	3.31	3.31
	r_S (AU)	4.00	4.00	4.00	4.00	4.00
	ΔV (m/s)	773.6	778.3	777.3	778.2	780.6
	α_S ($^\circ$)	53.2	54.8	54.5	54.7	55.7
	α_E ($^\circ$)	64.9	66.5	66.2	66.4	67.4

Table 4-1: Parameters for February-March 2004 Mission to Churyumov-Gerasimenko.

The parameters in the table have the following meaning:

- ΔV - size of manoeuvre
- α - Body aspect angle of manoeuvre = angle (ΔV -vector, spacecraft-to-Body vector); subscript E for Earth, and S for Sun.
- δ - declination of launch asymptote (MEEQ2000)
- V_{inf} - escape velocity or fly-by velocity

r - distance to Body; subscript E for Earth and S for Sun
 h_p - pericentre altitude.

MISSION TO 67P/C-G (LAUNCH: 2004/26/ 2 DURATION: 10.2 YEARS)

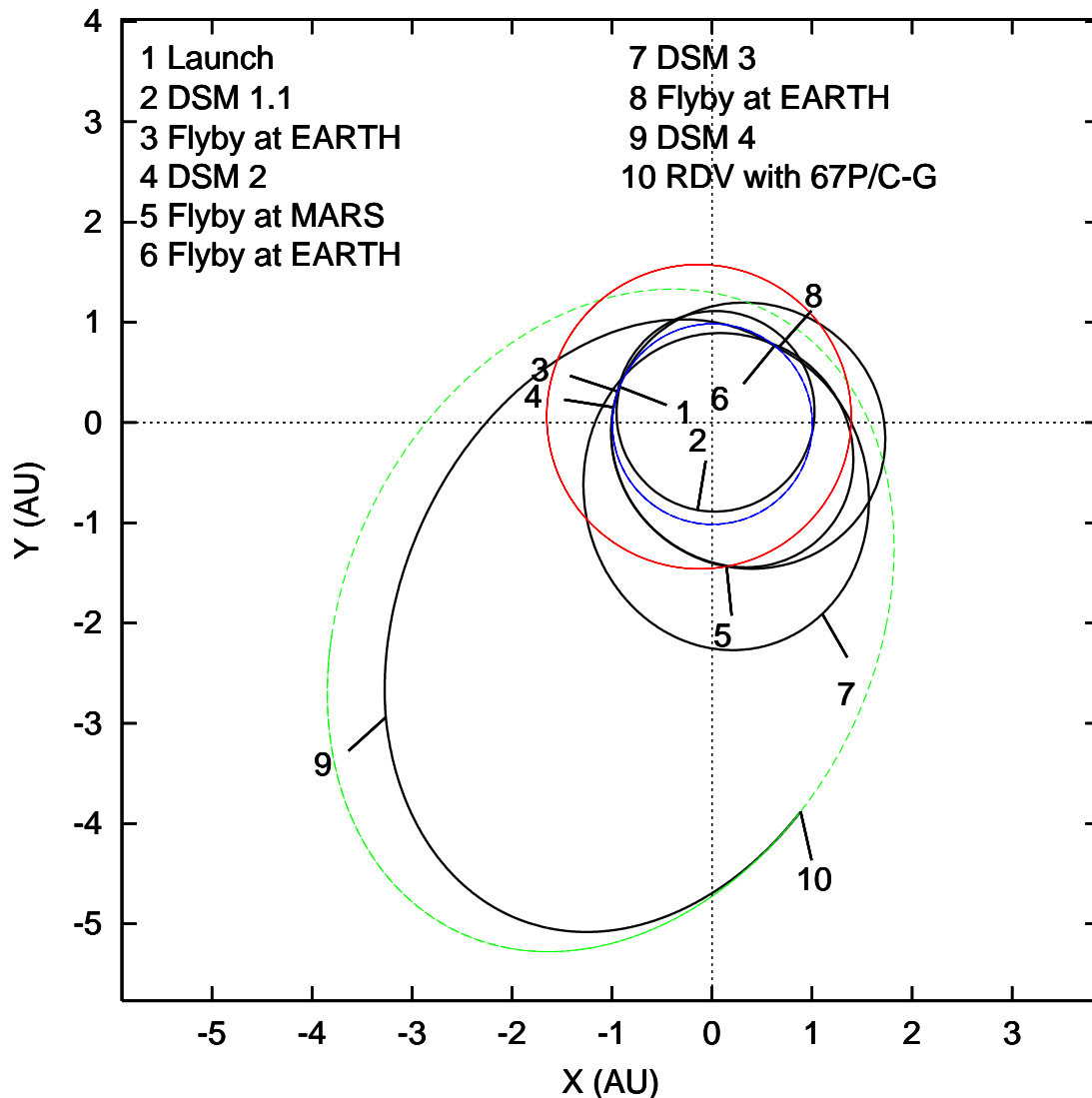


Figure 4-1: Ecliptic Projection of the Rosetta Trajectory (Launch 26/02/2004 – Only DSM 1.1).

The figure shows the projection on the Ecliptic Plane of the Rosetta baseline trajectory. The Rosetta trajectory is represented with solid line. The orbits of the Earth, Mars, and the asteroids are represented with dotted lines. The successive major events are numbered and displayed on the plot.

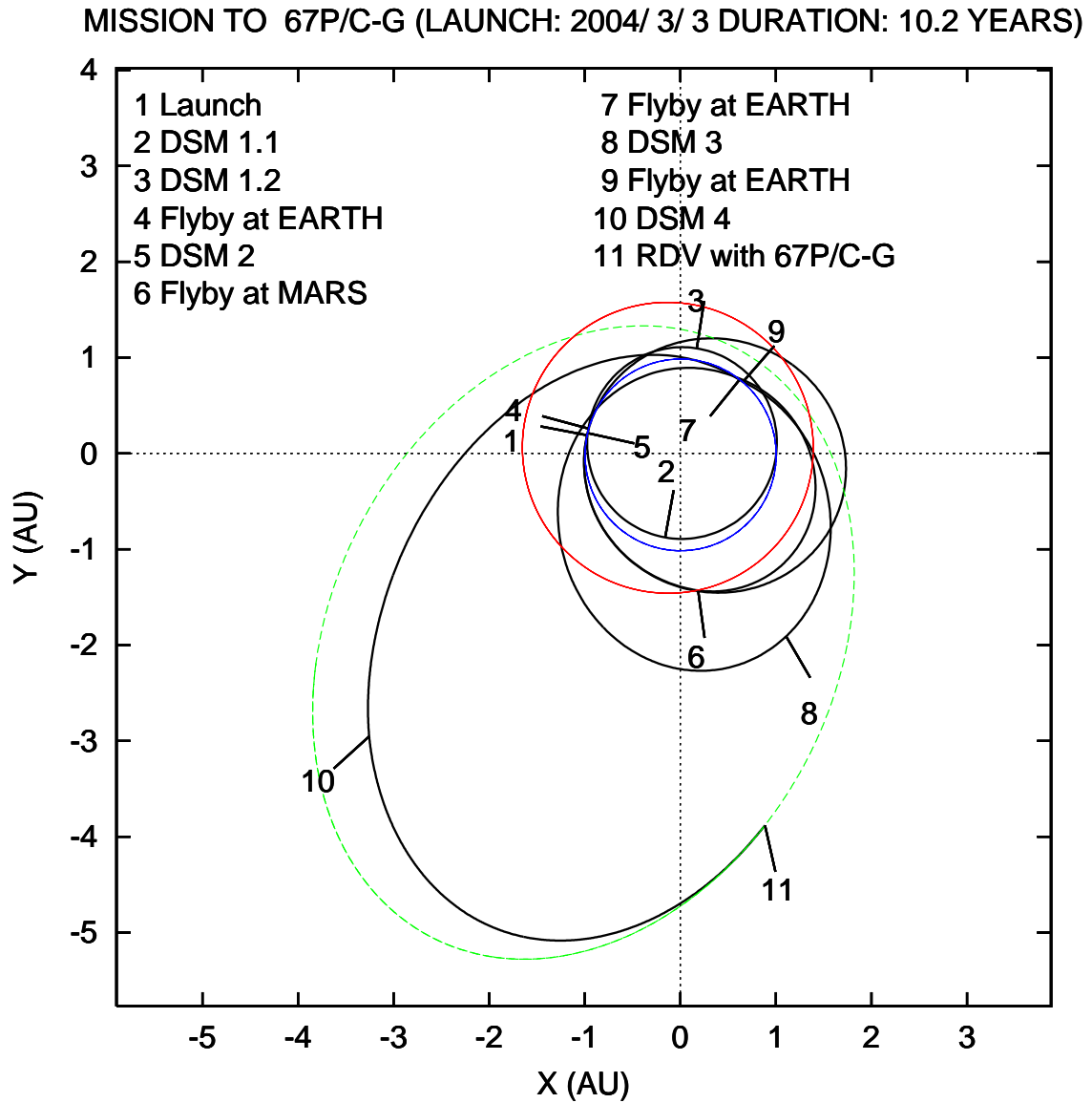


Figure 4-2: Ecliptic Projection of the Rosetta Trajectory (Launch 07/03/2004 – DSM 1.1 and DSM1.2) .

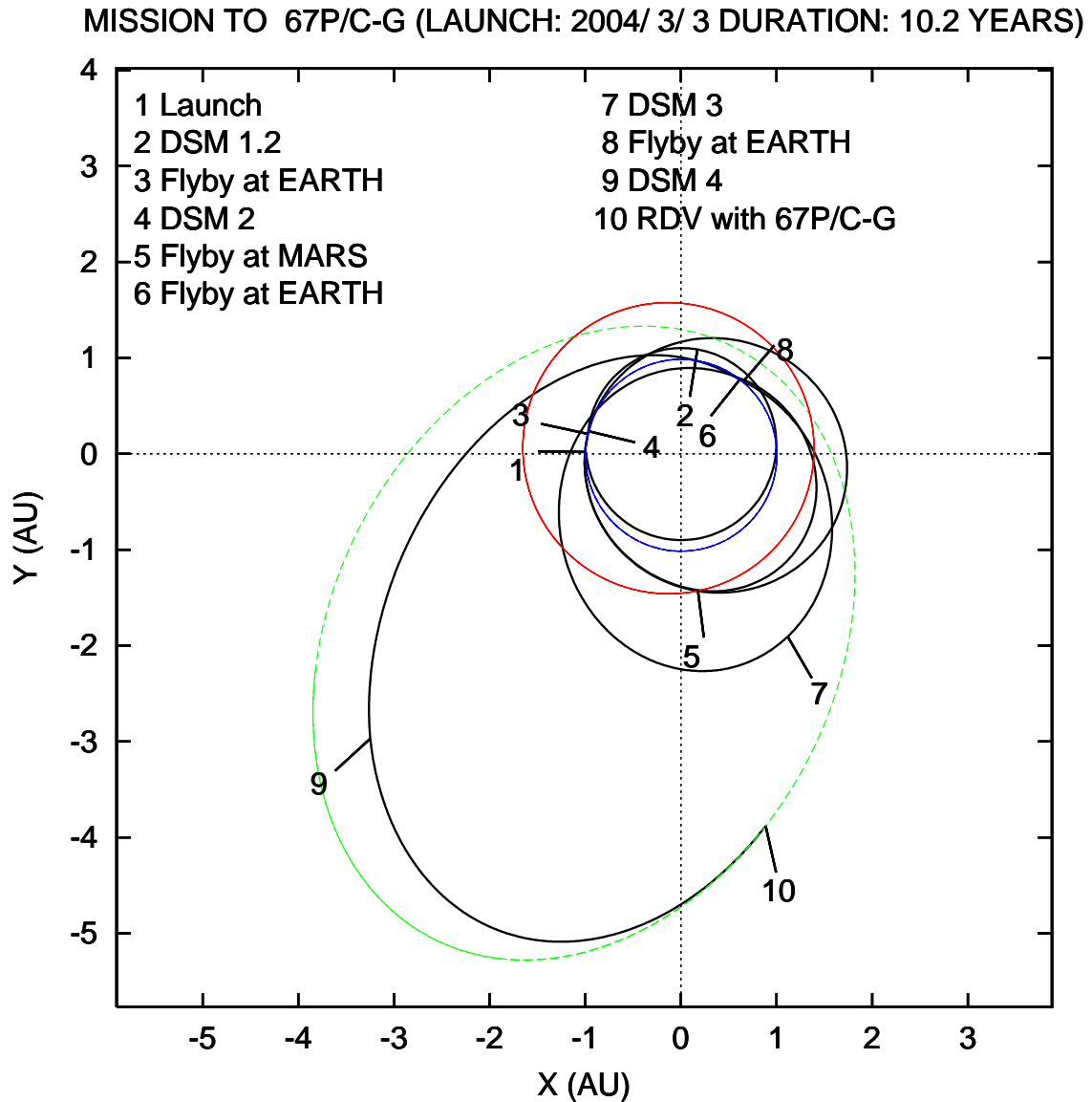


Figure 4-3: Ecliptic Projection of the Rosetta Trajectory (Launch 17/03/2004 – Only DSM 1.2).

4.2 Launcher Description

Rosetta will use the European launcher Ariane 5/G+ in a dedicated flight (single launch configuration). In Ariane 503 test flight both, delayed ignition and re-ignition of EPS stage have been demonstrated. The nominal characteristics and performances of Ariane 5 for the Rosetta launch have been provided by Arianespace {Ref. RD 12}. The launcher can be roughly described as consisting of:

Lower composite:

- EPC central cryogenic stage with approximately 155 tons of liquid hydrogen and oxygen (H155).
- Two EAP boosters with 230 tons of solid propellant (2 P230).

Upper Composite:

- EPS storable propellant stage with 9.7 tons (L9.7).
- VEB Vehicle equipment bay.
- Upper section consisting of Payload, Adaptor, and Fairing for the single launch case.

4.2.1 Launch Procedure

The target orbit is a hyperbolic escape orbit defined by an excess velocity of 3.545 km/s and a declination of the asymptote of -2.0° with respect to the equator. The injection of a payload of 3064 Kg in the target orbit, as required by the Rosetta mission, can only be achieved by inserting a coast phase of optimised duration before EPS ignition, and can not be reached by a direct launch. The consideration of a coast arc increases considerably the performance of the launcher for escape orbits.

The Ariane 5 ascent trajectory is defined by the target orbit and the launch vehicle constraints. The constraints applying to the launch vehicle are the following:

- Launch Azimuth: It is constrained for safety reasons between -10.5° and 91.5° . (The launch azimuth is defined as the angle between the north axis and the projection of the vehicle longitudinal axis on the local North-East plane frozen at the release of the inertial platform).
- Aerothermal Flux: It must be less than 1135 W/m^2 after fairing jettison.
- Central stage (H155) impact point: It must be in the Ocean at least 200 km away from the closest shoreline.
- Visibility: The launcher should be visible successively from the stations that compose the Launch Ground Stations Network (Kourou, Natal, Ascension, Libreville, Malindi and New Norcia).

4.2.2 Launcher Performances and Launch Dates

The performances of the Ariane 5 launcher for the Rosetta dedicated flight have been studied by Arianespace {Ref. RD 12}.

Arianespace has guaranteed a payload mass of 3242 kg in the hyperbolic escape trajectory for the Rosetta launch. The payload mass is the addition of the mass of the launcher adapter ACU1194V5 (123 kg) and the spacecraft mass. Therefore, the Rosetta maximum wet mass of 3064 kg can be injected into interplanetary orbit.

This performance is maintained during a launch window slot of 21 consecutive days between 26th of February and 17th of March 2004. In each of these days it is possible to launch at either time H01 or time H02, see Table 5-4. H01 and H02 are separated by 20 minutes but the flight of Ariane 5 compensates the rotation of the Earth during these 20 minutes, so that the trajectory conditions at escape from the Earth are the same for both lift-off times.

4.3 *Spacecraft Description*

The Rosetta spacecraft design will be based on existing technologies and on previous proven concepts.

The spacecraft platform will consist of three modules:

Bus Support Module (BSM): It accommodates most of the platform equipment.

Payload Support Module (PSM): It houses the science equipment, instruments and sensors.

Lander Support Module (LSM): The SSP will be placed in this module.

The **Mechanisms Subsystem** comprises the Solar Array Drive Mechanism (SADM), the Solar Array Hold down and Release Mechanism (SA-HRM), the High Gain Antenna-Antenna Pointing Mechanism (HGA-APM), the High Gain Antenna Hold down and Release Mechanism (HGA-HRM), two deployable experiment booms for Plasma Package Experiments, and the CONSERT antenna. The HGA, the SA, the experiment booms, and the CONSERT antenna are released at beginning of the mission, and the HGA-APM is extensively used during the comet phase.

The **Harness Subsystem** will interconnect all subsystem units with electrical connections.

Propulsion Subsystem. Rosetta will be equipped with a bipropellant (MMH as fuel and MON as oxidizer). It will cope with the requirements of the Rosetta mission, in particular the rendezvous manoeuvre (approx. 774 m/s) performed by four pairs of thrusters (10 N each) after about 3739 flight days.

For attitude control, and vector zed orbit manoeuvre, there are 12 pairs of 10 N thrusters. The location of these 10 N thrusters depends on the attitude manoeuvre requisites, and on minimization of contamination of the critical surfaces (SA, HGA dish, radiators, and sensors) due to mass flow ejected by the propulsion system.

Although based on concepts and elements already flown in other spacecraft, the **Thermal Control Subsystem** will fulfil the specific demands of the Rosetta mission, such as orbiting around the comet near perihelion, or Sun distances of 5.3 AU.

The **Power Subsystem** provides electrical power to the rest of subsystems, instruments and experiments. Power is generated by the solar arrays, and distributed to the elements. For

eclipses, power peaks, and emergency cases there are batteries. The management of the power supply is done by control units.

The **Solar Array Subsystem** consists of two solar array panel dimensioned to generate the electrical power needed by the spacecraft along the different mission phases. The solar energy per unit area at big Sun distances is very low, therefore special high performance cells will be used in the panels.

The **Telecommunications Subsystem** is composed of four antennae and the radio-frequency units necessary for the up and down links between the spacecraft and the ground stations. There is one High Gain Antenna (HGA), one Medium Gain Antenna (MGA) and two Low Gain Antennae (LGA). The HGA pointing requirement during the near comet operations will be fulfilled by the APM. The MGA is fixed with respect to the spacecraft and can be a back-up for the HGA. The LGAs are omni-directional and are diagonally opposed mounted on the satellite body. S-band will be used for the telecommand (up link) while the down link can be done in S-band and X-band, being the S-band dedicated to near Earth mission phases. The required performances of the telecommunications subsystem are listed Table 4-2.

TC/TM Subsystem	HGA			MGA			LGA		
	Station	Bit Rate	Dist.	Station	Bit Rate	Dist.	Station	Bit Rate	Dist.
Up Link	New Norcia 32 m	2000 bps	4.5 AU	New Norcia 32 m	16 bps	6.0 AU	DSN 70 m	7.8 bps	> 6.5 AU
							New Norcia 32 m	7.8 bps	1.1 AU
Down Link	New Norcia 32 m	5000 bps	4.5 AU	New Norcia 32 m	16 bps	4.0 AU	Kourou 15 m	16 bps	0.08 AU

Table 4-2: Rosetta Telecommunication Subsystem

The Avionics Subsystem includes the AOCMS and OBDH subsystems. The AOCMS subsystem has interfaces with most of the other spacecraft subsystems (i.e. with the Solar Array and Telecommunications subsystems for pointing purposes, or with the propulsion subsystem for the attitude control). The OBDH subsystem controls the telecommunications with the ground segment, managing the telecommand and telemetry traffic. The OBDH distributes the commands to the different subsystems, and receive from them their respective status and telemetry.

4.4 Mission Operation Phases

The different mission operation phases are directly derived from the successive mission events, identifying several operation modes and levels of ground activity.

The following major modes of nominal spacecraft operations and the corresponding ground activities can be identified.

LEOP: This phase last about 3 days, starting from a few hours before launch and ending with the first trajectory correction manoeuvre.

Commissioning and Verification Phase: The CVP follows the LEOP. It starts with the acquisition of RF link with the Earth via the HGA and it extends until completion of spacecraft check out and payload commissioning about 3 months later. The spacecraft is three axis stabilised. This mode is characterised by intensive ground activities during time intervals where communication with available ground stations is possible. During initial communications (few hours) the low gain antennas are used for S-band up and down link.

Cruise Phase: There are a number of cruise phases in the Rosetta mission between major mission events. Some of these phases can be longer than 2 years, and may include a long period of spacecraft near conjunction with the Sun, where RF communication with the spacecraft may be difficult or even impossible, (for 8-9 months the angular distance between the spacecraft and the centre of the Sun, as seen from the Earth, is less than 5°. The Cruise Phase is an operational mode where no routine control activities are assumed to be performed, and the spacecraft has to survive with a minimum of ground support.

Mars Gravity Assist: This phase starts 5-6 months before Mars swing-by with acquisition of the spacecraft, orbit determination, and navigation manoeuvres. At the end of this phase, further orbit determination, and navigation correction manoeuvres in preparation for the next Earth gravity assists will be performed.

Earth Gravity Assist: The three Earth gravity assists will be initiated about 1 month before the Earth swing-by with tracking and navigation manoeuvres, and they will last until about 1 month after the swing-by where any subsequent navigation manoeuvres are executed, and the spacecraft is prepared for the next cruise phase.

Asteroid Fly-by: The Asteroid Fly-by Mode is used before, during and after asteroid fly-by, (two asteroids fly-by are considered in the current baseline). The phase will start about 1-2 months before the fly-by with a check-out of the spacecraft, and of the payload. The navigation camera will be used to detect the asteroid several days before close encounter, so that the required fly-by conditions can be achieved by executing small navigation manoeuvres. The scientific payload will be operated during the pre-fly-by navigation and targeting and during the fly-by itself. Communications will use the high gain antenna except for a short period of time corresponding to the close fly-by during which loss of Earth pointing is allowed. The spacecraft shall rotate around its axis of lowest inertia to enable a fly-by at the shortest distance with the payload line of sight remaining asteroid pointing. Science data is recorded during this phase and transmitted after re-acquisition of the Earth after the fly-by.

Comet Rendezvous: The large comet velocity matching manoeuvre will be performed in steps of smaller manoeuvres to allow that the spacecraft arrives at good conditions for detection of the comet by the navigation camera. This also makes it possible to correct, without penalisation, manoeuvre execution errors, and comet ephemerides errors.

Details of this phase are presented in chapter 8.

Comet Approach: The Comet Approach includes a period waiting for enough power to be available, followed by an intensive phase of activities of comet characterisation and observation. The navigation camera will be used for comet detection and approach navigation. The instrument line of sight will remain pointing to the nucleus, while the high gain antenna is pointed to the Earth to maximise the down link capability and the solar arrays pointed to the Sun. At the end of this phase the spacecraft is manoeuvred into orbit around the comet nucleus.

Comet Mapping: In this phase more than 80% of the comet surface will be mapped, and several selected areas will be over-flown at low altitude. The comet nucleus characterisation will include all major parameters: size, rotation dynamics, gravity characteristics, outgassing, jets, etc. At the end of this phase, a suitable landing place for the Lander will be selected.

SSP Delivery and Relay: The orbiter will be manoeuvred to arrive at the proper conditions for delivery of the Lander. At a pre-set time the Lander will separate in the required attitude, and will start descending to the comet surface. The orbiter will autonomously manoeuvre to ensure proper communication conditions with the Lander for the relay phase where the Lander will perform its main scientific observation sequence.

Comet Escorting: This phase will extend up to the nominal end of the science mission at comet perihelion passage. The orbiter will orbit or escort the nucleus carrying out the various science objectives. Periodic contact with the Lander will allow recovering science data collected on the comet surface.

The spacecraft will switch between the different operation modes depending on the mission phases described in page 9. It has to be stressed that the operation timeline near the comet is very much dependent on decisions that will be taken when the spacecraft is close to the comet, based on spacecraft status, and comet detectability. The timeline described here assumes a late detection of the comet, and a quick sequence of phases thereafter to arrive at Lander ejection when the comet is at 3 AU from the Sun.

Table 4-3: Parameters of the Operation Phases of the Rosetta Mission

5. LAUNCH WITH ARIANE 5

5.1 Injection with Coast Arc

Figure 5-1 is a view of the Rosetta launch with coast arc for the 2004 launch window. After the cut-off of the EPC (H155), a ballistic phase of optimised duration follows before the ignition of the upper stage (L9.7). It should be noticed that the shorelines have been plotted at launch time.

The maximum payload injected into escape orbits by Ariane 5 can be considerably increased by the insertion of a coast arc. The effect is noticeable in particular for high declination target orbits, though the increase is also important for the selected Rosetta baseline mission, which has a low value of the asymptote declination. The drawback of inserting a coast arc is that it will require some extra equipment (e.g. to provide electrical power during the coast arc which may have a duration of about 2 hours, to respect the required thermal constraints, to maintain the attitude within the required accuracy, etc.) and it will complicate the operations (e.g. additional ground stations may be required, much longer time from lift-off to injection, etc.).

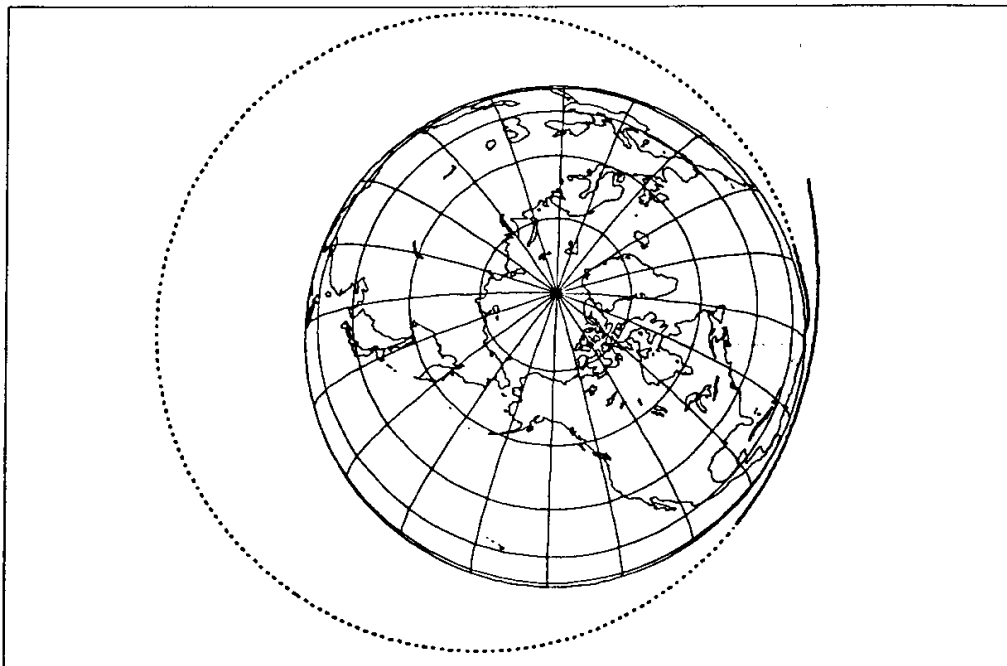


Figure 5-1: Rosetta Launch in January 2003 with Coast Arc.

The target escape orbit is $V_{\infty} = 3.545 \text{ km/s}$, $\delta = -2.0^\circ$. The trajectory is plotted in an inertial frame. The shorelines are represented at launch time.

5.1.1 Sequence of Events

The Ariane ascent trajectory is defined by the target orbit and the launch vehicle constraints, which leads to the following sequence of events:

- Vertical ascent during 5 seconds.
- Steering manoeuvre with constant pitch rate and constant yaw angle. The final pitch angle is optimised. The direction of the manoeuvre defines the launch azimuth (North to East). The axis of the rocket remains in the azimuth plane until the beginning of the optimised phase. This phase lasts 10 seconds.
- Atmospheric flight at zero angle of attack in pitch to minimise the aerodynamic loads until boosters (EAP) jettison.
- Optimised attitude during the EPC stable regime.
- Coast phase of optimised duration depending on the target orbit and trajectory constraints.
- Upper stage (EPS) stable regime until final injection.

The empty central stage EPC (H155) should re-enter and impact the surface of the Earth on the ocean, at least 200 km away from the nearest shoreline. To that end the maximum perigee altitude of the orbit of the empty stage is constrained to 50 km. It has been assumed that lower values are also allowed, though usually (but not always) they lead to poorer launcher performances.

5.1.2 Eclipses

An eclipse analysis has been done from the lift-off of the Ariane 5 launcher up to the injection in the escape hyperbola for the reference trajectory launch date at 26/02/2004. The two launch attempts which fulfils the necessary right ascension of the hyperbolic velocity vector have the following launch times: H01 - 7:24:09 and H02 - 7:44:09.

EPC cut-off (beginning of coast arc) occurs 591.7 s after lift-off.

EPS delayed ignition (end of coast arc) starts 6921.7 s after lift-off.

EPS cut-off occurs 7960.533 s after lift-off.

For the launch phase two eclipse periods have been detected as shown in the Table 5-1. The launch starts in the night of Kourou and the trajectory of Ariane 5 goes quickly into the sunshine. The launcher enters the shadow again during the coast arc for about 27 minutes and finally exits the eclipse before the end of the thrust phase of EPS. The spacecraft is injected during sunshine. The hour of launch is very similar for the different launch days, therefore the longitude of the Sun with respect to Kourou at launch is nearly the same and the eclipse periods have very small variations with the launch day, see Table 5-4.

Event	H01	H02
LAUNCHER IGNITION	07:24:09	07:44:09
EXIT SHADOW	07:32:58 DUR: 10:17	07:32:01 DUR: 27:22
BEGIN OF COAST PHASE	07:34:03	07:53:59
ENTRY SHADOW	09:08:15	09:27:23
END OF COAST PHASE	09:19:33	09:39:29
EXIT SHADOW	09:35:38 DUR: 27:22	09:55:03 DUR: 27:39
EPS CUT-OFF - INJECTION	09:36:52	09:56:48

Table 5-1: Eclipses during Launch Phase (UTC for 26/02/2004).

Figure 5-2 represents the arc of the trajectory in shadow on the coast phase ground track.

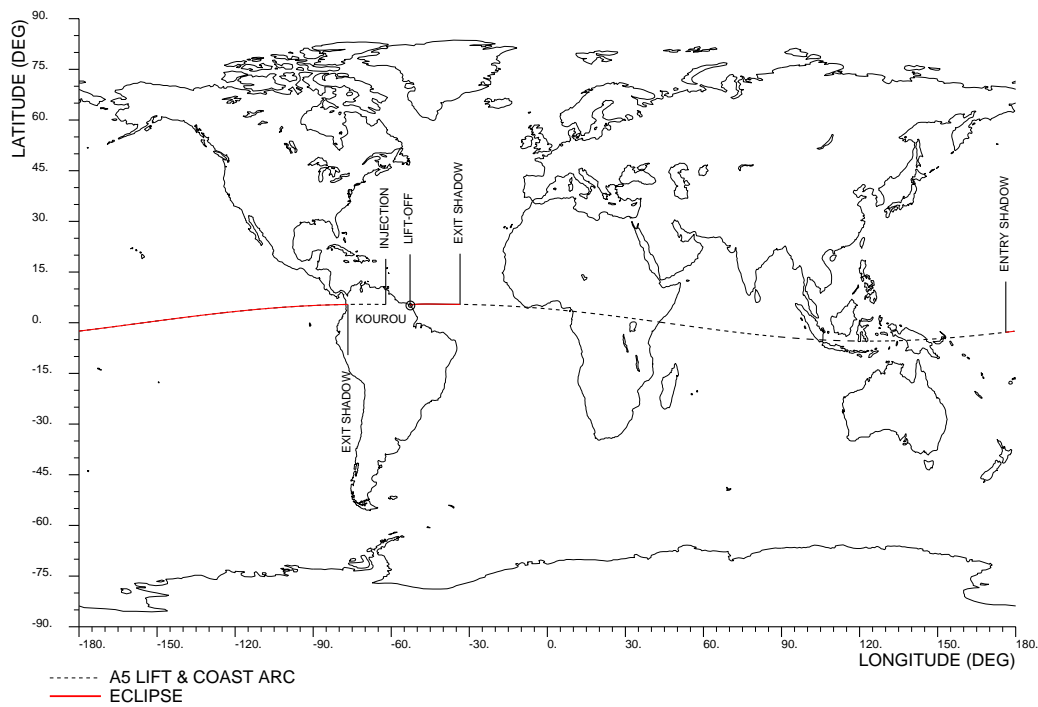


Figure 5-2: Eclipse Arc during Coast Arc.

5.1.3 Ground Station Coverage

The ground stations network for the launch trajectory is composed of Galliot (Kourou), Natal (Brazil), Ascension Island, Malindi (Kenya), Dongara (Australia) and South-Point (Hawaii, USA). Table 5-2 presents the visibility periods for each station (minimum elevation considered is 0°) for the two launch attempts. As the trajectories are fixed in the Earth rotating frame, the sequence of events is the same independently of the launch day. Coverage gaps occur between Dongara and Hawaii, and between Hawaii and the second pass of Kourou. Figure 5-3 represents the coast phase ground track with the visibility arcs from the different ground stations of the launch network.

Event	H01	H02
LAUNCHER IGNITION	0:00	0:00
AOS NATAL	0:08:30	0:08:34
LOS KOUROU	0:08:35 DUR: 8:35	0:08:38 DUR: 8:38
BEGIN OF COAST PHASE	0:09:52	0:09:52
AOS ASCENSION	0:12:17	0:12:12
LOS NATAL	0:13:47 DUR: 5:17	0:14:12 DUR: 5:37
AOS MALINDI	0:21:55	0:21:53
LOS ASCENSION	0:24:07 DUR: 11:50	0:24:47 DUR: 12:37
AOS DONGARA	0:47:52	0:48:14
LOS MALINDI	0:58:36 DUR: 36:41	0:59:47 DUR: 37:55
LOS DONGARA	1:35:05 DUR: 47:13	1:35:51 DUR: 47:37
AOS HAWAII	1:41:26	1:41:39
END OF COAST PHASE	1:55:22	1:55:22
LOS HAWAII	1:57:50 DUR: 16:24	1:58:07 DUR: 15:28
AOS KOUROU	2:11:06	2:11:13
INJECTION IN ESCAPE HYPERBOLA	2:12:41	2:12:41

Table 5-2: Ground Station Visibility during Launch Phase (ellapsed time from ignition).

Figure 5-4 presents the elevation of the visibility periods from all the ground stations during the coast arc and for the two launch attempts. The abscissas are the time since the engine ignition of Ariane 5. Kourou, Malindi and Dongara have very good visibility conditions with maximum elevations of 55, 76 and 31 degrees, respectively. The visibility passes from Ascension and Hawaii are short and with a maximum elevation about 13 degrees. The visibility from Natal is very short and with elevations bellow 3.4 degrees. Figure 5-5 presents the range for the coverage periods against time.

The EAP burn-out and separation is visible from Kourou (instant H1). The end of the main thrust phase of EPC and the EPC separation occurs during the visibility from Natal (instant H2). The second ignition of the upper stage, EPS, occurs during the visibility from Hawaii

(instant K2.1), while the shut down of the EPS and the injection into the final orbit is under coverage again from Kourou (instant H3).

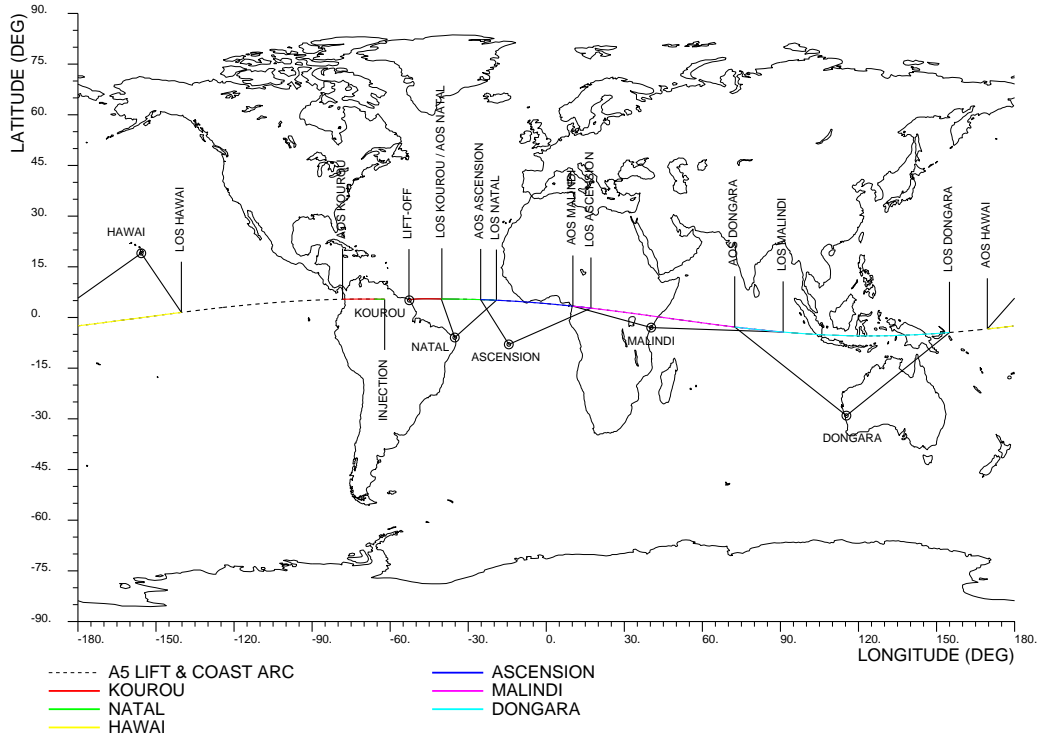


Figure 5-3: Launch Network. Ground Station Coverage during Coast Arc.

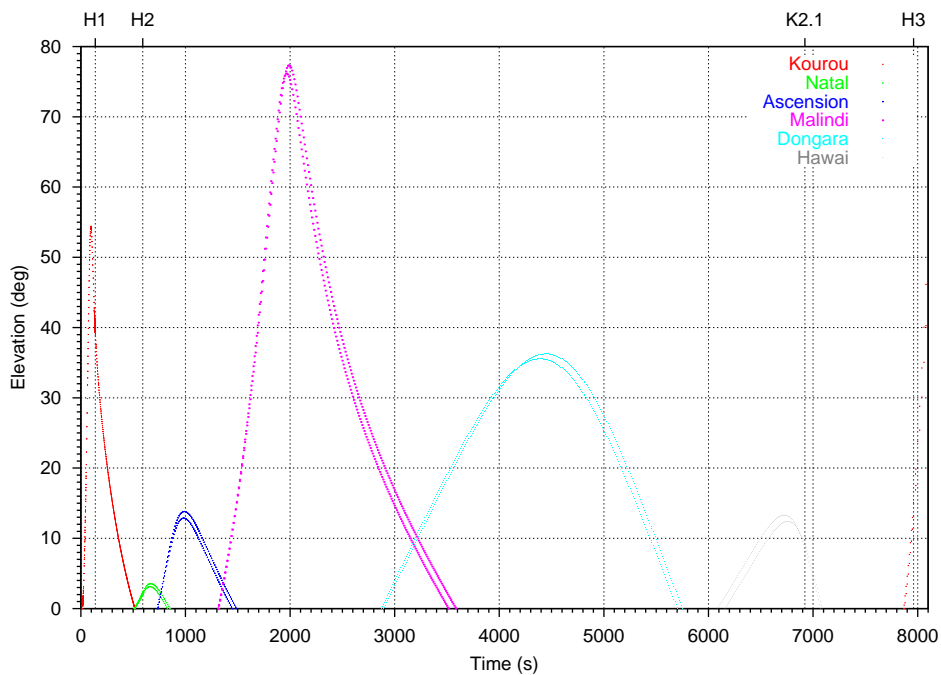


Figure 5-4: Launch Network. Elevation from Ground Stations during Coast Arc.

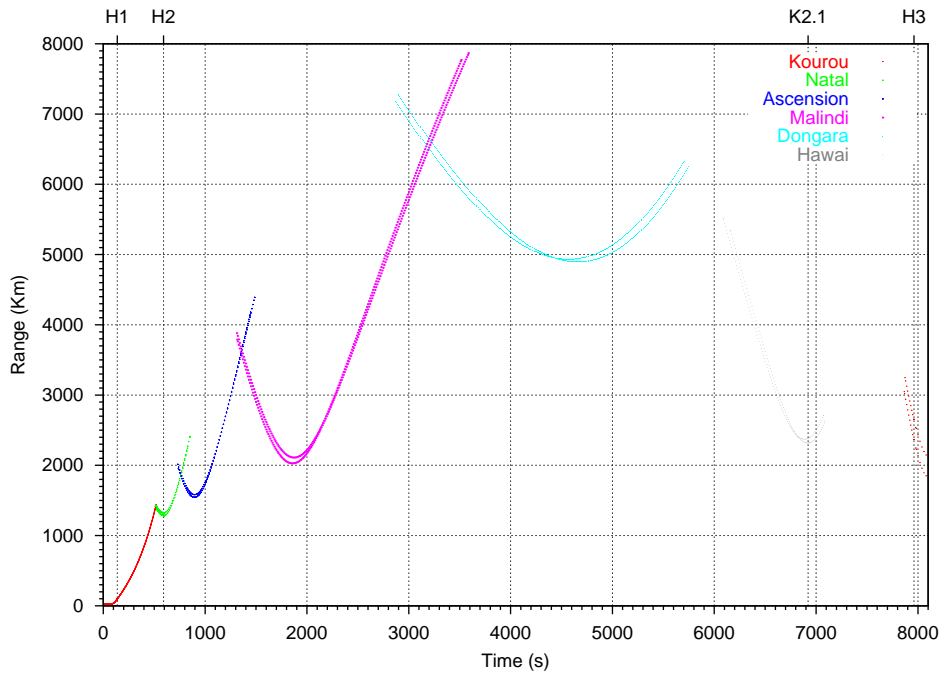


Figure 5-5: Launch Network. Range from Ground Stations during Coast Arc.

5.1.4 Injection Errors

Arianespace has provided a study on the injection errors by Ariane 5 for the Rosetta launch. The dispersions at injection for an optimal launch (no compensation for daily launch window) are given by Table 5-3:

Dispersions	Latitude (°)	Longitude (°)	Altitude (km)	V (m/s)	α (°)	β (°)
Nominal value at injection	5.681	-76.743	912	11031.10	17.714	89.295
Latitude	$0.545 \cdot 10^{-4}$	0.00116	0.027	-0.023	0.00045	$-0.273 \cdot 10^{-4}$
Longitude		0.0903	2.103	-1.80	0.0354	0.0089
Altitude			49.6	-42.2	0.836	0.207
V				36.4	-0.710	-0.177
α					0.014	0.00348
β						0.00165
σ	0.00737	0.3004	7.046	6.032	0.1186	0.0406

Table 5-3: Ariane 5 dispersion matrix for injection in escape orbit.

The parameters in the table have the following meaning:

V	--	Inertial Velocity
α	--	Angle between inertial velocity vector and local horizontal plane.
β	--	Azimuth angle of inertial velocity vector
σ	--	Typical Deviation

5.2 General Launch Window

The spacecraft mass after comet rendezvous is one of the most important parameters in the design of the Rosetta mission. Once the general trajectory strategy has been fixed, (gravity assist conditions, trajectory correction manoeuvres, ephemerides of celestial bodies, etc.), there is an optimum day and time of launch such that the mass delivered at the comet is maximised. Due to the high probability of a launch hold on any launch attempt, it is important to ensure that it is possible to launch at least in a period of a few days near the nominal optimum day, and within each particular day, in a period of several minutes around the optimum lift-off time of that particular day (daily launch window).

The definition of the launch window has been carried out by means of an end-to-end numerical optimisation of the precise trajectory to maximise the wet mass of Rosetta after the rendezvous with 67P/Churyumov-Gerasimenko. The special properties of the Δ VGA Earth-Earth first arc of the trajectory allows to use the same value of hyperbolic escape velocity and declination for every day. The manoeuvre or pair of manoeuvres after the departure ensures the adequate arrival conditions at the Earth first swing-by to match the rest of the trajectory to the comet rendezvous. The lift-off time for each launch day is fixed so that the trajectory of Ariane 5 in the fixed Earth matches the optimum right ascension of the departure hyperbola.

The launch conditions are:

Modulus of hyperbolic velocity	–	$V = 3.545 \text{ Km/s}$
Declination of hyperbolic velocity	–	$d = -2.0^\circ \text{ (MEEQ2000)}$

The launch window extends from the nominal launch day at 26th February 2004 for 21 days until the 17th of March. The total deterministic delta-V for the trajectory along the 21-day launch period is shown in Figure 5-6. The variations of the mass at rendezvous with the comet with respect to the first day of the launch window (OPEN – 26/02/2004), considered as baseline, are presented in Figure 5-7. The maximum performance is foreseen for the 02/03/2003 launch day, with an over-performance of 10 Kg with respect to the baseline.

For the first days of the launch window, the optimum strategy consists on a 1-DSM arc between departure and the 1st Earth swing-by. This manoeuvre is implemented near the perihelion of the 1:1 resonant orbit with Earth's period. From 03/03/2003 to 14/03/2003 the optimum strategy has a 2-DSM arc, one manoeuvre at perihelion and one manoeuvre at aphelion. For the end of the launch window, it is again optimum a 1-DSM strategy with only the aphelion manoeuvre. In the abovementioned two figures, manoeuvres at perihelion are shown by a looking-down

triangle and manoeuvres at aphelion by a looking-up triangle. Figure 5-8 presents the ΔV for the manoeuvre at perihelion, DSM1.1, and the manoeuvre at aphelion, DSM1.2.

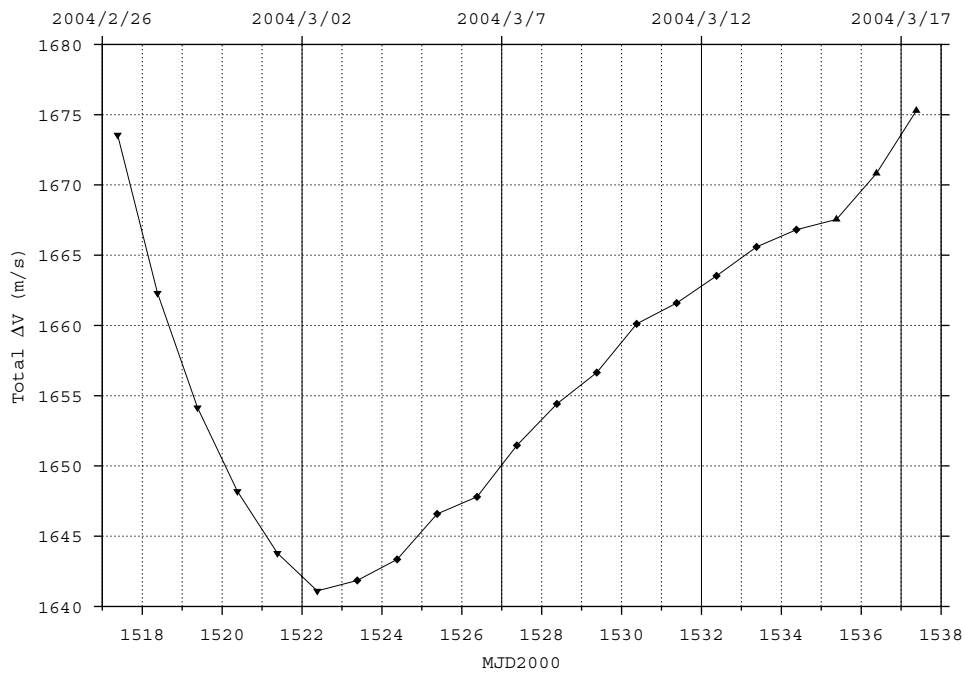


Figure 5-6: Total trajectory ΔV as function of the Launch Day.

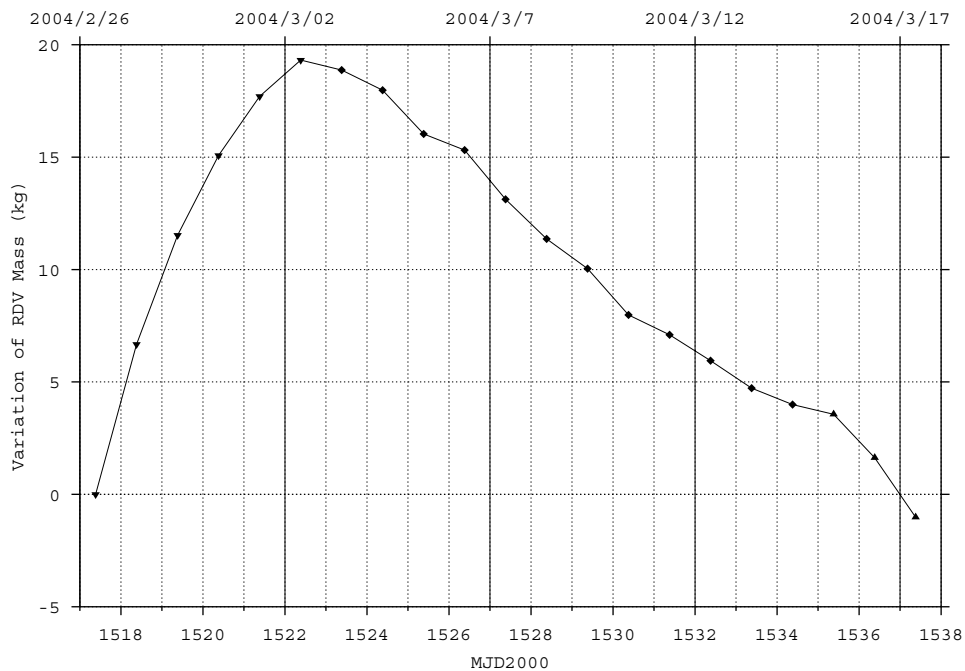


Figure 5-7: Variation of mass after Rendezvous Manoeuvre as function of the Launch Day.

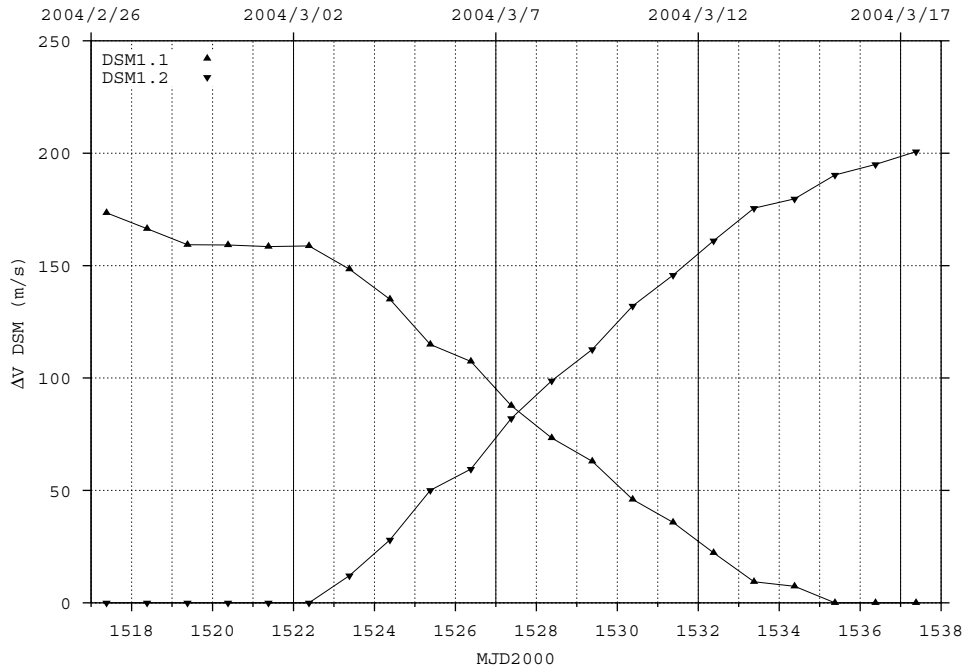


Figure 5-8: ΔV of first arc manoeuvres as a function of Launch Date.

The right ascension of the departure asymptote increases from -18° to about 0° , see Figure 5-9, which means about one degree per day to compensate the rotation movement of the Earth around the Sun.

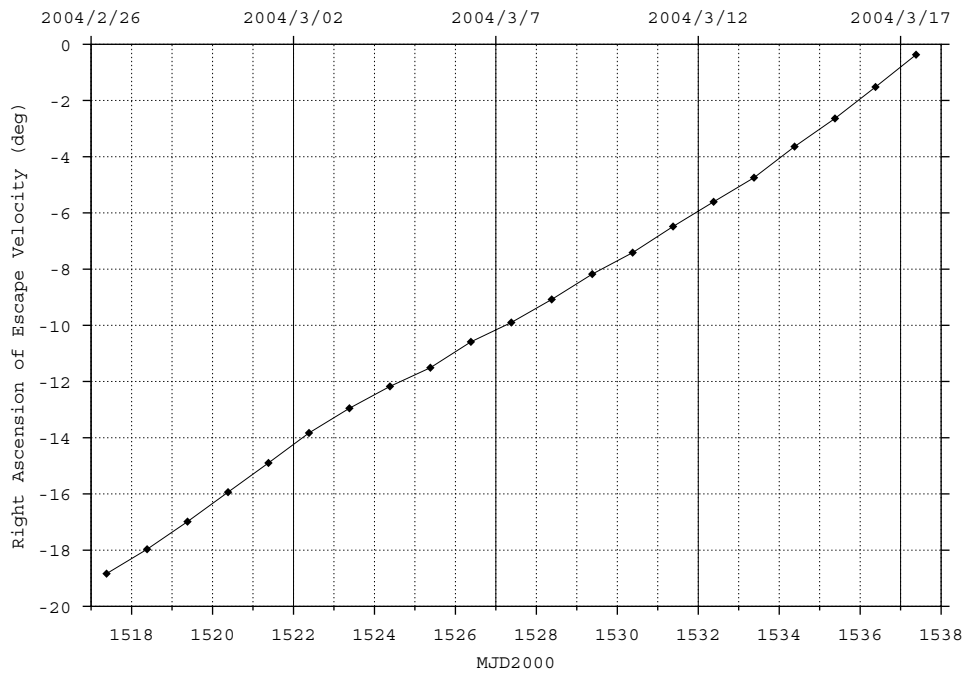


Figure 5-9: Right Ascension of Earth departure hyperbolic velocity (osculating at injection).

Together with the two DSM performed in the first trajectory arc, the altitude of the first swing-by of the Earth is one of the parameters most affected by the launch date. The pericentre height of this swing-by is presented in Figure 5-10 and ranges from 4300 km to 1200 km. The swing-by of Mars and the third Earth swing-by must be performed to give the maximum deflection of the velocity, therefore these two swing-by have constant altitudes of the pericentre equal to the minimum advisable to ensure the integrity of the spacecraft. However, the second Earth swing-by presents a small variation of the pericentre height with the launch date, see Figure 5-11.

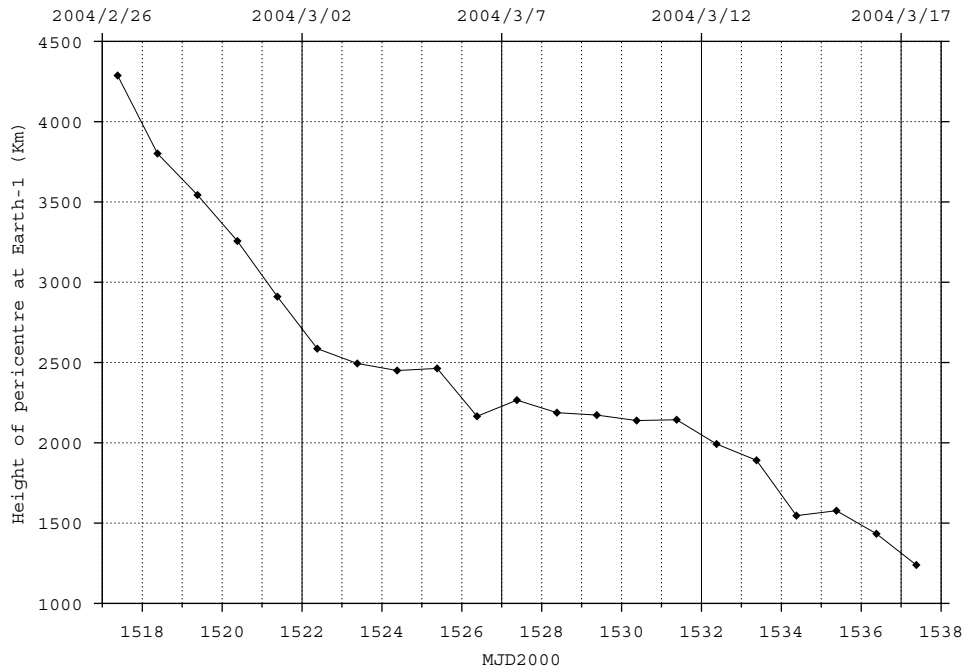


Figure 5-10: Pericentre height of first Earth swing-by as a function of Launch Date.

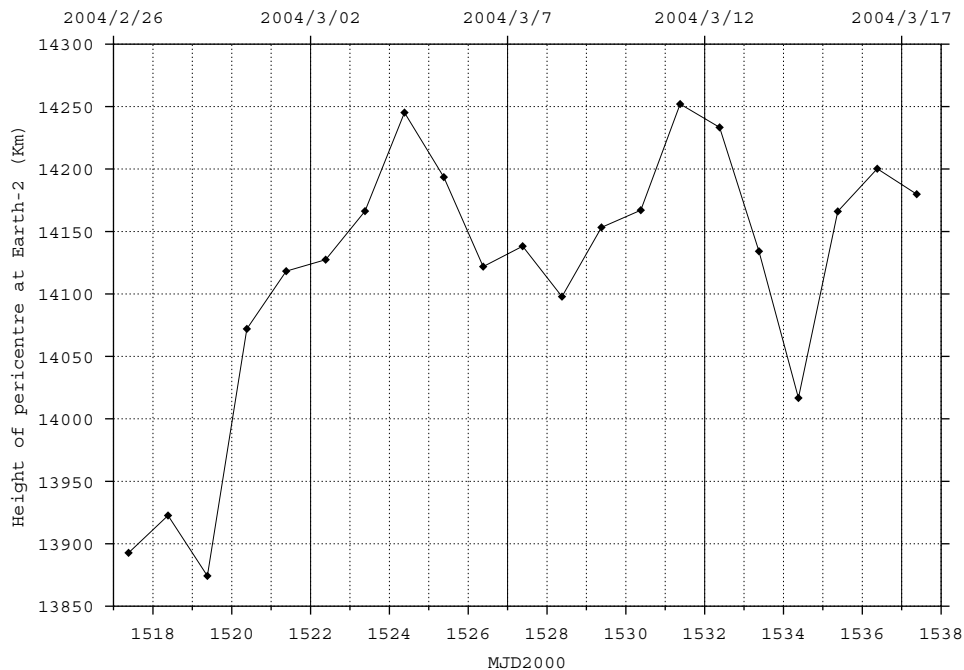


Figure 5-11: Pericentre height of second Earth swing-by as a function of Launch Date.

The cross point of the asymptote to the arrival hyperbola with the B-plane is a design parameter for a swing-by. This plane is defined as the plane orthogonal to the arrival velocity, which passes through the centre of the central body and the reference X-Axis is the intersection of this plane with the planet Equator. Figure 5-12 to Figure 5-15 present the position of the impact vectors for all the launch days for the three Earth and the Mars swing-by. The impact vectors are more concentrated for the Mars and third Earth swing-by, showing that a very good precision of these must be obtained.

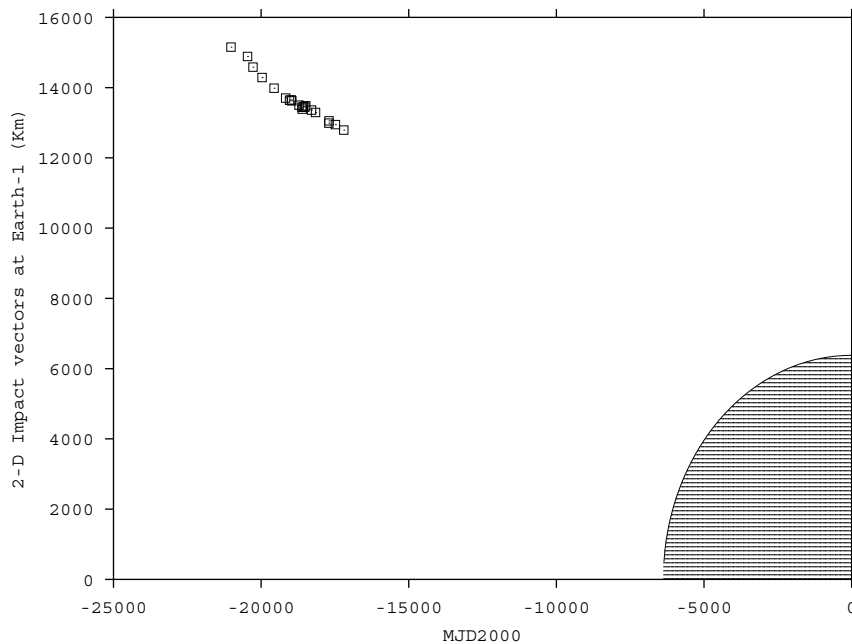


Figure 5-12: Impact vectors on B-plane of first Earth swing-by.

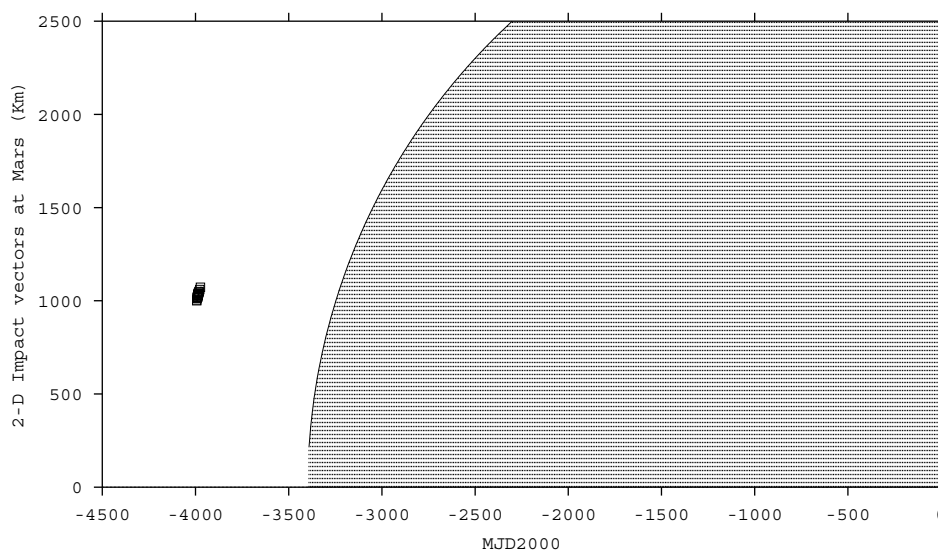


Figure 5-13: Impact vectors on B-plane of Mars swing-by.

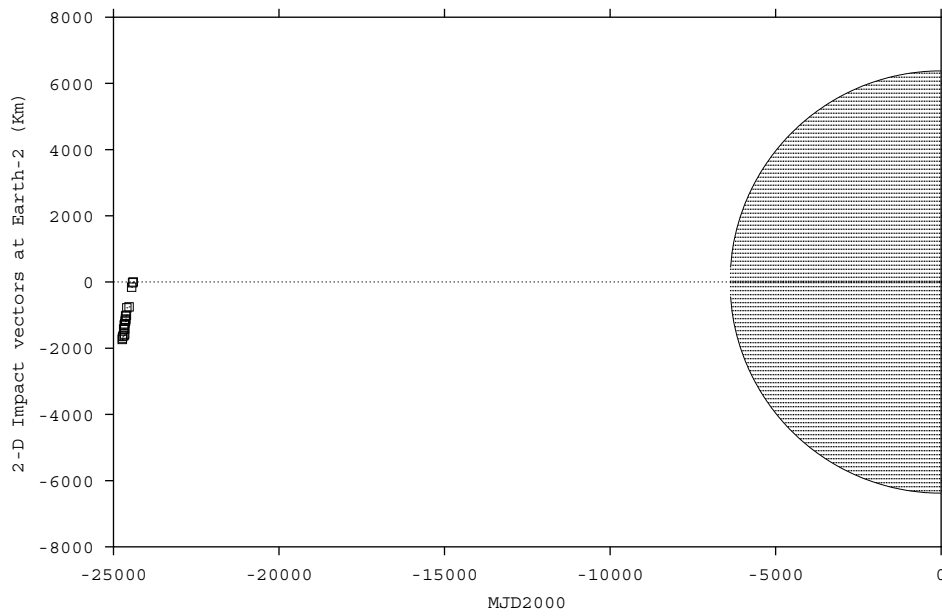


Figure 5-14: Impact vectors on B-plane of second Earth swing-by.

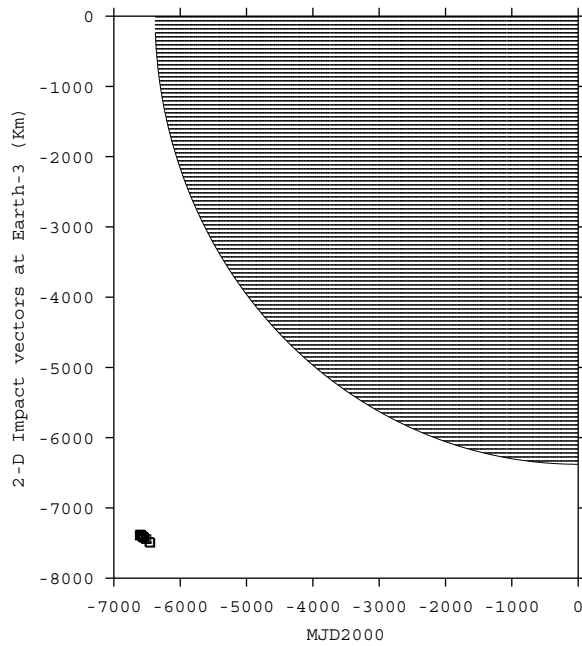


Figure 5-15: Impact vectors on B-plane of third Earth swing-by.

5.3 Daily Launch Window

The daily launch window is the daily limited period of time during which spacecraft injection into the required orbit is achievable. If the launch is not performed at the optimum launch time the rotation of the Earth changes the right ascension of the obtained excess velocity vector with respect to the optimum one, defined in an inertial non-rotating frame.

As stated by Arianespace in the document {Ref. RD 12} Ariane 5 can re-optimize its trajectory as a function of the launch time to correct for the Earth rotation and achieve the required right ascension of the escape velocity at any time of the window. The flight reserve of the launcher allows a 20-min launch slot. Two launch attempts are possible every launch day, the first at H01 before the optimum launch hour H0*, and the second at H02 after the optimum launch hour. The Ariane 5 launcher flies a slightly different trajectory for every launch attempt and corrects the right ascension deviation of the departure asymptote due to the difference of launch hour. In order to balance the performance between these two trajectories of the launcher, H01 and H02 are not symmetric around H0*. H01 is 12 minutes before optimum hour and H02 is 8 minutes after optimum hour.

5.4 Non-Optimal Ariane 5 Flight Program Launch

NOT APPLICABLE

5.5 Maximum Spacecraft Mass and Launch Window

The launch window for Rosetta covers a period of 20 days. Following the latest results provided by Arianespace, the maximum spacecraft mass injected into interplanetary orbit by Ariane 5 is 3064 kg.

Only one flight program will be used for the launch of the Rosetta mission. The modulus and declination of the escape velocity are fixed. The right ascension of the escape velocity is set in order to optimize the delivered mass at rendezvous with the comet for every launch day. The launch hour is set in order to match the required asymptotic right ascension.

The following table shows a preliminary launch hour for every day of the launch window. This value is an estimation computed with an interpolation model of the Ariane 5 injection parameters. The actual launch hour is to be confirmed by Arianespace. The preliminary data provided by Arianespace shows that the lift-off time can be about 7 minutes before the values given in the table. Therefore, these values should be considered as having a precision of 7-10 minutes. The final values will be provided by Arianespace at the RAMF.

In the following table:

α – Right ascension of osculating departure hyperbola in MEEQ2000 at injection point.

Launch Day	α (°)	H0* (UTC)	H01	H02
26-Feb-04	341.244	7:36:09	7:24:09	7:44:09
27-Feb-04	342.250	7:36:14	7:24:14	7:44:14
28-Feb-04	343.275	7:36:24	7:24:24	7:44:24
29-Feb-04	344.321	7:36:38	7:24:38	7:44:38
1-Mar-04	345.413	7:37:04	7:25:04	7:45:04
2-Mar-04	346.521	7:37:33	7:25:33	7:45:33
3-Mar-04	347.659	7:38:09	7:26:09	7:46:09
4-Mar-04	348.616	7:38:02	7:26:02	7:46:02
5-Mar-04	349.377	7:37:09	7:25:09	7:45:09
6-Mar-04	350.131	7:36:13	7:24:13	7:44:13
7-Mar-04	350.938	7:35:30	7:23:30	7:43:30
8-Mar-04	351.734	7:34:45	7:22:45	7:42:45
9-Mar-04	352.556	7:34:06	7:22:06	7:42:06
10-Mar-04	353.378	7:33:27	7:21:27	7:41:27
11-Mar-04	354.207	7:32:49	7:20:49	7:40:49
12-Mar-04	355.043	7:32:13	7:20:13	7:40:13
13-Mar-04	355.875	7:31:37	7:19:37	7:39:37
14-Mar-04	356.553	7:30:23	7:18:23	7:38:23
15-Mar-04	357.542	7:30:24	7:18:24	7:38:24
16-Mar-04	358.678	7:31:00	7:19:00	7:39:00
17-Mar-04	359.844	7:31:43	7:19:43	7:39:43

Table 5-4: Launch hour as function of launch date, and escape right ascension.

5.6 Cost of Delayed Launch

In case of an hypothetical delay of the launch date, one of the possibilities could be to launch the spacecraft after the planned 21-days launch window. Obviously, such a delayed launch would require additional ΔV that was planned for another tasks different than the trajectory. Therefore, there could be a degradation of the performances of the mission.

Figure 5-16 presents the total ΔV required for the trajectory from the departure to the comet rendezvous for the period from 22/02/2004 to 16/04/2004. The 21-days launch window ends at

17/03/2004. For the days afterwards, the total ΔV increases continuously, and quickly reaches a variation rate of about 23 m/s per day. Launching at the 27/03/2004 with a 10 days delay will require an additional ΔV of 125 m/s. The optimum strategy for these launches consists on giving only a manoeuvre at the aphelion of the arc from the launch to the Earth (DSM1.2) with an increasing ΔV for this manoeuvre.

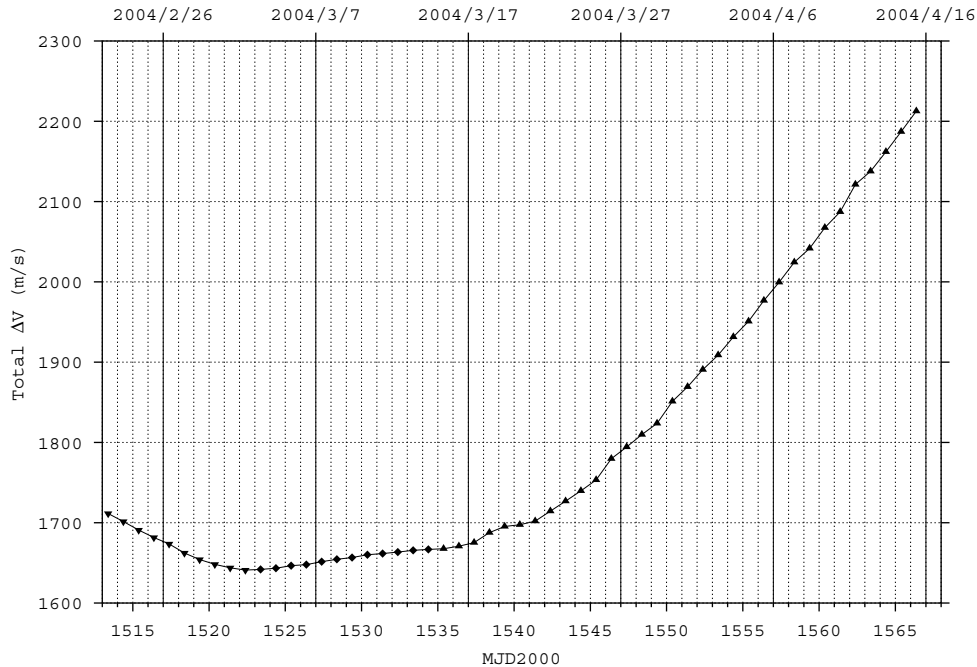


Figure 5-16: Total trajectory ΔV for delayed launch.

The right ascension of the departure asymptote increases at a rate of about 1 degree per day, see Figure 5-9. However, for the days 19 and 20 of March the departure hyperbola from the Earth passes close to the Moon. The influence of the Moon gravity attraction forces a variation of the injection conditions, in particular, the optimum right ascension of the departure asymptote. The launch at either of these days is not recommended due to the large injection dispersion errors and the high risk that the real trajectory passes closer to the Moon than the nominal one, which could derive in extra ΔV for the navigation correction manoeuvres.

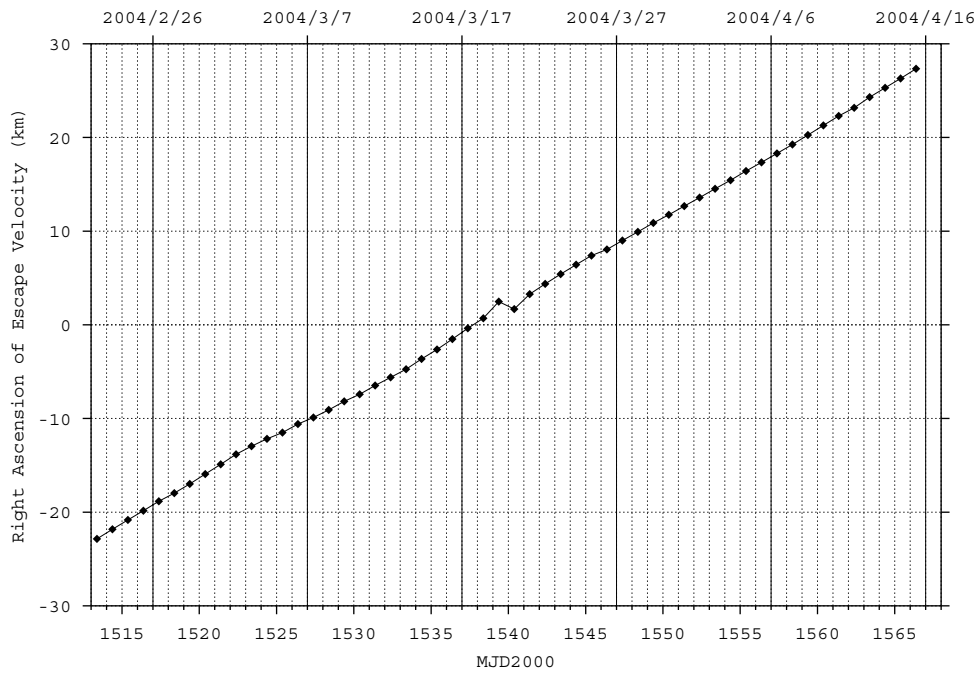


Figure 5-17: Right Ascension of Earth departure hyperbolic velocity (osculating at injection).

6. INTERPLANETARY TRAJECTORY

This chapter describes the trajectory from Earth departure on February 26, 2004 up to arrival to comet 67P/Churyumov-Gerasimenko on May 2014. The details of the trajectory depend not only on the ephemerides that are used for the planet and small bodies, but also on the selected strategy for manoeuvres, (manoeuvres at swing-by, deep space manoeuvres, distance to Earth or Sun, etc), and on the model of the Ariane 5 performances. The function to be optimised is, of course, the spacecraft mass after rendezvous with the comet.

The global parameters describing the trajectory do not change very much when the normal variation on ephemerides, and numerical calculation is considered. So that the range of parameters variation will be the same for distances, distance rates, angles, duration of eclipses, communication black-out, etc. However, some trajectory manoeuvres can be split and moved to other dates without changing more than a few m/s the total ΔV needed for the mission.

In this chapter numerical trajectory data is presented for the whole mission. This trajectory is consistent in the sense that for the force model, and ephemerides used, it is possible to integrate numerically from beginning to end of each phase, and, after introducing a negligible small manoeuvre that corrects numerical noise, to integrate up to the end of the new phase. In this form the integration proceeds from phase to phase up to the end. The phases are defined by trajectory arcs, which are either in the sphere of influence of a planet, or are in interplanetary region, or approaching or going away from one of the small bodies.

Event	Date	ΔV (m/s)	Relative velocity (km/s)	Pericentre height (km)
Earth	2004/02/26		3.545	
Deep Space Manoeuvre 1.1	2004/05/25	173.5		
Earth gravity assist	2005/03/02	0	3.90	4287
Deep Space Manoeuvre 2	2006/10/21	64.3		
Mars gravity assist	2007/02/27	0	8.77	200
Earth gravity assist	2007/11/15	0	9.33	13893
Deep Space Manoeuvre 3	2009/03/16	129.4		
Earth gravity assist	2009/11/11	0	9.98	300
Deep Space manoeuvre 4 (4.4 AU)	2011/05/10	532.6		
Rendezvous with 67P/C-G (4.0 AU)	2014/05/23	773.6		
Start near nucleus operations at 3.25 AU	2014/10/03			
Perihelion pass	2015/08/11			

Table 6-1: Major events of the Rosetta mission

6.1 Detailed Mission Description

6.1.1 Numerical Trajectory Data

Appendix A presents the detailed phase-by-phase data from the injection of the escape hyperbola of the Earth to the rendezvous manoeuvre with 67P/Churyumov-Gerasimenko. For each phase and leg, it is given the initial/final orbital state and the associated dates, as well as the forces considered for the propagation.

When a manoeuvre is required is listed under "Manoeuvre Applied". A manoeuvre of less than a few mm/s indicates a manoeuvre that probably is due to numerical noise. If a slightly different force model or numerical integration scheme is used, the manoeuvre will remain small but will be different, or even disappear.

For the legs which are close to a planet, parameters relative to the planet are also given, like: impact vector, arrival and departure conditions, pericentre altitude, etc.

6.1.2 Geometrical Data

General Trajectory

The ecliptic projection of the complete trajectory is presented in Figure 4-1. For this trajectory, the evolution of the spacecraft distance to the Sun and the Earth is presented in Figure 6-1. For the first four and half years the spacecraft remains at distances between 1 to 2 AU from the Sun, and up to 3 AU from the Earth. A minimum distance to the Sun of 0.88 AU is reached after the second Earth swing-by. The arc between the second and third Earth swing-by has an aphelion at 2.29 AU. Afterwards, the spacecraft goes up to 5.3 AU from the Sun and up to 6.2 AU from the Earth and reaches the comet at 4.0 AU from the Sun and 3.3 AU from the Earth..

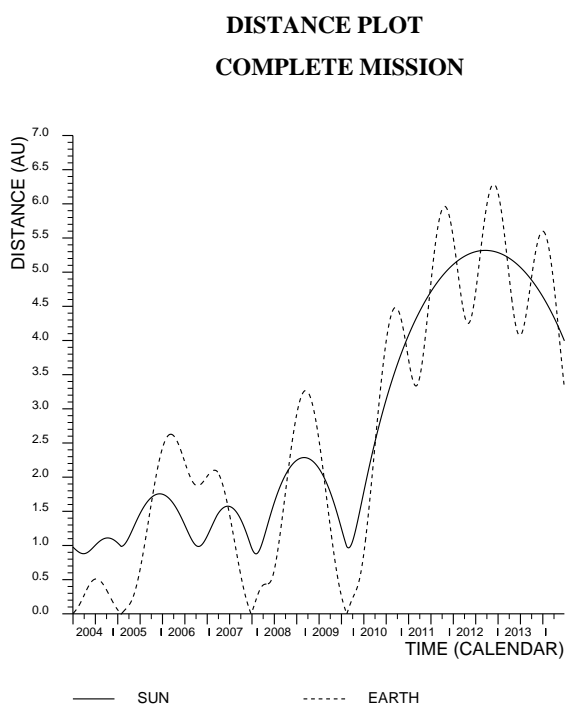


Figure 6-1: Evolution of spacecraft distance to Sun and Earth

The evolution of the angle Earth-Spacecraft-Sun, and the angle Spacecraft-Earth-Sun is presented in Figure 6-2. The last angle is important for radio communication with the spacecraft. For some months during 2004, and a few days during 2008, 2009, and 2010, the spacecraft will be near conjunction, and radio communication could be difficult.

ANGLES PLOT COMPLETE MISSION

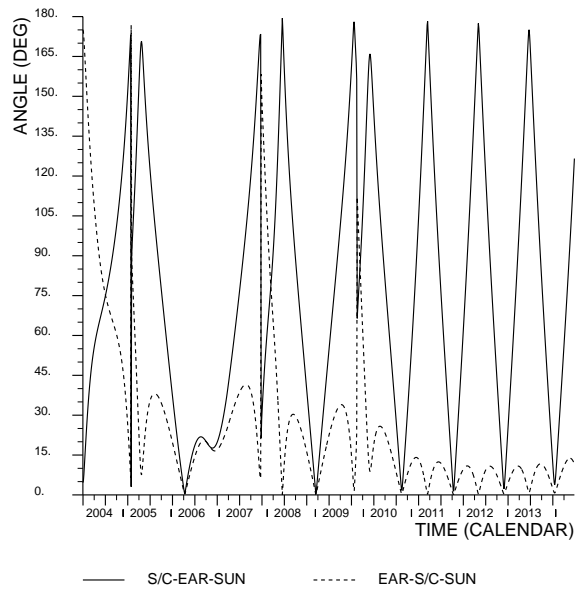


Figure 6-2: Evolution of Spacecraft communication angles

Figure 6-3 presents the variation of the spacecraft declination. For long periods of time, and after 2011 in particular, the spacecraft declination is negative, and, therefore, well in view of a southern ground station. Small values of the declination of the spacecraft produce larger errors of the orbit determination as the component of the position normal to the ecliptic plane cannot be properly obtained. The declination passes through zero value once in the arc from launch to Earth, twice from Earth to Mars, once from Mars back to the Earth and once before and once after the third Earth swing-by.

ANGLES PLOT COMPLETE MISSION

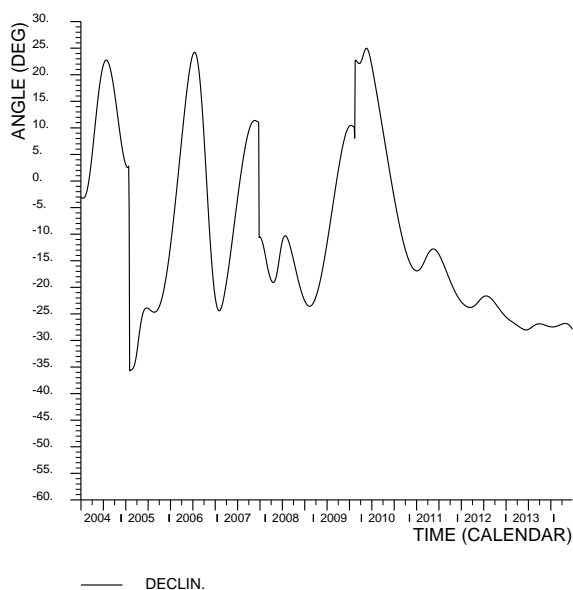


Figure 6-3: Evolution of spacecraft declination

Phase from Launch to Earth

The launcher delivers the spacecraft in a heliocentric trajectory of a period very similar to the translation period of the Earth. The spacecraft must perform one or two deep space manoeuvres in order to encounter again the Earth with the proper arrival conditions. These manoeuvres can be given at perihelion or aphelion of the orbit. Due to this variability, this arc and the following swing-by of the Earth are the most dependant part of the trajectory to the launch day.

Figure 6-4 presents the ecliptic projection of this part of the trajectory. Figure 6-5 gives the evolution of the spacecraft distance to the Sun and the Earth for this period.

The evolution of the declination is given in Figure 6-6.

The evolution of the angle Earth-Spacecraft-Sun and the angle Spacecraft-Earth-Sun is presented in Figure 6-7. For the first days of the trajectory, the Earth is nearly between the Sun and the Spacecraft. During the LEOP the angle Spacecraft-Earth-Sun reaches a minimum in about one to three days, which could difficult the communication with the spacecraft. The value of this minimum depends strongly on the launch date, see Figure 6-8 and Figure 6-9. At launch window open the minimum angle is above 4 degrees, but it is less than 2 degrees for the middle.

**XY PLOT. MEAN ECLIPTIC OF DATE
PHASE LAUNCH - EARTH 1**

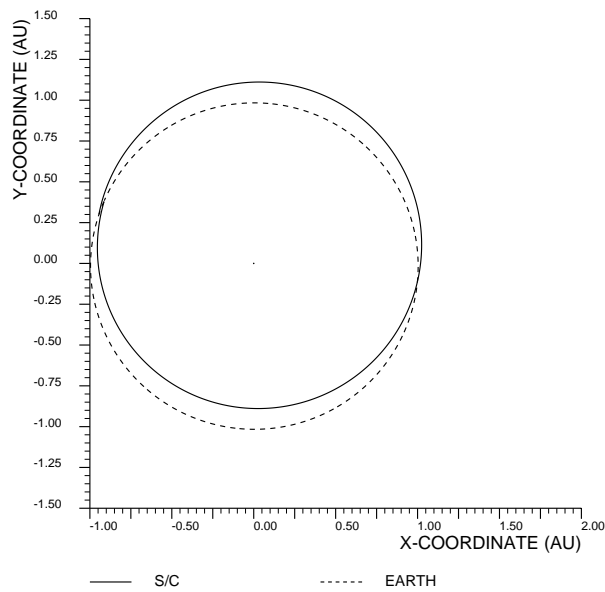


Figure 6-4: Phase from Launch to Earth. Ecliptic projection of the trajectory

**DISTANCE PLOT
PHASE LAUNCH - EARTH 1**

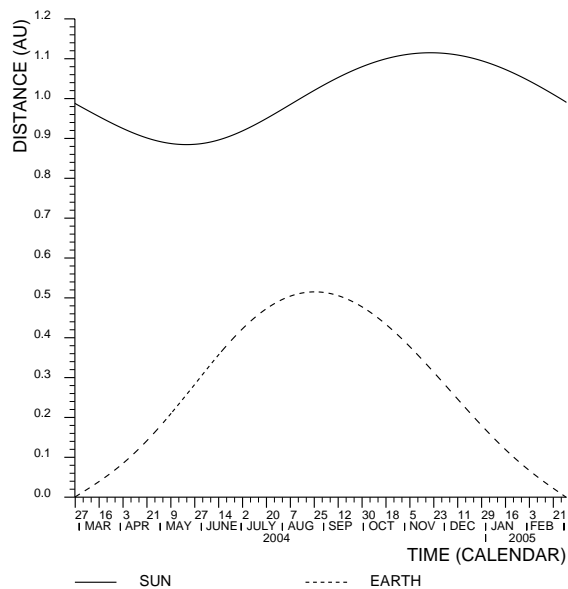


Figure 6-5: Phase from Launch to Earth. Spacecraft distance to Sun and Earth

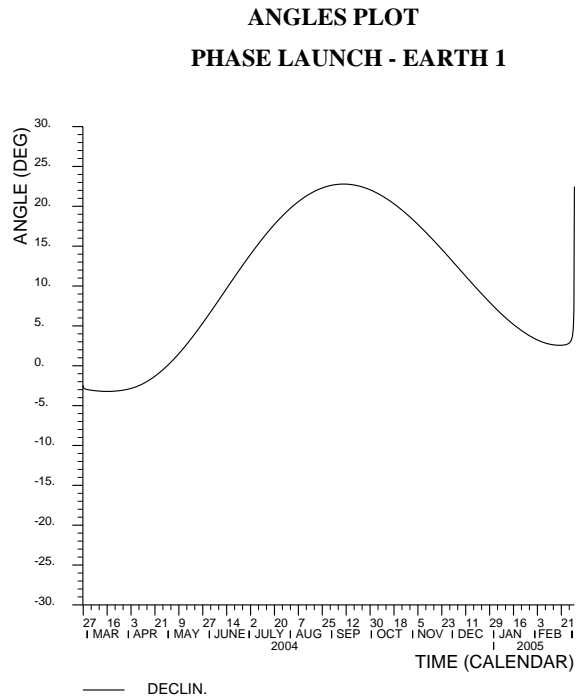


Figure 6-6: Phase from Launch to Earth. Spacecraft declination

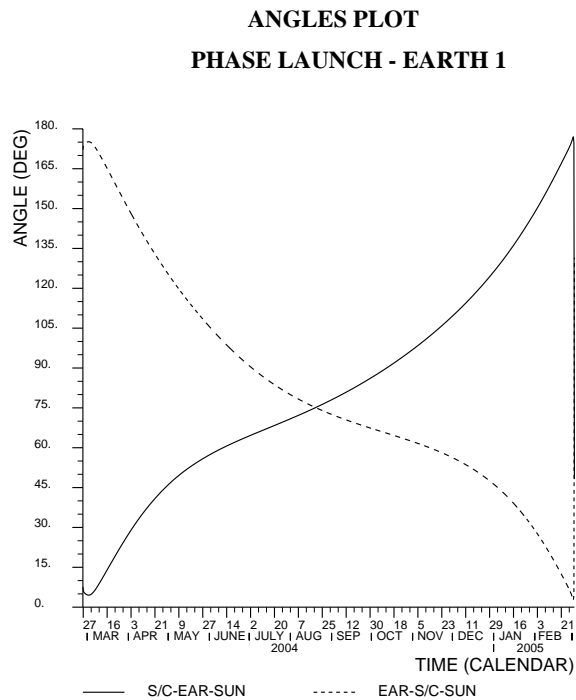


Figure 6-7: Phase from Launch to Earth. Spacecraft communication angle

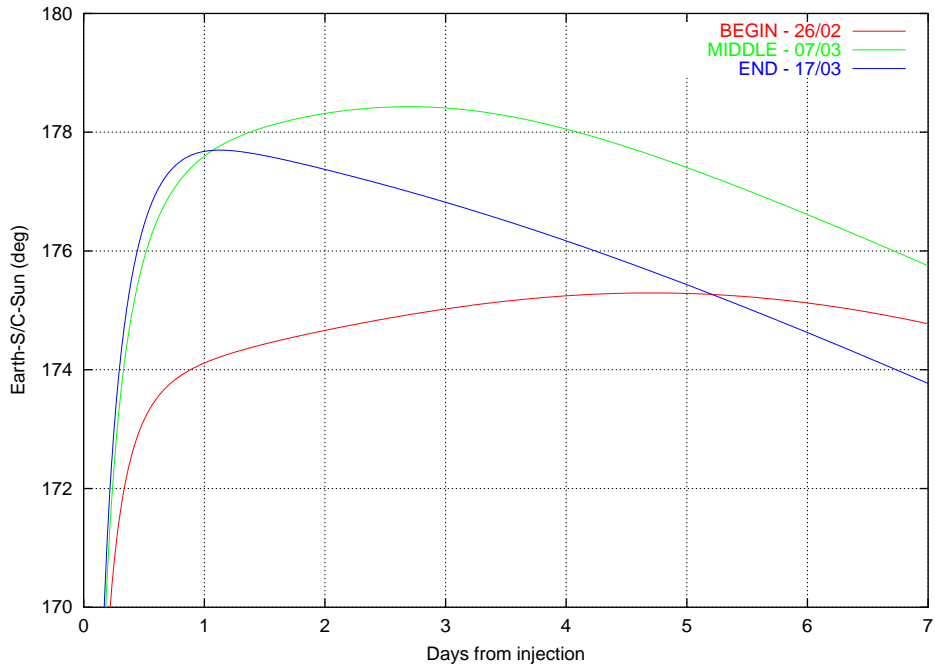


Figure 6-8: Phase from Launch to Earth. Angle Earth-S/C-Sun during LEOP.

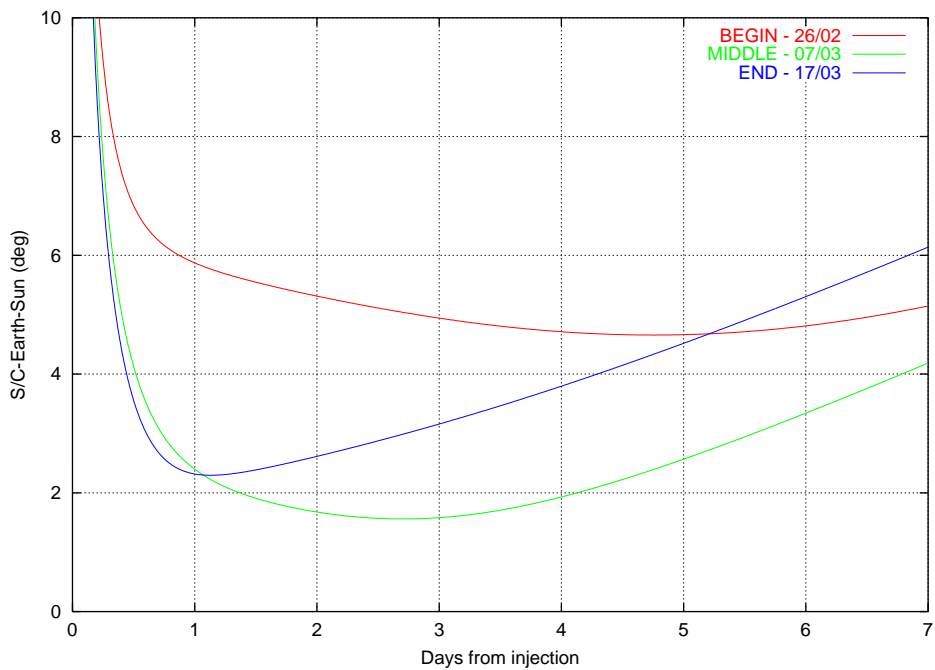


Figure 6-9: Phase from Launch to Earth. Angle S/C-Earth-Sun during LEOP.

Phase First Swing-by of the Earth

The first Earth swing-by is performed at a minimum altitude of more than 1530 km from the surface. Figure 6-10 presents the equatorial projection of the trajectory relative to the Earth for a period of 8 hours. The relative approach and departure velocity is about 3.9 km/s. There are no manoeuvres to be performed except for normal navigation manoeuvres far away from the

Earth. The swing-by takes place with a Sun elongation of about 168° , good conditions for radio telecommunications, Figure 6-11, and in less than 5 hours it changes to about 72° . There is no eclipse in this swing-by, see Figure 6-12.

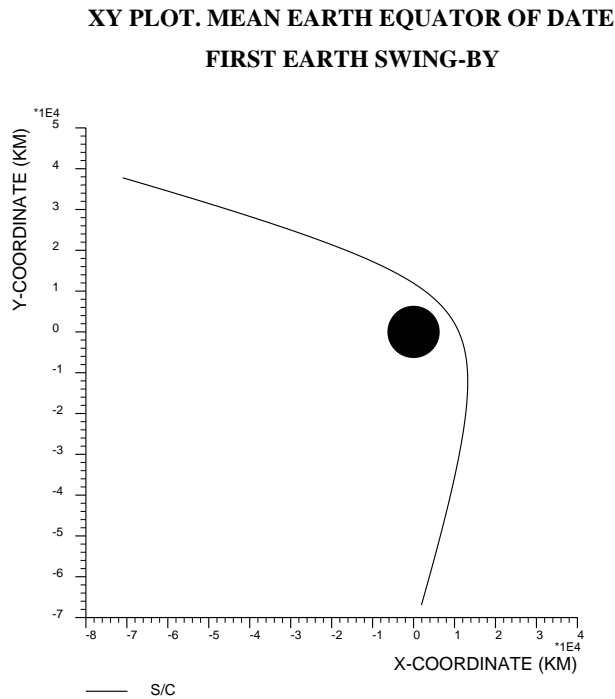


Figure 6-10: Phase First Earth swing-by. Trajectory relative to the Earth.

ANGLES PLOT
FIRST EARTH SWING-BY

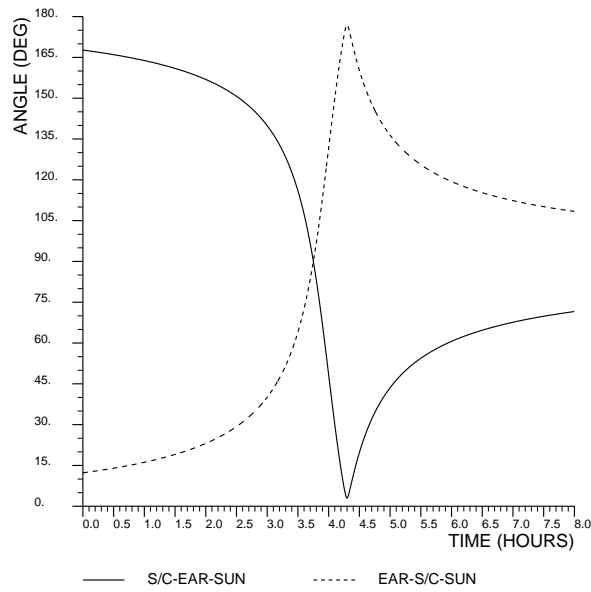


Figure 6-11: Phase First Earth swing-by. Spacecraft communication angle.

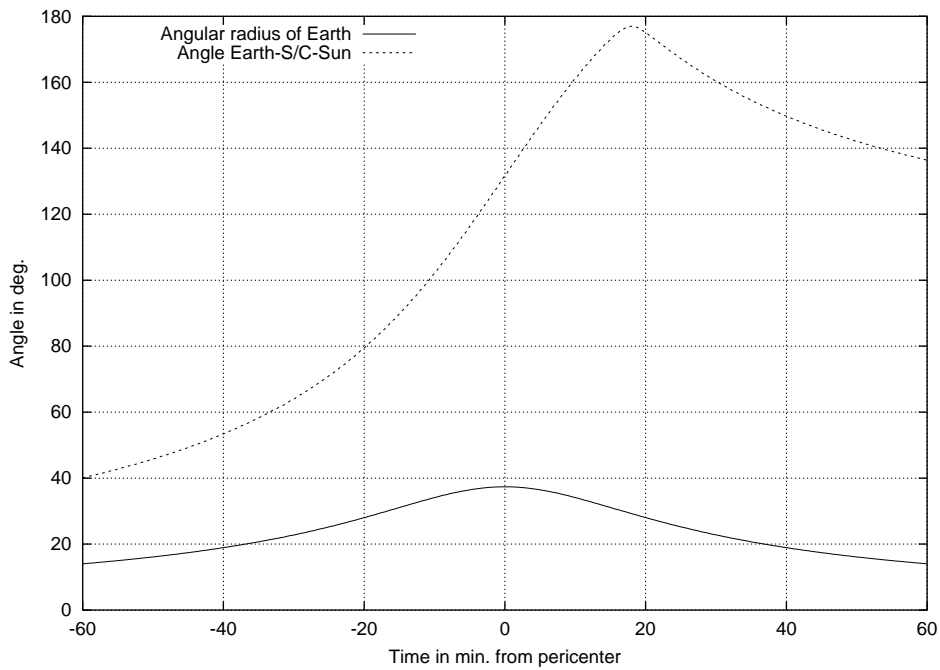


Figure 6-12: Phase First Earth swing-by. Eclipse condition.

Phase from Earth to Mars

After leaving the Earth, the spacecraft makes one revolution around the Sun, and in the second arc from perihelion to aphelion makes a swing-by of Mars. Figure 6-13 presents the ecliptic projection of this part of the trajectory. Figure 6-14 gives the evolution of the spacecraft distance to the Sun and the Earth for this period.

The evolution of the declination is given in Figure 6-15.

The evolution of the angle Earth-spacecraft-Sun, and the angle spacecraft-Earth-Sun is presented in Figure 6-16. The spacecraft has a conjunction with the Sun with both communication angles having a value less than 5° for a period of almost one month in April of 2006.

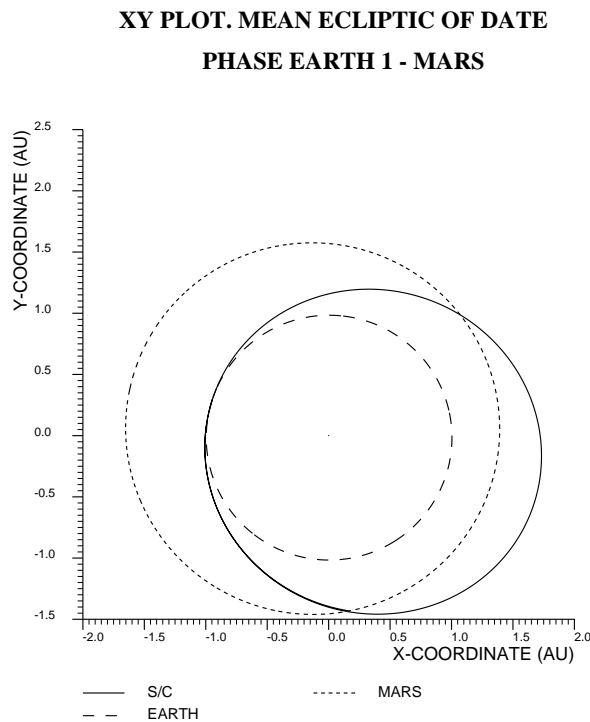


Figure 6-13: Phase from Earth to Mars. Ecliptic projection of the trajectory

DISTANCE PLOT
PHASE EARTH 1 - MARS

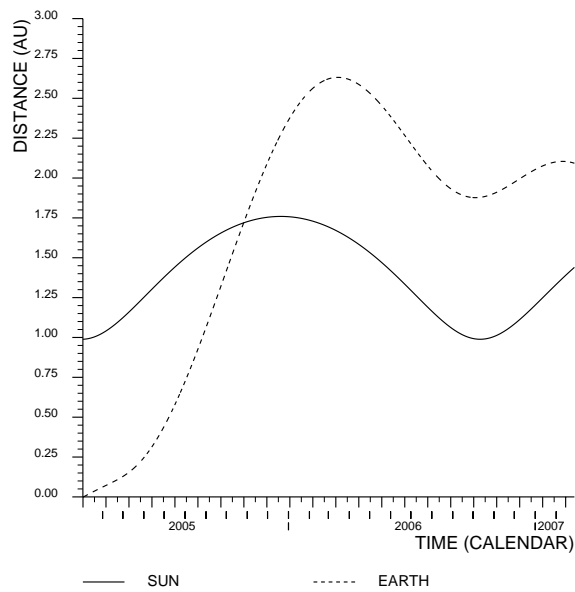


Figure 6-14: Phase from Earth to Mars. Spacecraft distance to Sun and Earth

ANGLES PLOT
PHASE EARTH 1 - MARS

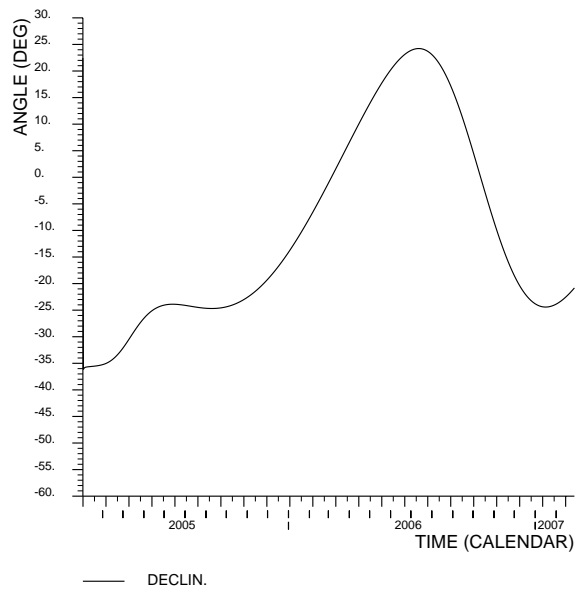


Figure 6-15: Phase from Earth to Mars. Spacecraft declination

ANGLES PLOT PHASE EARTH 1 - MARS

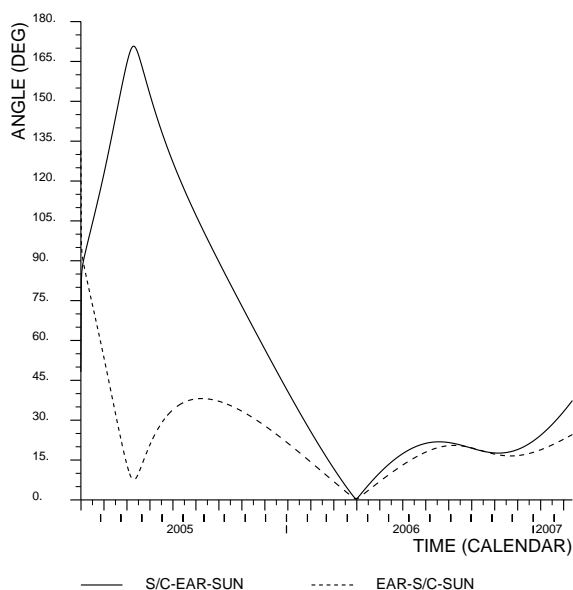


Figure 6-16: Phase from Earth to Mars. Spacecraft communication angle

Phase Swing-by Mars

The Mars swing-by must be performed as close to the planet as possible, the minimum distance has been fixed as 200 km. Figure 6-17 and Figure 6-18 presents the trajectory relative to Mars for a short period of time near the pericentre passage. The relative approach and departure velocity is about 8.77 km/s. Figure 6-19 shows the distance of the Spacecraft to Mars centre of masses and also to the satellites Phobos and Deimos.

Table 6-2 presents the orbital and physical parameters of Phobos and Deimos. A close encounter with the satellite Phobos will occur about 13 minutes after the pericentre pass. The minimum distance to Phobos will be of 3362 Km. Then the minimum distance to Deimos of 10974 Km will be reached 32 minutes after the pericentre pass. However, the fast movement of the satellites of Mars cause that the small variations of the swing-by date change completely this geometrical configuration. In fact, a deterministic variation on the swing-by date is expected during the launch window and the stochastic variations due to the navigation uncertainties will also play an important roll.

Property	Phobos	Deimos
Semi-major axis (km)	9378	23459
Sidereal orbit period (days)	0.31891	1.26244
Sidereal rotation period (days)	0.31891	1.26244
Orbital inclination (deg)	1.08	1.79
Orbital eccentricity	0.0151	0.0005
Major axis radius (km)	13.4	7.5
Median axis radius (km)	11.2	6.1
Minor axis radius (km)	9.2	5.2
Mass (10^{15} kg)	10.6	2.4
Mean density (kg/m^3)	1900	1750
Geometric albedo	0.07	0.08
Visual magnitude	11.8	12.89
Apparent visual magnitude	11.3	12.4

Table 6-2: Orbital and Physical properties of Mars Satellites.

No manoeuvre is performed during the Martian swing-by. The elongation of the Sun during the encounter is about 25° providing good visibility and telecommunications conditions, Figure 6-21. Near the pericentre, there is an occultation of the spacecraft by Mars that lasts about 14 minutes and an eclipse of about 24 minutes, see Figure 6-22.

XY PLOT. MEAN EARTH EQUATOR 2000

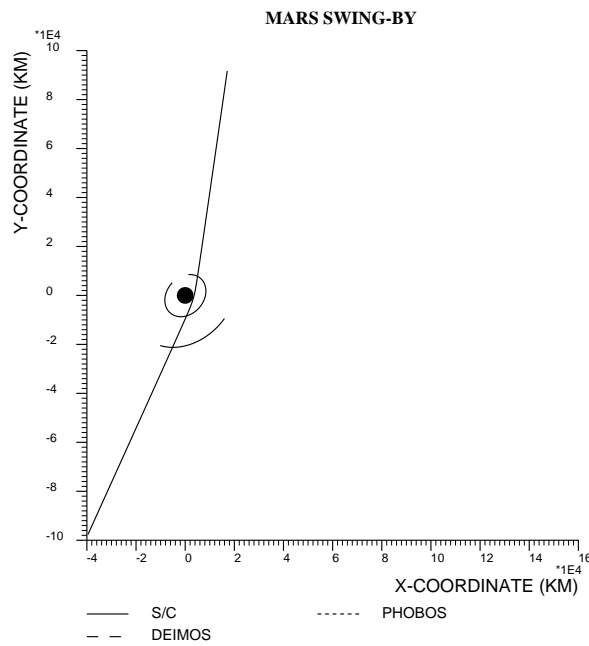


Figure 6-17: Phase Swing-by Mars. Spacecraft trajectory XY projection relative to Mars

XZ PLOT. MEAN EARTH EQUATOR 2000

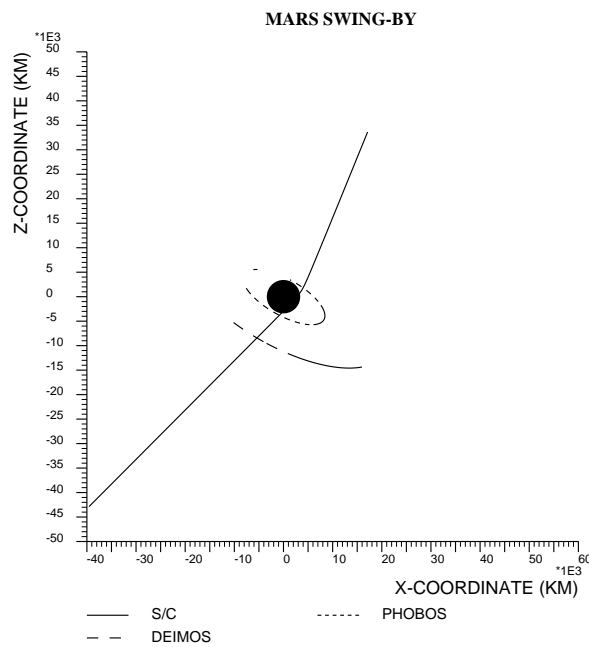


Figure 6-18: Phase Swing-by Mars. Spacecraft trajectory XZ projection relative to Mars

DISTANCE PLOT

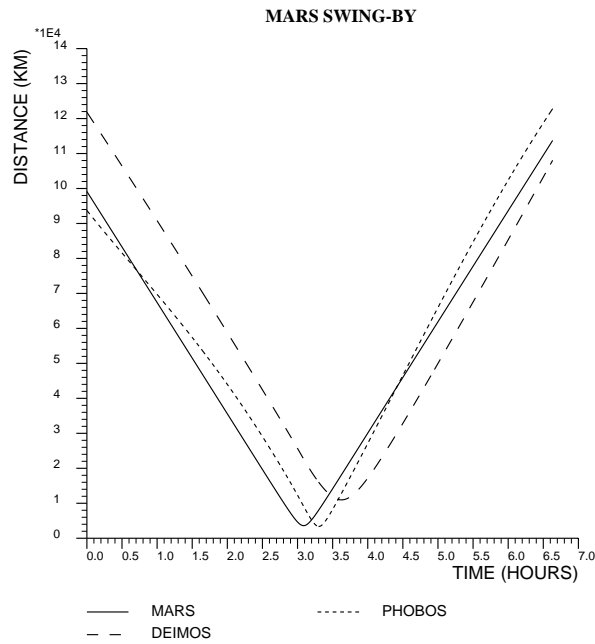


Figure 6-19: Phase Swing-by Mars. Spacecraft distances to Mars, Phobos and Deimos.

ANGLES PLOT

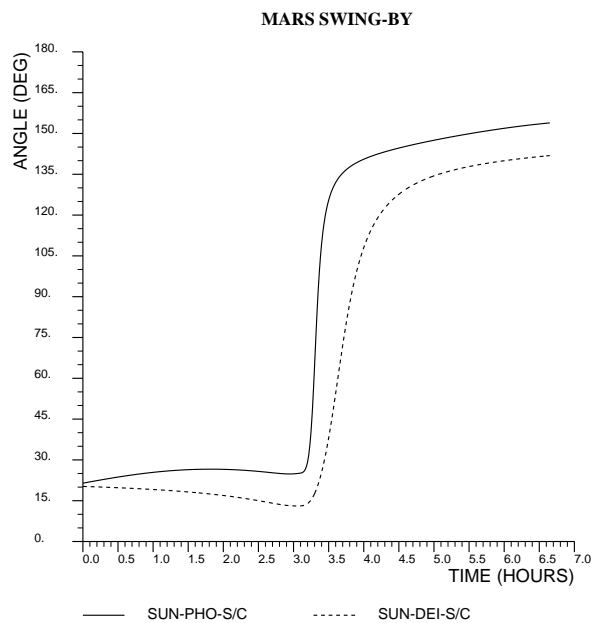


Figure 6-20: Phase Swing-by Mars. Illumination angles to Phobos and Deimos.

**ANGLES PLOT
 MARS SWING-BY**

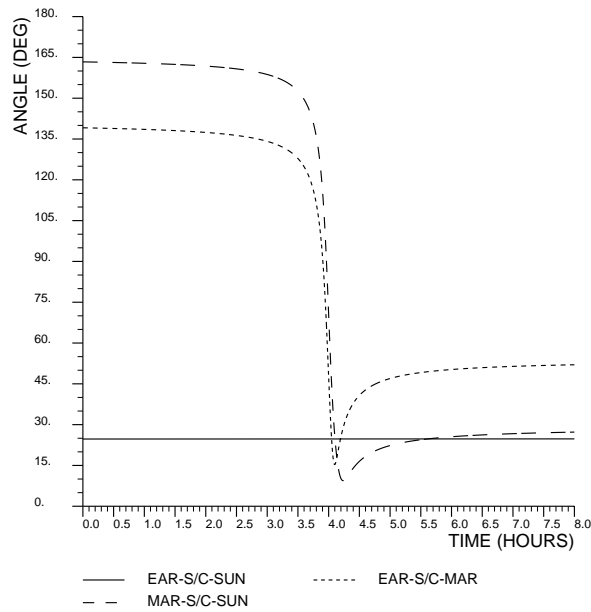


Figure 6-21: Phase Swing-by Mars. Spacecraft communication angles.

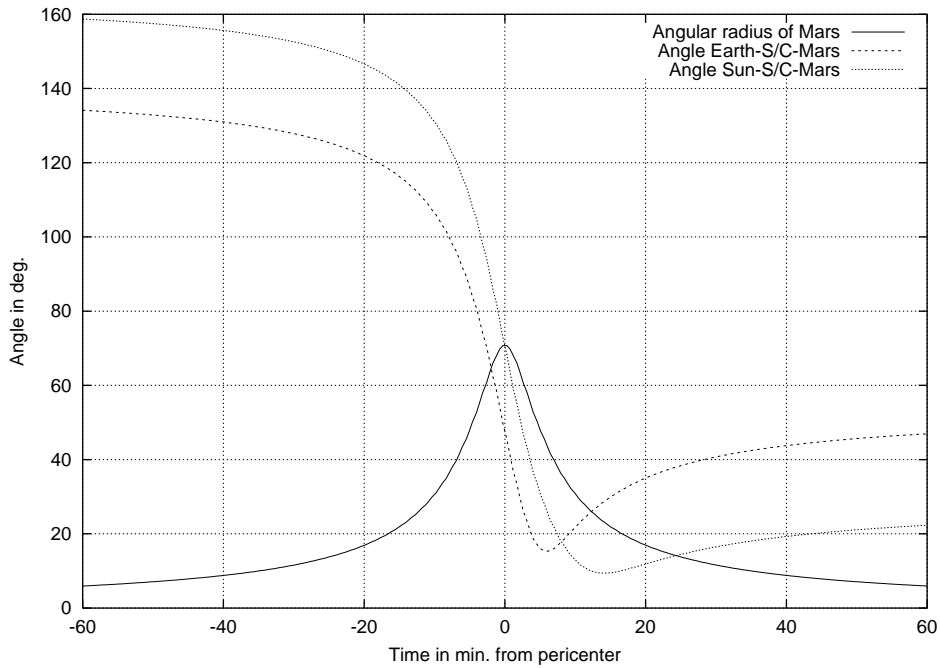


Figure 6-22: Phase Swing-by Mars. Communication black-out due to spacecraft occultation by Mars.

Phase from Mars to Earth

This phase is an arc of about 9 months that joins Mars with the second swing-by of the Earth. No DSM is needed for this arc.

Figure 6-23 presents the ecliptic projection of this part of the trajectory.

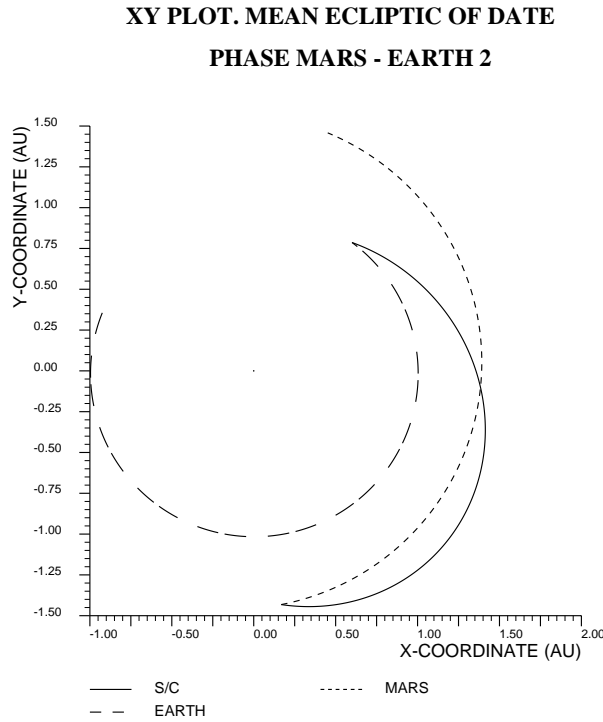


Figure 6-23: Phase from Mars to Earth. Ecliptic projection of the trajectory.

DISTANCE PLOT
PHASE MARS - EARTH 2

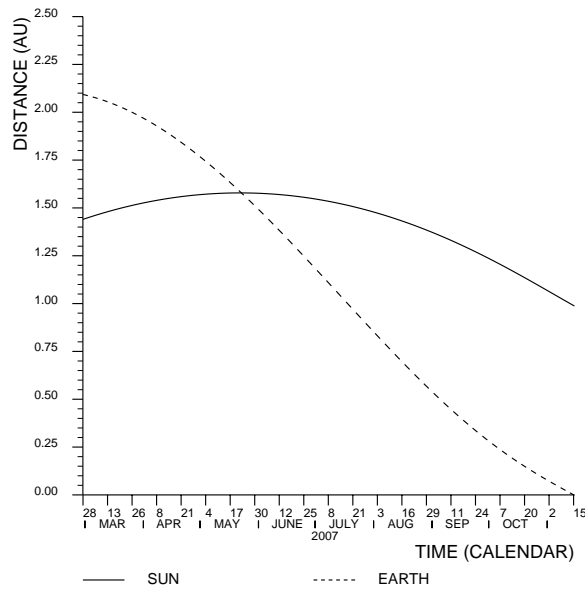


Figure 6-24: Phase from Mars to Earth. Spacecraft distance to Sun and Earth

ANGLES PLOT
PHASE MARS - EARTH 2

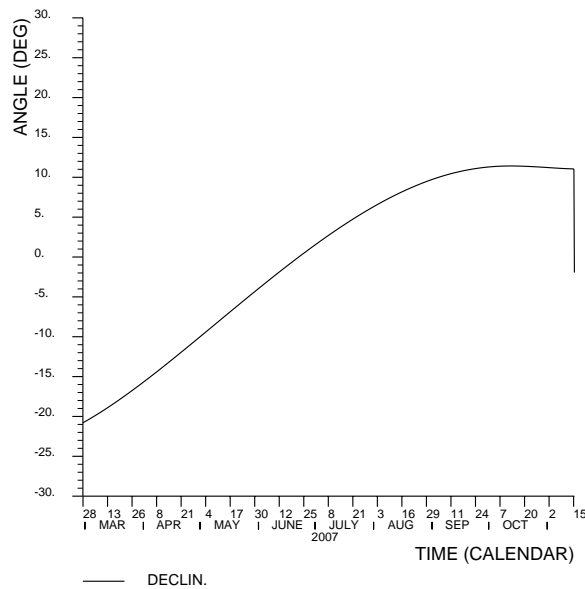


Figure 6-25: Phase from Mars to Earth. Spacecraft declination

ANGLES PLOT
PHASE MARS - EARTH 2

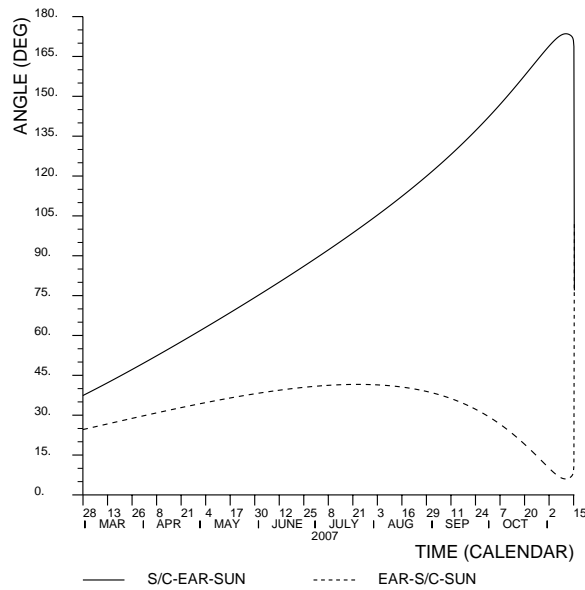


Figure 6-26: Phase from Mars to Earth. Spacecraft communication angle

Phase Second Earth swing-by

The Earth swing-by is performed at a minimum altitude of about 13870 km from the surface. Figure 6-27 presents the equatorial projection of the trajectory relative to the Earth for a period of 8 hours. The relative approach and departure velocity is about 9.3 km/s. There are no manoeuvres to be performed except for normal navigation manoeuvres faraway from the Earth. The swing-by takes place with a Sun elongation of about 166° , good conditions for radio telecommunications, Figure 6-28, and in less than 4 hours it changes to about 16° . There is no eclipse in this swing-by, see Figure 6-29.

XY PLOT. MEAN EARTH EQUATOR OF DATE SECOND EARTH SWING-BY

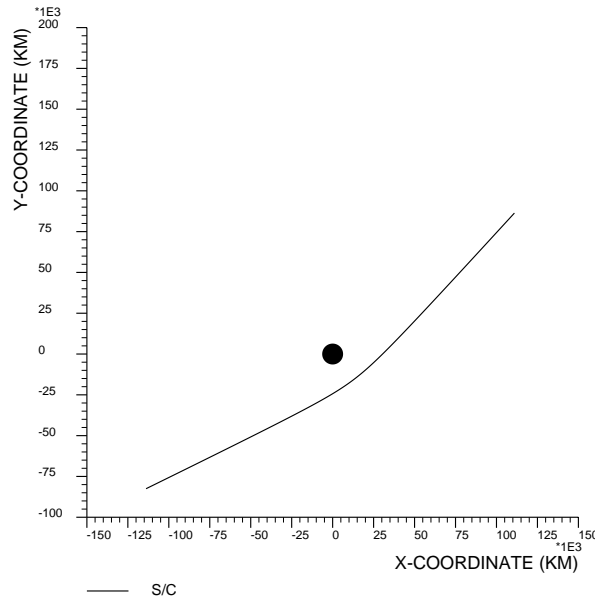


Figure 6-27: Phase Second Earth swing-by. Trajectory relative to the Earth.

ANGLES PLOT SECOND EARTH SWING-BY

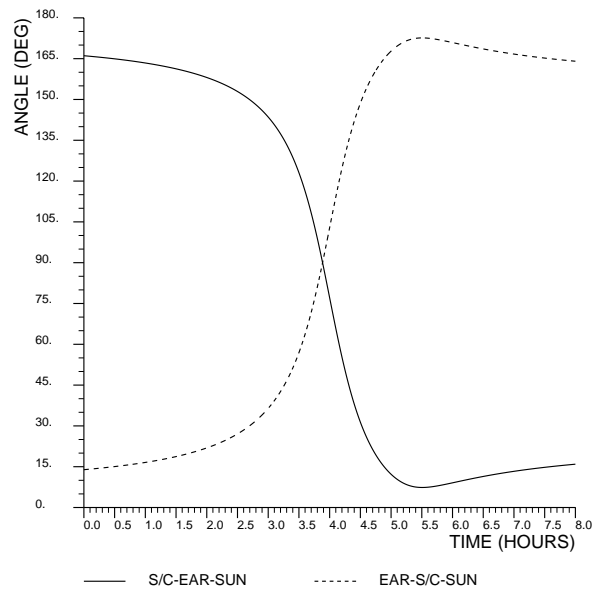


Figure 6-28: Phase Second Earth swing-by. Spacecraft communication angle.

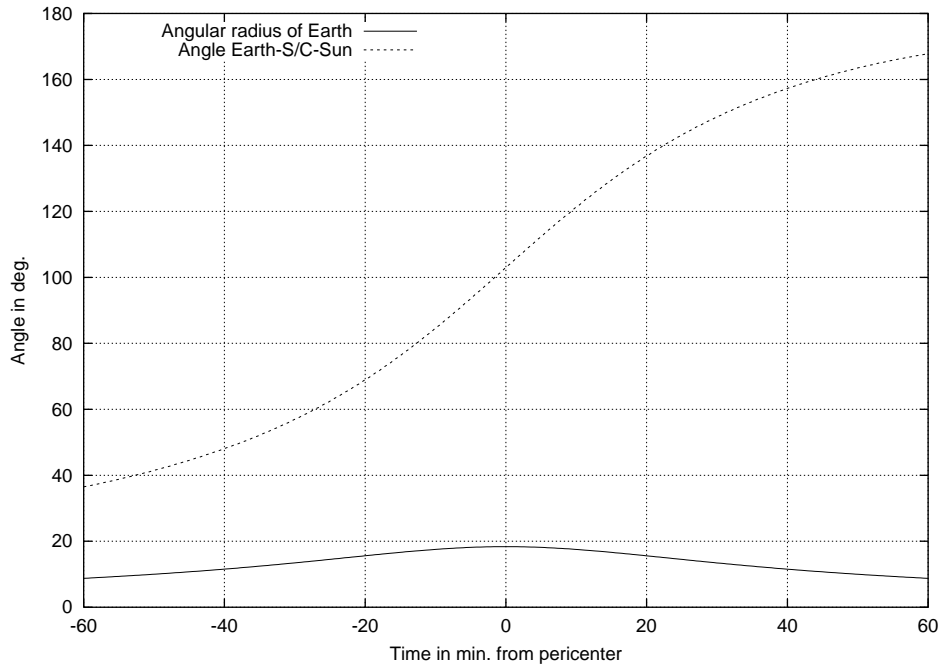


Figure 6-29: Phase Second Earth swing-by. Eclipse condition.

Phase from Earth to Earth

In this phase the spacecraft makes a revolution around the Sun, ecliptic projection is presented in Figure 6-30, and goes to distances of up to 2.3 AU from the Sun, and 3.3 AU from the Earth, Figure 6-31. The relative velocity while leaving or approaching the Earth is about 9.9 km/s. A manoeuvre of more than 100 m/s is scheduled near the aphelion of this arc in order to obtain the proper arrival conditions at the Earth.

The evolution of the declination is given in Figure 6-32. It is seen that most of the time the spacecraft is at negative declinations, except for the period of the approach to the third Earth swing-by.

The evolution of the angle Earth-spacecraft-Sun, and the angle spacecraft-Earth-Sun is presented in Figure 6-33. There is a period of about 18 days where the angle spacecraft-Earth-Sun is smaller than 5° two months before the DSM3.

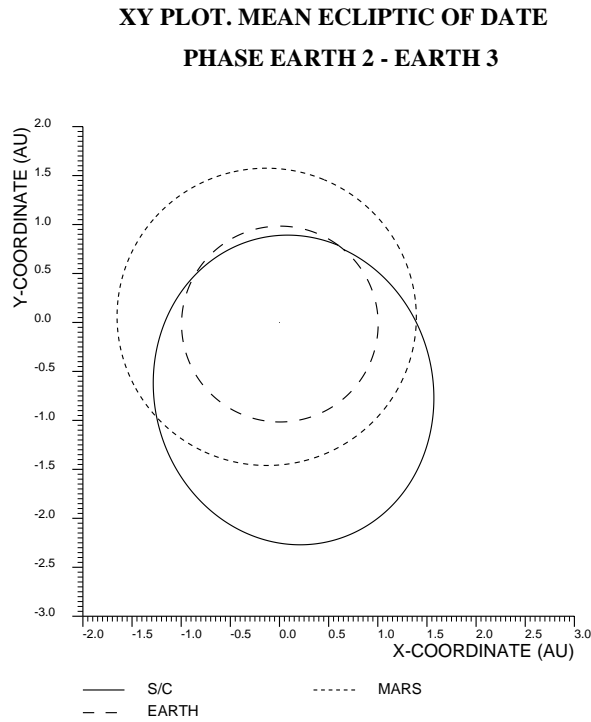


Figure 6-30: Phase from Earth to Earth. Ecliptic projection of the trajectory.

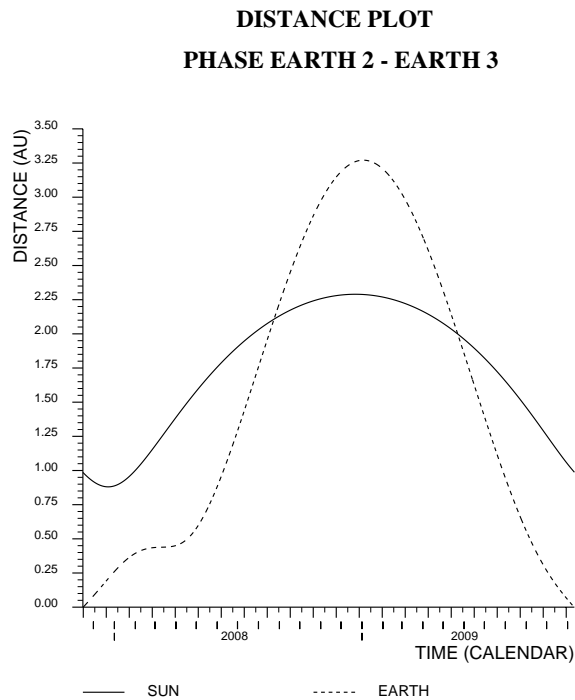


Figure 6-31: Phase from Earth to Earth. Spacecraft distance to Sun and Earth.

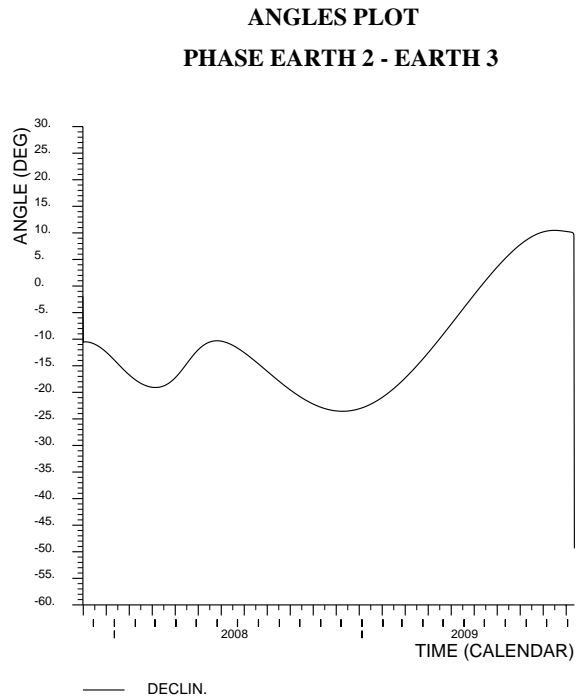


Figure 6-32: Phase from Earth to Earth. Evolution of spacecraft declination.

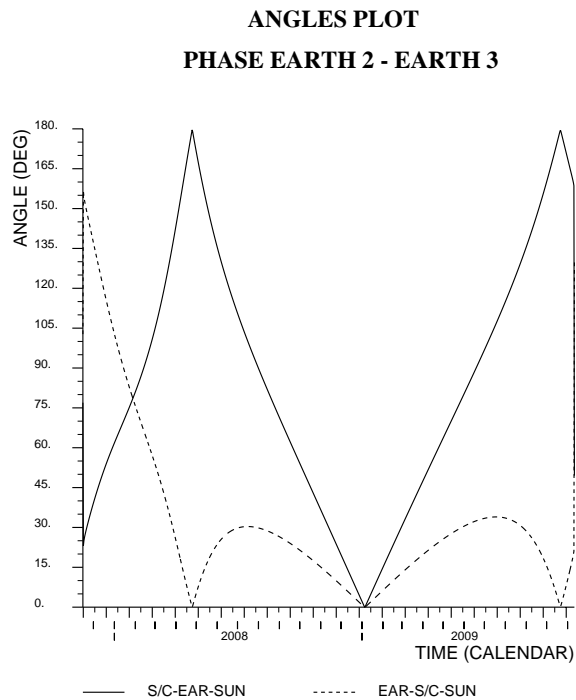


Figure 6-33: Phase from Earth to Earth. Communication angles.

Phase Third Earth swing-by

The Earth swing-by should be performed so close to the Earth as possible. For the nominal trajectory computation a minimum altitude at swing-by of 300Km has been used. Figure 6-34 presents the equatorial projection of the trajectory relative to Earth for a period of 8 hours. The relative approach and departure velocity is about 9.9 km/s.

The swing-by takes place with a Sun elongation of about 156°, good conditions for radio telecommunications, Figure 6-35, and in less than 3 hours it changes to about 60°. There is no eclipse in this swing-by, see Figure 6-36.

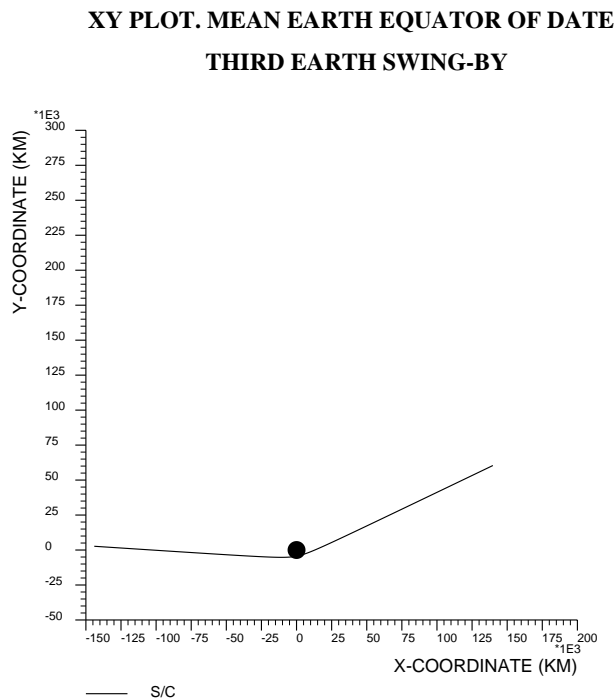


Figure 6-34: Phase Third Earth swing-by. Trajectory relative to the Earth

**ANGLES PLOT
 THIRD EARTH SWING-BY**

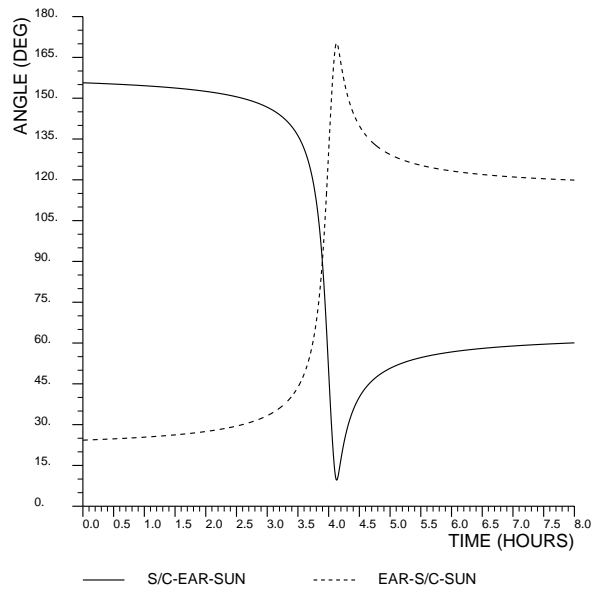


Figure 6-35: Phase Third Earth swing-by. Spacecraft communication angle.

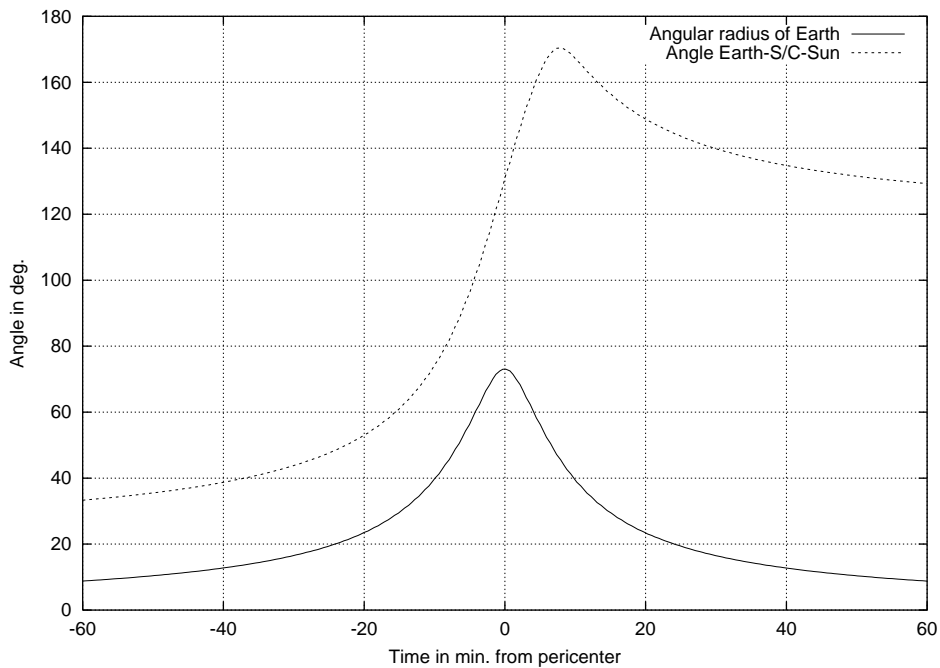


Figure 6-36: Phase Third Earth swing-by. Eclipse condition.

Phase from Earth swing-by to Churyumov-Gerasimenko

Figure 6-37 and Figure 6-38 presents the ecliptic projection of the trajectory. The spacecraft goes to the capture of Churyumov-Gerasimenko in a less elongated orbit in a near orbital plane. Near the rendezvous the comet is behind the spacecraft and by means of a manoeuvre it must increase the velocity to rendezvous the comet. The final relative velocity with respect to the comet at rendezvous is 774 m/s.

The distance to the Sun and to the Earth keeps increasing up to their maximum values of 5.3 AU and 6.3 AU, respectively. See Figure 6-39. A Deep Space Manoeuvre will be performed when the spacecraft has reached a distance to the Sun of 4.4 AU and then put to hibernation for its aphelion pass. The manoeuvre will be executed in May 2011, and requires a ΔV of about 530 m/s.

The spacecraft is almost in conjunction with the Sun in Oct. 2010, Nov. 2011, Dec. 2012 and Dec. 2013, Figure 6-41, but in all cases the period where the Sun elongation is less than 5° is less than 2 weeks. The spacecraft declination is always negative after Aug. 2010. The beginning of the rendezvous will start at the end of May, 2014, and the detailed implementation is described in chapter 8.

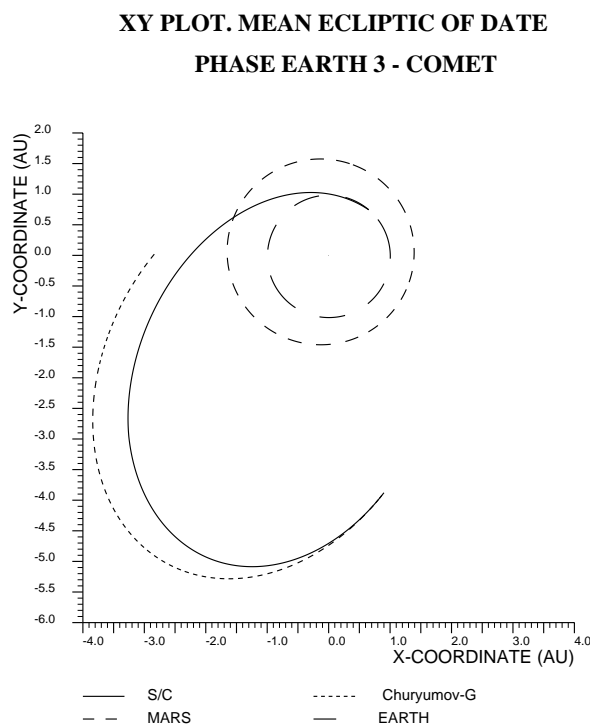


Figure 6-37: Phase from Earth to 67P/C-G. Ecliptic projection of the trajectory.

**XZ PLOT. MEAN ECLIPTIC OF DATE
PHASE EARTH 3 - COMET**

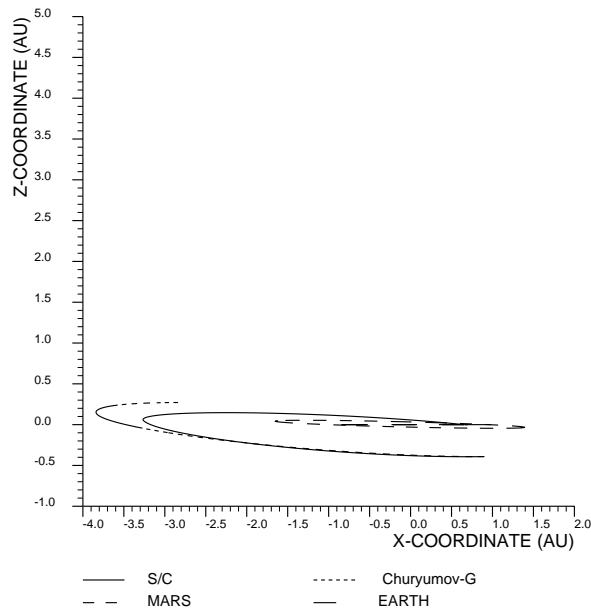


Figure 6-38: Phase from Earth to 67P/C-G. Out ecliptic projection of the trajectory.

**DISTANCE PLOT
PHASE EARTH 3 - COMET**

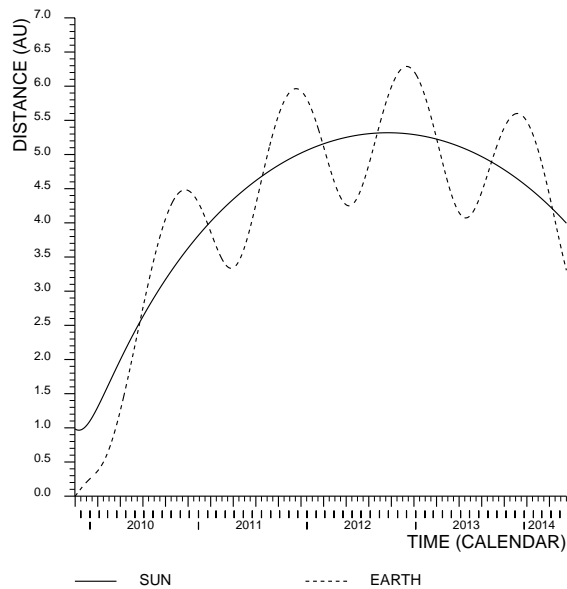


Figure 6-39: Phase from Earth to 67P/C-G. Spacecraft distance to Sun and Earth

ANGLES PLOT
PHASE EARTH 3 - COMET

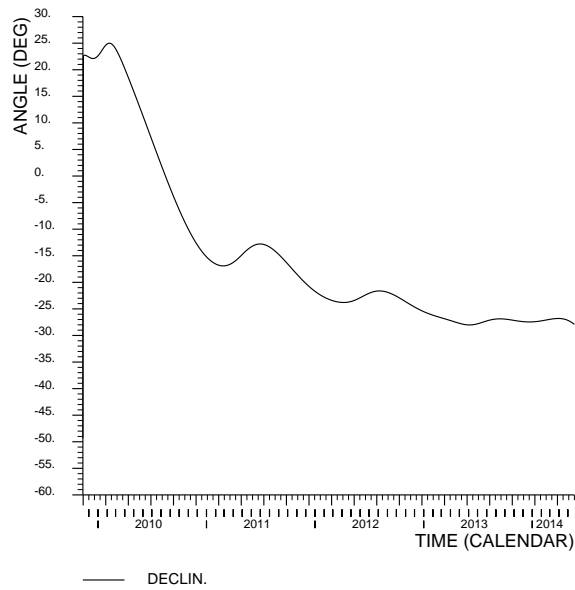


Figure 6-40: Phase from Earth to 67P/C-G. Evolution of spacecraft declination

ANGLES PLOT
PHASE EARTH 3 - COMET

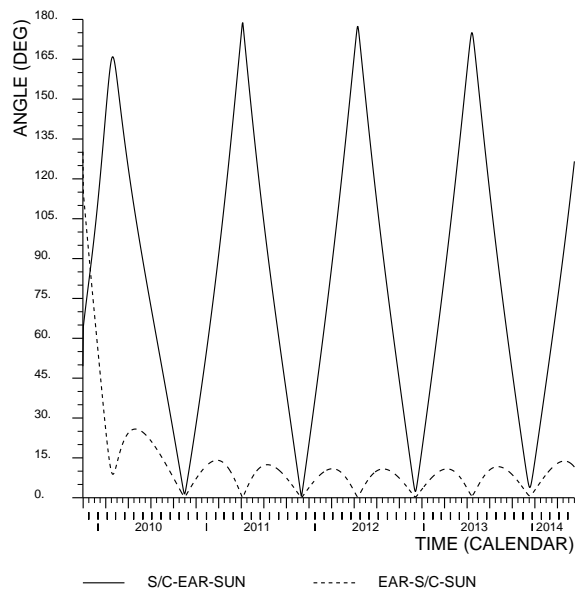


Figure 6-41: Phase from Earth to 67P/C-G. Communication angles

Phase from Churyumov-Gerasimenko RDV to Perihelion

The spacecraft orbits the comet and moves around the Sun along the trajectory of the comet. Figure 6-42 presents the ecliptic projection of this trajectory. Figure 6-43 shows the variation of the position out of the ecliptic plane from below to above.

The distance to the Sun decreases as the comet reaches the perihelion at 1.24 AU. The perihelion is also near the minimum distance to the Earth. At this point the distance is 1.77 AU. See Figure 6-44.

The declination remains negative during almost the whole period until about five months before the perihelion, see Figure 6-45.

Figure 6-46 presents the communication angles during this period. The spacecraft is nearly in conjunction with the Sun in Feb. 2015, but the Sun elongation is less than 5 degrees only for 2 days.

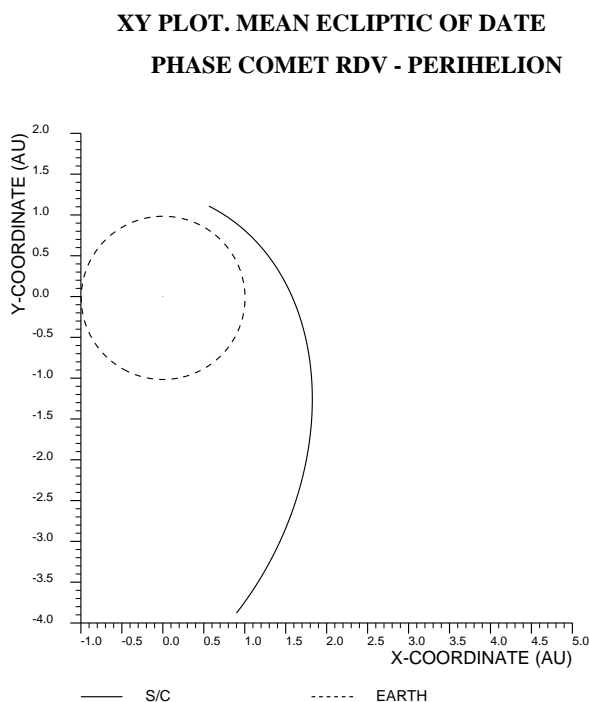


Figure 6-42: Phase from 67P/C-G RDV to Perihelion. Ecliptic projection of the trajectory.

**XZ PLOT. MEAN ECLIPTIC OF DATE
PHASE COMET RDV - PERIHELION**

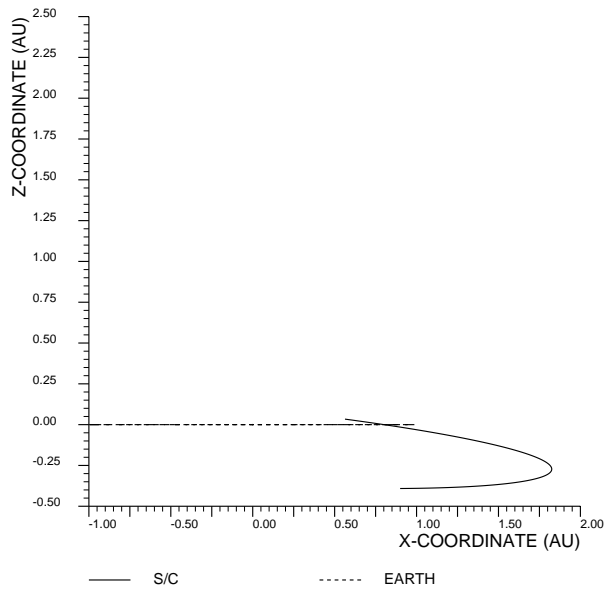


Figure 6-43: Phase from 67P/C-G RDV to Perihelion. Out ecliptic projection of the trajectory.

**DISTANCE PLOT
PHASE COMET RDV - PERIHELION**

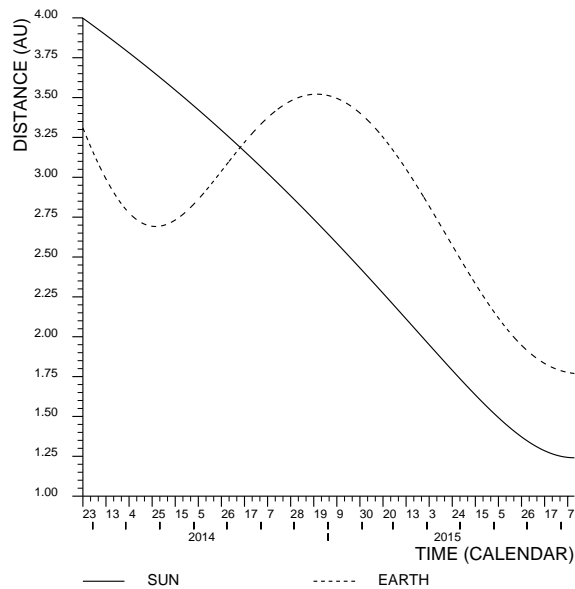


Figure 6-44: Phase from 67P/C-G RDV to Perihelion. Spacecraft distance to Sun and Earth

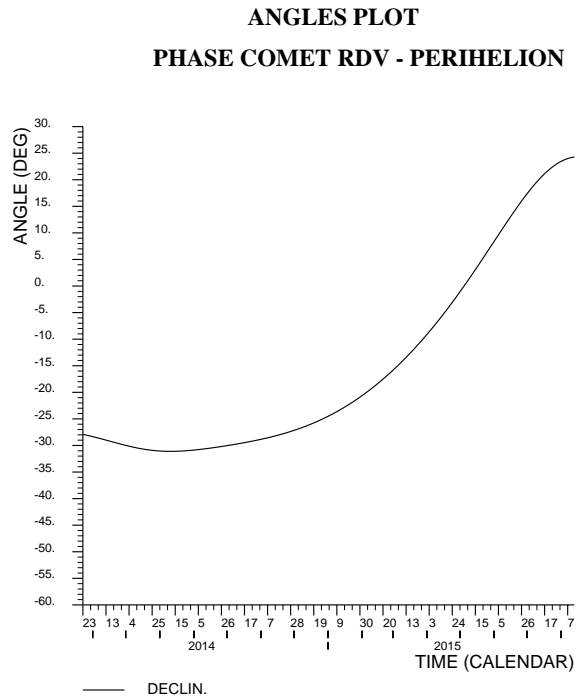


Figure 6-45: Phase from 67P/C-G RDV to Perihelion. Evolution of spacecraft declination.

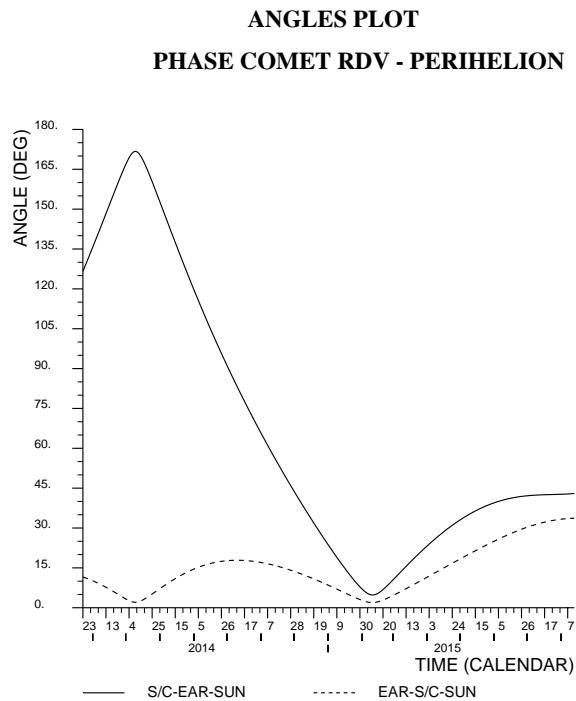


Figure 6-46: Phase from 67P/C-G RDV to Perihelion. Communication angles

6.1.3 Ground Station Coverage

A visibility study has been done along the interplanetary arcs during the whole mission duration. The ground stations selected are: New Norcia (New Norcia), and Kourou. Results are presented here in two different ways:

1. The entry and exit in the visibility interval during the day for each ground station versus calendar date.
2. The visibility duration versus calendar date.

Minimum elevation considered in all the cases is: 5°. At this minimum elevation it is most likely possible to communicate with the spacecraft, however, in the worst case, the minimum elevation that needs to be maintained for communication is 10° for commanding, and no protection is given to the deep space frequency band below 10°. The difference in duration of the daily pass for the two elevations can be up to 1 hour.

In the following plots, visibility from the ground station is obtained in the dashed zone. The continuous lines show the acquisition and loss of signal for a minimum elevation of 5°, while the dashed lines are the AOS/LOS for a minimum elevation of 10°.

Phase from Launch to 1st Earth swing-by

This arc has been considered from the exit of the sphere of influence of the Earth up to the entry again of this the sphere of influence of Mars. Figure 6-47 and Figure 6-48, show the entry-exit in the visibility interval during the day, and Figure 6-49 the visibility duration of the two stations along this phase.

Phase from Earth to Mars

This arc has been considered from the exit of the sphere of influence of the Earth at the first swing-by up to the entry in the sphere of influence of Mars. Figure 6-50 and Figure 6-51, show the entry-exit in the visibility interval during the day, and Figure 6-52 the visibility duration of the two stations along this phase.

Phase from Mars to 2nd Earth swing-by

This arc has been considered from the exit of the sphere of influence of Mars up to the entry in the sphere of influence of the Earth before the 2nd swing-by. Figure 6-53 and Figure 6-54 show the entry-exit in the visibility interval during the day, and Figure 6-55 the visibility duration of the two stations along this phase.

Phase from 2nd Earth swing-by to 3rd Earth swing-by

This arc has been considered from the exit of the sphere of influence at the 2nd swing-by of the Earth up to the entry in the sphere of influence of the Earth before the 3rd swing-by. Figure 6-56

and Figure 6-57 show the entry-exit in the visibility interval during the day, and Figure 6-58 the visibility duration of the two stations along this phase.

Phase from 3rd Earth swing-by to Deep Space Manoeuvre

This arc has been considered from the exit of the sphere of influence of the Earth at the third swing-by up to the Deep Space Manoeuvre execution at 4.4 AU. Figure 6-59 and Figure 6-60 show the entry-exit in the visibility interval during the day, and Figure 6-61 the visibility duration of the two stations along this phase.

Phase from Deep Space Manoeuvre to Churyumov-Gerasimenko

This arc has been considered from the Deep Space Manoeuvre up to the rendezvous manoeuvre with 67P/Churyumov-Gerasimenko. Figure 6-62 and Figure 6-63 show the entry-exit in the visibility interval during the day, and Figure 6-64 the visibility duration of the two stations along this phase.

Phase Churyumov-Gerasimenko to Perihelion

This arc has been considered from rendezvous manoeuvre with 67P/Churyumov-Gerasimenko up to perihelion. During this arc the spacecraft orbits the comet and moves along the trajectory of the comet around the Sun. Figure 6-65 and Figure 6-66 show the entry-exit in the visibility interval during the day, and Figure 6-67 the visibility duration of the two stations along this phase.

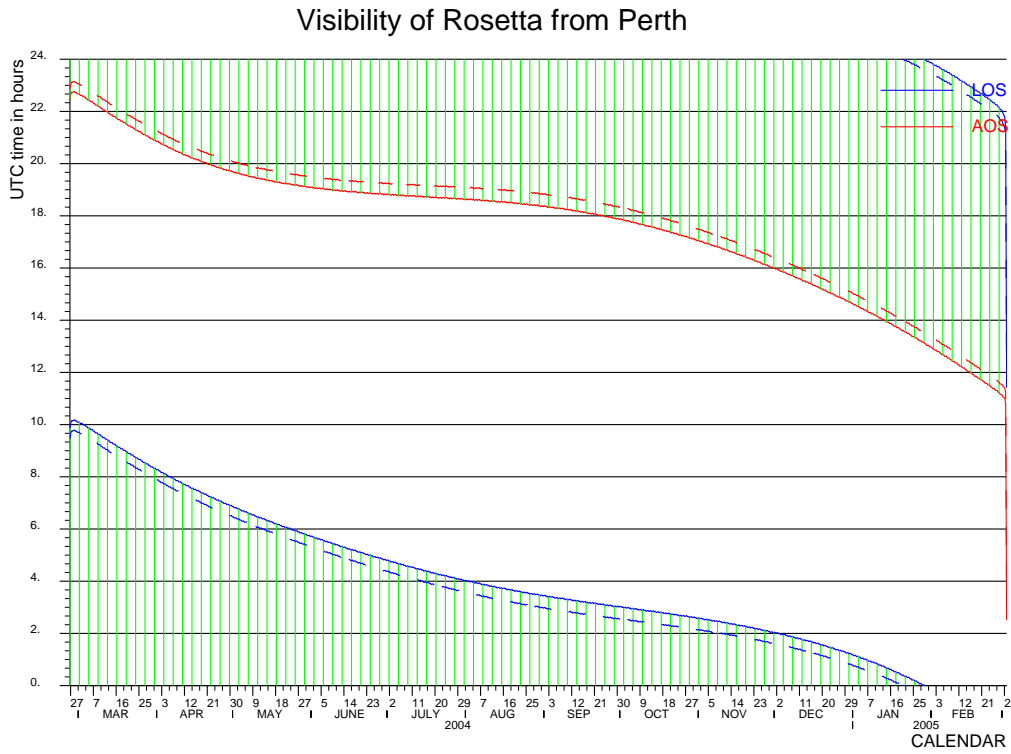


Figure 6-47: Phase from Launch to Earth. Beginning and End of Visibility Interval from New Norcia during the Day versus Calendar Date.

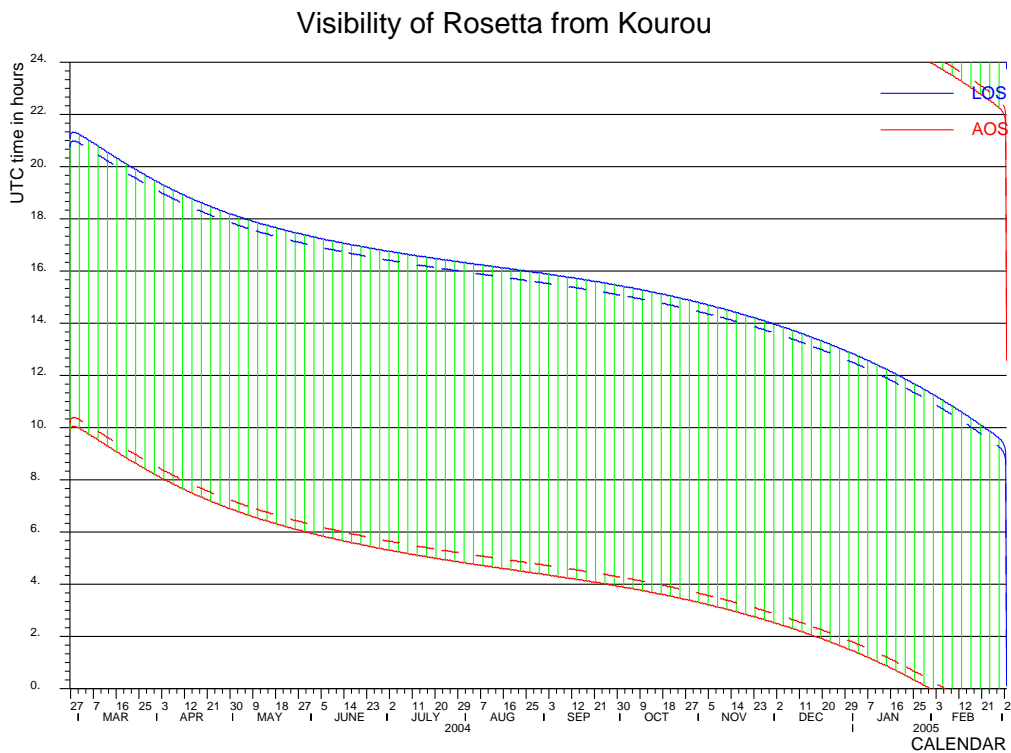


Figure 6-48: Phase from Launch to Earth. Beginning and End of Visibility Interval from Kourou during the Day versus Calendar Date.

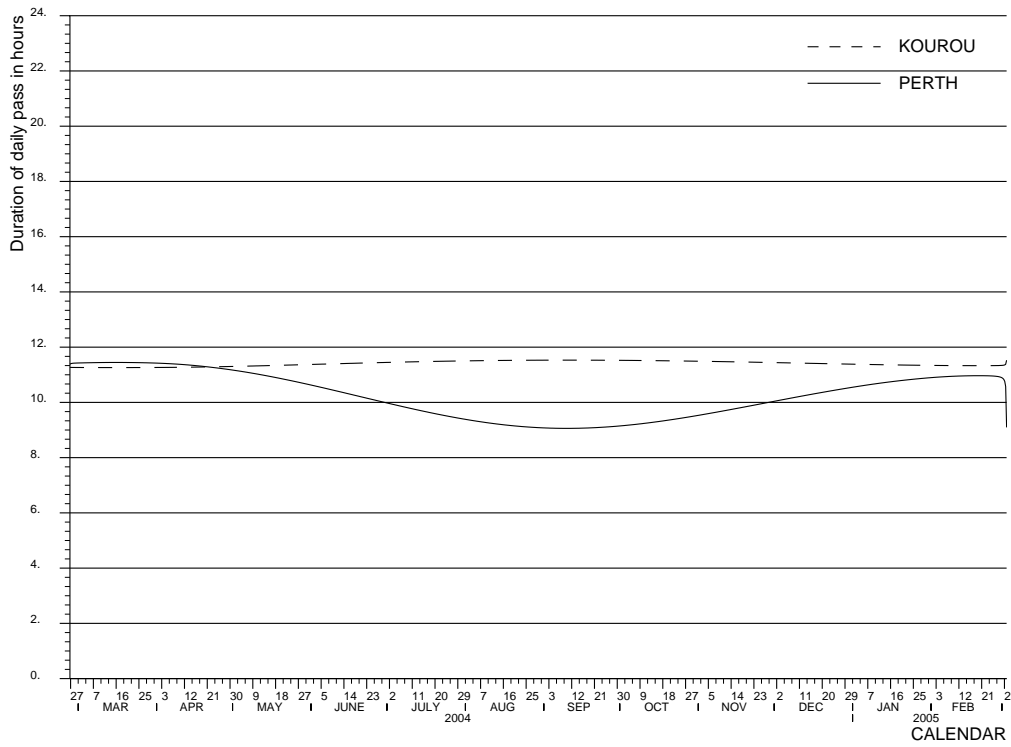


Figure 6-49: Phase from Launch to Earth. Visibility Duration for the two Ground Stations versus Calendar Date.

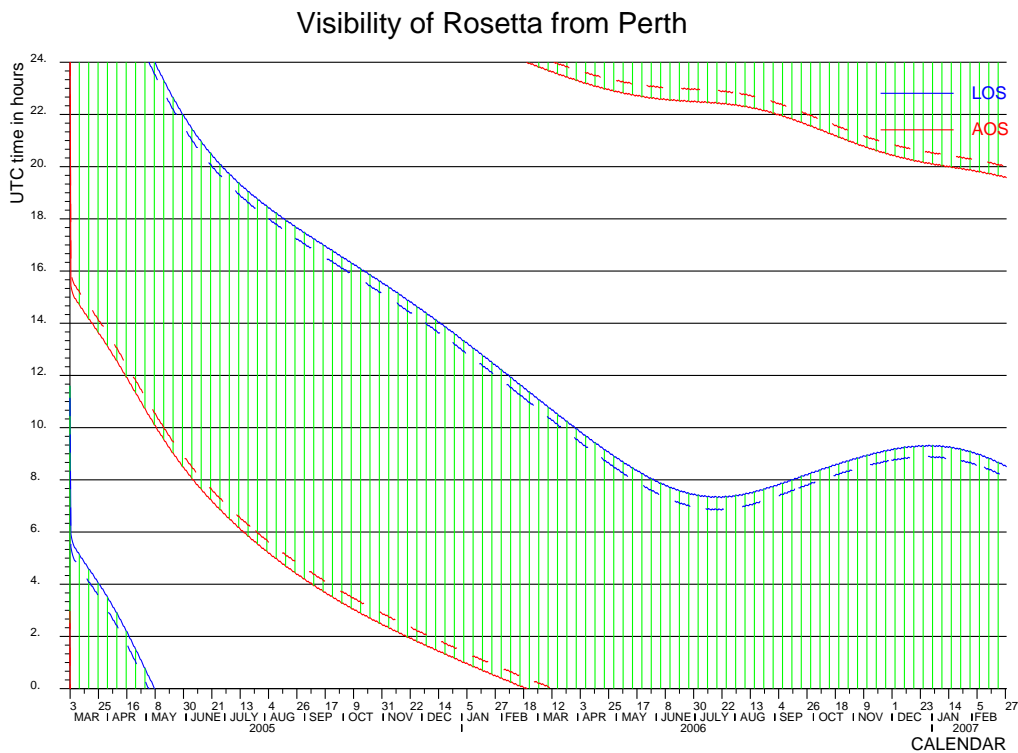


Figure 6-50: Phase from Earth to Mars. Beginning and End of Visibility Interval from New Norcia during the Day versus Calendar Date.

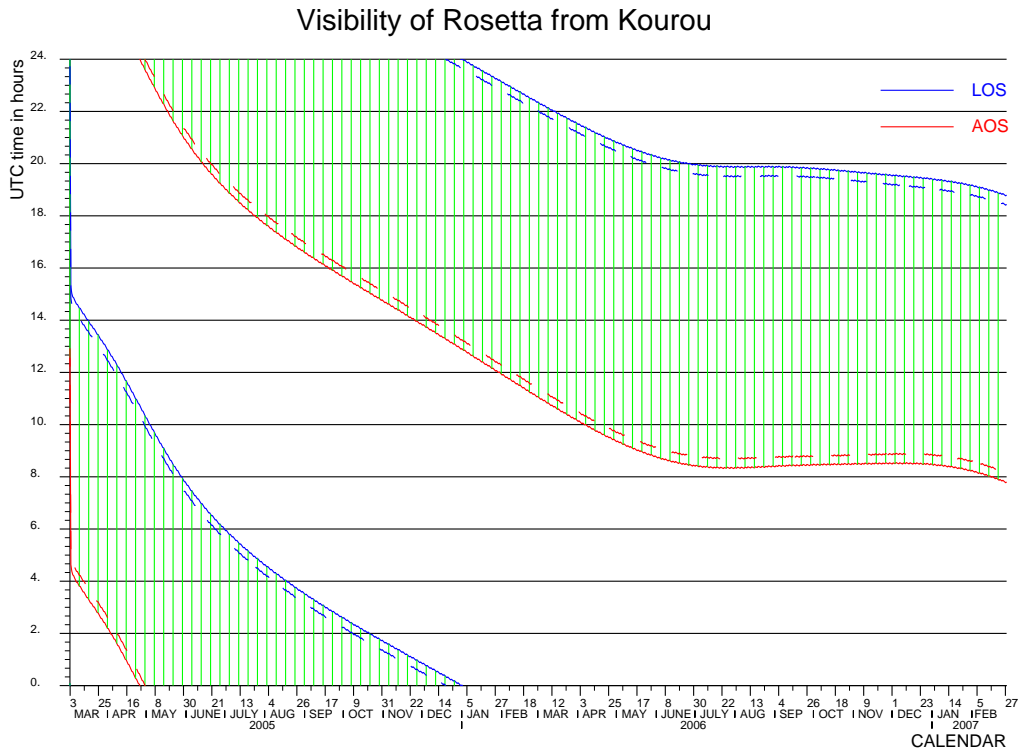


Figure 6-51: Phase from Earth to Mars. Beginning and End of Visibility Interval from Kourou during the Day versus Calendar Date.

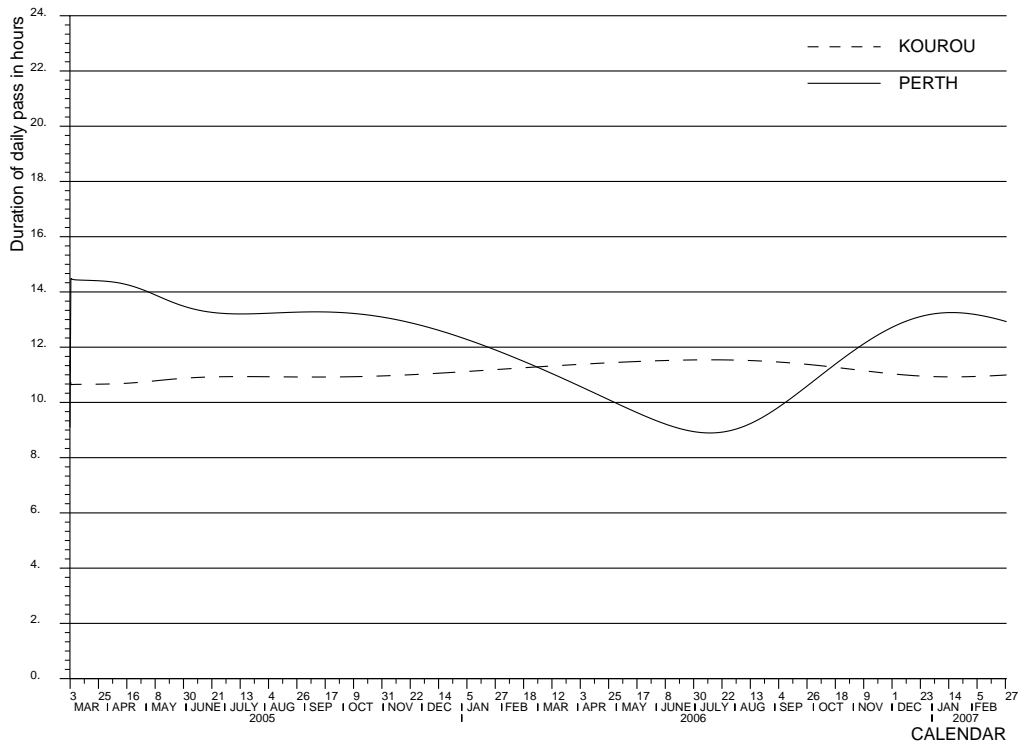


Figure 6-52: Phase from Earth to Mars. Visibility Duration for the two Ground Stations versus Calendar Date.

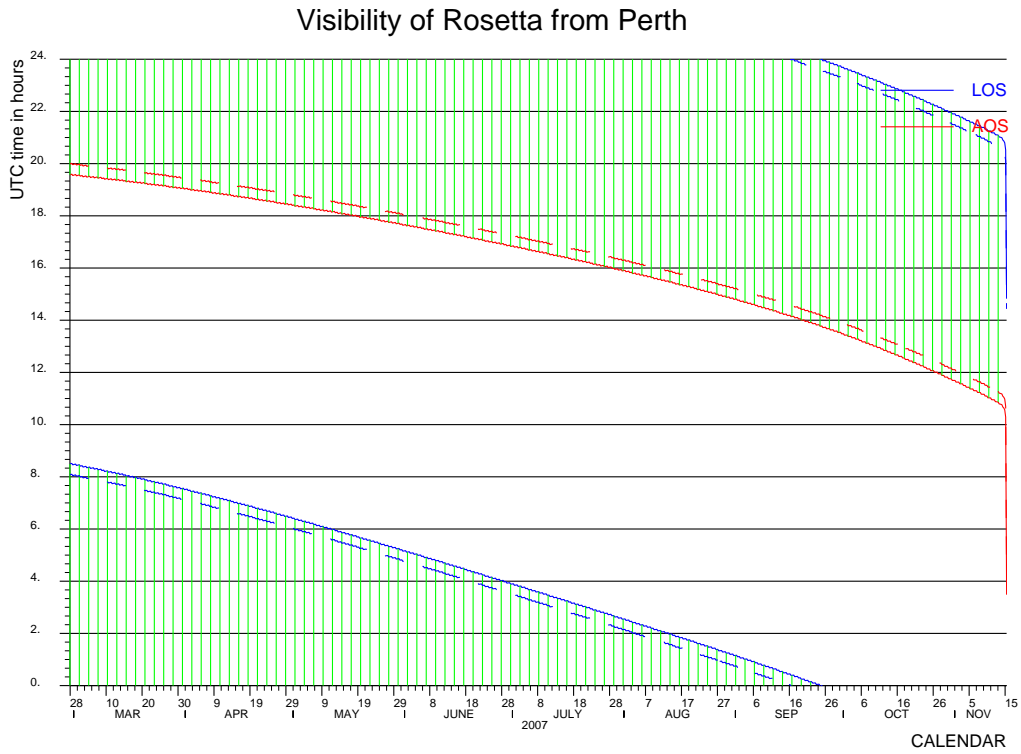


Figure 6-53: Phase from Mars to Earth. Beginning and End of Visibility Interval from New Norcia during the Day versus Calendar Date.

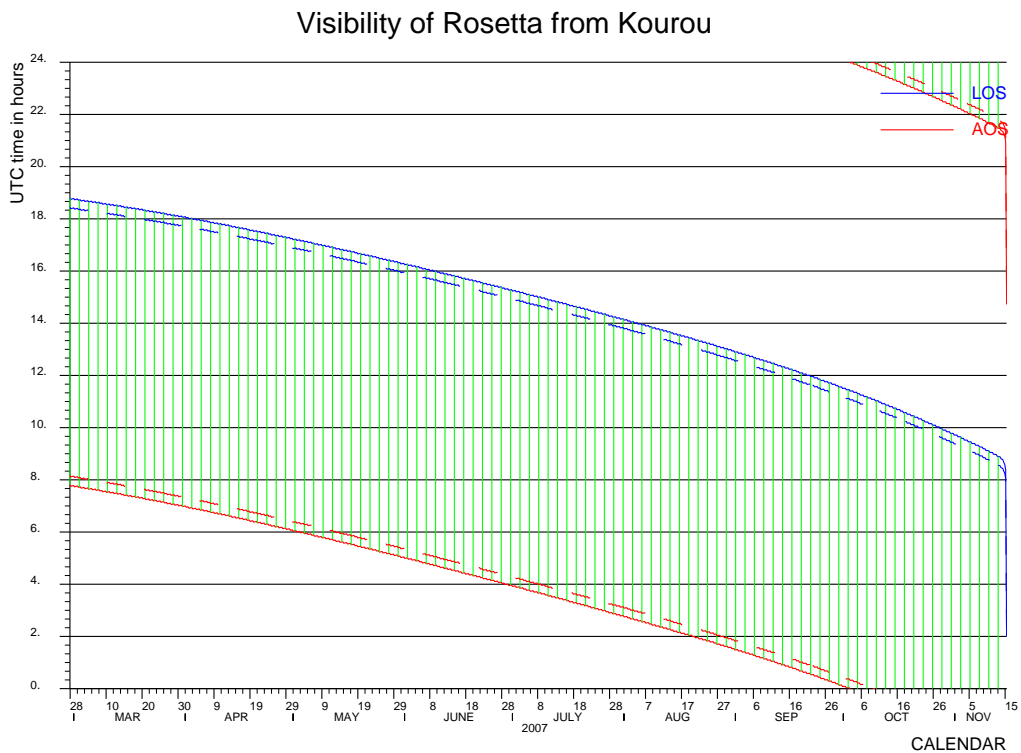


Figure 6-54: Phase from Mars to Earth. Beginning and End of Visibility Interval from Kourou during the Day versus Calendar Date.

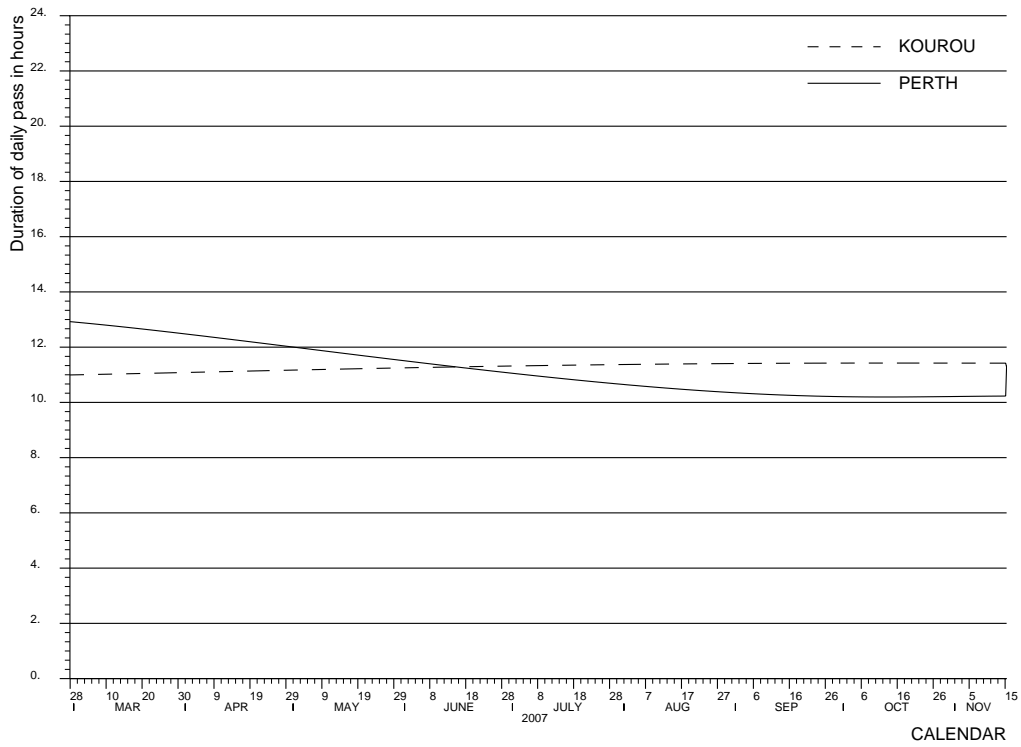


Figure 6-55: Phase from Mars to Earth. Visibility Duration for the two Ground Stations versus Calendar Date.

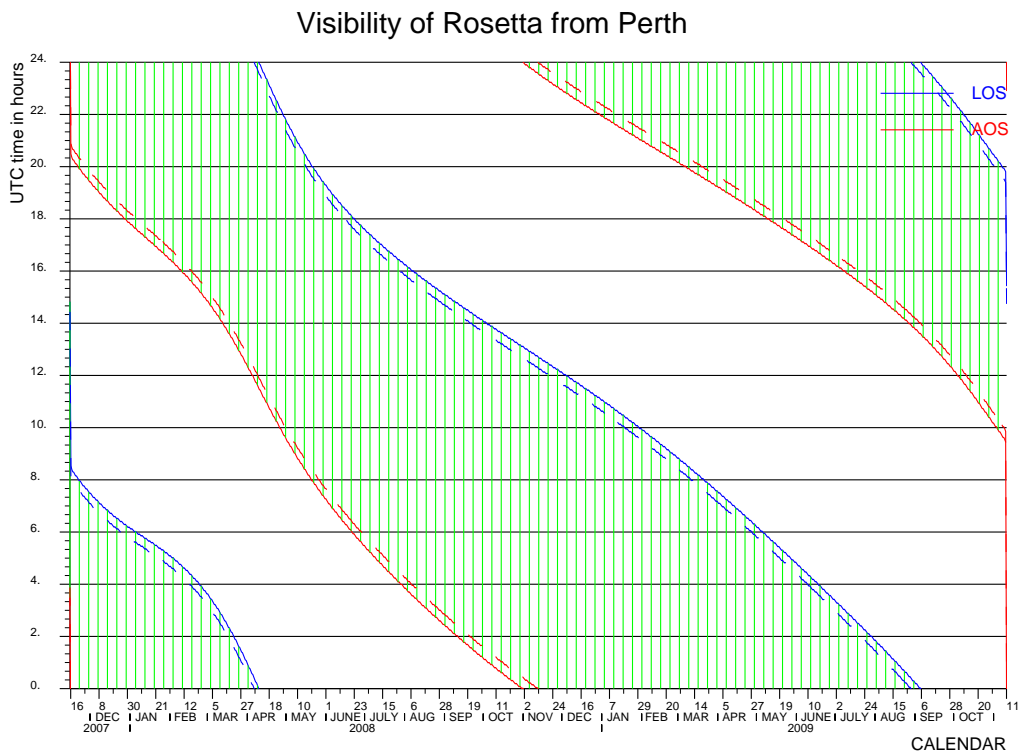


Figure 6-56: Phase from Earth to Earth. Beginning and End of Visibility Interval from New Norcia during the Day versus Calendar Date.

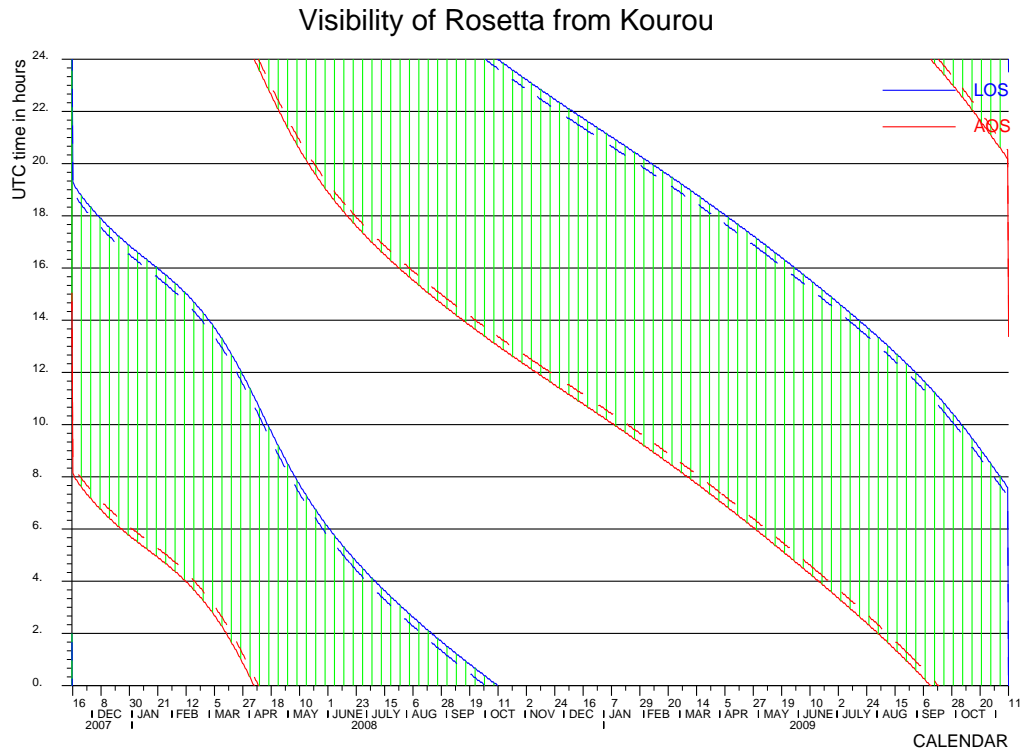


Figure 6-57: Phase from Earth to Earth. Beginning and End of Visibility Interval from Kourou during the Day versus Calendar Date.

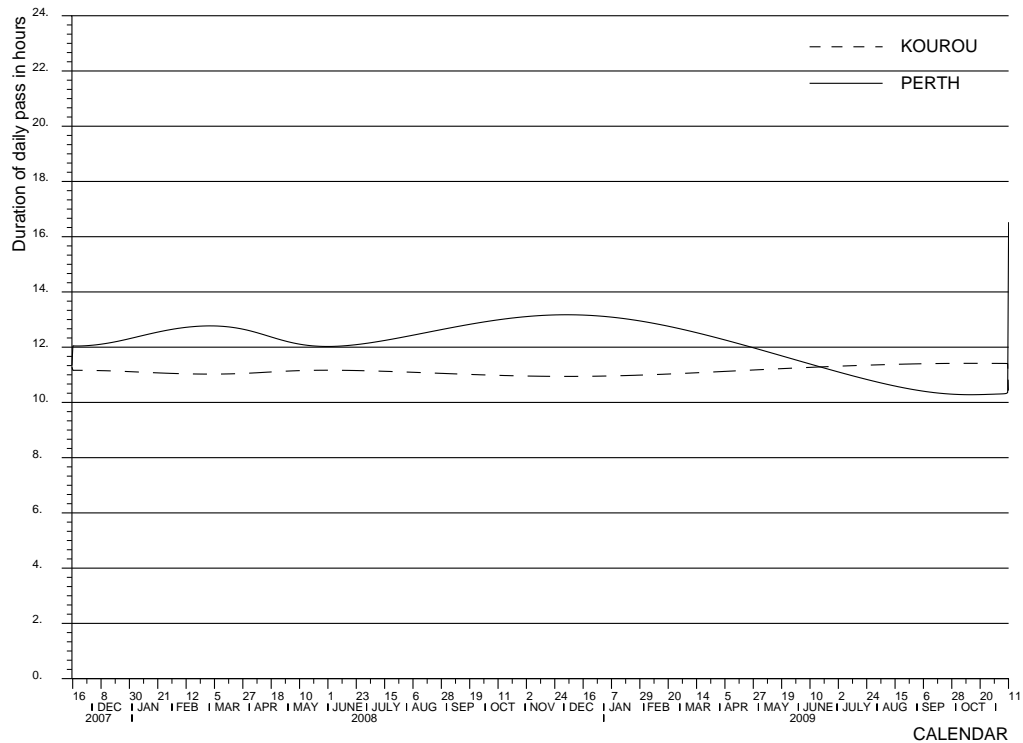


Figure 6-58: Phase from Earth to Earth. Visibility Duration for the two Ground Stations versus Calendar Date.

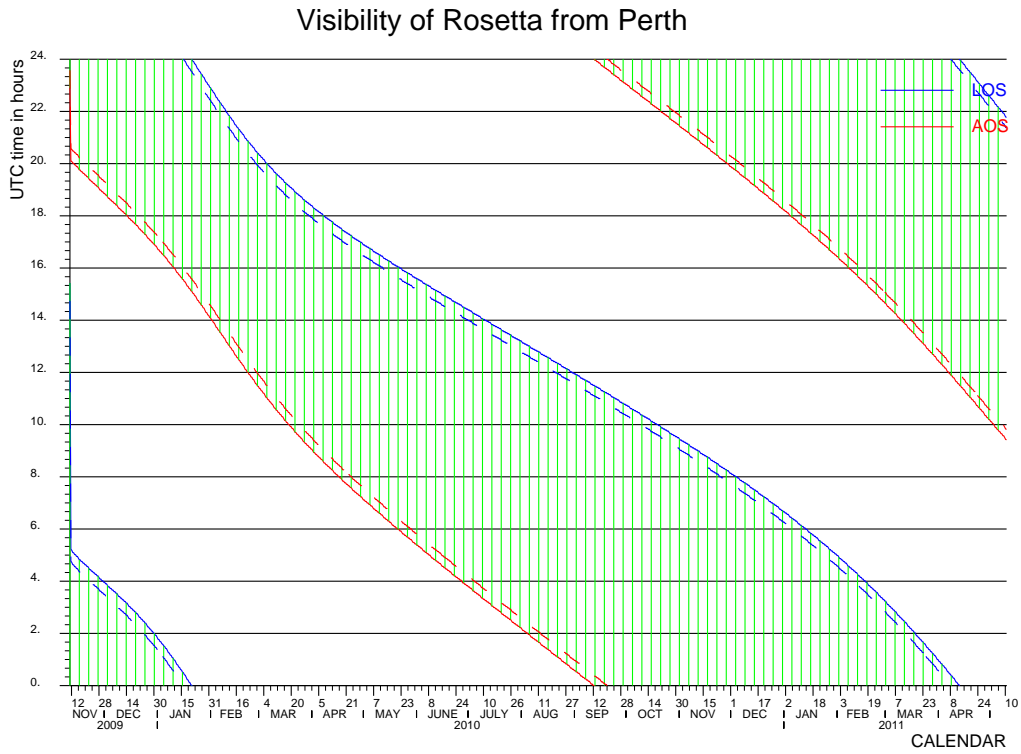


Figure 6-59: Phase from Earth to DSM 4. Beginning and End of Visibility Interval from New Norcia during the Day versus Calendar Date.

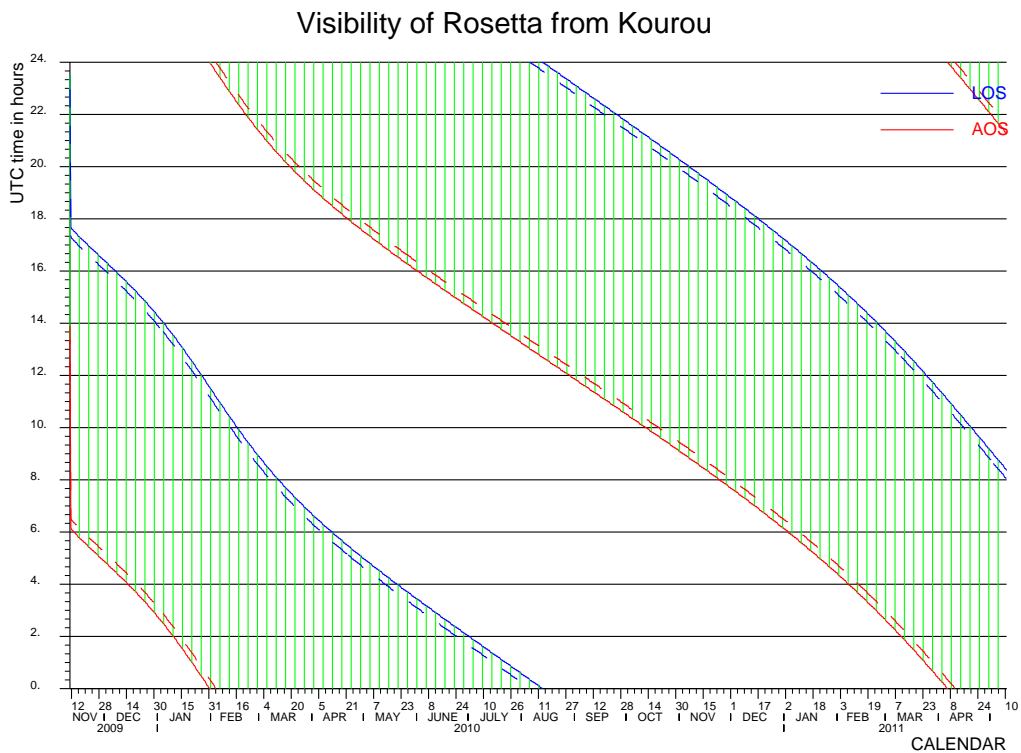


Figure 6-60: Phase from Earth to DSM 4. Beginning and End of Visibility Interval from Kourou during the Day versus Calendar Date.

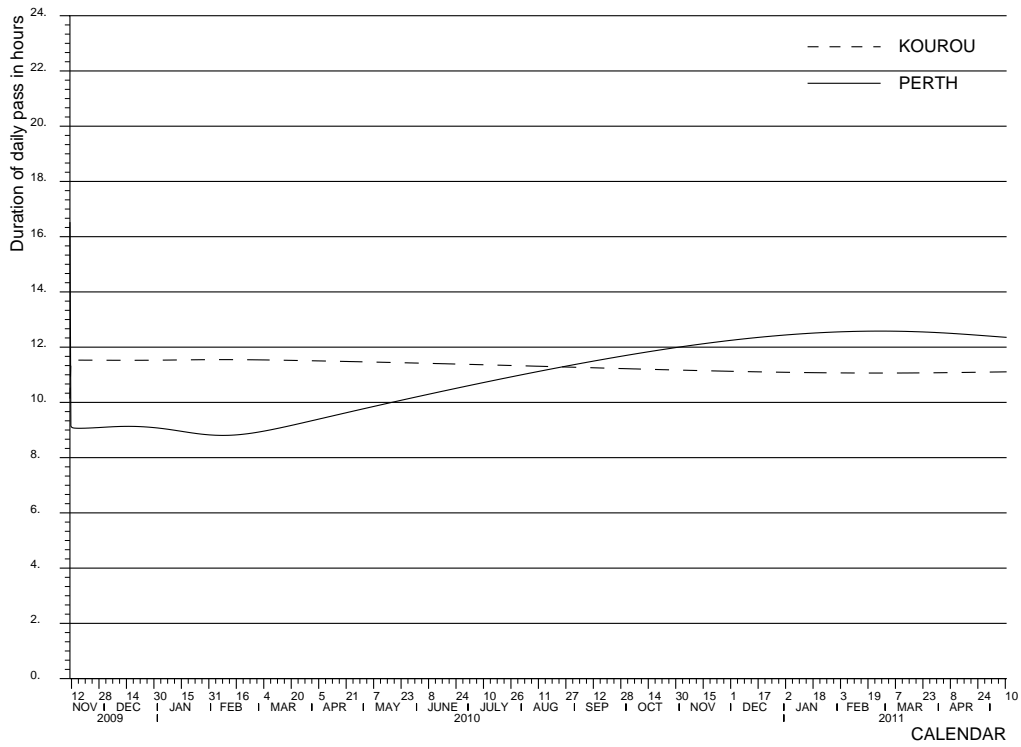


Figure 6-61: Phase from Earth to DSM 4. Visibility Duration for the two Ground Stations versus Calendar Date.

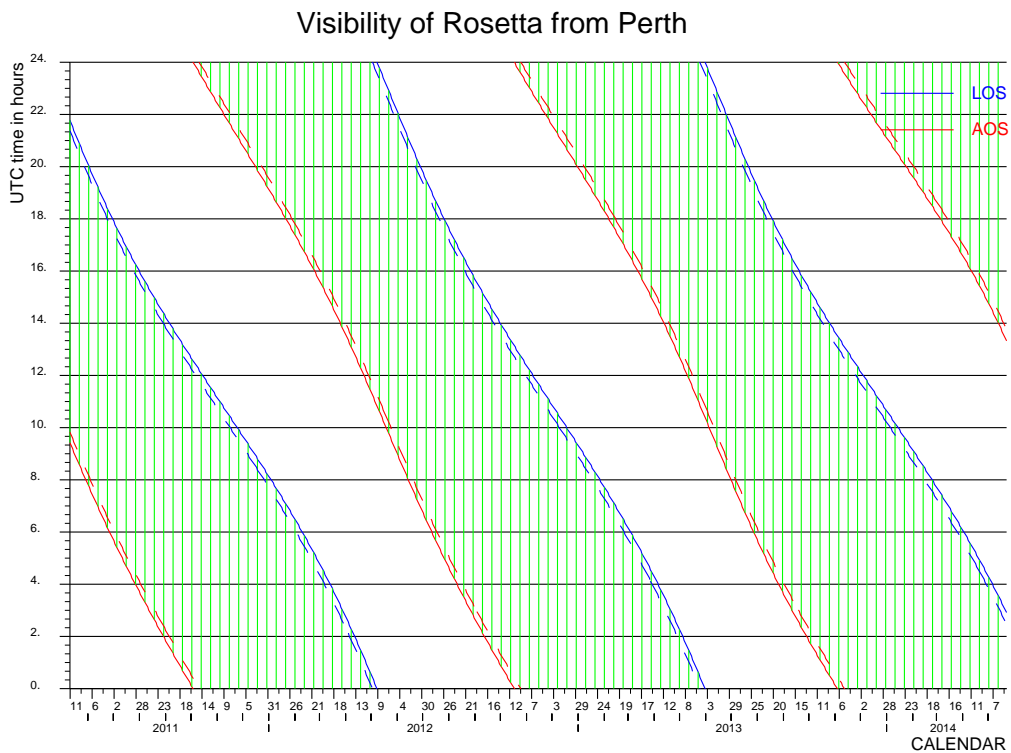


Figure 6-62: Phase from DSM 4 to 67P/C-G. Beginning and End of Visibility Interval from New Norcia during the Day versus Calendar Date.

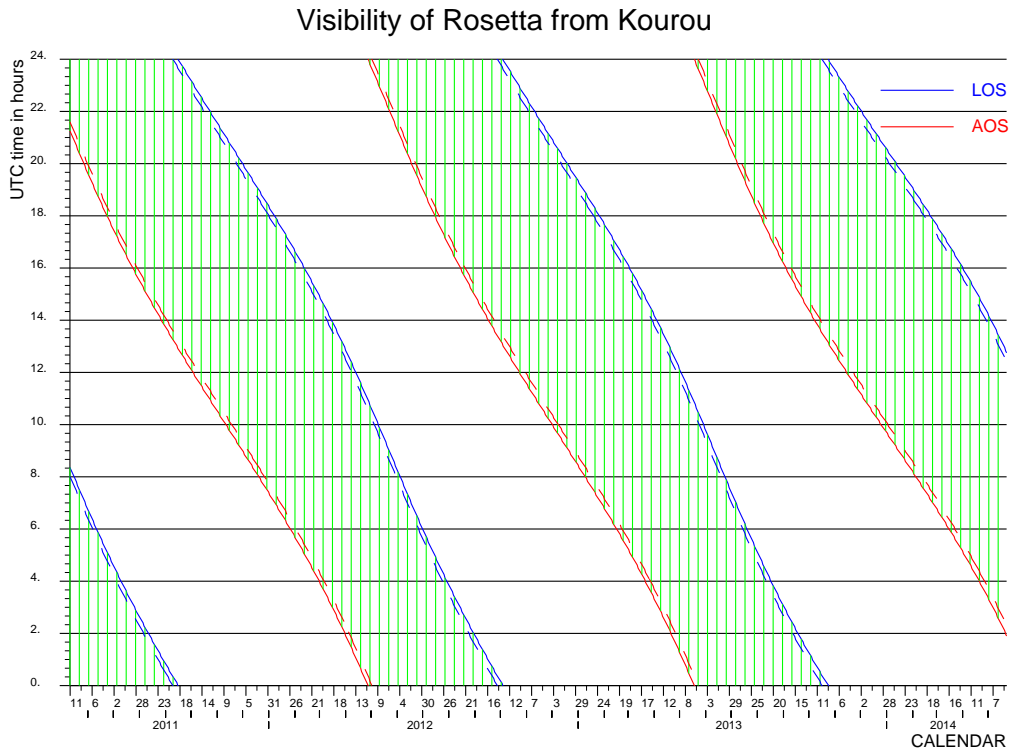


Figure 6-63: Phase from DSM 4 to 67P/C-G. Beginning and End of Visibility Interval from Kourou during the Day versus Calendar Date.

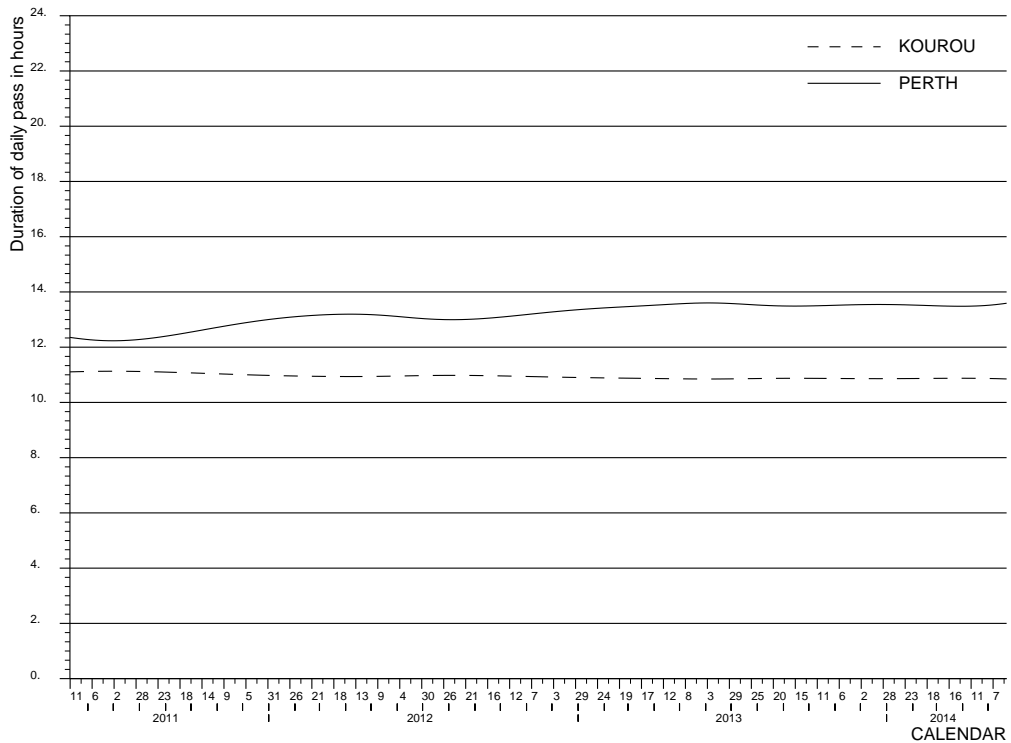


Figure 6-64: Phase from DSM 4 to 67P/C-G. Visibility Duration for the two Ground Stations versus Calendar Date.

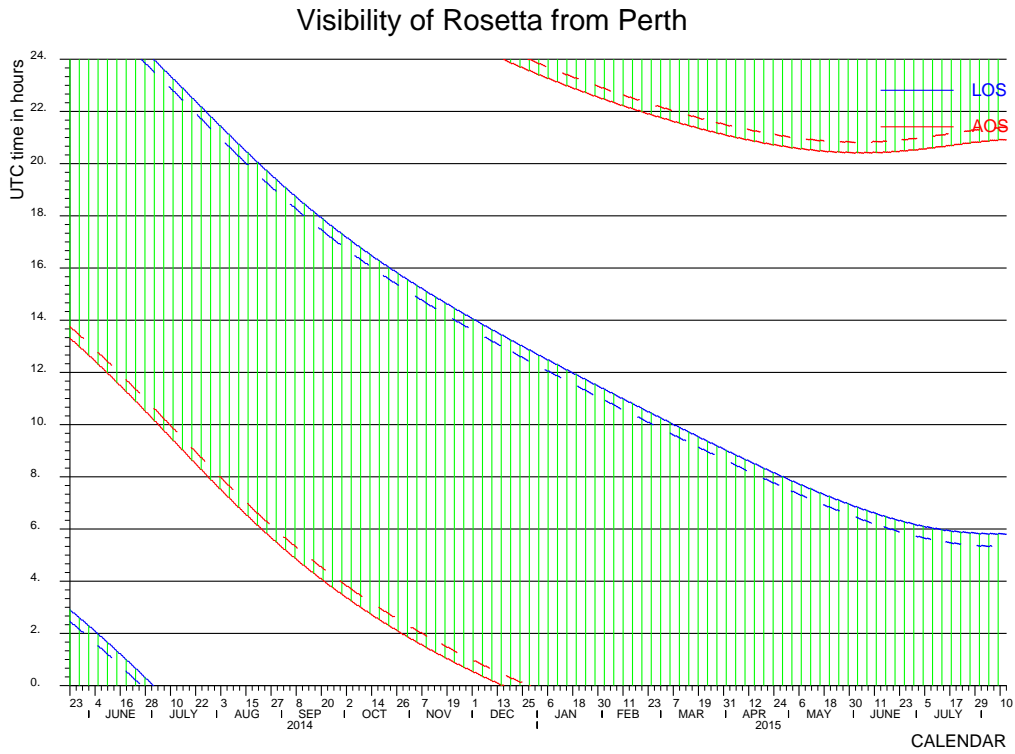


Figure 6-65: Phase 67P/C-G to Perihelion. Beginning and End of Visibility Interval from New Norcia during the Day versus Calendar Date.

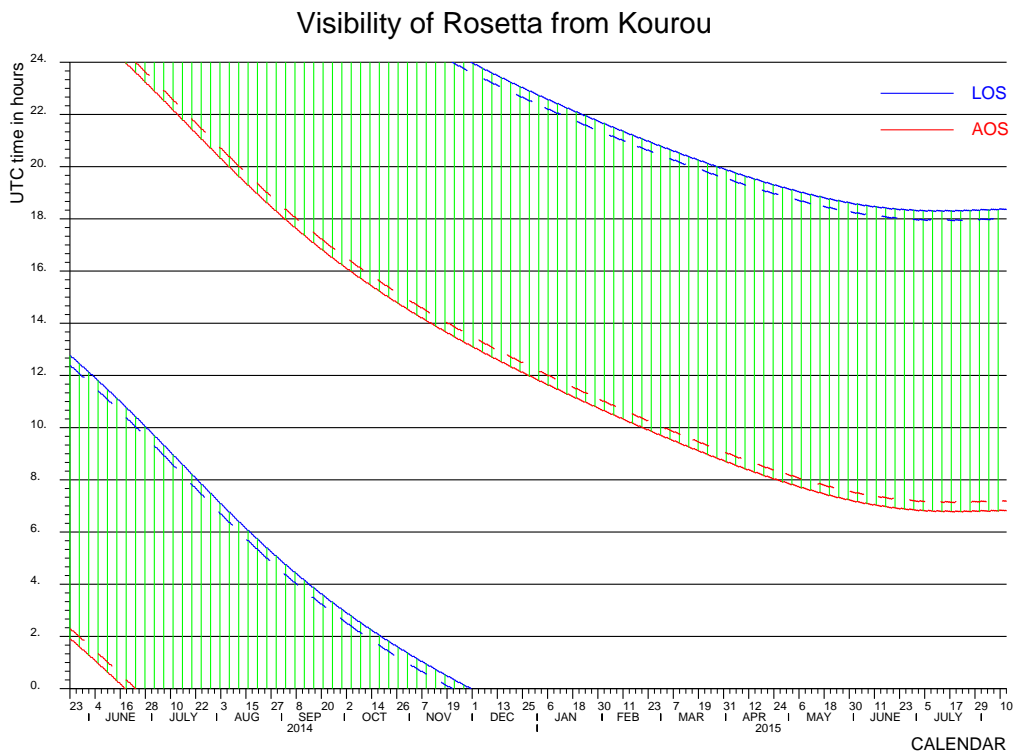


Figure 6-66: Phase 67P/C-G to Perihelion. Beginning and End of Visibility Interval from Kourou during the Day versus Calendar Date.

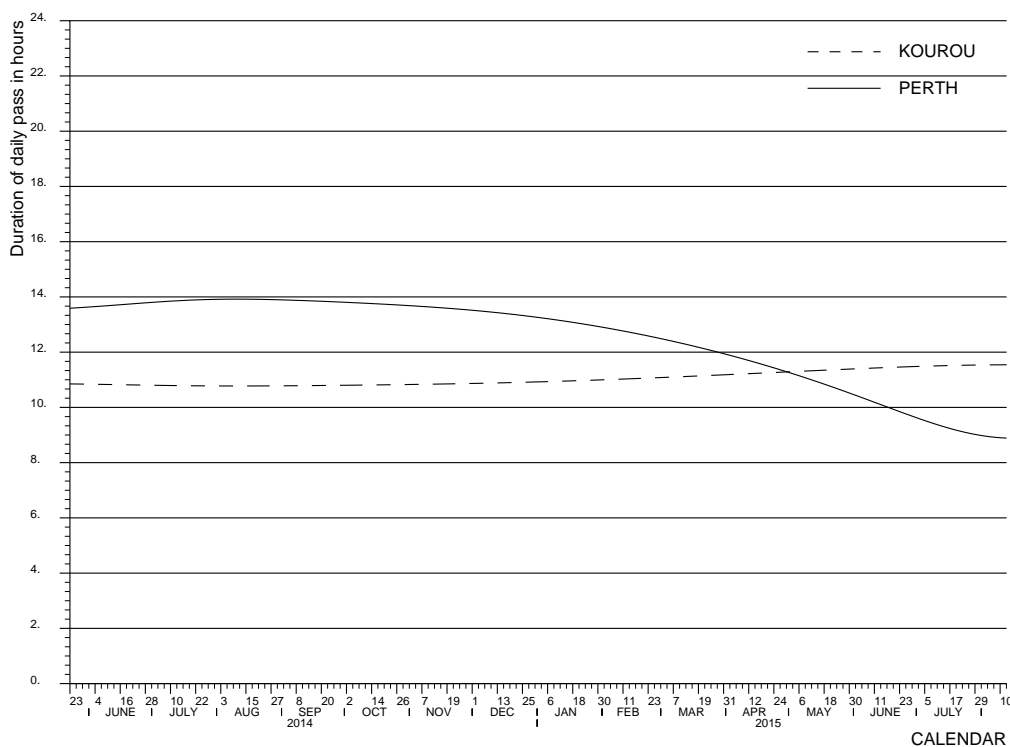


Figure 6-67: Phase 67P/C-G to Perihelion. Visibility Duration for the two Ground Stations versus Calendar Date.

Ground Station Coverage Summary and Visibility from Cebreros

Figure 6-68 and Figure 6-69 provide a complete overview of the visibility of Rosetta from New Norcia and Kourou respectively. The entry and exit events of the visibility for each daily pass are plotted for minimum elevations of 5 and 10 degrees.

The new ESA deep space ground station of Cebreros (Avila, Spain), which is planned to become operational in September 2005, could help as back-up to the current ground stations in New Norcia and Kourou. The daily entry and exit of the visibility from Cebreros for the duration of the mission from launch to rendezvous with the comet are presented in Figure 6-70.

Figure 6-71 and Figure 6-72 show a comparison of the duration of the daily visibility pass from New Norcia and Kourou and from New Norcia and Cebreros, respectively. The duration of the pass from Cebreros suffers more changes due to the big latitude, while the duration of the pass from Kourou is more constant.

Finally, Table 6-3 presents the duration of the minimum and maximum gaps and overlaps of the daily passes of the two ground station couples: New Norcia and Kourou, and New Norcia and Cebreros. The different arcs of the trajectory have been considered in order to give an idea of the possible variation of these magnitudes during the mission.

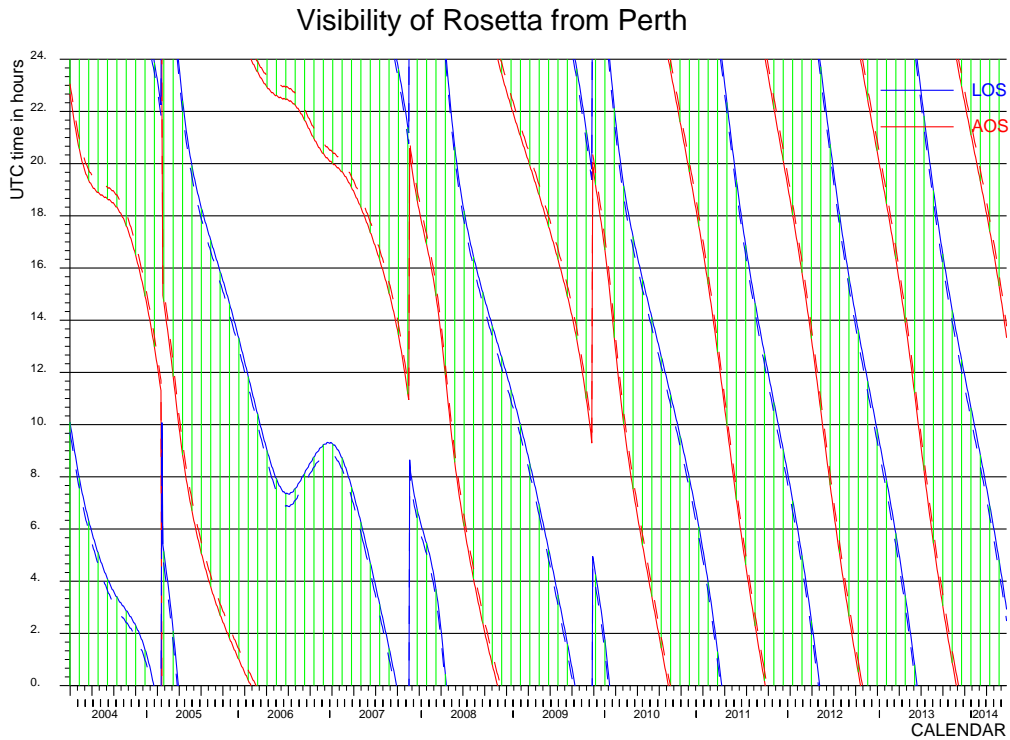


Figure 6-68: Phase Launch to Perihelion. Beginning and End of Visibility Interval from New Norcia during the Day versus Calendar Date.

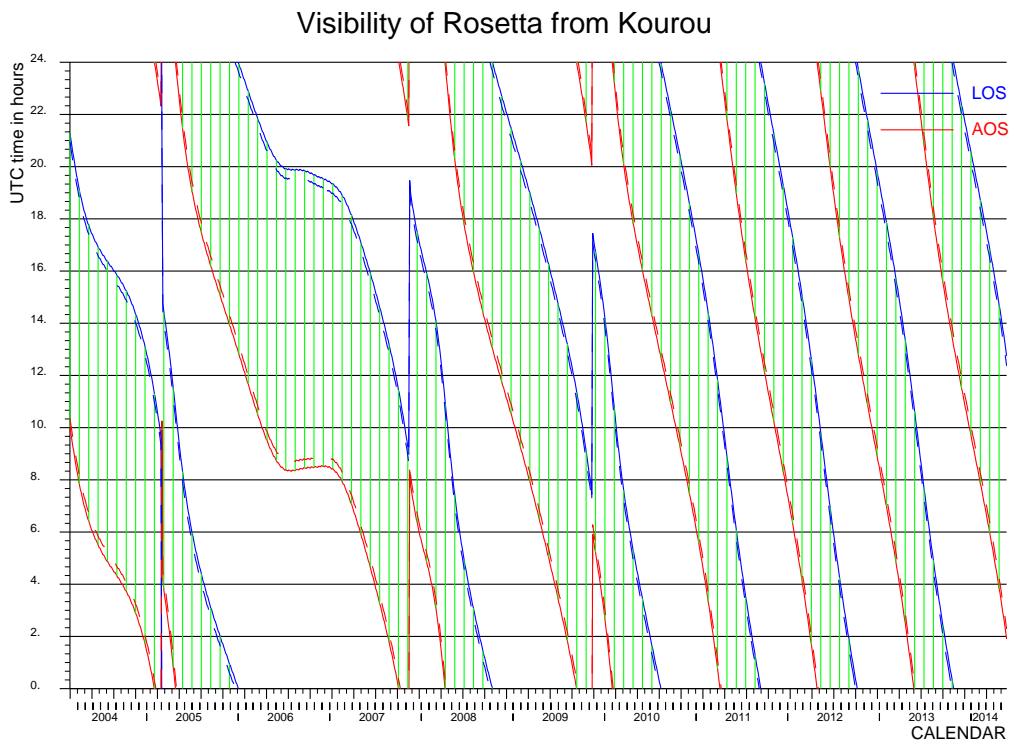


Figure 6-69: Phase Launch to Perihelion. Beginning and End of Visibility Interval from Kourou during the Day versus Calendar Date.

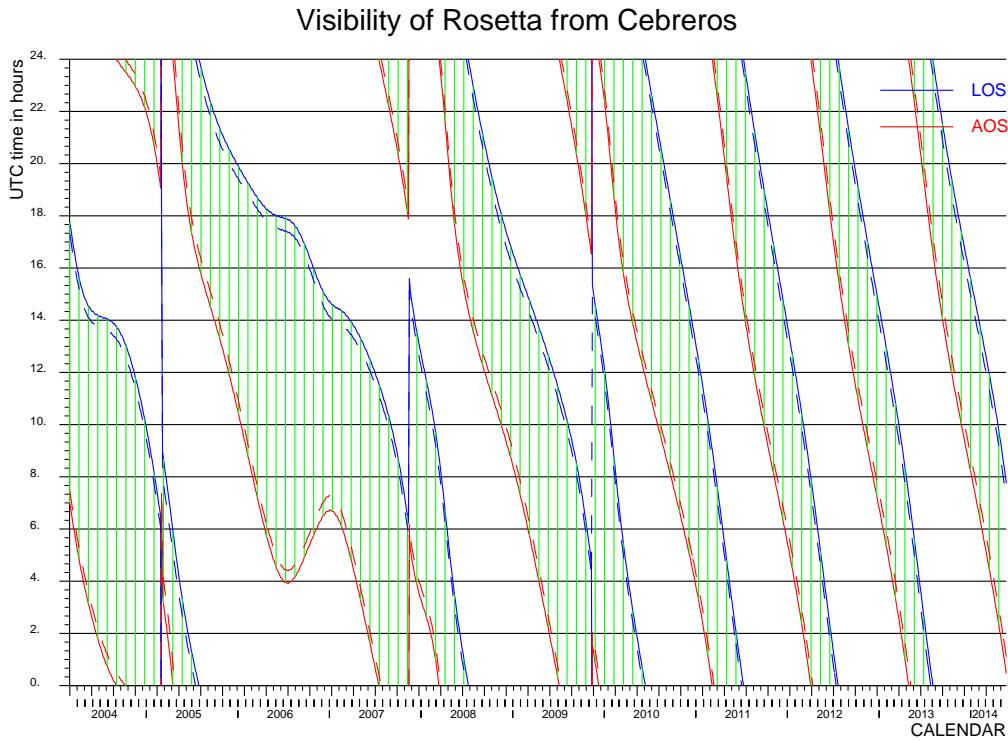


Figure 6-70: Phase Launch to Perihelion. Beginning and End of Visibility Interval from Cebreros during the Day versus Calendar Date.

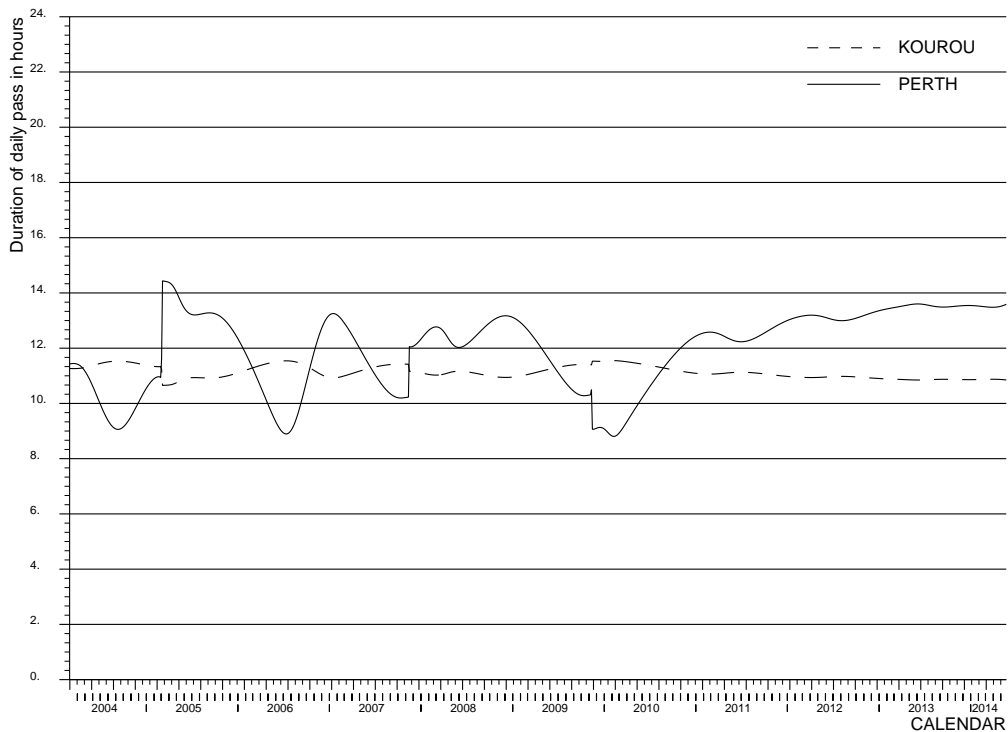


Figure 6-71: Phase Launch to Perihelion. Visibility Duration from New Norcia and Kourou versus Calendar Date.

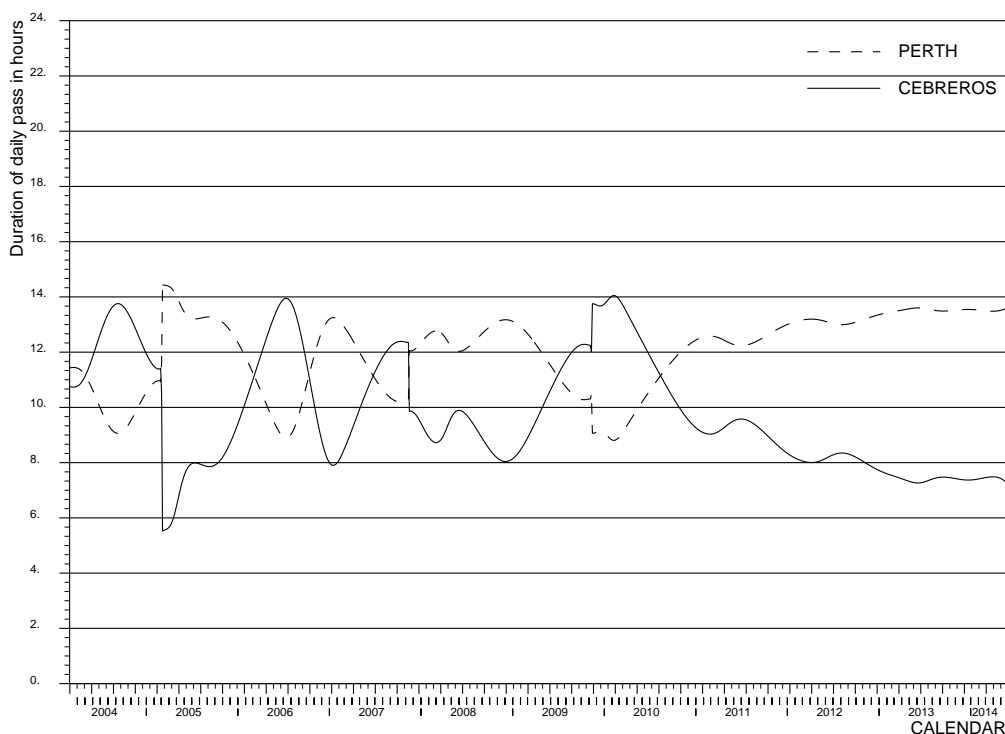


Figure 6-72: Phase Launch to Perihelion. Visibility Duration from New Norcia and Cebberos versus Calendar Date.

	ARC	MIN GAP (h)	MAX GAP (h)	MIN OVERLAP (h)	MAX OVERLAP (h)
NEW NORCIA & CEBREROS	LAUNCH-EAR1	5.47	5.76	2.20	2.48
	EAR1-MARS	5.48	7.51	0.42	2.48
	MARS-EAR2	5.51	6.26	1.70	2.45
	EAR2-EAR3	5.51	6.40	1.56	2.44
	EAR3-DSM4	5.54	6.18	1.91	2.56
	DSM4-RDV	5.91	6.66	1.29	2.04
	RDV-PERIH.	5.47	6.91	1.05	2.48
NEW NORCIA & KOUROU	LAUNCH-EAR1	2.74	5.06	0	0
	EAR1-MARS	1.08	5.25	0	0.44
	MARS-EAR2	1.63	3.89	0	0
	EAR2-EAR3	1.47	3.80	0	0.06
	EAR3-DSM4	1.87	5.35	0	0
	DSM4-RDV	1.33	2.12	0	0.19
	RDV-PERIH.	1.24	5.25	0	0.29

Table 6-3: Duration of visibility gaps and overlaps (Min. elevation: 10 deg)

6.1.4 Early Orbit Determination and First Correction Manoeuvre

First Kourou Pass

The elevation of Rosetta from Kourou at separation reaches 90 degrees after the separation. During this close to Zenith pass, the achievement of the communications link with the spacecraft can be problematic.

Furthermore, another problem at the start of the first Kourou pass comes from the launch vehicle injection dispersion errors. Figure 6-73 presents the evolution of the pointing dispersions after spacecraft separation projected onto the plane-of-sky, which is normal to the line of sight of the spacecraft from Kourou. The $3\text{-}\sigma$ semi-major axis of the error ellipse has a maximum value of more than 5 degrees. Figure 6-74 presents the $3\text{-}\sigma$ range rate errors caused by the launch vehicle injection dispersion. The uncertainty in the Doppler frequency shift is also big for the beginning of the pass.

Considering the previous points, the establishment of AOS from Kourou should be delayed for about 10 minutes after the separation.

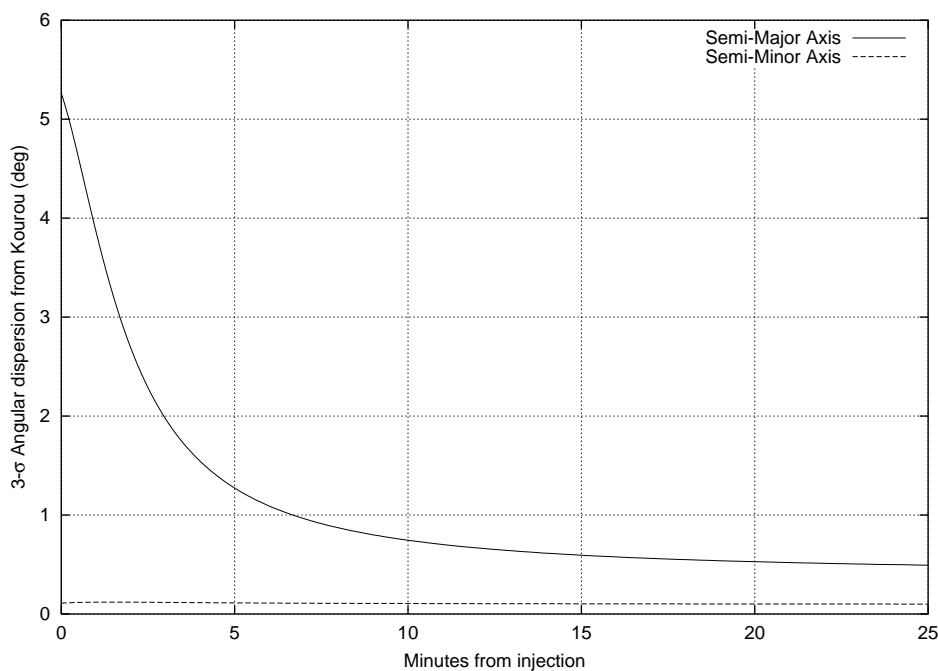


Figure 6-73: Evolution with time of pointing dispersion from Kourou at first pass.

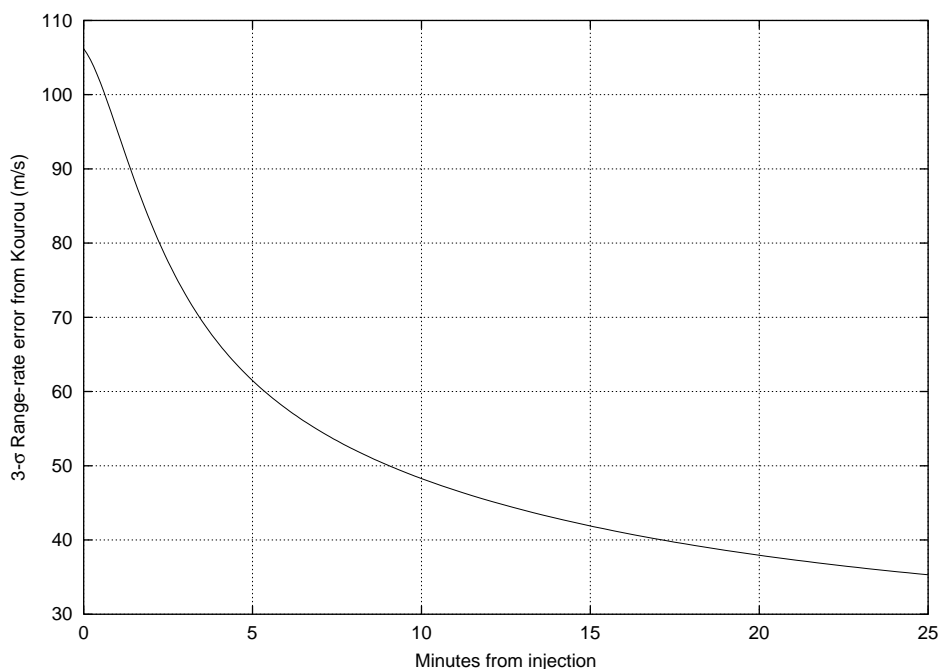


Figure 6-74: Evolution with time of range-rate dispersion relative to Kourou at first pass.

Early Orbit Determination

Once injected into its escape trajectory, Rosetta departs from the Earth rather quickly, and in only 7 days is at a distance of about 2 millions of km from the Earth, Figure 6-75 and Figure 6-76. During the nominal launch window from 26/02/2004 to 17/03/2004, the Moon is far away and to the opposite direction to the departure hyperbola. There are no effects to the trajectory or the orbit determination caused by the Moon. However, for a possible extension of the launch window duration, the departure trajectory will pass near the Moon and be affected by its gravity attraction for periods of few days.

The orbit injection errors at the spacecraft separation from Ariane 5 for the case with coast phase are much larger than for a direct injection. The Ariane 5 dispersion matrix in Table 5-3 is transformed to errors in the position and velocity in an intrinsic reference. This reference is formed by the Radial direction, the Cross-Track direction is perpendicular to the orbit plane and the Along-Track direction completes the tri-orthogonal frame following the direction of the velocity vector. The 1-σ injection errors are:

	Position (km)	Velocity (m/s)
Along Track	38	5.1
Cross Track	1	5.4
Radial	7	35.4

Table 6-4: Ariane 5 Injection Accuracy for Rosetta Escape Mission with Coast Arc

XY PLOT. MEAN EARTH EQUATOR OF DATE
EPOCH: 2004: 2:26 ; 9:10:15.10

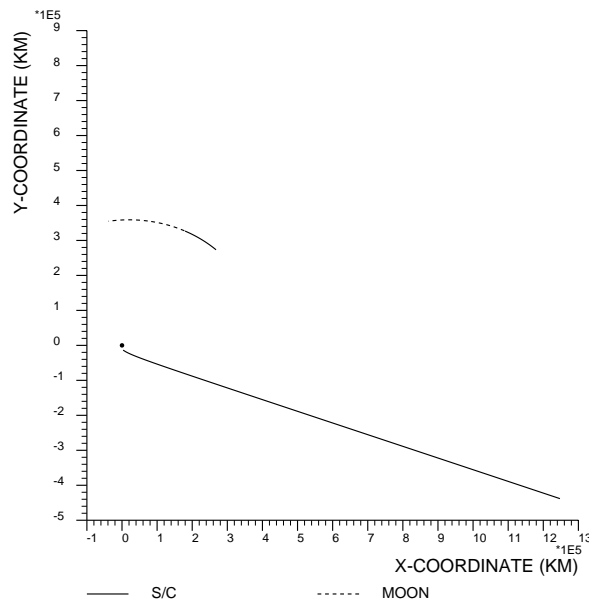


Figure 6-75: Early Orbit Trajectory. Equatorial projection.

DISTANCE PLOT
EPOCH: 2004: 2:26 ; 9:10:15.10

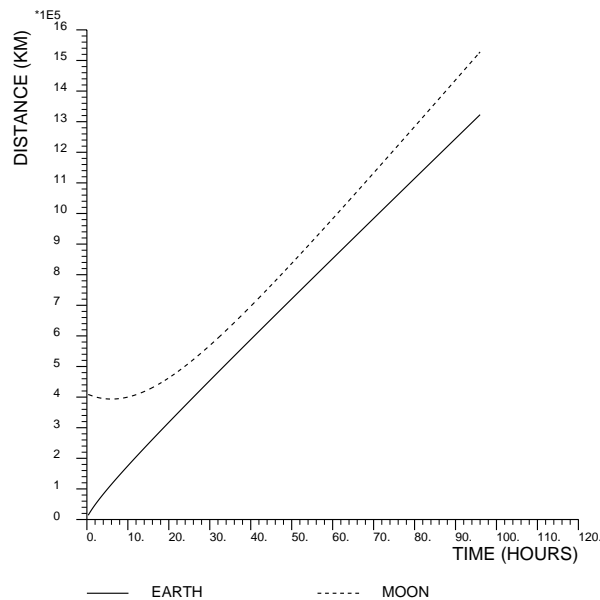


Figure 6-76: Early Orbit Trajectory. Distance to Earth and Moon.

For the analysis of the early orbit determination, it is assumed that New Norcia and Kourou are intensively dedicated to tracking the spacecraft for a period of a few weeks after launch. Both stations perform range, and range rate measurements.

In the first 0.5 days the relative velocity with respect to Kourou, decreases from 8.3 km/s to 4.5 km/s and this part of the trajectory is in full visibility from Kourou ground station, Figure 6-77. Thereafter, New Norcia and Kourou alternate in their period of visibility, and between both stations an almost continuous coverage of the spacecraft is obtained.

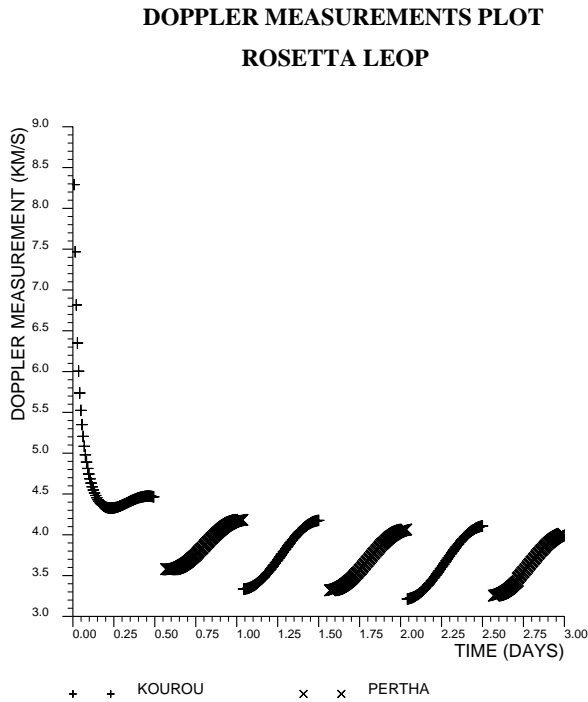


Figure 6-77: Early Orbit Trajectory. Range Rate Measurements from Kourou and New Norcia

A range measurement is supposed to be taken every hour with typical 1- σ errors of 10 m as random noise, and 10 m as fixed bias. Range rate measurements will be obtained continuously and used in the orbit determination process as interpolated measurements every 10 to 30 minutes.

After the first day, the position of the spacecraft is estimated with an error of about 1 km. Thereafter, the position error grows slightly with the distance to the Earth, Figure 6-78. 10 days after the injection the error is about 2 km (1- σ), with the bigger error in the orbital cross track direction. The velocity is estimated to less than 1 cm/s, Figure 6-79.

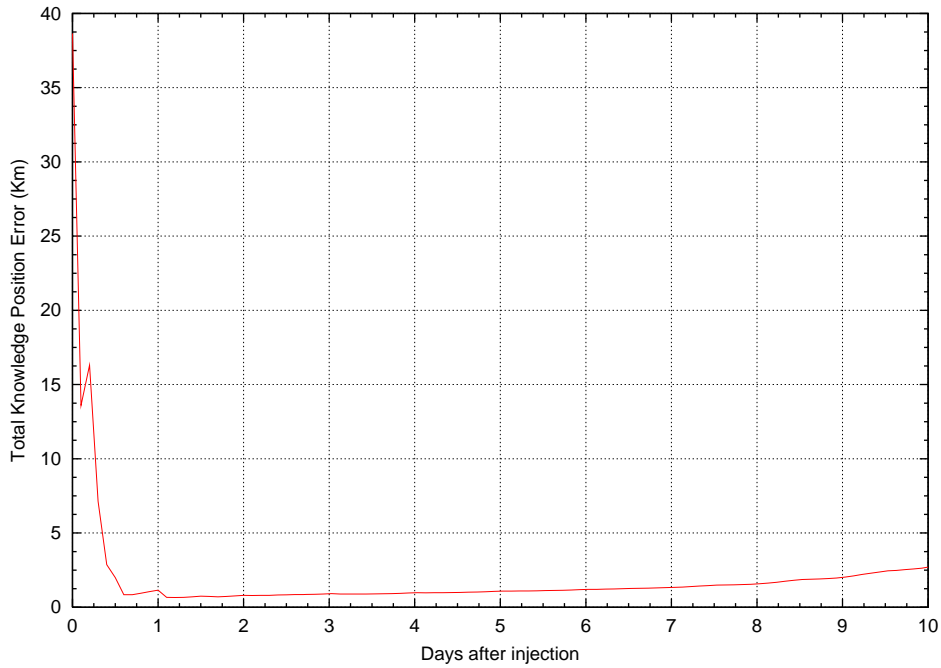


Figure 6-78: Early Orbit Trajectory. Orbit Determination Position Error

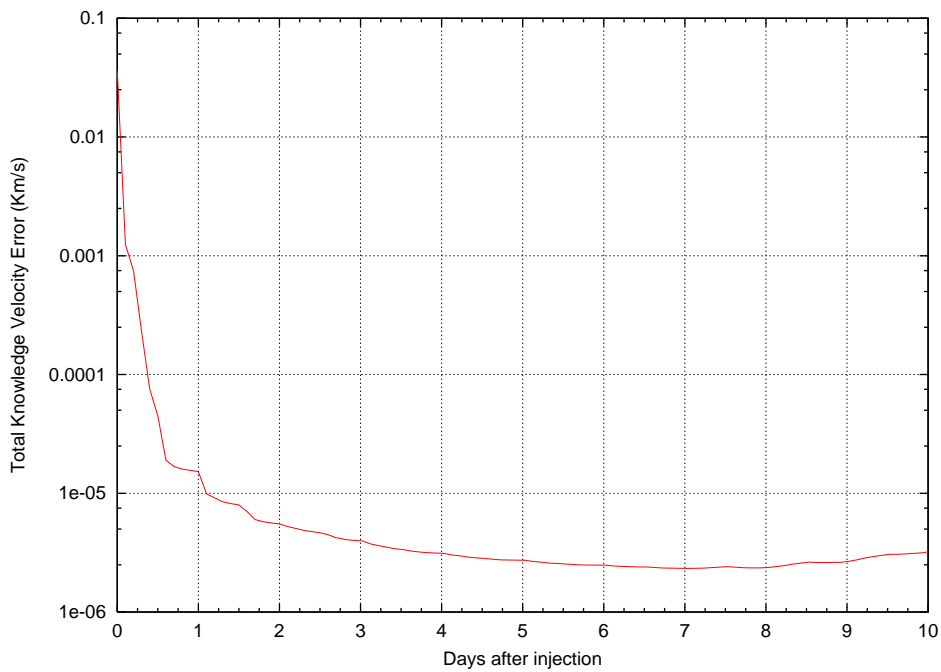


Figure 6-79: Early Orbit Trajectory. Velocity Error

First Correction Manoeuvre

A first correction manoeuvre has to be performed to correct the injection errors due to the dispersion on the ascent trajectory of Ariane 5. In a first step the position and velocity of the spacecraft must be determined to a good level during the early orbit phase. Considering a direct guidance strategy, the correction manoeuvre targets a given point of the nominal trajectory in order to maintain a trajectory very near the nominal. Subsequent small trim manoeuvres correct the arrival conditions at the next Earth pericentre passage to minimise the dispersion errors at the swing-by.

There are three possible target points for this manoeuvre: the DSM1.1 near perihelion, the DSM1.2 near aphelion and the pericentre of the Earth at the first swing-by. In the first case there are about only 90 days from injection to perihelion. The first correction must be implemented soon after launch, otherwise the required delta-V becomes very big as a great part of the time to reach the target has already elapsed. If the correction targets the pericentre of the Earth, then the delta-V required have a big variation with the launch date due to the different distributions of the delta-V among DSM1.1 and DSM1.2 for the whole launch window.

The first correction manoeuvre targeting the aphelion of the nominal trajectory presents several advantages. The delta-V required diminishes as the implementation day is delayed and it is stable when considering different launch days, in fact the statistical variation over the launch window is of only a few m/s. Table 6-5 presents the statistical analysis of the first correction manoeuvre implemented at different dates, based on the previous early orbit determination process and on a 10000 Monte Carlo analysis for the manoeuvre implementation errors. The injection dispersion errors considered are only the Along-Track, Cross-Track, and Radial position and velocity errors of the covariance matrix of the errors provided by Arianespace in ref. {Ref. RD 12}.

The sooner this manoeuvre is implemented, then the value of the delta-V required is bigger. However, the dispersion errors also become bigger and the following trajectory is far from the nominal one and the velocity dispersion errors at the pericentre of the first Earth increase. Then, big trim manoeuvres would be needed to correct these errors for the swing-by. Therefore, the first correction manoeuvre should be implemented soon after the injection. To ensure a probability of success of 99 %, at least 140 m/s have to be allocated for the correction of injection errors.

The particular configuration for the first arc of the trajectory with an orbital period resonant with the Earth, 2 DSM manoeuvres and a swing-by with a relatively high perigee altitude permits another guidance strategy that has been investigated. This strategy consists on the full optimisation of this trajectory arc including the first correction manoeuvre, two possible deep space manoeuvres and the swing-by conditions in order to obtain the nominal departure conditions from the first Earth swing-by. Therefore, the initial dispersion error is corrected by not only the first correction manoeuvre, but also a redistribution of the delta-V in the DSM1.1 and the DSM1.2 and the variation of the perigee altitude at the swing-by. This strategy can be called a combined guidance strategy.

FIRST CORRECTION MANOEUVRE STATISTICS (M/S) – DIRECT GUIDANCE						
Days after injection	Mean	1- σ	Min	91%	99%	Max
3	45.7	30.9	0.75	93.7	140.1	222.0
4	45.4	30.5	0.75	92.7	138.6	219.6
5	44.9	30.1	0.76	91.6	137.0	217.0
6	44.5	29.7	0.76	90.4	135.3	214.3
8	43.7	28.9	0.77	88.2	131.8	208.8
10	42.8	28.1	0.79	85.9	128.5	203.4
12	42.1	27.3	0.80	83.7	125.2	198.2
15	41.0	26.2	0.82	80.6	120.5	190.8
20	39.5	24.6	0.86	76.1	113.7	180.0
25	38.6	23.3	0.91	74.4	108.5	171.7

Table 6-5: Statistical Results of Manoeuvre for Correction of Injection Errors

The initial dispersion model for the Ariane 5 dispersion errors have been taken as input for a Monte Carlo simulation of this guidance strategy. In order to simplify the problem and obtain a first estimation of the propellant requirement, the orbit determination errors have been considered negligible and a full optimisation of the trajectory has been made for every of the 10000 cases of the Monte Carlo analysis.

The results of this study are presented in Table 6-6 and Table 6-7. The first table shows that the ΔV required for this guidance is much lower than a direct guidance, as expected. The mean, standard deviation and maximum values are smaller as those in Table 6-5. Moreover, the minimum ΔV has negative values that shows that the initial dispersion due to the launcher injection errors can be used to fly similar trajectories with less propellant than the nominal. The maximum value throughout the launch window of about 164 m/s is at day 10/03/2004.

ΔV REQUIRED (M/S) FOR COMBINED GUIDANCE						
LAUNCH	MEAN	1- σ	MIN	95%	99%	MAX
26/02	11.5	19.6	-31.7	50.1	68.4	109.3
07/03	12.0	27.0	-48.7	66.2	94.5	139.7
10/03	12.6	27.6	-48.7	68.1	95.7	163.7
17/03	7.9	17.8	-30.7	42.1	62.9	117.9

Table 6-6: Statistics of required ΔV for trajectory guidance of arc from launch to Earth.

The altitude of the perigee can vary up to about 150 km in either direction to re-optimize the trajectory, while this altitude is always over 970 Km. This altitude change modifies the deflection to the trajectory provided in the gravity assist. A very effective velocity change due to the swing-by can be used to reduce the ΔV required for the guidance of the trajectory.

PERIGEE ALTITUDE CHANGE (KM) FOR COMBINED GUIDANCE						
LAUNCH	MEAN	1- σ	MIN	MAX	NOM-MIN	MAX-NOM
26/02	3610.8	23.2	3475.3	3667.4	144.2	47.8
07/03	1789.3	22.0	1695.7	1867.9	96.3	75.9
10/03	1623.3	26.7	1525.8	1748.2	107.1	115.2
17/03	1081.8	33.7	970.5	1201.5	83.7	147.3

Table 6-7: Statistics of required perigee altitude change of 1st Earth swing-by for trajectory guidance.

6.1.5 Interplanetary Navigation

The interplanetary navigation will be based on radio tracking using range and range-rate measurements. Intensive campaign will be needed for calibration of the tracking system, for trajectory determination in critical phases, for preparation of trajectory correction manoeuvres, for estimation of unknown parameter, etc.

The analysis of the navigation pretends to estimate the delta-V required to correct the dispersion errors at the major events during the trajectory – planetary swing-by, asteroids fly-by and comet rendezvous. The dispersion errors achieved at these events are also an important output of this study. The number and the implementation date of the trim correction manoeuvres have been selected based on the experience of previous similar studies. An optimisation of the guidance strategy and the dates of the trim manoeuvres is a non-trivial problem out of the scope of a preliminary analysis.

A covariance analysis is used to estimate the position and velocity of the spacecraft. The measurements incorporated to the orbit determination are supposed to be range and Doppler with the same assumptions stated in the previous section. The frequency of the measurements depends on the trajectory segment considered, increasing when close to an active phase such as the DSM or a swing-by. The following variables are considered parameters included as bias in the estimation process: Solar Radiation Pressure (1- σ 0.1% of nominal value), position of selected ground stations (1- σ 1-3 metres) and Measurements biases (1- σ 10 m of range bias).

The guidance correction manoeuvres are supposed to be implemented with a Gaussian error of 1% ($1-\sigma$) in manoeuvre modulus and 0.5° ($1-\sigma$) in the conic angle. A stochastic error has been added to every DSM to model the implementation errors of such kind of manoeuvres, with a component in the modulus of the ΔV vector and a component due to the angular error.

Phase from LIC to 1st Earth swing-by

During this phase, the orbit determination will be achieved by Range and Doppler measurements. The guidance strategy to arrive to the Earth after launch and the first correction manoeuvre of the launcher injection dispersion consists on four trim manoeuvres: one after the LIC to correct its implementation errors, one after the DSM1.1 and two at the arrival arc to the Earth.

The estimated values for the magnitudes of the correction manoeuvres up to the 1st Earth swing-by are shown in the Table 6-8. Every manoeuvre has been estimated by means of a Monte Carlo analysis. The last row shows the accumulated values for the four correction manoeuvres considered.

NAVIGATION TO 1 ST EARTH SWING-BY MANOEUVRE STATISTICS (M/S)				
	Mean	1- σ	99%	Max
MC1	0.07	0.03	0.15	0.23
MC2	1.95	1.3	5.94	9.4
MC3	0.24	0.18	0.78	1.25
MC4	0.03	0.02	0.08	0.12
Total	2.29	1.31	7.0	11.0

Table 6-8: Statistics of the Mid-Course Correction Manoeuvres up to 1st Earth swing-by.

Table 6-9 shows the position $1-\sigma$ dispersion errors at the perigee of the 1st Earth swing-by. Figure 6-80 shows the dispersion ($1-\sigma$) ellipses on the pericentre target plane. In order to view the effect of the last MC before the swing-by of the Earth, both ellipses before and after the manoeuvre are plotted. The radial vector of the position of the nominal pericentre is presented as well.

Intrinsic components		Projection on target plane	
Along-Track (Km)	3.61	SMA (Km)	2.57
Cross-Track (Km)	1.97	SMI (Km)	0.50
Radial (Km)	1.73	α ($^\circ$)	-74.7
Total (Km)	4.46	LTF (s)	0.38

Table 6-9: Position dispersion errors at pericentre 1st Earth swing-by

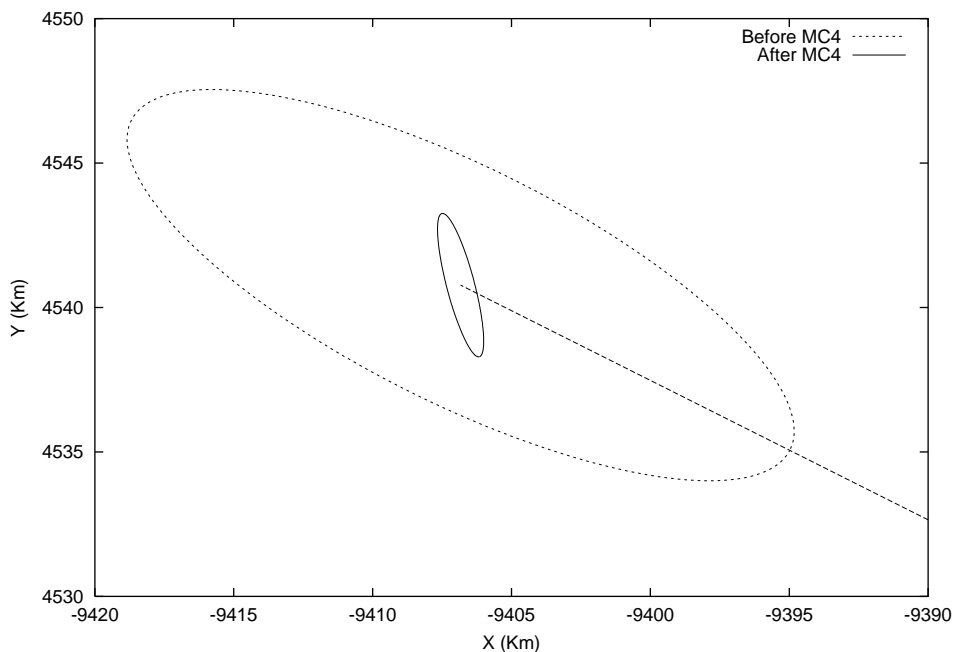


Figure 6-80: Dispersion 1- σ ellipses at 1st Earth pericentre target plane

Phase from Earth to Mars

One of the critical phases is the swing-by of Mars. The pericentre altitude must be as low as possible to maximise the swing-by effect, but a limit of 200 Km to the minimum altitude is needed to avoid the Mars atmosphere. Variations of the pericentre altitude of the passage of Mars have great effect in the trajectory and bear significant ΔV penalties. Any guidance strategy for the Rosetta trajectory phase from the Earth to Mars shall minimise the dispersion errors at the pericentre at Mars. Therefore, the guidance considered consists of a series of manoeuvres targeting the pericentre of the hyperbola at Mars swing-by.

The guidance strategy to reach Mars swing-by with an adequate precision consists of 4 trim manoeuvres targeting the conditions at the pericentre of Mars. The first is implemented as soon as possible after the 1st swing-by of the Earth, then two other intermediate manoeuvres follow and a final manoeuvre about 20 days before the swing-by of Mars reduces the dispersion errors at the pericentre.

The statistics of the guidance manoeuvres are shown in Table 6-10. The only correction manoeuvre of this phase that has a big magnitude is the MC just after the swing-by of the Earth, which could require about 6 m/s

NAVIGATION TO MARS - MANOEUVRE STATISTICS (M/S)				
	Mean	1- σ	99%	Max
MC5	1.37	0.75	3.61	5.7
MC6	0.02	0.01	0.06	0.09
MC7	0.07	0.04	0.18	0.27
MC8	0.1	0.08	0.34	0.54
Total	1.56	0.76	4.19	6.60

Table 6-10: Statistics of the Mid-Course Correction Manoeuvres from Earth to Mars

Table 6-11 shows the position 1- σ dispersion errors at the perigee of the Mars swing-by. Figure 6-81 shows the dispersion (1- σ) ellipses on the pericentre target plane before and after the MC7, which is implemented to correct the errors after the DSM2. This correction has a great effect on the dispersion reducing the great initial errors, especially removing the radial component. Figure 6-82 shows the dispersion (1- σ) ellipses on the pericentre target plane before and after the MC8. The correction reduces the cross-track component of the dispersion to about the same level of the radial error.

Intrinsic components		Projection on target plane	
Along-Track (Km)	3.14	SMA (Km)	8.71
Cross-Track (Km)	7.35	SMI (Km)	2.33
Radial (Km)	5.21	α (°)	-68.4
Total (Km)	9.54	LTF (s)	0.31

Table 6-11: Position dispersion errors at pericentre of Mars swing-by

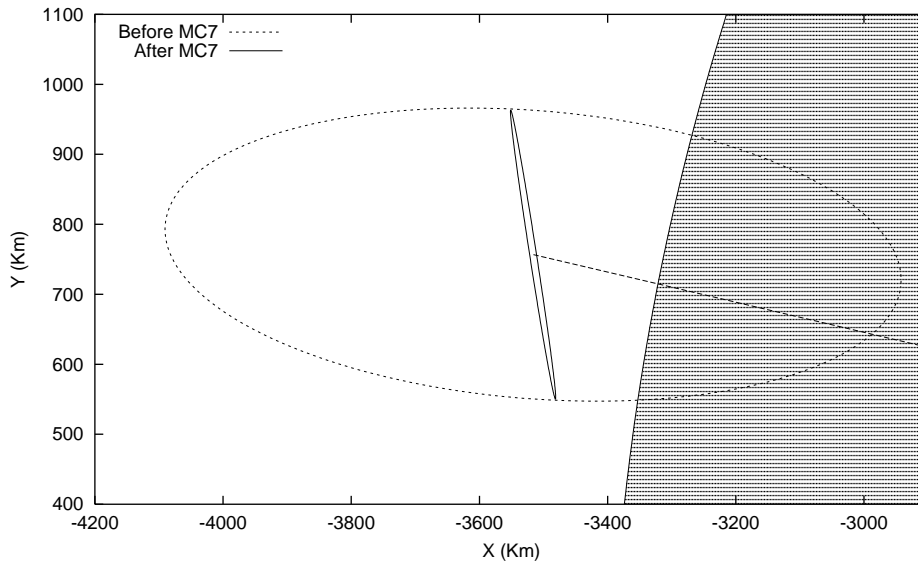


Figure 6-81: Dispersion 1- σ ellipses at Mars pericentre target plane

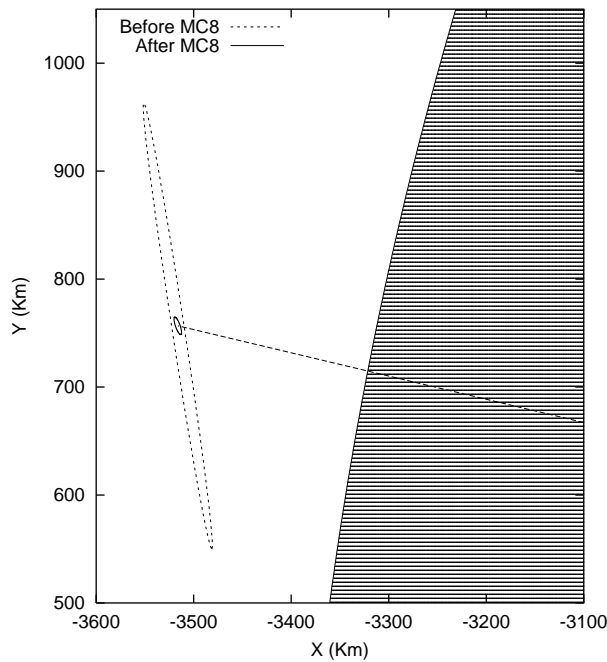


Figure 6-82: Dispersion 1- σ ellipses at Mars pericentre target plane

Phase from Mars to 2nd Earth swing-by

Two correction manoeuvres have been considered for this phase. The first is implemented about 10 days after the swing-by of Mars and corrects the errors at the departure of this swing-

by. The second manoeuvre performs a fine reduction of the dispersion at the pericentre of the 2nd Earth swing-by. The statistics of the guidance manoeuvres are shown in Table 6-12. The correction manoeuvre after the swing-by of Mars is very big and could reach about 22 m/s. The correction to fine target the pericentre of the Earth swing-by has also a rather big magnitude of up to 5 m/s.

NAVIGATION TO 2 ND EARTH SWING-BY MANOEUVRE STATISTICS (M/S)				
	Mean	1- σ	99%	Max
MC9	4.66	3.15	14.23	22.56
MC10	1.12	0.74	3.39	5.36
Total	5.78	3.24	17.62	27.92

Table 6-12: Statistics of the Mid-Course Correction Manoeuvres from Mars to Earth

Table 6-13 shows the position 1- σ dispersion errors at the perigee of the 2nd Earth swing-by. In this case, the pericentre altitude of the swing-by is high and the exact position of the pericentre is quite flexible. The dispersion errors does not produce great velocity errors at the departure of the swing-by, therefore the dispersion level acquired is not so good as for the other swing-by. The evolution of the dispersion at the Earth pericentre is presented in Figure 6-83.

Intrinsic components		Projection on target plane	
Along-Track (Km)	19.96	SMA (Km)	20.97
Cross-Track (Km)	19.96	SMI (Km)	14.55
Radial (Km)	15.90	α (°)	-62.7
Total (Km)	36.15	LTF (s)	1.78

Table 6-13: Position dispersion errors at pericentre of 2nd Earth swing-by

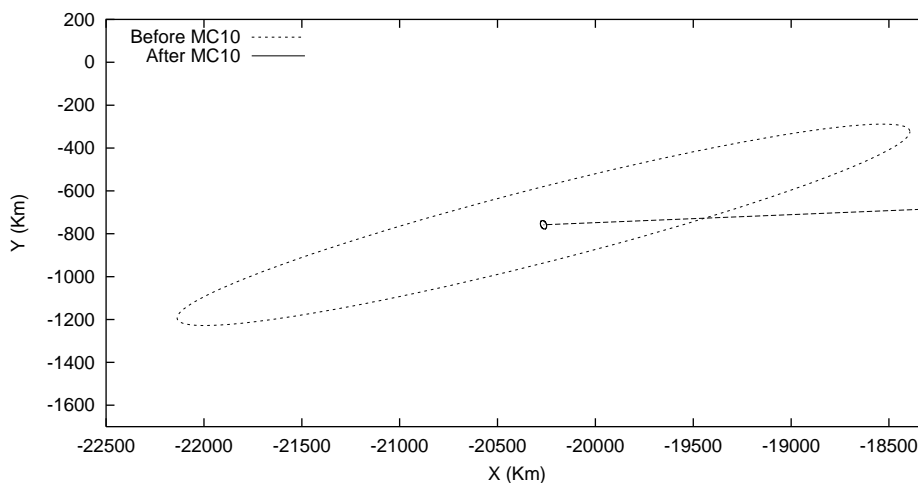


Figure 6-83: Dispersion 1- σ ellipses at 2nd Earth pericentre target plane

Phase from 2nd Earth swing-by to 3rd Earth swing-by

A total of 5 correction manoeuvres have been considered for this phase. The first is implemented about 10 days after departure from the Earth to vanish the great velocity dispersions. One MC is given prior to the DSM3 that performs a trajectory change to reach again the Earth with the appropriate velocity. One MC is given after the DSM3 to correct its errors. The last two manoeuvres, implemented quite close to the swing-by, successively diminish the dispersion errors at the 3rd Earth pericentre. The statistics of the guidance manoeuvres are shown in Table 6-13. The correction after the 2nd swing-by of the Earth can become quite big, about 9 m/s, while the other intermediate manoeuvres are small.

NAVIGATION TO 3 RD EARTH SWING-BY MANOEVRE STATISTICS (M/S)				
	Mean	1- σ	99%	Max
MC11	1.93	1.25	5.75	9.09
MC12	0.03	0.02	0.08	0.13
MC13	0.06	0.03	0.16	0.24
MC14	0.27	0.2	0.88	1.4
MC15	0.14	0.1	0.44	0.7
Total	2.43	1.27	7.31	11.56

Table 6-14: Statistics of the Mid-Course Correction Manoeuvres from 2nd Earth to 3rd Earth swing-by

The swing-by of the Earth makes use of all the possible deflection provided by the gravity effect of the planet. The altitude of the pericentre is rather low and must be achieved with great precision in order to avoid following correction manoeuvres after the swing-by. Table 6-15 shows the position 1- σ dispersion errors at the perigee of the 2nd Earth swing-by. The evolution of the dispersion at the Earth pericentre is presented in two steps with Figure 6-84 after the MC14 and with Figure 6-85 after the final MC15.

Intrinsic components		Projection on target plane	
Along-Track (Km)	2.96	SMA (Km)	3.70
Cross-Track (Km)	2.41	SMI (Km)	1.85
Radial (Km)	3.35	α (°)	78.0
Total (Km)	5.08	LTF (s)	0.20

Table 6-15: Position dispersion errors at pericentre of 3rd Earth swing-by

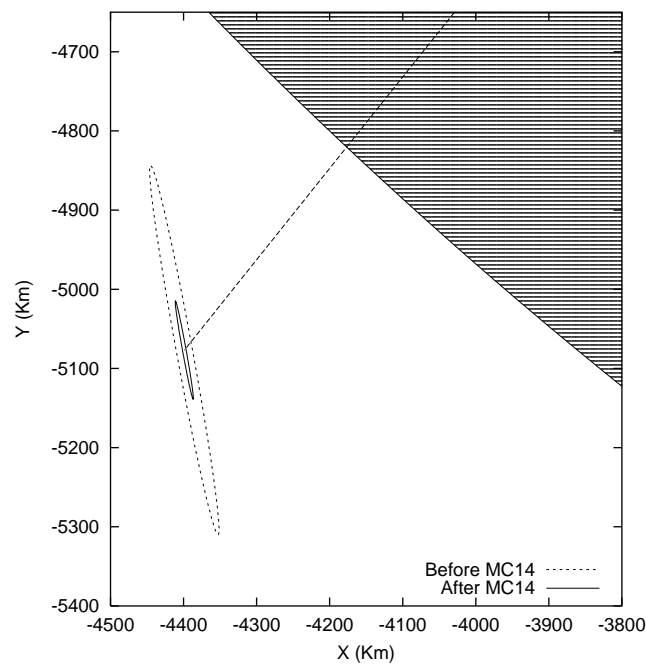


Figure 6-84: Dispersion 1- σ ellipses at 3rd Earth pericentre target plane

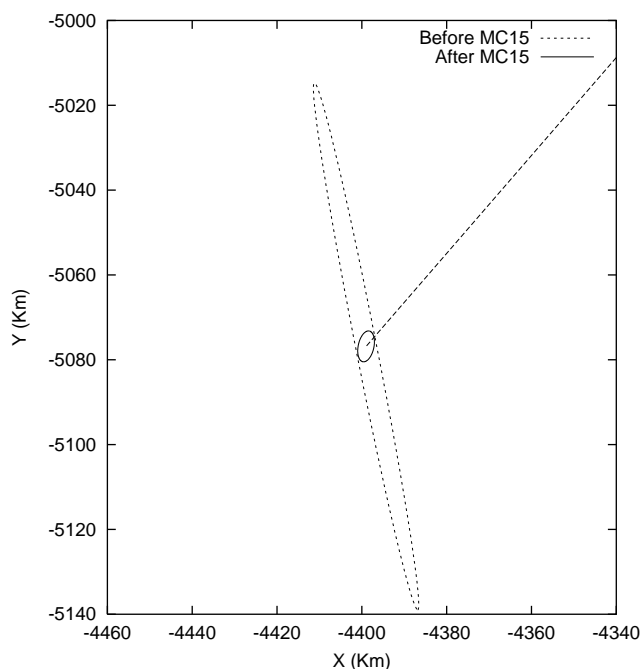


Figure 6-85: Dispersion 1- σ ellipses at 3rd Earth pericentre target plane

Phase from 3rd Earth swing-by to comet rendezvous

The final arc of the trajectory is controlled by a manoeuvre after the swing-by of the Earth, which targets the conditions at the DSM4, and a correction just after the DSM4 to reduce the dispersion due to the implementation errors of this big manoeuvre. Then, the spacecraft will enter a large hibernation phase and finally reach the comet.

The statistics of the guidance manoeuvres are shown in Table 6-16. The correction manoeuvre after the 3rd swing-by of the Earth is big, with a maximum about 17 m/s. The final dispersion errors at the approach to 67P/Churyumov-Gerasimenko are of about 2000 Km, which is similar to the order of magnitude supposed for the initialisation of the studies of the close approach to the comet.

NAVIGATION TO COMET RENDEZVOUS MANOEUVRE STATISTICS (M/S)				
	Mean	1- σ	99%	Max
MC16	4.01	2.26	10.86	16.88
MC17	0.42	0.22	1.05	1.61
Total	4.43	2.27	11.91	18.49

Table 6-16: Statistics of the Mid-Course Correction Manoeuvres from 3rd Earth swing-by to comet

Table 6-17 below shows a summary of the requirements of ΔV for the navigation and guidance of the different phases of the Rosetta baseline trajectory.

MANOEUVRE STATISTICS (M/S)				
Phase	Mean	1- σ	99%	Max
Earth – Earth 1	2.29	1.31	6.95	11.0
Earth 1 – Mars	1.56	0.76	4.19	6.60
Mars – Earth 2	5.78	3.24	17.6	27.9
Earth 2 – Earth 3	2.43	1.27	7.31	11.6
Earth 3 – 67P/Churyumov-G.	4.43	2.27	11.9	18.5
Interplanetary Navigation	16.5	4.42	48.0	75.6

Table 6-17: Accumulated ΔV statistics of the trim correction manoeuvres

7. ASTEROID FLY-BY POSSIBILITIES

The scientific return of the mission can be improved by the fly-by of one or two asteroids. The new mission baseline to 67P/Churyumov-Gerasimenko with launch in early 2004 does not allow to reach the previous selected asteroids Otawara and Siwa. The current trajectory offers multiple fly-by possibilities, however only a few are feasible in terms of required delta-V for the trajectory modification in order to fly-by the asteroid or in terms of the visibility and communication constraints during the fly-by.

Some of the selected asteroids require large amounts of additional propellant w.r.t. the baseline mission, therefore compromising the fuel budget of the mission. However, it is still possible to reach these asteroids once the launcher injection correction manoeuvre has been performed and its value has been adequately small.

Instead of giving a mission baseline including asteroids fly-by, it has been decided to study the single and double fly-by alternatives that could be flown. The final decision on the asteroids to be flown-by will be taken after the implementation of the launcher injection correction manoeuvre.

7.1 *Extra Delta-V Assessment*

Two trajectory arcs are appropriate for asteroid fly-by. The arc between the 2nd and 3rd Earth swing-by and the arc between the Earth and the comet. The first arc presents more flexibility due to the fact that the spacecraft will encounter the Earth twice in a very similar position with respect to the Sun. Therefore, the inclination of the orbital plane of this arc is a free parameter that can be used to search asteroids. On the other hand, the trajectory of the last arc is well determined between the Earth and the comet. The arrival date is fixed and changes of the orbital plane to reach asteroids can only be achieved by large manoeuvres. All of which reduces the possible asteroids during this part of the trajectory to only a few.

Table 4-1 below shows a list of all the asteroids that Rosetta could fly-by. The additional ΔV required to reach the asteroid is presented in the last column. The results have been obtained by numerical propagation including all relevant orbit perturbations. The first set of asteroids is the ones visited in the arc between the two Earth swing-by and the three asteroids at the end are visited at the arc between the Earth and the comet.

Some asteroids mentioned in the preliminary studies of the mission have been discarded due to a conjunction preventing the communications during the fly-by. This is the case of 1063/Aquilegia (ϕ 18Km) and 5668/Foucault in the arc between the Earth, and 767/Bondia (ϕ 40Km) and 1033/Simona (ϕ 25Km) in the arc to the comet. Also unfavourable illumination conditions during the fly-by force to reject the asteroids 1831/Nicholson (ϕ 18Km) and Abashiri, both in the arc between the 2nd and 3rd Earth swing-by.

ASTEROID	#	ϕ (Km)	Total ΔV (m/s)			Extra DV (m/s)
			OPEN: 26/02	MID: 07/03	CLOSE: 17/03	
None			1682	1664	1688	
Rhodia	437	14.3	1786	1747	1775	98
Sofala	1393	0	1855	1795	1817	167
Sy	1714	19.2	1682	1667	1693	5
Baetsle	2513	0	1699	1677	1706	18
Steins	2867	0	1756	1731	1757	69
Carrera	3050	0	1818	1787	1789	130
Luichewoo	5538	0	1705	1691	1719	31
Lutetia	21	99.5	1773	1777	1827	139
Fogelin	2181	0	1692	1677	1702	14
Izvekov	3418	21.1	1685	1669	1696	8

Table 7-1: Single asteroid fly-by missions.

Table 7-2 presents a summary of the parameters of the fly-by of the selected asteroids: date, relative velocity, distances to Earth and Sun and also illumination and communication angles. The high illumination angle during the fly-by of Sy can present problems to the NAVCAM and this fly-by is still under investigation (TBD).

Table 7-3 presents the additional ΔV required for double fly-by missions including two of the selected asteroids. Asteroids Lutetia and Izvekov are the most interesting for the final arc. The best combinations are with the asteroid Sy in the arc between the 2nd and 3rd Earth swing-by.

Meaning of the parameters in the next table:

ϕ – Asteroid diameter.

V_R – Relative velocity between spacecraft and asteroid at fly-by.

r_E, r_S – Distance to Earth and Sun, respectively.

α – Illumination Angle: angle Sun-Asteroid-Spacecraft at the approach to the asteroid fly-by.

β – Angle Sun-Spacecraft-Earth at the approach to the asteroid fly-by.

δ – Angle Earth-Asteroid-Spacecraft at the approach to the asteroid fly-by.

ASTEROID	#	ϕ (Km)	Fly-By Date	Vr (Km/s)	r_E (AU)	r_S (AU)	α (deg)	δ (deg)	β (deg)
Rhodia	437	14.3	2008/09/17	11.254	2.64	2.14	41.2	31.0	21.2
Sofala	1393	0	2008/09/22	6.577	2.52	2.18	60.7	37.8	23.2
Sy	1714	19.2	2009/03/06	8.211	2.98	2.22	126.6	139.0	14.3
Baetsle	2513	0	2008/10/04	8.578	2.68	2.21	34.6	14.5	21.0
Steins	2867	0	2008/09/06	8.571	2.42	2.13	38.5	15.9	24.6
Carrera	3050	0	2008/08/04	11.143	1.77	2.04	26.1	4.0	29.9
Luichewoo	5538	0	2009/04/03	5.499	2.61	2.14	105.6	125.8	21.6
Lutetia	21	99.5	2010/07/10	15.007	3.04	2.72	11.1	8.5	19.3
Fogelin	2181	0	2010/05/25	13.559	2.00	2.37	21.5	17.1	25.3
Izvekov	3418	21.1	2010/12/04	11.291	4.45	3.68	20.0	28.5	8.6

Table 7-2: Fly-by parameters of asteroid candidates.

Asteroid in arc E2-E3	#	Asteroid in arc E3-C	#	Total ΔV (m/s)			Extra ΔV (m/s)
				OPEN: 26/02	MID: 07/03	CLOSE: 17/03	
None				1682	1664	1688	-
Sy	1714	Lutetia	21	1688	1673	1700	12
Rhodia	437	Lutetia	21	1852	1839	1869	181
Steins	2867	Lutetia	21	1796	1791	1829	141
Luichewoo	5538	Lutetia	21	1786	1782	1816	128
Rhodia	437	Izvekov	3418	1792	1770	1797	110
Sy	1714	Izvekov	3418	1684	1670	1696	8
Baetsle	2513	Izvekov	3418	1945	1930	1947	266
Steins	2867	Izvekov	3418	1789	1742	1815	127
Luichewoo	5538	Izvekov	3418	1709	1695	1721	33

Table 7-3: Double asteroid fly-by missions. Additional delta-V required.

The following table summarizes the available possibilities as a function of the additional ΔV needed.

Extra ΔV (m/s)	Fly-by Opprtunities	
	Single	Double
20	Sy	Sy – Izvekov
	Izvekov	
	Baetsle	
	Fogelin	
40	Luichewoo	Luichewoo – Izvekov
80	Carrera	
	Steins	
	Rhodia	
100	Sofala	Rhodia – Izvekov
		Steins – Izvekov
130	Lutetia	Luichewoo – Lutetia
		Steins – Lutetia
200		Rhodia – Lutetia
		Baetsle – Izvekov

Table 4: Asteroid fly-by opportunities as a function of available ΔV .

7.2 Effect to Interplanetary Trajectory

This section covers a brief study on the variations of the mission parameters due to the fly-by of one asteroid.

7.2.1 Asteroid fly-by in phase from 2nd Earth to 3rd Earth swing-by

The trajectory between the 2nd and 3rd Earth swing-by including one asteroid can change considerably due to the fact that the orbital plane and the position of the pericentre are not totally determined for a double swing-by. However, the asteroids that are reachable at a low delta-V cost are the closest ones to the baseline trajectory and modify only slightly the trajectory. Only the asteroids 437/Rhodia and 2867/Steins have considerable effects on all the mission parameters during this arc of the trajectory.

Figure 7-1 shows the distance from Rosetta to the Sun for the mission without asteroid and the different asteroids that can be visited in this period. Figure 7-2 presents an analogue plot for the distances to the Earth. For most of the asteroids the evolution of these distances is the same as

without asteroid fly-by. The trajectories including Rhodia and Steins have smaller eccentricity, which translates into higher perihelion and lower aphelion distances.

A comparison of the evolution of the declination is presented in Figure 7-3. This plot shows the differences of inclination of the orbital planes of the different trajectories with and without asteroid. Again Rhodia and Steins presents the bigger variations. The declination including these asteroids begins with positive values instead of the negative values of the trajectory without asteroid. At the 3rd Earth swing-by, the declination is negative instead of positive. Also for Sofala and Luichewoo appear rather big differences in the declination.

Figure 7-4 and Figure 7-5 present the evolution of the Spacecraft-Earth-Sun angle and the Earth-Spacecraft-Sun angle, respectively. The evolution agrees for nearly all the asteroids except for Rhodia and Steins. In this case, the effect of the asteroid is beneficial as the conjunctions almost disappear. This is especially true for the spacecraft as the first and third conjunctions during this arc disappear. The third conjunction before the 3rd Earth swing-by also disappears flying-by other asteroids like Sofala, Luichewoo and Carrera.

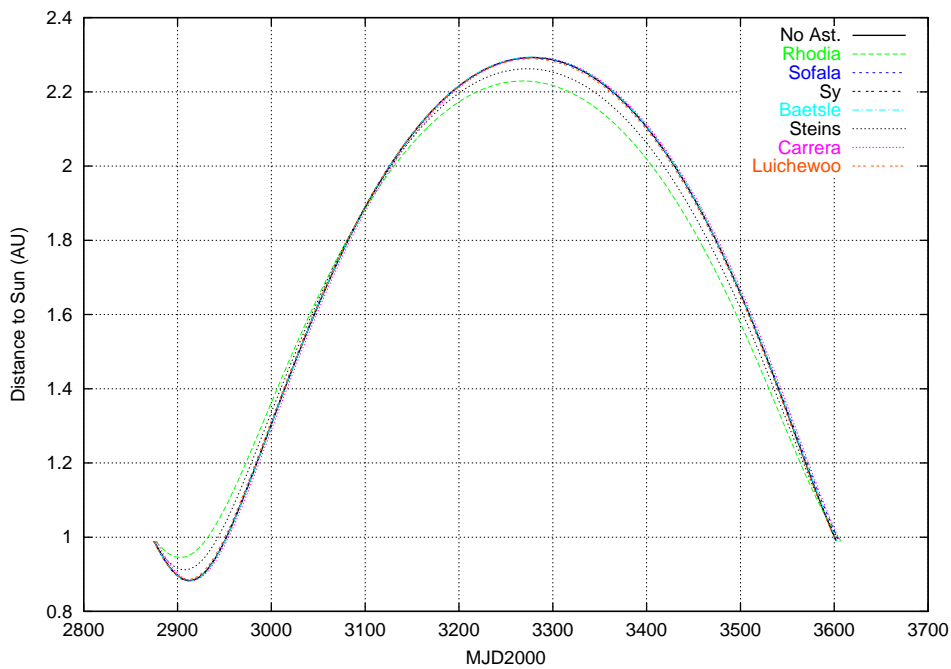


Figure 7-1: Distances to the Sun during phase EAR2-EAR3.

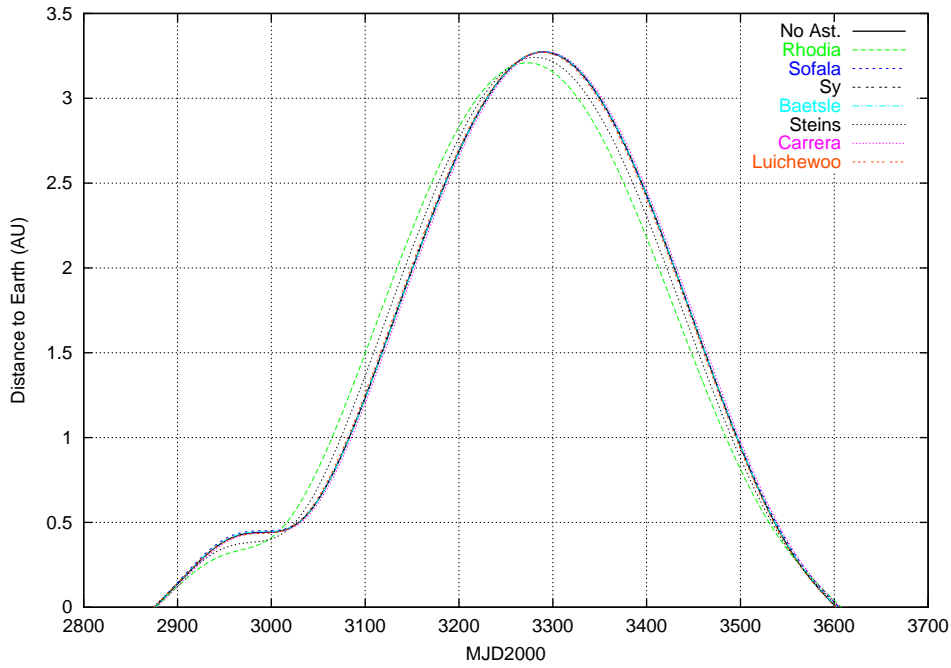


Figure 7-2: Distances to the Earth during phase EAR2-EAR3.

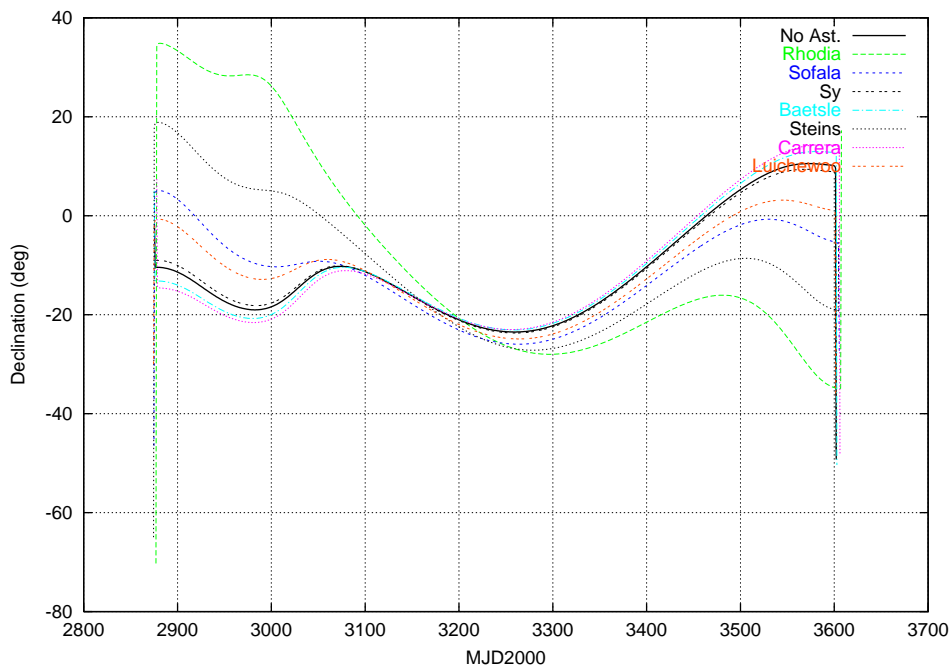


Figure 7-3: Equatorial declination during phase EAR2-EAR3.

Figure 7-6 shows the ecliptic projection of the trajectories without asteroid and with the selected asteroids for the arc between the Earth swing-by. The trajectories with Rhodia and Steins are clearly different as they are less eccentric and the argument of perihelion has diminished.

Figure 7-7 presents the XZ-projection of the trajectories. This plot shows the inclination of the different orbits. The inclination of the orbit is the parameter that changes slightly for all the asteroid. The trajectory with Rhodia has the biggest inclination, while for Steins it is also considerable.

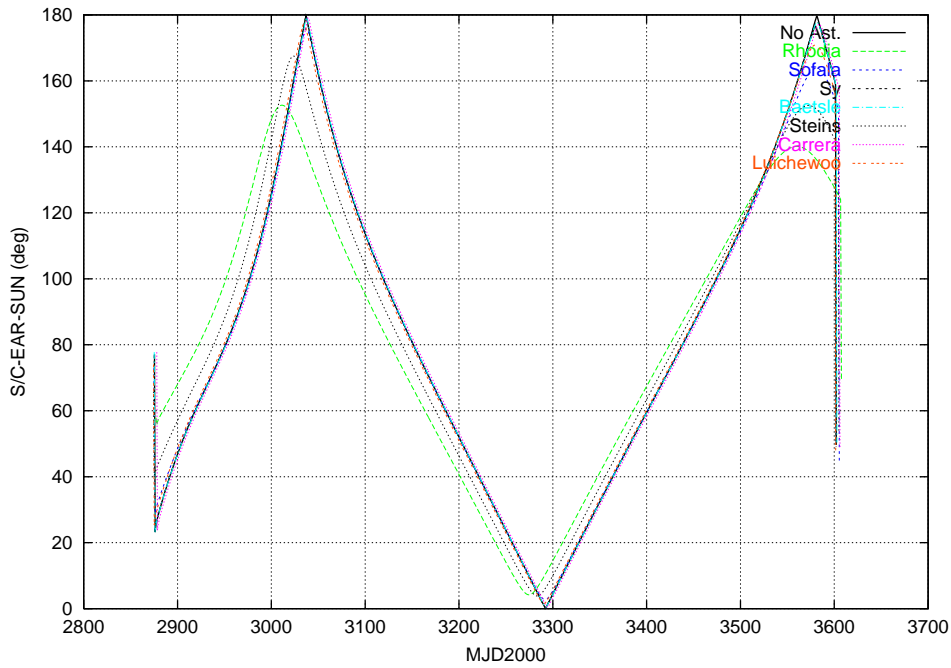


Figure 7-4: Angle Spacecraft-Earth-Sun during phase EAR2-EAR3.

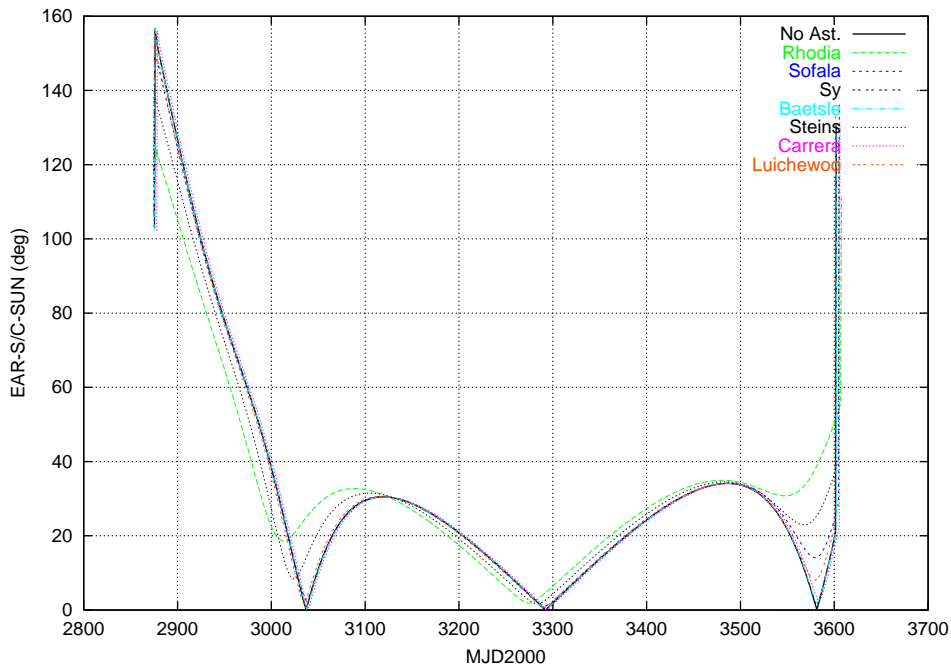


Figure 7-5: Angle Earth-Spacecraft-Sun during phase EAR2-EAR3.

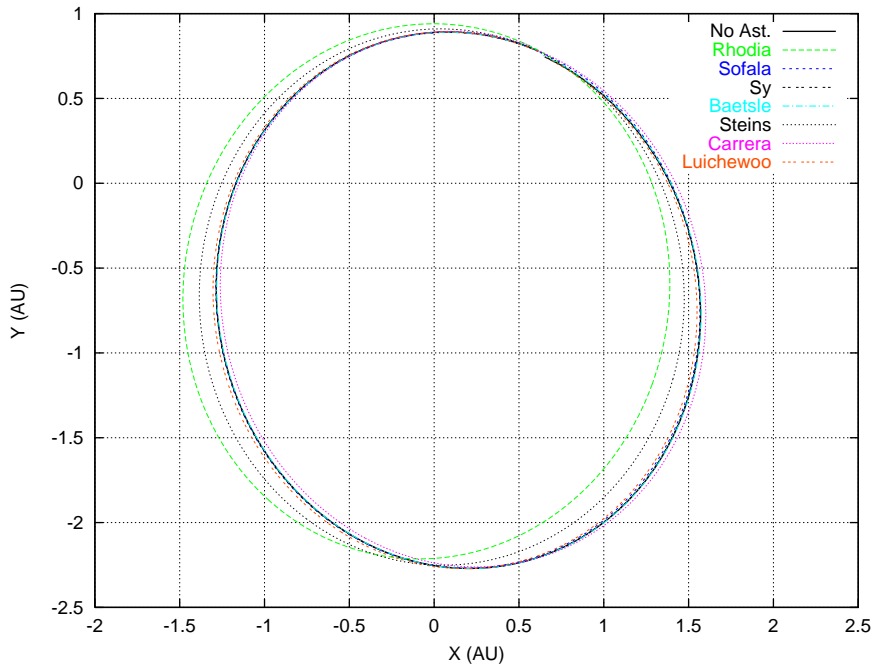


Figure 7-6: Ecliptic XY projection of the trajectory of phase EAR2-EAR3.

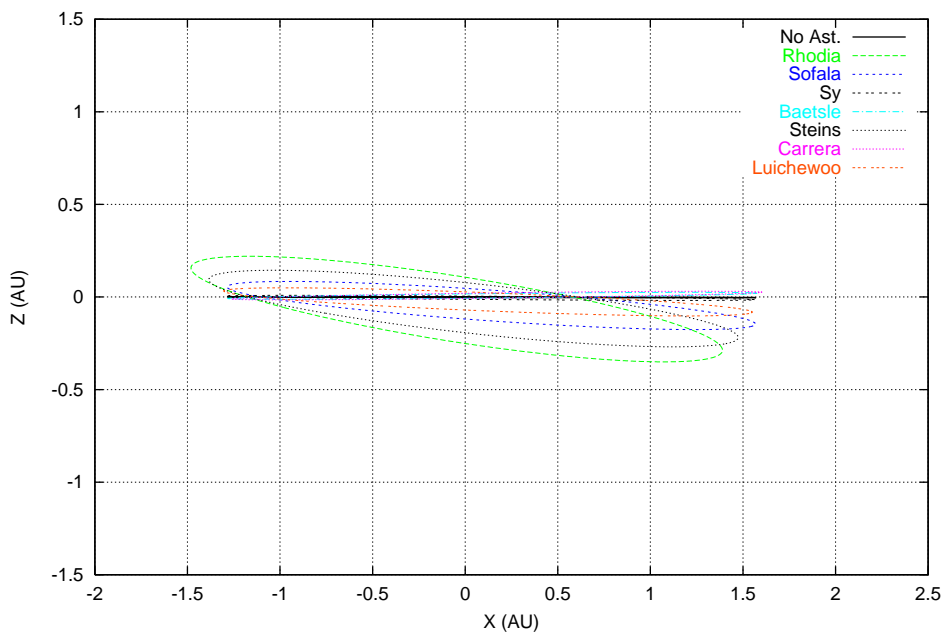


Figure 7-7: Ecliptic XZ projection of the trajectory of phase EAR2-EAR3.

7.2.2 Asteroid fly-by in phase from 3rd Earth swing-by to comet

The following figures present the parameters and the projection of the trajectories during the arc from the Earth to the comet without asteroid and with an asteroid fly-by. The asteroids presented are: 21/Lutetia, 2181/Fogelin and 3418/Izvekov. The figures show that the effect of these asteroids on the trajectory is very small.

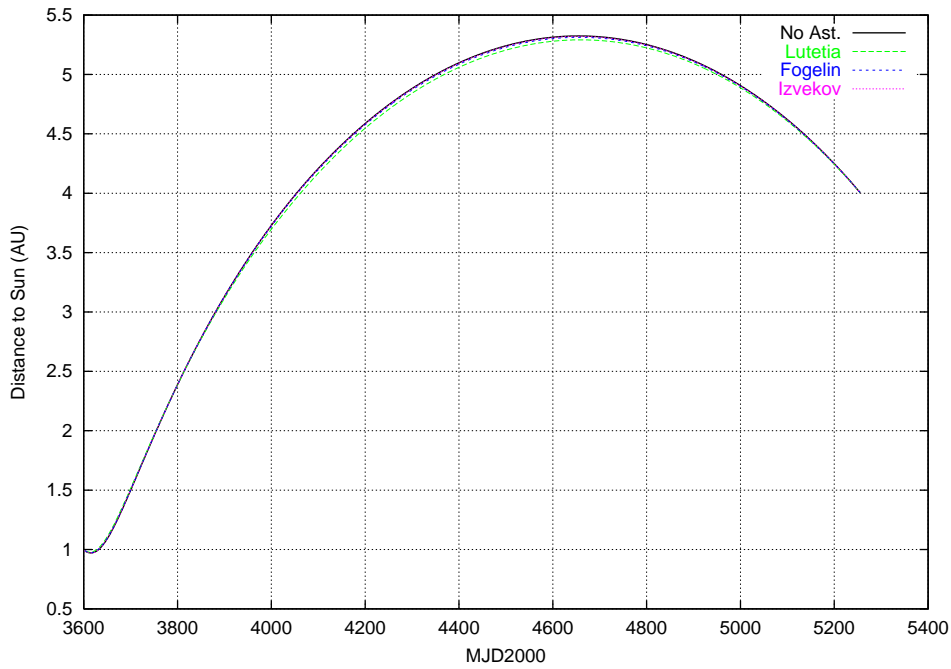


Figure 7-8: Distances to the Sun during phase EAR3-Comet.

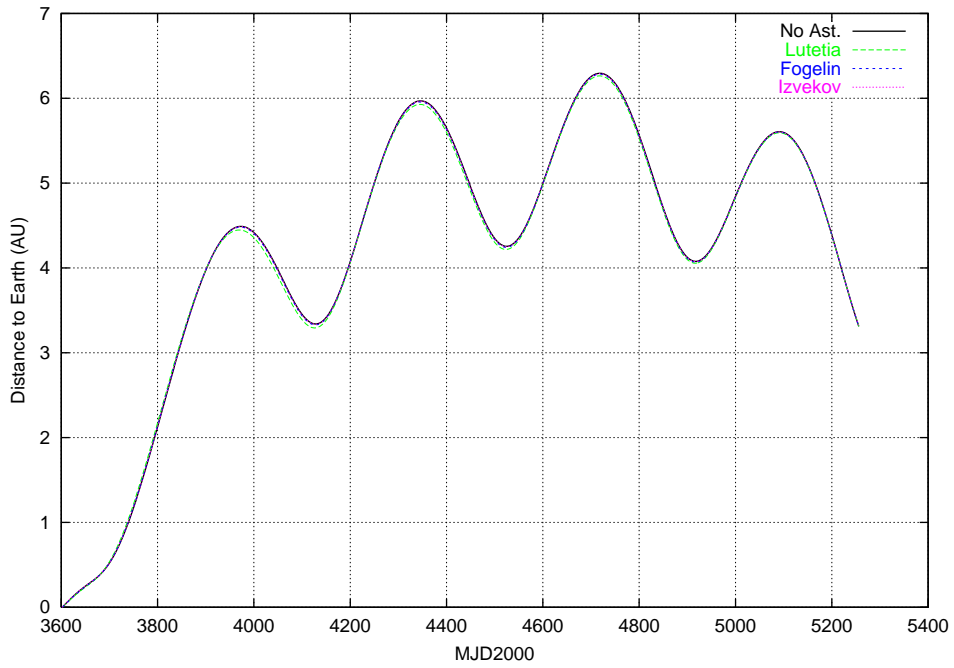


Figure 7-9: Distances to the Earth during phase EAR3-Comet.

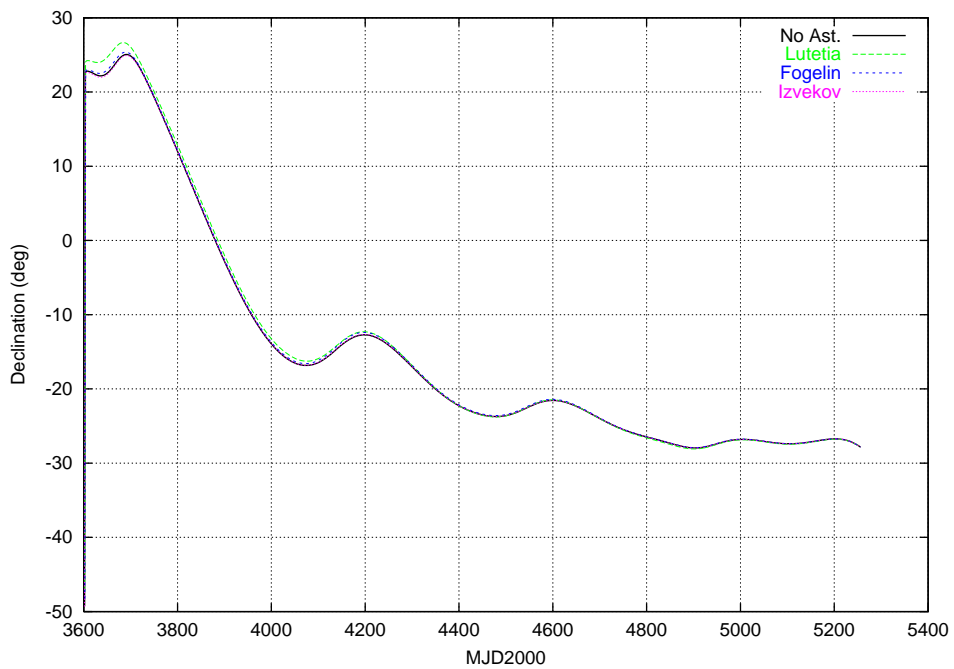


Figure 7-10: Equatorial declination during phase EAR3-Comet.

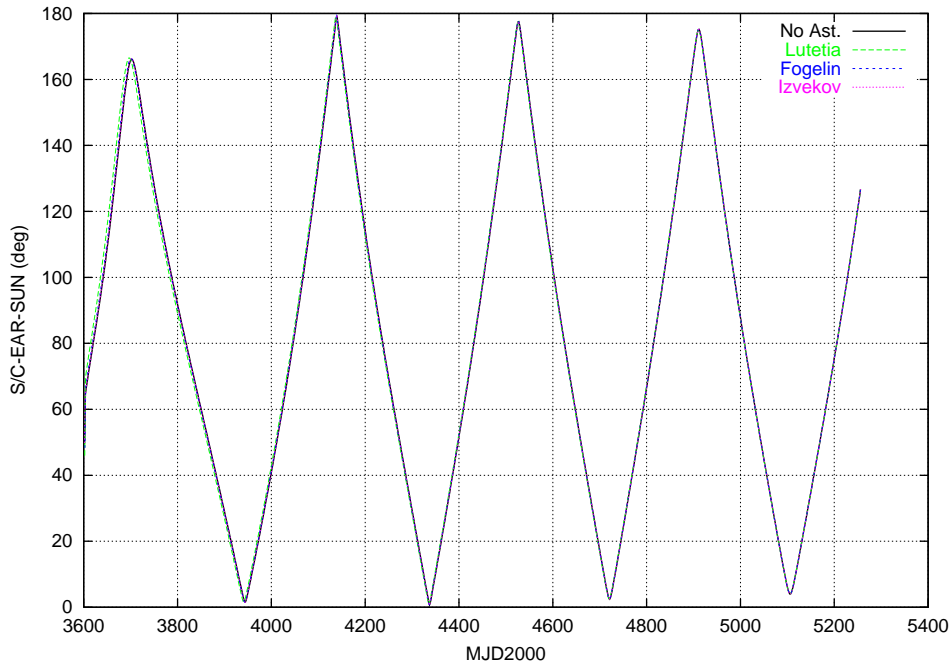


Figure 7-11: Angle Spacecraft-Earth-Sun during phase EAR3-Comet.

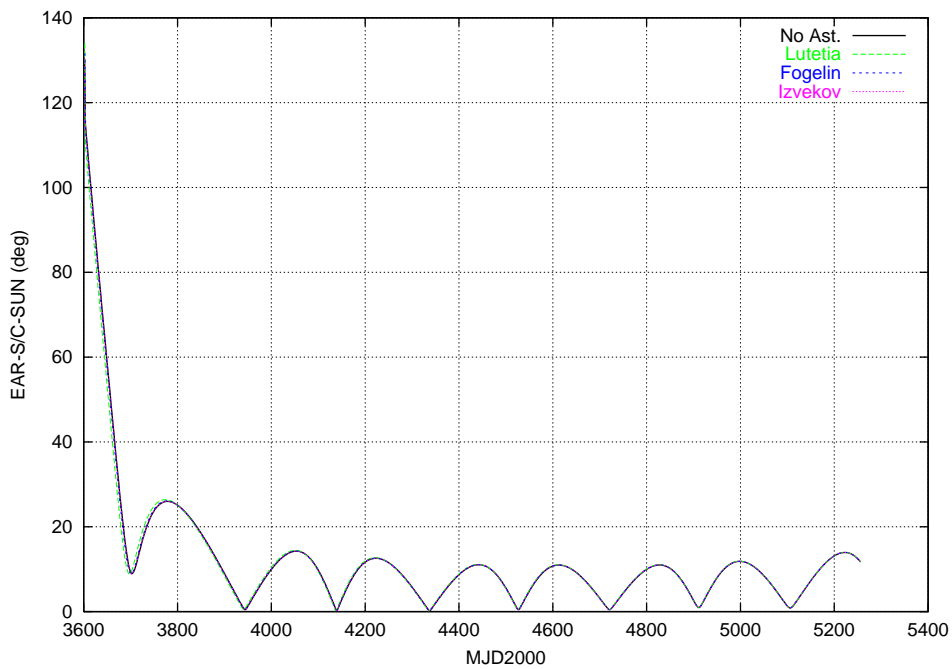


Figure 7-12: Angle Earth-Spacecraft-Sun during phase EAR3-Comet.

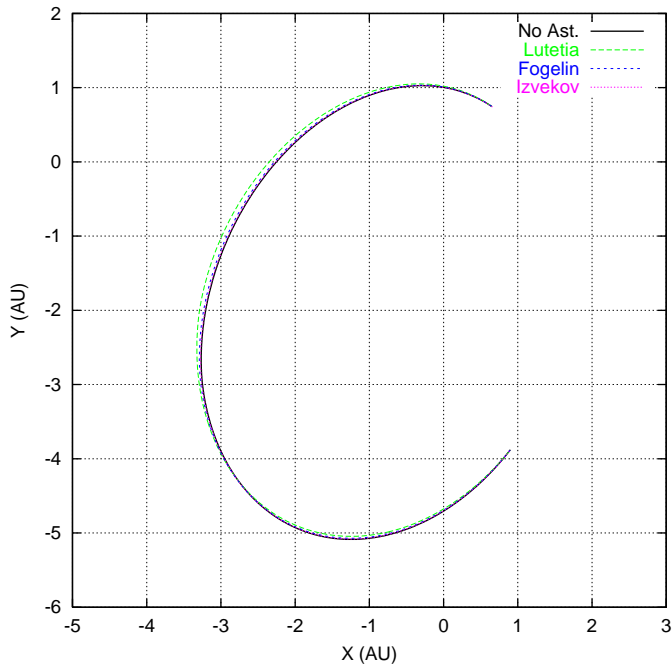


Figure 7-13: Ecliptic XY projection of the trajectory of phase EAR3-Comet.

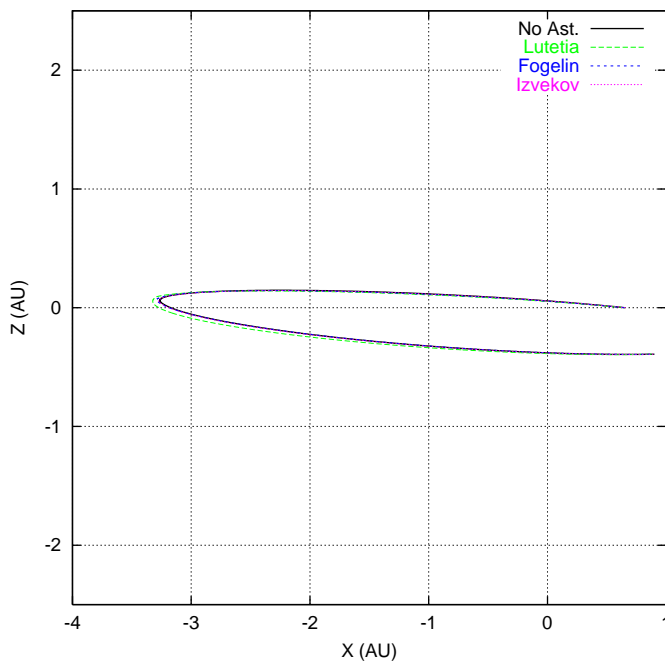


Figure 7-14: Ecliptic XZ projection of the trajectory of phase EAR3-Comet.

8. NEAR COMET OPERATIONS

8.1 Comet Model

An engineering model of the comet covering all important characteristics of the real comet was developed in RD 10 and it was used in RD 8, RD 9, and RD 11 to analyse the different reference cases including several comet sizes, nucleus kinematics, shapes, mass distributions, albedo, comet spin axis orientation, etc, representing all kind of possible comets.

The results presented in the following sections have been obtained using that model, and adjusting the parameters to the best known values of comet P67/Churyumov-Gerasimenko. The comet P67 has been observed from the European Southern Observatory, and from the Hubble Space Telescope, and it is now well characterized in respect to gas production rate, structures in the gas near the comet, size, and shape. The nucleus is an irregular elongated body with a size estimated to be about five by three kilometre.

In this work the nucleus of the comet is supposed to have a constant density of 1000 kg/m^3 , and an irregular shape based on an ellipsoid with craters and mountains on its surface. The equivalent radius of the comet, radius of a sphere with the same volume as the comet nucleus, has been taken as 2 km. The comet final shape is stored in a tabular function that provides the radius as a function of longitude and latitude. The use of this surface grid, simulates the operational environment during the comet approach. The engineering model of the comet will be updated by analysing the images provided by the on board cameras. An example of a possible comet shape is shown in Figure 8-1.

The gravitational field around the comet is obtained by numerical integration of each of the integrals of inertia of the nucleus. Terms up to forth order have been taken into account. In addition to the gravitational forces, there are forces on the orbiter due to the cometary activity, and a model of comet outgassing, with gas and dust, has been included. This model considers a radial flux and concentrated areas of higher activity (jets) both generating forces over the spacecraft. 67P/Churyumov-Gerasimenko has a level of activity similar to the one of Wirtanen. An analysis of the effect of different levels of activities and its influence on the operations near the comet is presented in RD 11.

The kinematics of the comet has also a very big influence in the design of the orbital strategy, mainly in the phases of surface observation and surface probe delivery. Since the torques acting on the comet are very small (only due to the out gassing) the rotation will be very similar to a free motion of a rigid body and consequently, the motion of the comet with respect of its centre of gravity can be modelled as a nutation.

The main parameters of the rotation are the orientation of the angular momentum and the maximum value of the nutation angle. Several values for these parameters have been also taken into account. The rotation period of 67P/Churyumov-Gerasimenko is currently estimated at about 12 hrs.

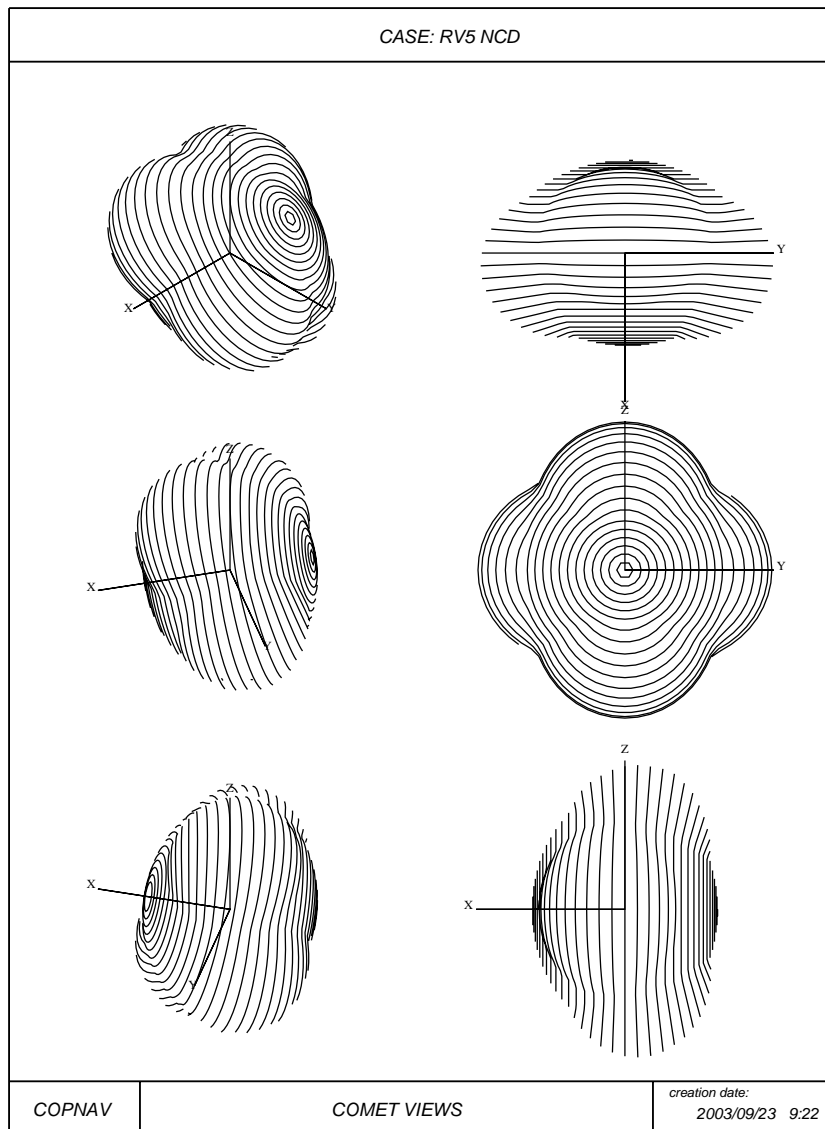


Figure 8-1: Model of Comet shape

8.2 *Range of Comet Models*

In RD 8, RD 9, and RD 11, detailed results are available for the following range of parameters defining the comet nucleus:

- Comet size (equivalent radius):
 - Small: $R_{eq} = 0.5$ km
 - Baseline: $R_{eq} = 0.6$ km
 - Big: $R_{eq} = 2.5$ km
- Comet Density:
 - Low: $\rho = 0.2$ gr/cm³
 - Baseline: $\rho = 0.75$ gr/cm³
 - High: $\rho = 1.5$ gr/cm³
- Rotation period:
 - Baseline: $T = 7$ hr
 - Quick: $T = 10$ hr
 - Medium: $T = 14$ hr
 - Slow: $T = 240$ hr
- Nutation (Maximum angle of nutation)
 - No Nutation: $\gamma = 0^\circ$
 - Baseline: $\gamma = 5^\circ$
 - Big Nutation: $\gamma = 10^\circ$
- Angular Momentum Orientation with respect to the Sun and orbital plane
 - Baseline: Perpendicular to the orbital plane
 - Inclined: 45° Inclined w.r.t the sun and 45° out of the orbital plane
 - In orbit: Perpendicular to the sun direction and contained in the orbital plane
 - Towards the sun: 30° away from the sun direction within the orbital plane
- Irregularity of the comet shape, (defined by the ratio of the axis of an ellipsoid)
 - Baseline (2-3-4)
 - Low Irregular (5-6-7)
 - High Irregular (1-2-3)
- Level of comet activity, (as described in RD 10, with an active surface of a given percentage of the total comet area)
 - Baseline, 2 %
 - High Activity, 20 %

- Low Activity, 0.2 %

Data presented in this chapter summarise the results obtained for the simulations performed for the baseline case of 67P/Churyumov-Gerasimenko defined in section 8.1 above.

The initial estimates of the value of the comet nucleus parameters needed for the near comet operations will be obtained from the information provided by the camera images acquired during a certain time. Camera images taken over at least one revolution period will be needed. The first images acquired by the on board imaging system will only provide information about relative position and velocity of the Rosetta S/C with respect to the comet. When the comet image extends over 100 pixels on the camera screen, the surface details and landmark position can be identified. At this moment the navigation filter will use the line of sight to landmarks. The estimation of the comet kinematics will be performed in the following sequence of events:

- Identification of the comet surface landmark by visual inspection of the images. The selection will take into account that the landmark is visible in as many images as possible in order to increase the number of measurements. Small landmarks are desirable in order to minimize the center finding error.
- Identify in the sequence of images of the trajectory of each of the landmarks selected.
- These sequences of positions together with the errors in the different involved parameters (i.e. pointing error, position error, geometrical-optical centre offset) will be the input for a minimization error algorithm (Least Squares Estimation Filter). This algorithm will filter the measurements and will obtain the initial estimation required for the navigation filter. Assuming M landmarks and N images the parameters to be estimated will be the following:
 - Initial values of the Euler angles (3)
 - Initial values of the angular velocity (3)
 - Values of the ratios I_y/I_x and I_z/I_x (2)
 - Landmarks coordinates with respect to a comet fixed reference system having its XZ plane containing one landmark ($3M - 1$) (The "Y" coordinate of one landmark will be zero).
 - Error in the camera pointing axis at each image (2N)

The total number of parameters to estimate will be $2N+3M+7$. The expected error in this initial estimation for the different parameters is presented in Table 8-1.

The approach to the comet is divided into phases selected to achieve given objectives:

- The Near Comet Drift, NCD, is the phase where the spacecraft comes near the comet without previous onboard observation. Therefore, a safe distance must be maintained and the relative velocity reduced to a few tens of meters per second.
- In the Far Approach Trajectory, FAT, the comet nucleus is observed with more or less resolution with the onboard camera. In successive steps the distance and relative velocity are reduced while information on the comet nucleus and environment is obtained.

- The Close Approach Trajectory, CAT, is the phase where the comet kinematics state is observed, and the spacecraft comes closer to the comet.
- In the Transition to Global Mapping, TGM, the objective is to bring the spacecraft to the injection point into the required orbit for observing the comet surface. In this phase the distance to the comet is reduced to values such that the gravity of the nucleus can be estimated.
- The Global Mapping Phase, GMP, serves to obtain full information on the surface, comet activity, and topography of the nucleus comet.
- In the Close Observation Phase, COP, selected areas of the comet will be observed at short distance so that they can be mapped to high accuracy.
- The Surface Package Delivery, SPD, is dedicated to bringing the spacecraft to the position required to eject the Lander.
- The Surface Package Relay, SPR, is designed to perform dedicated communication with the Lander for a period of a few days.

In all these phases it is very important to ensure the safety of the spacecraft, while observations are made to obtain information about the comet nucleus and the environment. The duration of the first 2 phases is fixed here to 60 days, but can be fixed to other values by selecting different parameters than the ones proposed here. The duration of the other phases will be very similar to the duration presented here, but they can be repeated, or waiting phases can be included between them.

8.3 *Near Comet Drift Phase*

The main objective of the Near Comet Drift, NCD, phase is to transfer the Rosetta spacecraft from the interplanetary phase, far from the comet, to a given safe distance to the comet using a sequence of manoeuvres that reduce the relative velocity to a safe value. For the mission to 67P/Churyumov-Gerasimenko, the total Rosetta mass after rendezvous with the comet, decreases when the rendezvous is performed at earlier dates, or equivalently, when the distance to the Sun at start of the NCD is larger. This behaviour is different than it was for the original mission to comet Wirtanen. For Wirtanen less ΔV was needed when the rendezvous was performed at larger distance from the Sun. Table 8-2 and Figure 8-2 present the distances spacecraft-Sun and spacecraft-Earth from the rendezvous manoeuvre up to perihelion.

Parameter	1 σ
α (°)	5.5
β (°)	1.5
γ (°)	5
ω_x (%)	1
ω_y (%)	3

ω_z (%)	3
Ix/Iy (%)	3.5
Ix/Iz (%)	5
Offset x(m)	25
Offset y(m)	25
Landmark x(m)	35
Landmark y(m)	30
Landmark z(m)	25

Table 8-1: Initial Estimation errors of Comet Kinematics

Given the Rosetta ΔV capabilities, the distance to the Sun at start of NCD must be smaller than 4.0 AU. This ensure power supply (the distance to the Sun must be less than 4.2 AU), and is a compromise between the ΔV used and the time left for operations up to perihelion. Therefore, a distance to the Sun of 4.0 AU at start of NCD has been selected. It is supposed that during this phase, Rosetta approaches the comet without observing the comet with the navigation camera. The errors in the estimated position of the comet can still be several tens of thousand km.

In this work, the total duration of this phase is fixed 26 days from the date at which the distance to the Sun is 4.0 AU (nominal rendezvous manoeuvre).

The NCD is designed to arrive at the CAP (Comet Acquisition Point) with a given condition relative to the comet.

The nominal distance at which it is expected to acquire the comet is estimated at 100.000 km, and the safety bias for this distance has been set to 10.000 km.

A sequence of 4 manoeuvres will reduce the relative velocity with respect to the comet from 780 m/s to 50 m/s.

The phase angle, (in the figures denoted illumination angle and defined as the angle Sun-comet-S/C), is about 51° at the beginning of this phase and decreases to 46° at the end of this phase. This value, far from the maximum allowed for comet detection (70°), has been selected to account for expected errors up to 20° .

The proposed strategy for this phase is to perform a sequence of manoeuvres (with decreasing magnitude) which progressively turn the trajectory of the last interplanetary arc towards the comet, and such that the comet acquisition point is reached with the desired target bias and relative velocity to the comet. The number of manoeuvres has been fixed to four. All manoeuvres are performed in the direction of the vector difference between the initial and the final velocity. A scheme of the proposed strategy and the numerical trajectory obtained are shown in Figure 8-3 and Figure 8-4. The RST frame has been used for trajectory representation. The R axis has the

Calendar Date	S/C-Sun Distance (AU)	S/C-Earth Distance (AU)	Calendar Date	S/C-Sun Distance (AU)	S/C-Earth Distance (AU)
2014/05/23	4.000	3.312	2015/01/03	2.628	3.511
2014/05/28	3.973	3.222	2015/01/08	2.589	3.498
2014/06/02	3.946	3.137	2015/01/14	2.550	3.480
2014/06/08	3.919	3.058	2015/01/19	2.510	3.459
2014/06/13	3.891	2.986	2015/01/25	2.471	3.433
2014/06/18	3.863	2.921	2015/01/30	2.431	3.403
2014/06/24	3.835	2.863	2015/02/04	2.390	3.369
2014/06/29	3.807	2.813	2015/02/10	2.350	3.331
2014/07/04	3.778	2.772	2015/02/15	2.309	3.290
2014/07/10	3.749	2.740	2015/02/20	2.268	3.246
2014/07/15	3.720	2.716	2015/02/26	2.227	3.198
2014/07/21	3.690	2.701	2015/03/03	2.186	3.148
2014/07/26	3.660	2.694	2015/03/09	2.145	3.095
2014/07/31	3.630	2.696	2015/03/14	2.104	3.039
2014/08/06	3.600	2.705	2015/03/19	2.062	2.982
2014/08/11	3.569	2.721	2015/03/25	2.021	2.922
2014/08/16	3.538	2.743	2015/03/30	1.979	2.862
2014/08/22	3.507	2.772	2015/04/04	1.938	2.800
2014/08/27	3.475	2.805	2015/04/10	1.897	2.737
2014/09/02	3.443	2.842	2015/04/15	1.856	2.674
2014/09/07	3.411	2.883	2015/04/20	1.815	2.611
2014/09/12	3.379	2.927	2015/04/26	1.774	2.548
2014/09/18	3.346	2.972	2015/05/01	1.734	2.485
2014/09/23	3.313	3.019	2015/05/07	1.695	2.423
2014/09/28	3.280	3.066	2015/05/12	1.656	2.363
2014/10/04	3.246	3.114	2015/05/17	1.617	2.304
2014/10/09	3.212	3.160	2015/05/23	1.580	2.247
2014/10/15	3.178	3.205	2015/05/28	1.544	2.192
2014/10/20	3.143	3.249	2015/06/02	1.508	2.139
2014/10/25	3.108	3.291	2015/06/08	1.474	2.090
2014/10/31	3.073	3.330	2015/06/13	1.442	2.043
2014/11/05	3.038	3.366	2015/06/19	1.411	2.000
2014/11/10	3.002	3.399	2015/06/24	1.382	1.960
2014/11/16	2.966	3.429	2015/06/29	1.356	1.924
2014/11/21	2.930	3.455	2015/07/05	1.331	1.892
2014/11/26	2.893	3.477	2015/07/10	1.310	1.864
2014/12/02	2.856	3.495	2015/07/15	1.291	1.839
2014/12/07	2.819	3.509	2015/07/21	1.275	1.819
2014/12/13	2.781	3.518	2015/07/26	1.262	1.802
2014/12/18	2.743	3.523	2015/08/01	1.252	1.789
2014/12/23	2.705	3.523	2015/08/06	1.246	1.779
2014/12/29	2.667	3.519	2015/08/11	1.243	1.773

Table 8-2: Distances S/C-Sun and S/C-Earth from Rendezvous Manoeuvre to Perihelion.

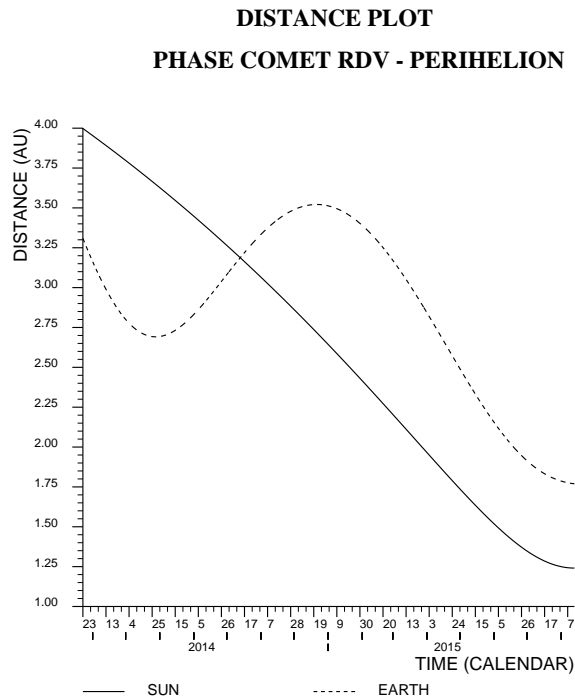


Figure 8-2: Evolution of the Distances from the Earth and the Sun to the Rosetta S/C.

direction of the position vector of the comet (vector Sun-comet), the S axis is perpendicular to the previous one and contained in the plane of motion of the comet and the T axis makes a right-handed frame with the R and S axis.

The Figure 8-5 shows the evolution of other interesting parameters such as distances of the S/C to the comet, Earth or Sun, phase angle and velocity relative to the comet.

The following list summarises the values of the main parameters along the trajectory for a typical case, where, DIS, and SUND are distances from the spacecraft to the comet and to the Sun, respectively. V0 is the relative velocity with respect to the comet, DV is the planned manoeuvre, and VF the actual relative velocity after the manoeuvre was performed.

REAL WORLD MANOEUVRES FOR THE NEAR COMET DRIFT PHASE
 =====

DATE (MJD2000)	T (DAYS)	MASS (KG)	DIS (KM)	SUND (AU)	V0 (M/S)	DV (M/S)	VF (M/S)
5248.0000000	0.000	1500.000	538141.8	4.03775	777.401		
5250.9938777	2.994	1318.894	337531.4	4.02383	777.392	366.059	413.618
5253.9877554	5.988	1223.425	231114.0	4.00981	413.610	213.761	200.848
5256.9816331	8.982	1179.729	179507.6	3.99571	200.843	103.468	97.775
5259.9755108	11.976	1160.103	154397.0	3.98151	97.768	47.727	50.251
5274.0000000	26.000	1160.103	93794.6	3.91379	50.222		

TOTAL NEAR COMET DRIFT DELTA-V (M/S) : 731.01

It is assumed that during this phase there will not be onboard optical measurements of the comet available and consequently there will not be a reduction in the errors of the relative spacecraft-comet position and velocity. At the end of the Near Comet Drift phase, the 1- σ error in position and in velocity of the spacecraft with respect to the comet is estimated as 13000 km, and 0.9 m/s, respectively. The values of the main parameters of this phase are the following ones:

- Duration: 26 days.
- Nominal required ΔV : 731 m/s

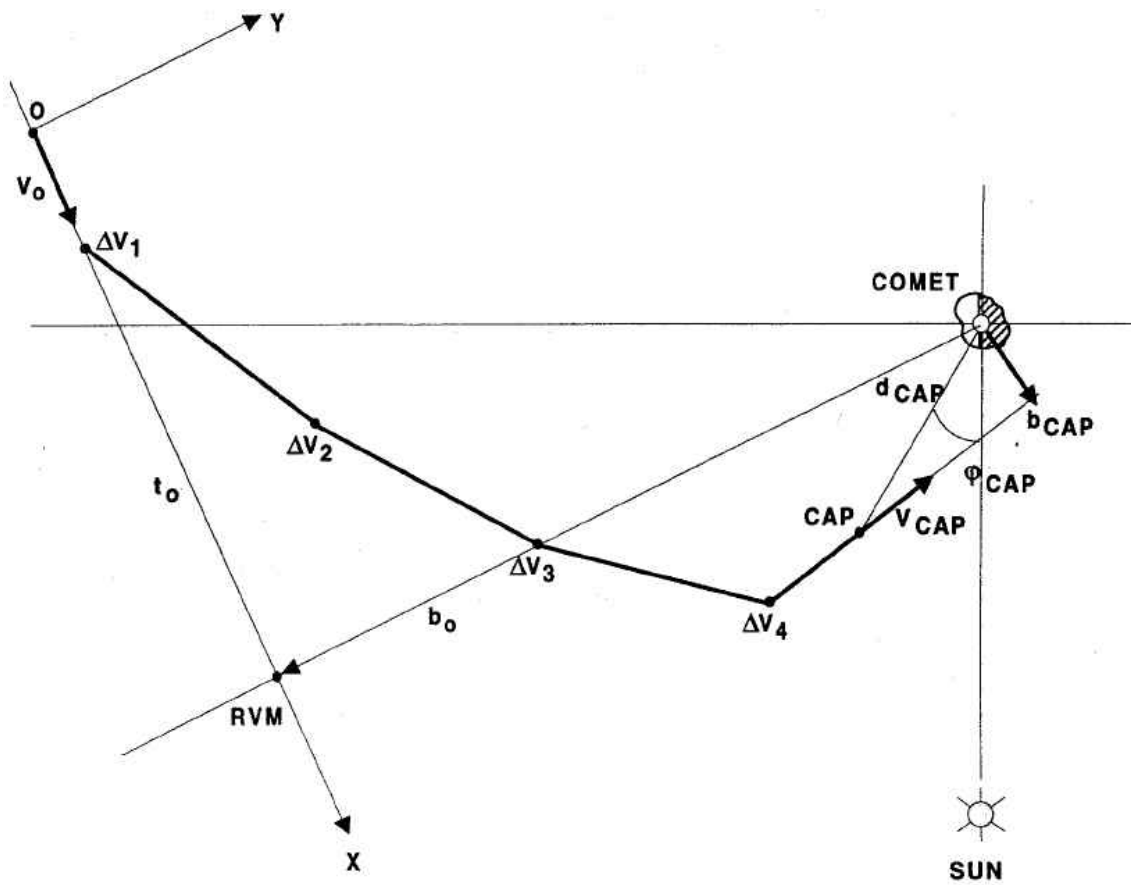


Figure 8-3: NCD Strategy

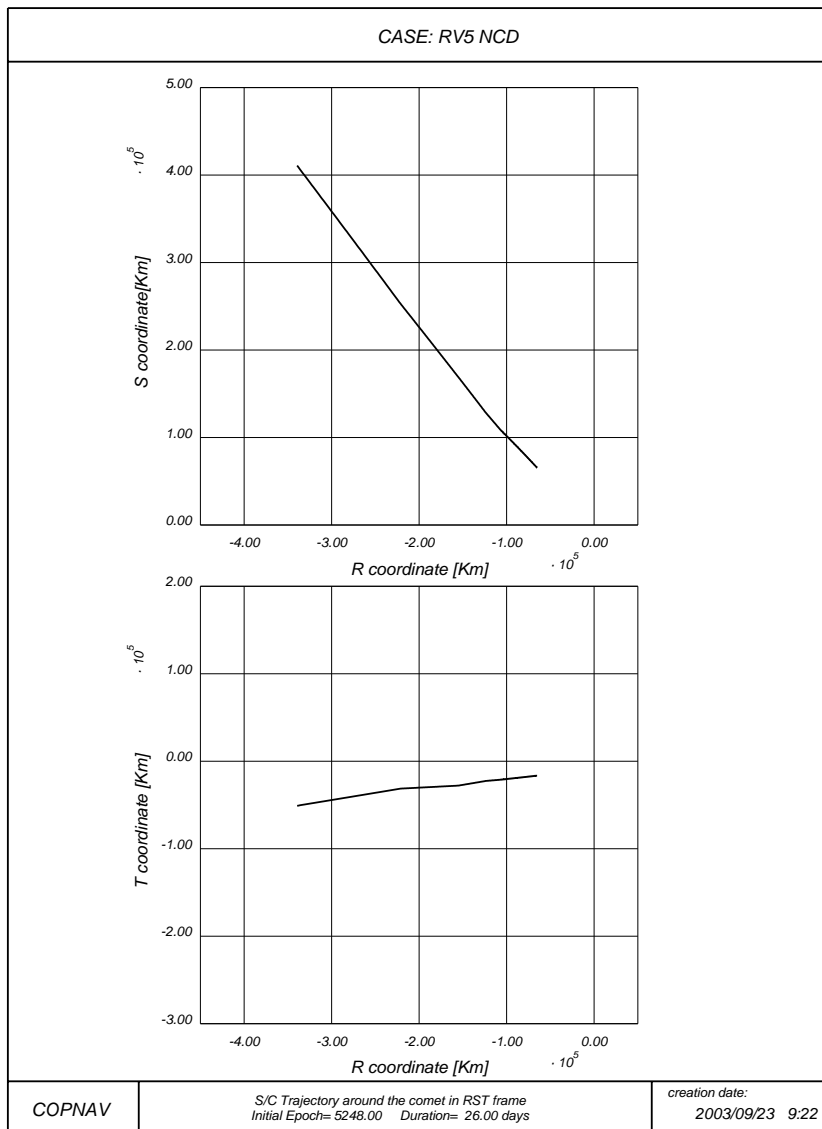


Figure 8-4: Numerical Trajectory (RST Frame)

The R axis has the direction of the position vector of the comet, the S axis is perpendicular to the previous one and contained in the plane of motion of the comet and the T axis makes a right-handed frame with the R and S axis.

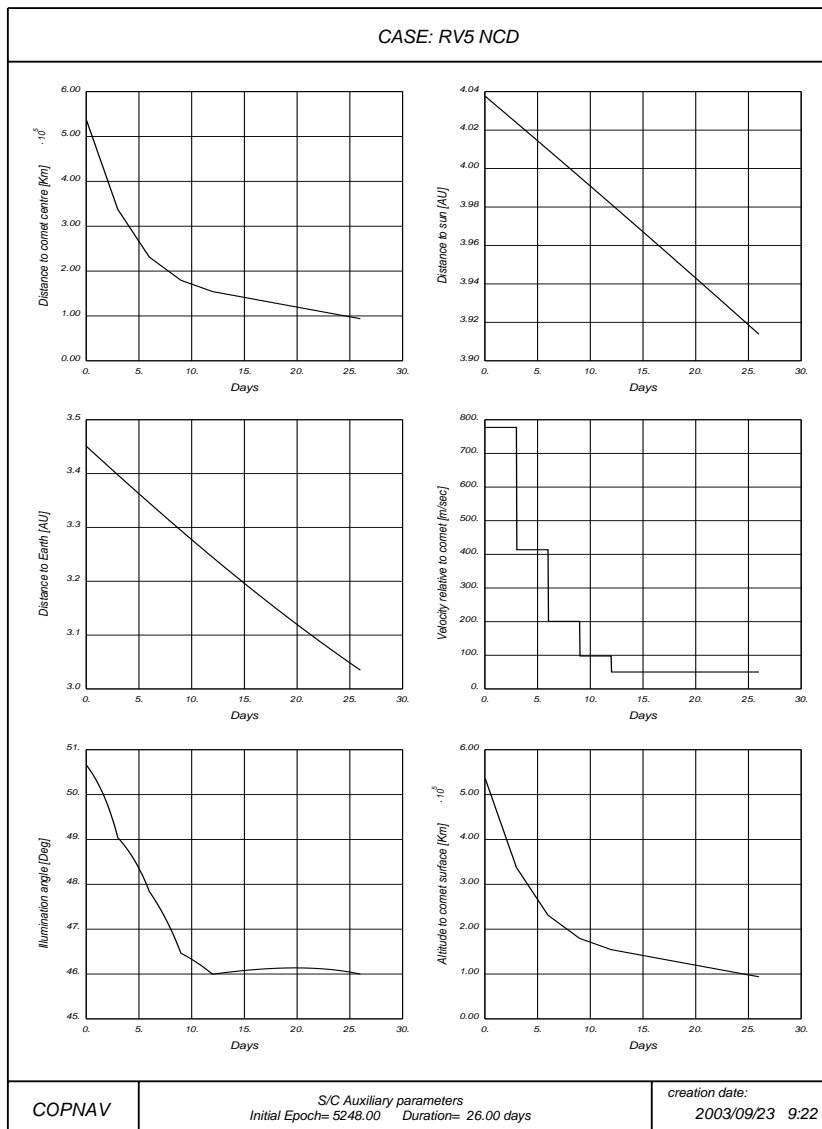


Figure 8-5: S/C Auxiliary Parameters during Near Comet Drift.

8.4 Far Approach Trajectory

During this phase the S/C continues its approximation to the comet from the CAP (Comet Acquisition Point) up to the ATP (Approach Transition Point) that is situated about 1000 comet radii from the comet nucleus. A series of manoeuvres is performed to progressively reduce the

relative velocity and arrive to the ATP. The impact vector is situated at 50 comet radii from the nucleus for safety reasons and the relative velocity is 3.1 m/s. The Earth communications requirements at ATP define a maximum distance to the Earth of 3.25 AU. This requirement is always satisfied for this mission, Table 8-2. The phase angle has been set to zero at ATP in order to optimise the visibility conditions during the following phase. This is very important from the point of view of the nucleus kinematics estimation. The number of manoeuvres during this phase has been set to 4. The first manoeuvre is close to the beginning of this phase in order to reduce the dispersion error as soon as the first estimation of the relative position is provided.

A scheme of the proposed strategy and the numerical trajectory (in RST Frame) obtained are shown in Figure 8-6 and Figure 8-7. The following list summarises the values of the main parameters along the trajectory for a typical case.

REAL WORLD MANOEUVRES FOR THE FAR APPROACH PHASE
 =====

DATE (MJD2000)	T (DAYS)	MASS (KG)	DIS (KM)	SUND (AU)	V0 (M/S)	DV (M/S)	VF (M/S)
5274.0000000	0.000	1160.103	93794.6	3.91379	50.222		
5281.0000000	7.000	1154.617	63753.1	3.87923	50.212	13.484	37.806
5291.0000000	17.000	1149.903	31286.5	3.82896	37.800	11.641	26.548
5301.0000000	27.000	1145.288	8623.7	3.77762	26.554	11.439	15.318
5306.0000000	32.000	1140.023	2512.6	3.75155	15.327	13.109	3.095
5308.0000000	34.000	1140.023	1978.6	3.74104	3.100		

TOTAL FAR APPROACH DELTA-V (M/S) : 49.67

The Figure 8-8 shows the evolution of other interesting parameters such as distances of the S/C to the comet, Earth or Sun, phase angle and velocity relative to the comet.

It can be seen that the phase angle tends to 0° at the end of this phase.

During this phase the first images of the comet are obtained with the optical measurement system. This fact provides the first estimate of the relative position S/C-comet and the combination of Earth measurements and on board measurements improves the knowledge in the comet ephemerides. At the beginning of this phase, the distance to the comet is too big to provide enough accuracy on the pictures to estimate the rotation kinematics of the nucleus. The accuracy in the determination of the S/C relative position will increase continuously in the following phases until the SSP delivery.

At the end of this phase, the values of the main parameters are:

- Duration: 34 days.
- Nominal required ΔV : 50 m/s.
- S/C relative position estimation error: 2.3 km (1 σ).
- S/C relative velocity estimation error: 2.1 cm/s (1 σ).
- Comet position estimation error: 151 km (1 σ).

- Comet velocity estimation error: 6 cm/s (1σ).

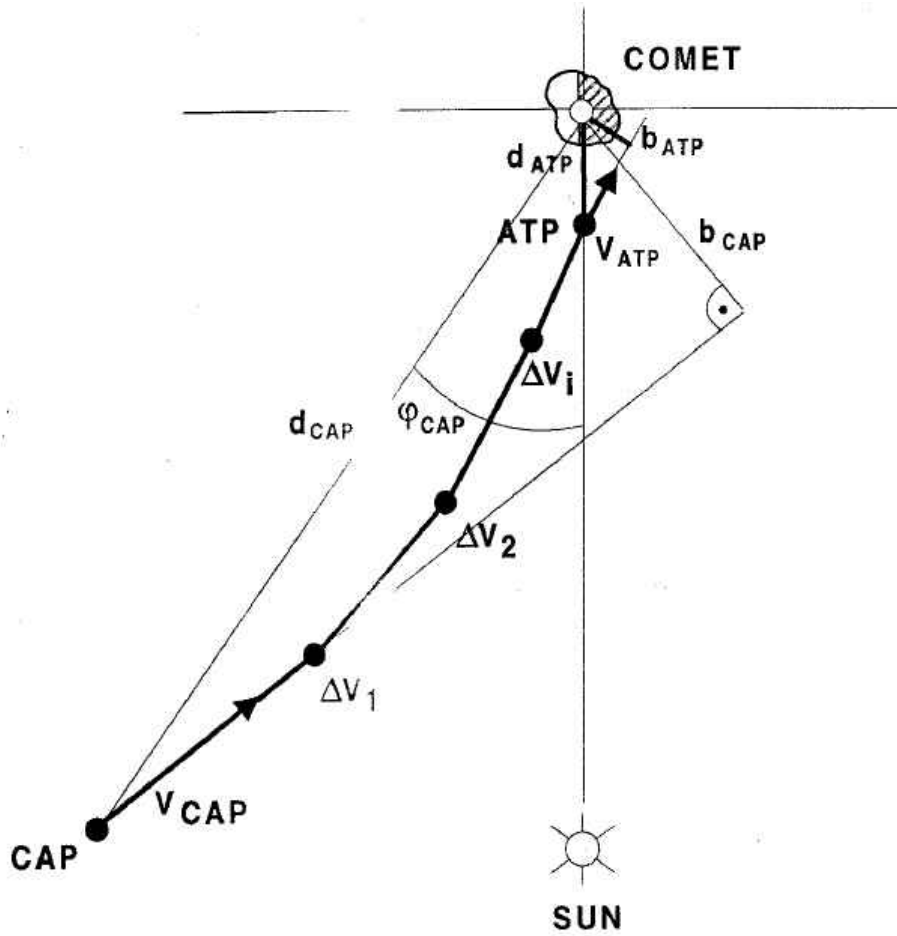


Figure 8-6: FAT Strategy

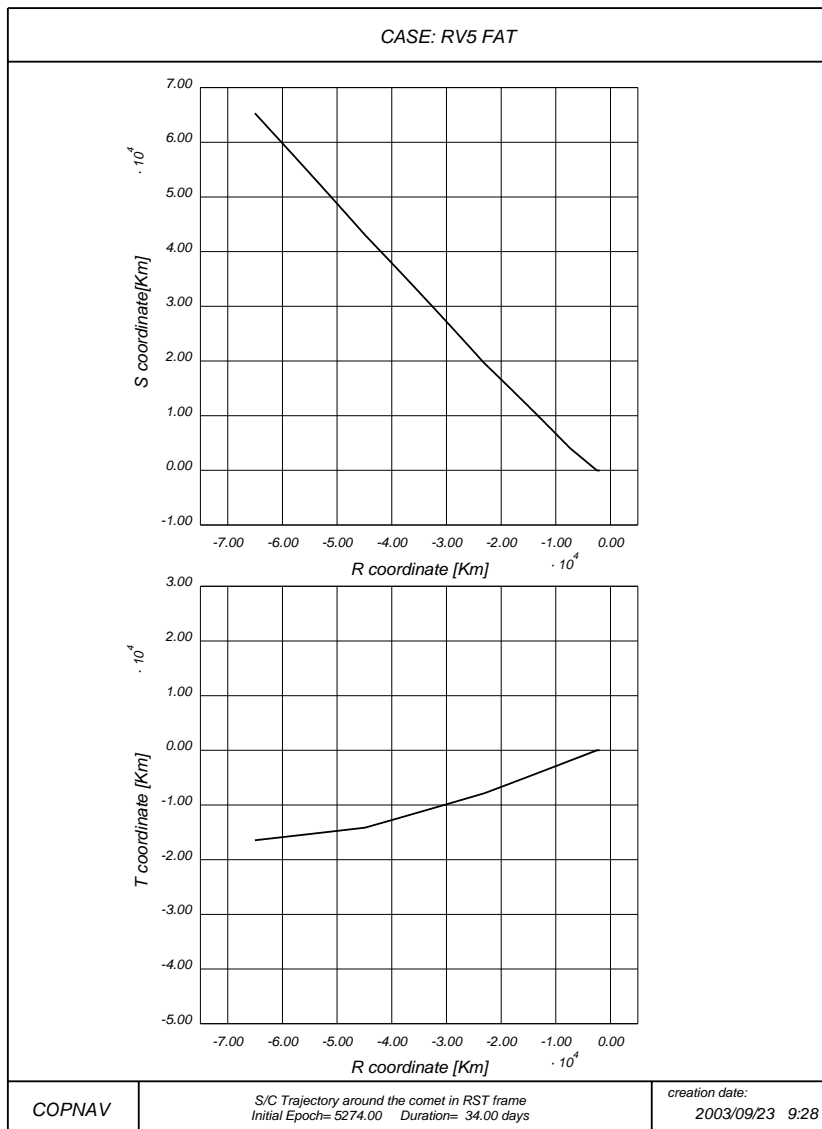


Figure 8-7: FAT Numerical Trajectory (RST Frame)

The R axis has the direction of the position vector of the comet, the S axis is perpendicular to the previous one and contained in the plane of motion of the comet and the T axis makes a right-handed frame with the R and S axis.

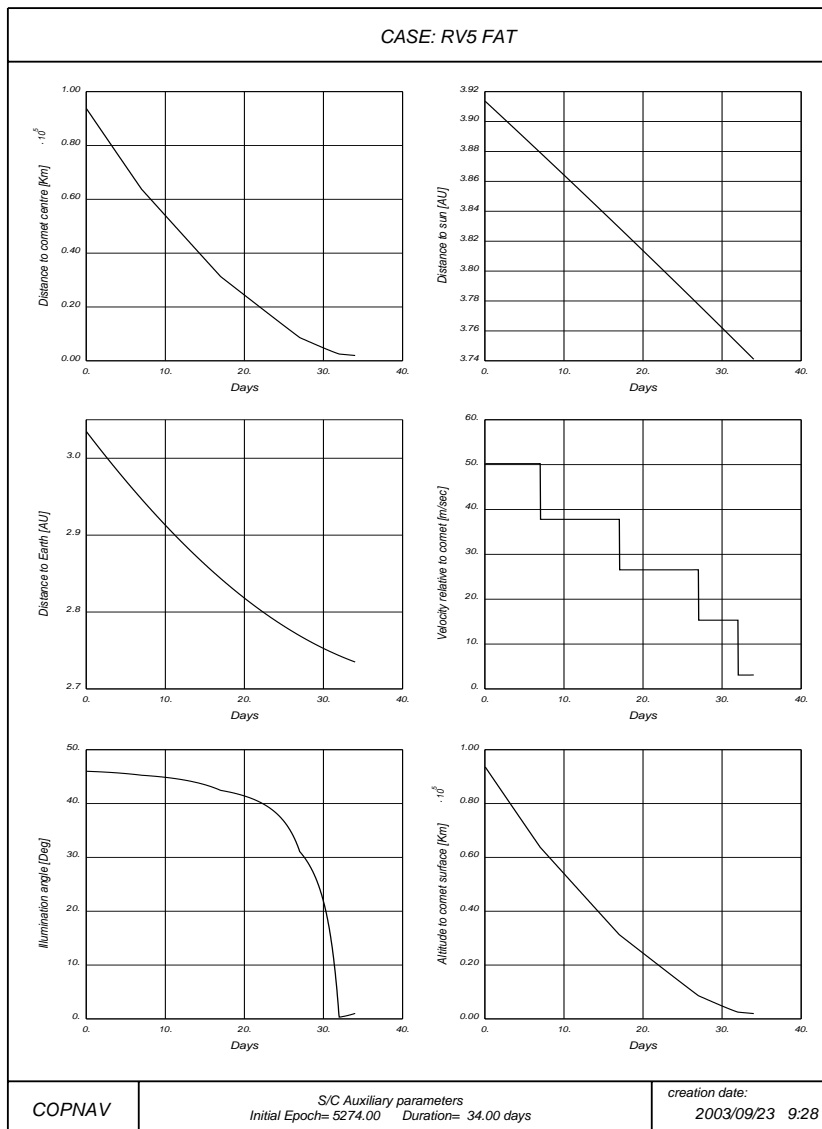


Figure 8-8: S/C Auxiliary Parameters during Far Approach Trajectory.

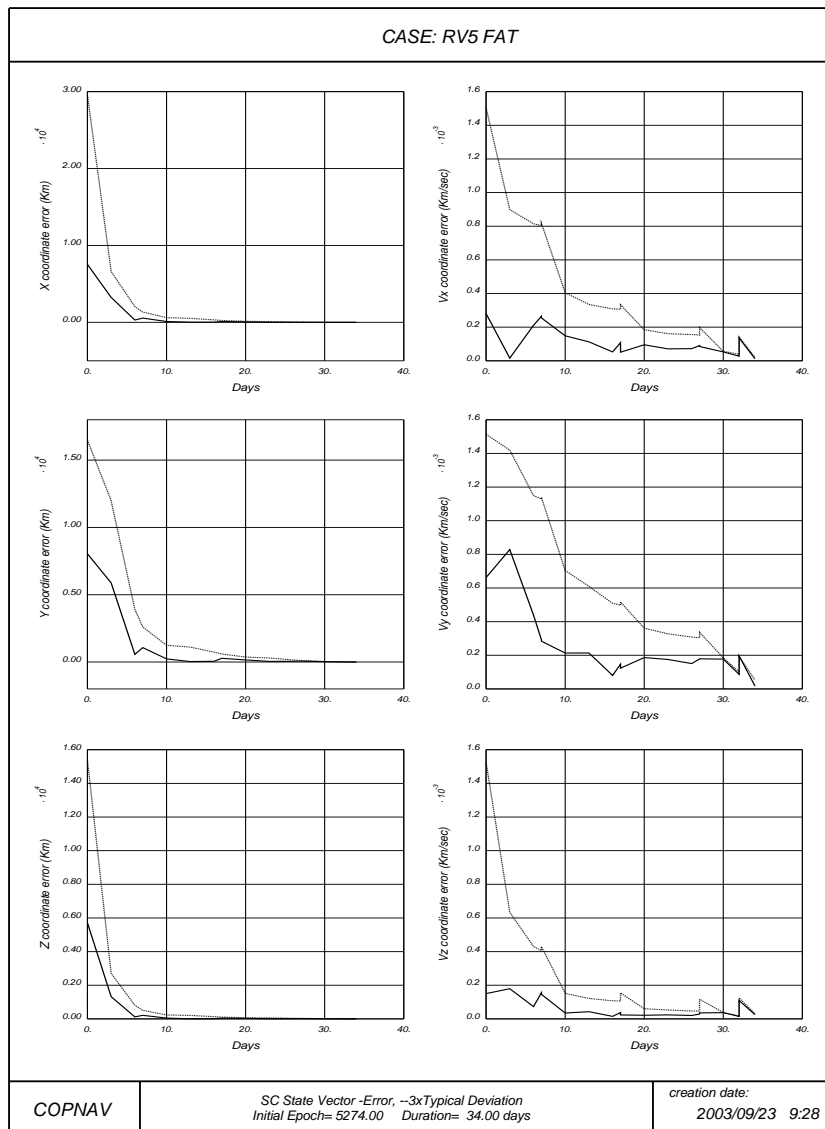


Figure 8-9 Estimation of spacecraft relative state with respect to comet

8.5 Close Approach Trajectory

During this phase the S/C finishes its approximation to the comet at a distance of 40 nucleus radii and with an impact vector of 35 comet radii. The final point of this phase is called OIP (Orbit Insertion Point) and is the point where the S/C starts orbiting the comet.

The S/C has to change the plane of motion to reach the final orbit plane of the global mapping phase. The number of manoeuvres has been set to 3. The injection is performed by means of a hyperbolic orbit with a pericentre of 25 comet radii that is the maximum distance of the global mapping phase.

A scheme of the proposed strategy and the numerical trajectory (RST Frame) obtained are shown in Figure 8-10 and Figure 8-11. The following list summarises the values of the main parameters along the trajectory for a typical case.

REAL WORLD MANOEUVRES FOR THE CLOSE APPROACH PHASE
 =====

DATE (MJD2000)	T (DAYS)	MASS (KG)	DIS (KM)	SUND (AU)	V0 (M/S)	DV (M/S)	VF (M/S)
5308.0000000	0.000	1140.023	1978.6	3.74104	3.100		
5308.0000000	0.000	1139.542	1978.6	3.74104	3.100	1.159	1.953
5313.6471483	5.647	1139.250	1024.6	3.71114	1.961	0.704	1.258
5319.3964147	11.396	1139.061	398.9	3.68034	1.271	0.458	0.814
5324.1526296	16.153	1139.061	77.9	3.65458	0.859		

TOTAL CLOSE APPROACH DELTA-V (M/S) : 2.32

Figure 8-12 shows the evolution of other interesting parameters such as distances of the S/C to the comet, Earth or Sun, phase angle, and velocity relative to the comet. The distance S/C-comet decreases enough to provide by means of the optical measurements to the landmarks, the first estimation of the nucleus attitude, nucleus spin rate, comet inertia tensor, and landmarks position. The gravitational field, however, cannot be estimated on this phase.

At the end of this phase, the values of the main parameters are:

- Duration: 17 days.
- Nominal required ΔV : 2.4 m/s.
- S/C relative position estimation error: 350 m (1σ).
- S/C relative velocity estimation error: 1.8 mm/s (1σ).
- Comet position estimation error: 130 km (1σ).
- Comet velocity estimation error: 25 mm/s (1σ).
- Euler angles estimation error: 0.95° - 1.20° (1σ).
- Comet rotation period estimation error: 0.08 % (1σ).
- Maximum inertia momentum estimation error: 10 % (1σ).
- Landmark position estimation error: 6-10 m (1σ).

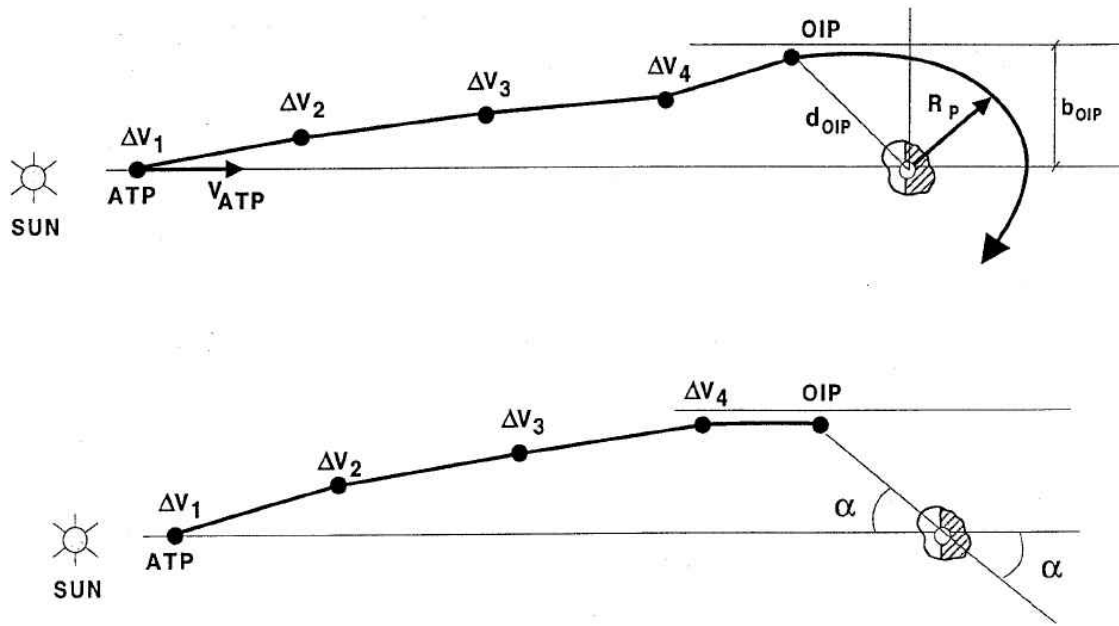


Figure 8-10: CAT Strategy

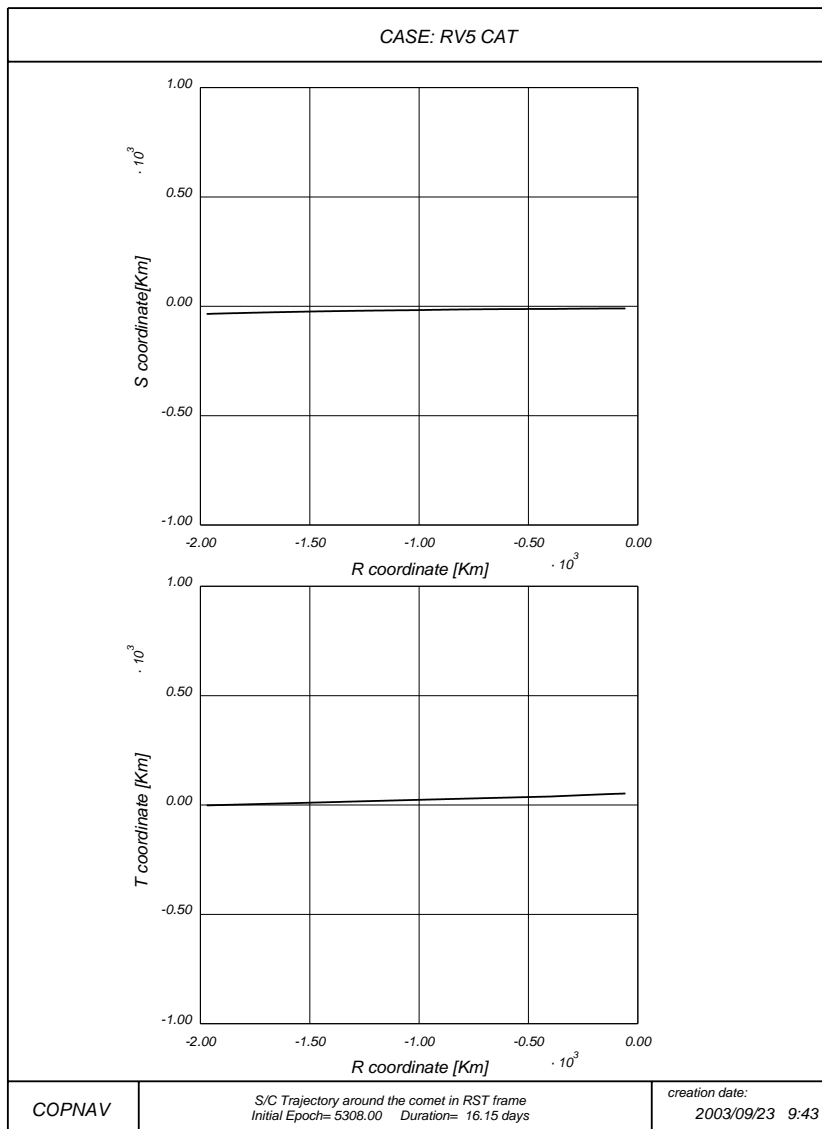


Figure 8-11: CAT Numerical Trajectory (RST Frame)

The R axis has the direction of the position vector of the comet, the S axis is perpendicular to the previous one and contained in the plane of motion of the comet and the T axis makes a right-handed frame with the R and S axis.

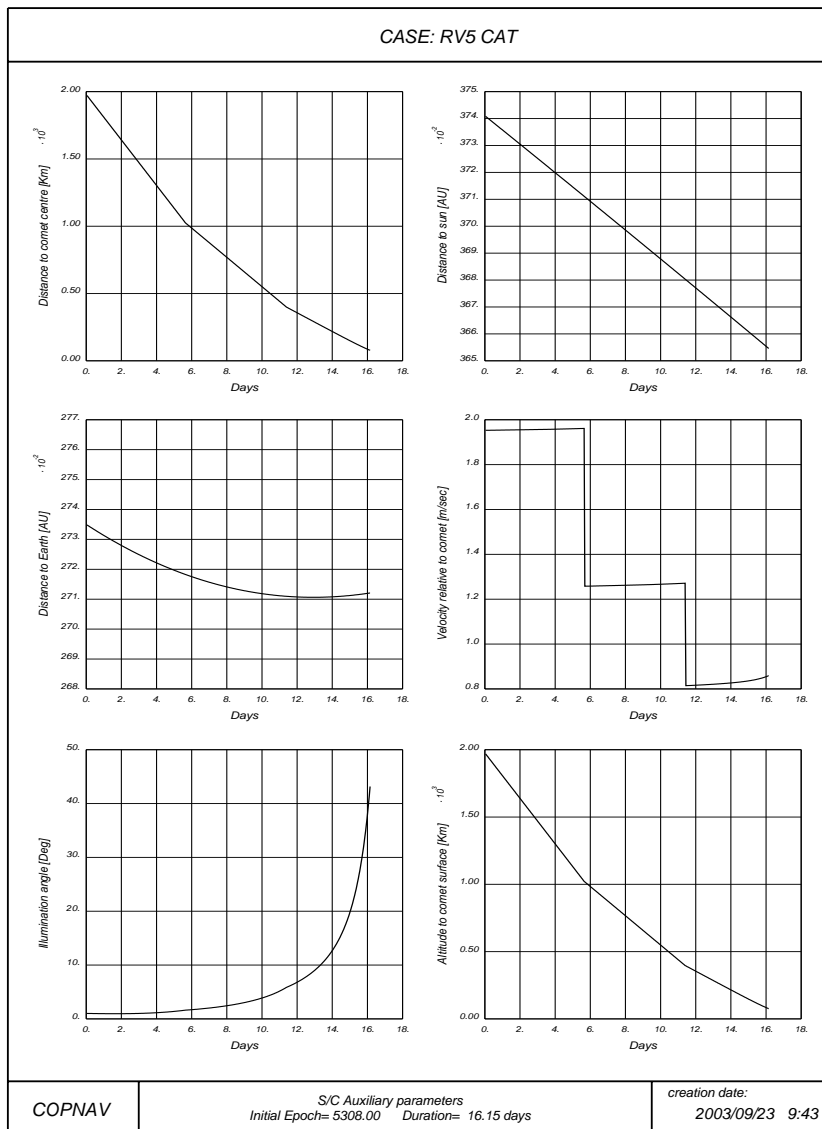


Figure 8-12: S/C auxiliary parameters during Close Approach Trajectory.

8.6 Transition to Global Mapping

This phase consists on a series of manoeuvres that starts at OIP (Orbit Insertion Point) and ends at the starting point of the global mapping phase. The sequence of manoeuvres must reduce the orbit distance from its value at OIP (40 comet radii) down to the distance of the global mapping

phase (10 - 25 comet radii). The sequence starts at the pericentre of the incoming hyperbola where the orbit is circularised by means of a first ΔV . A second manoeuvre injects the S/C into a Hohmann transfer orbit that injects the S/C into the final mapping orbit by means of a third circularisation manoeuvre.

A scheme of the proposed strategy and the numerical trajectory obtained are shown in Figure 8-13 and Figure 8-14.

The following list summarises the values of the main parameters along the trajectory for a typical case.

REAL WORLD MANOEUVRES FOR THE TRANS. TO GLOBAL MAPPING
 =====

DATE (MJD2000)	T (DAYS)	MASS (KG)	DIS (KM)	SUND (AU)	V0 (M/S)	DV (M/S)	VF (M/S)
5324.1526296	0.000	1138.841	77.9	3.65458	0.859	0.531	0.373
5325.2391475	1.087	1138.780	52.7	3.64866	0.419	0.146	0.498
5326.1087927	1.956	1138.668	40.4	3.64391	0.532	0.270	0.271
5328.1387980	3.986	1138.656	41.8	3.63280	0.265	0.029	0.261
5330.9280002	6.775	1138.656	40.1	3.61745	0.269	0.000	0.269
5333.6567011	9.504	1138.655	40.7	3.60235	0.260	0.003	0.258
5336.4805431	12.328	1138.652	38.9	3.58663	0.272	0.007	0.267
5338.9776775	14.825	1138.652	37.1	3.57265	0.283		

TOTAL TRANS. TO GLOBAL MAP. DELTA-V (M/S) : 0.99

The Figure 8-15 shows the evolution of other interesting parameters such as distances of the S/C to the comet, Earth or Sun, phase angle, and velocity relative to the comet.

It can be seen that there is a strong reduction in the relative velocity at the beginning of the phase to inject the S/C into the orbit around the comet. The distance to the comet also decreases deeply at the beginning until the injection. On the sixth plot small irregularities on the distance to the comet surface can be observed. They are due to the craters and mountains existing on the comet surface.

During this phase, the processing of on ground and on board measurements continues, and the estimation of all the comet kinematics and gravitational parameters will be improved. The Figure 8-16, Figure 8-17 and Figure 8-18 show the evolution of the estimation errors in Euler angles and angular rate, Landmark position and gravitational field parameters during this phase. The dotted line represents the 3σ error while the continuous line represents the real error during the simulation. The estimation of the Euler angles, which started during the previous phase, continues during the Transition to Global Mapping reducing the 3σ by a factor of around 5 times the initial value. The components of the rotational velocity in the plane perpendicular to the axis with maximum inertia momentum can be estimated now, while the error of the main component continues decreasing. The landmark position knowledge is also improved reaching during this phase values around several meters. Due to the information provided by the rotation of the comet, the coordinates in the plane perpendicular to the rotation axis are better known than along this axis. At this phase, since the distance to the comet has been reduced sufficiently, the estimation of the gravitational field can start. Both the gravitational constant and inertial momentum rates (I_{yy}/I_{xx} , I_{zz}/I_{xx}) errors are reduced but the knowledge of inertial momentum I_{xx} is not increased yet.

At the end of this phase, the values of the main parameters are:

- Duration: about 15 days.
- Required ΔV : 1 m/s.
- S/C relative position estimation error: 50 m (1σ).
- S/C relative velocity estimation error: 0.6 mm/s (1σ).
- Comet position estimation error: 110 km (1σ).
- Comet velocity estimation error: 27 mm/s (1σ).
- Euler angles estimation error: 0.3° (1σ).
- Comet rotation period estimation error: 0.3 % (1σ).
- Gravitational cte. estimation error: 0.1 % (1σ).
- Maximum inertia momentum estimation error: 8.6 % (1σ).
- Landmark position estimation error: 5-13 m (1σ).

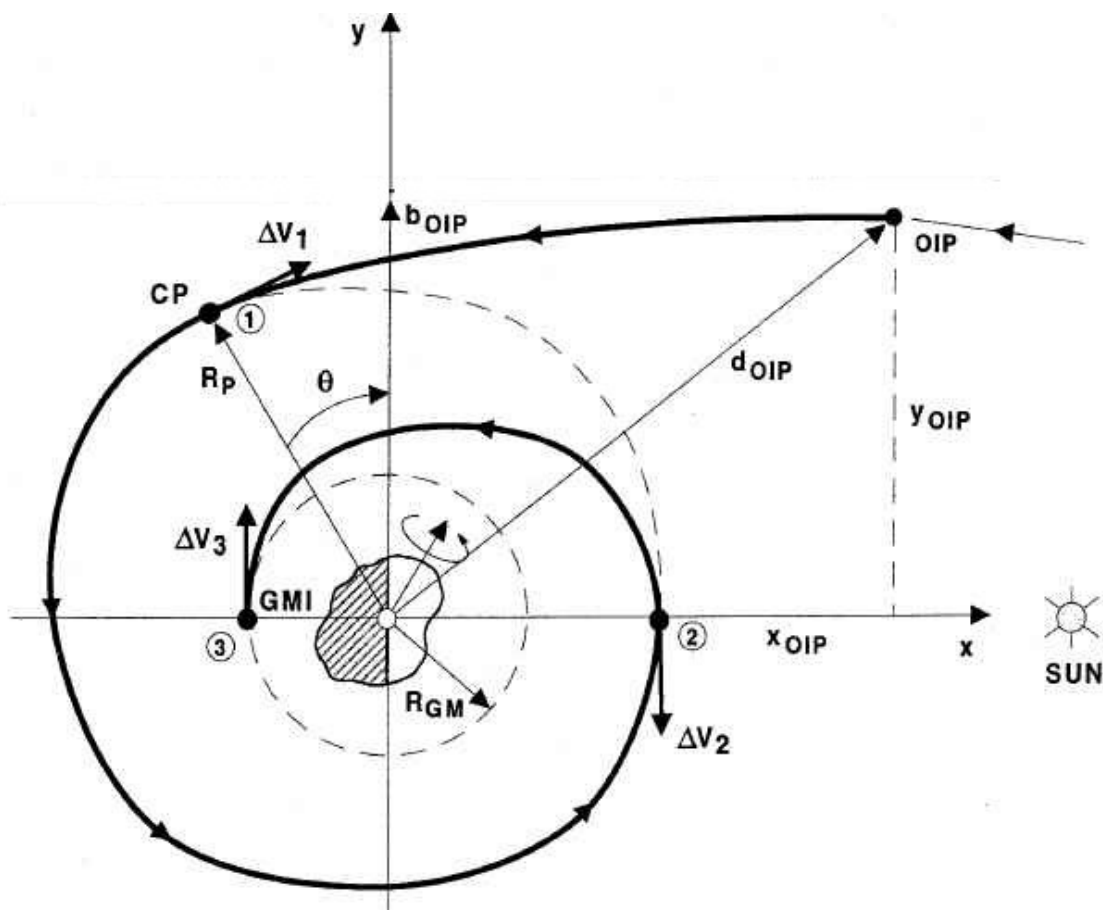


Figure 8-13: TGM Strategy

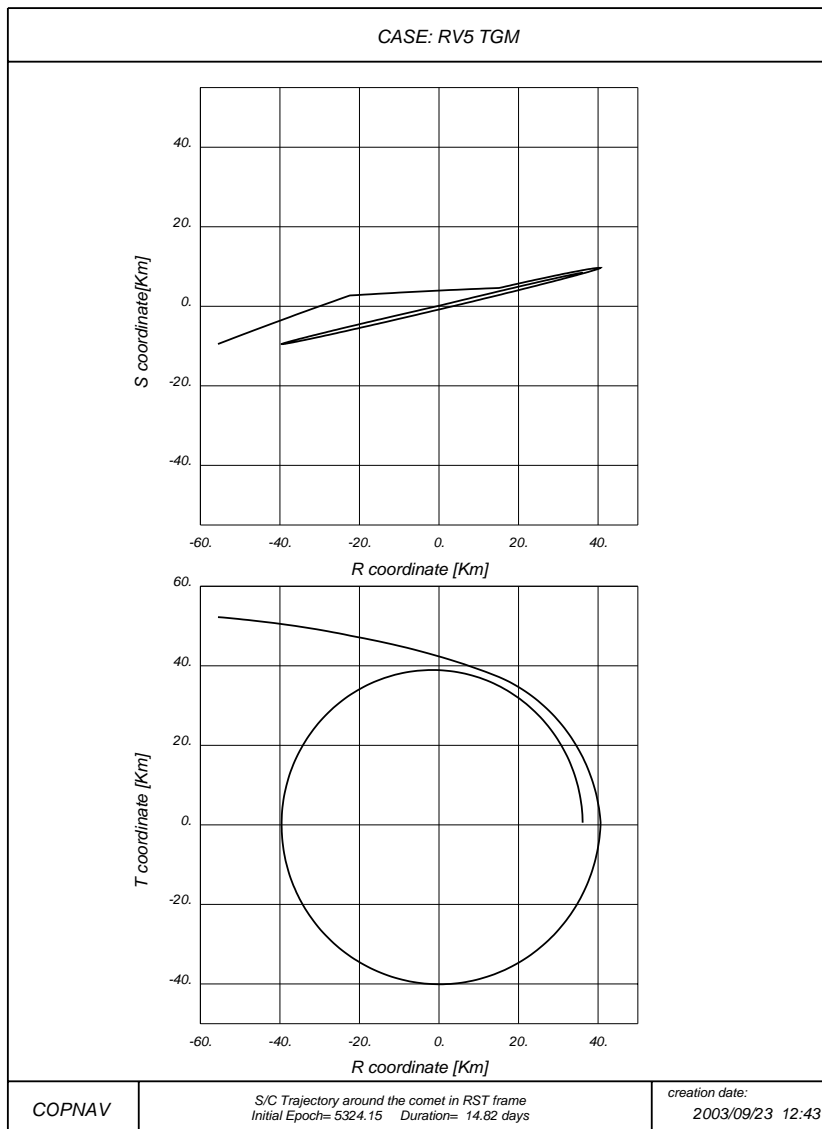


Figure 8-14: TGM Numerical Trajectory (RST Frame)

The R axis has the direction of the position vector of the comet, the S axis is perpendicular to the previous one and contained in the plane of motion of the comet and the T axis makes a right-handed frame with the R and S axis.

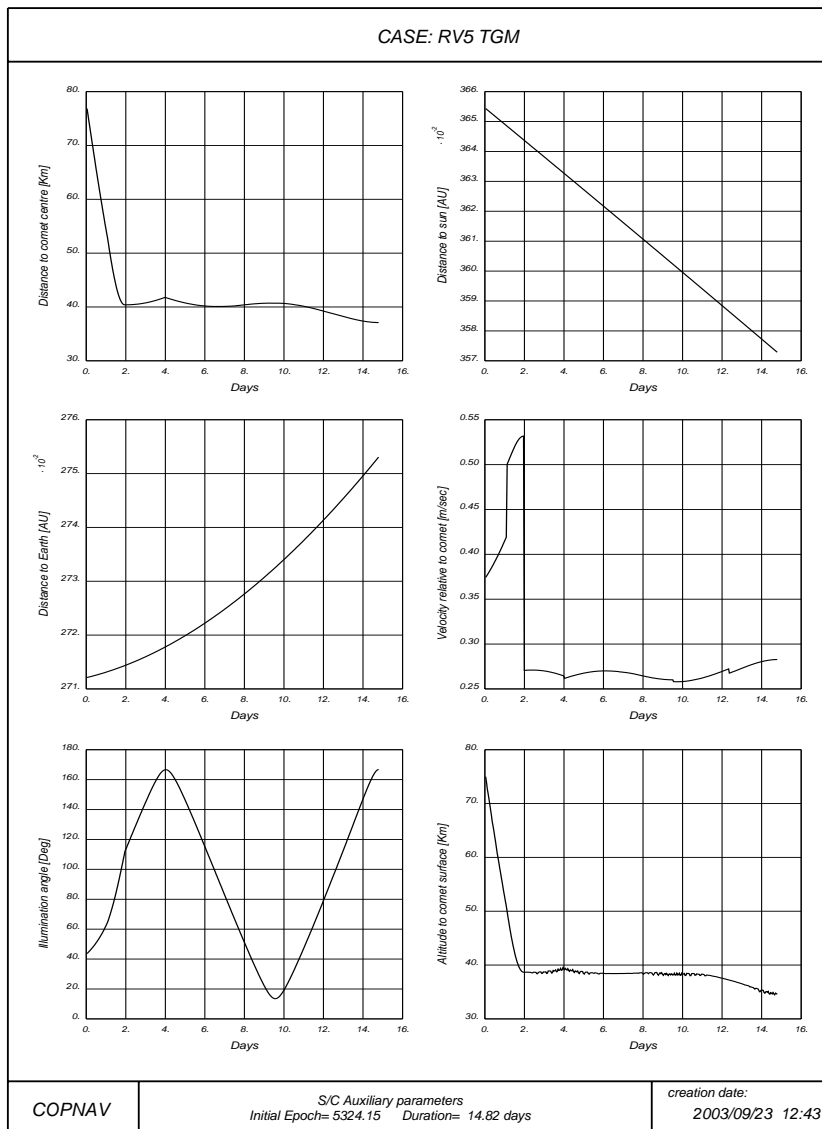


Figure 8-15: S/C Auxiliary Parameters during Transition to Global Mapping phase.

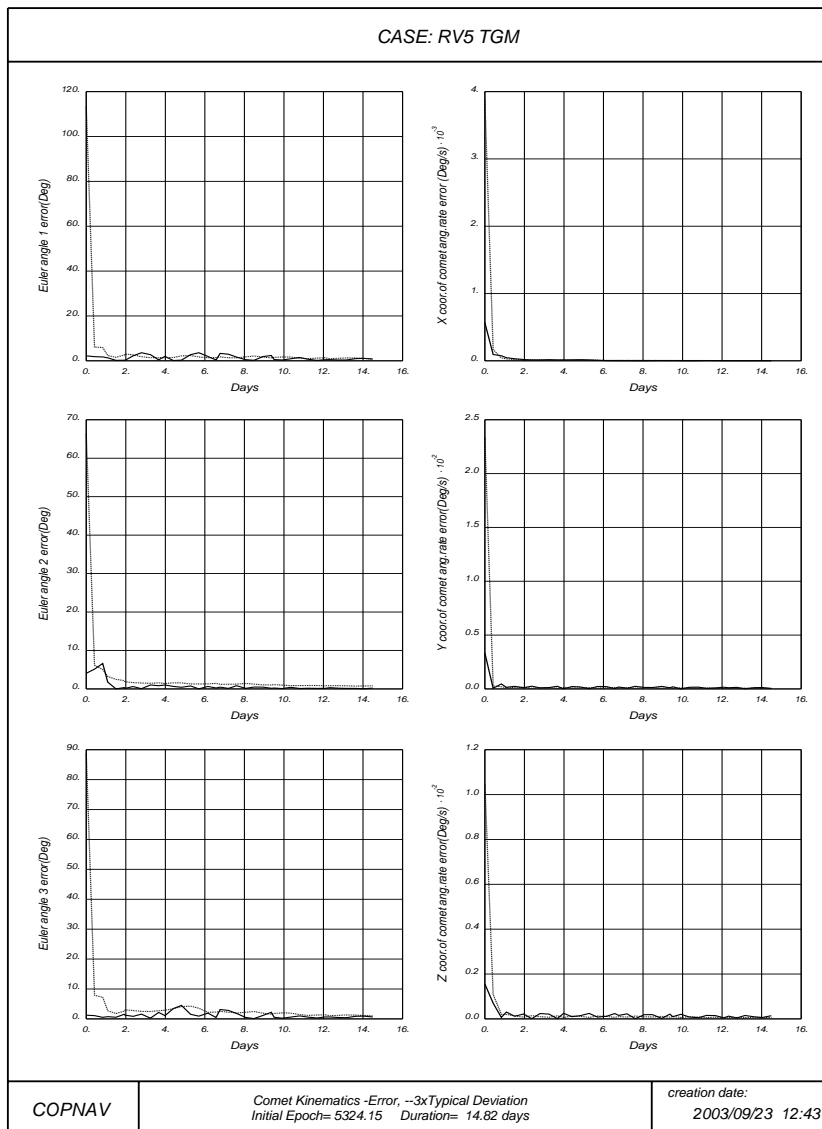


Figure 8-16: Comet Kinematics Estimation Errors during Transition to Global Mapping.

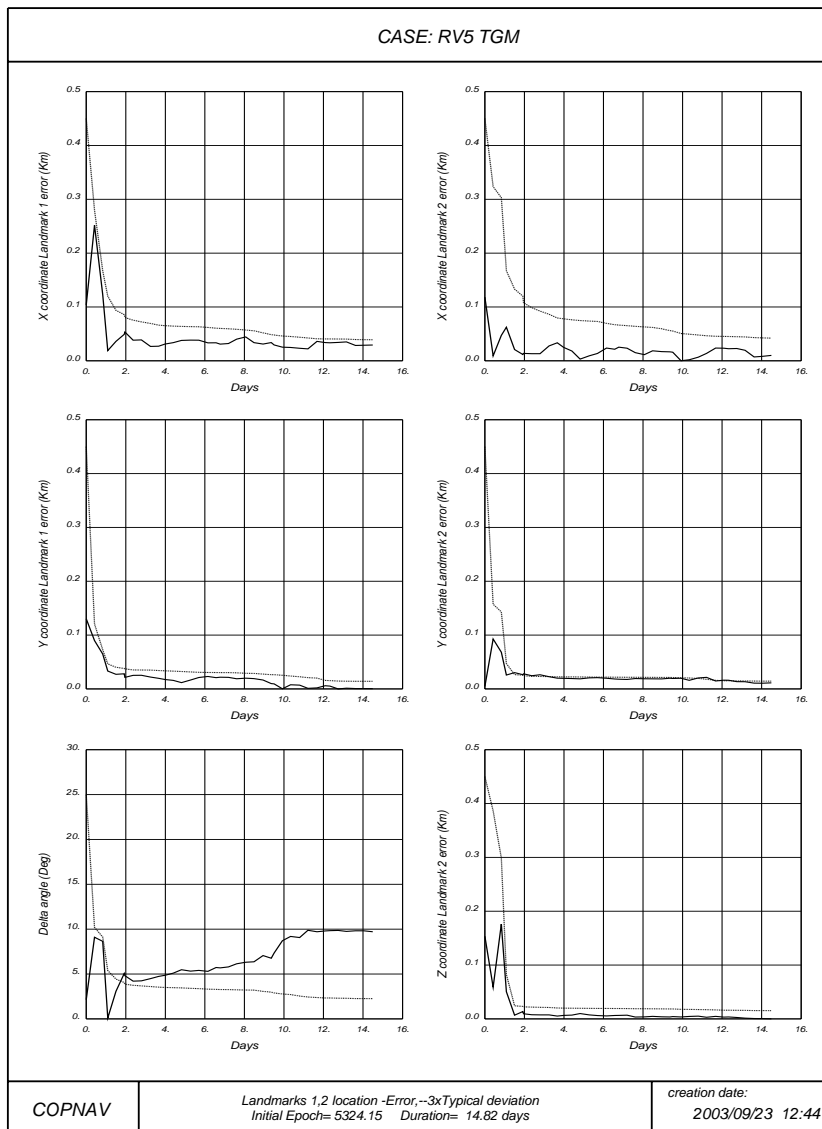


Figure 8-17: Landmark Position Estimation Errors during Transition to Global Mapping.

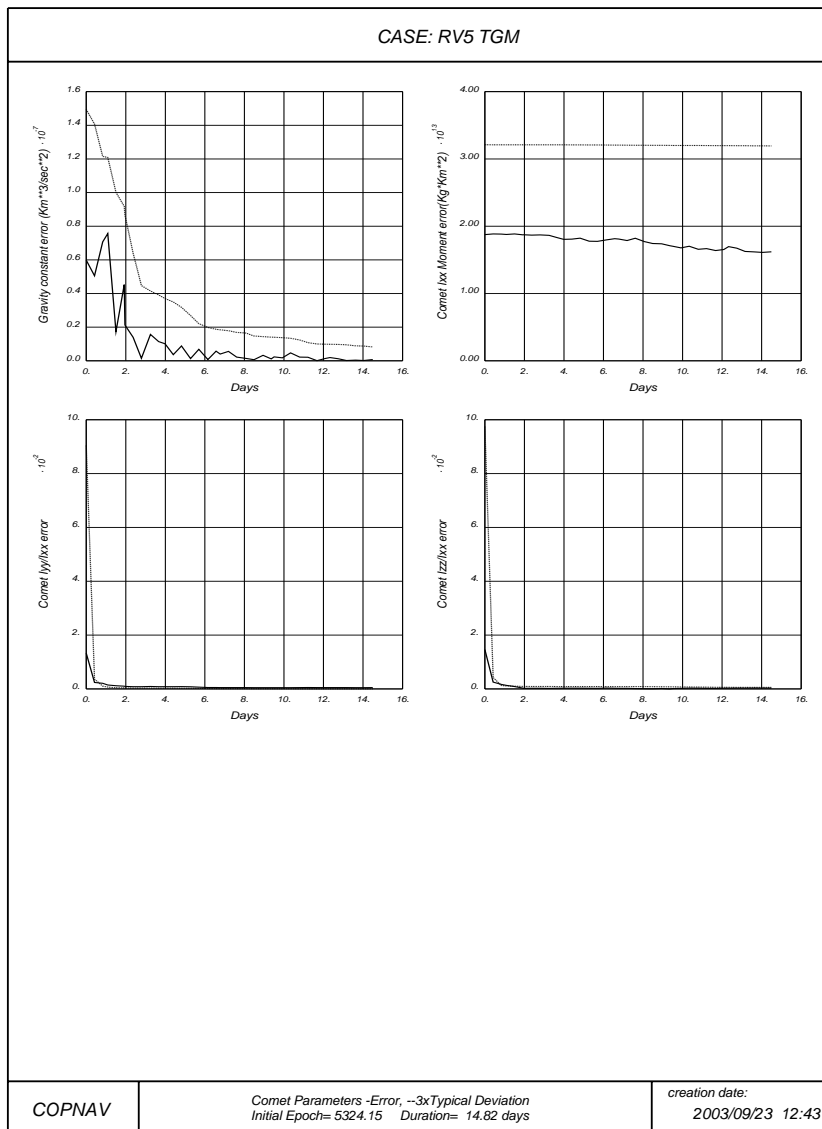


Figure 8-18: Gravitational Field Estimation Errors during Transition to Global Mapping.

8.7 Global Mapping Phase

The objective of this phase is to perform a mapping of at least 80 % of the comet surface satisfying the following requirements:

- The comet surface shall be covered with a minimum resolution of 2000 pixels across the smallest diameter.
- The orbit shall be safe.
- The volume of the acquired data during one day, shall not exceed the spacecraft memory size, and shall not exceed the data volume that can be transmitted within this day.
- The angle between the viewing direction and the mapped surface normal shall be less than 70° .

The selection of the orbital plane for the nucleus mapping must be such that Sun eclipses and Earth occultation are avoided. The recommended strategy is the following (Figure 8-19). The intersection of the plane defined by the comet angular momentum (\vec{L}) and the Sun direction with the plane perpendicular to the Sun direction defines the axis around which the orbital plane is rotated to satisfy the eclipse and Earth occultation constraints.

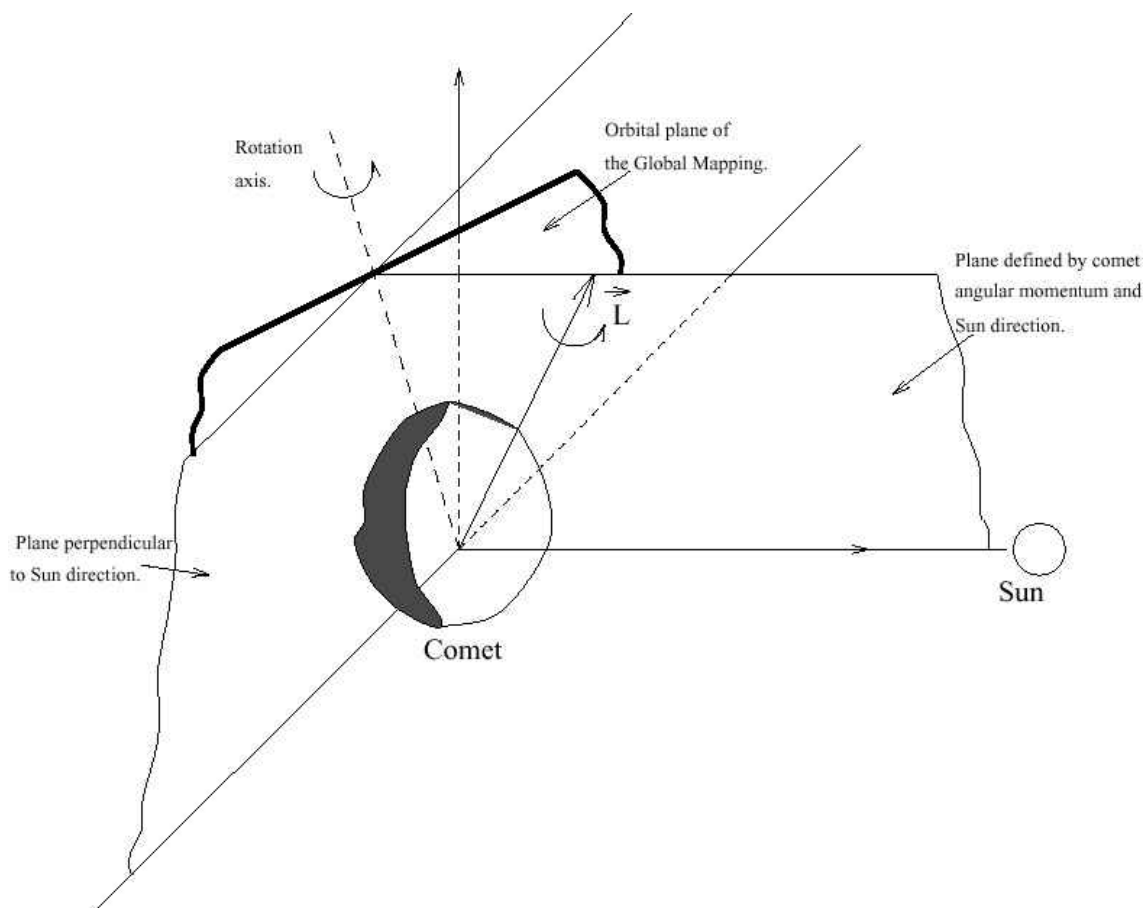


Figure 8-19: Global Mapping Orbital Plane Selection

In case of slow rotating comets it can be necessary to perform several orbits to cover the entire comet surface. This makes the strategy duration very sensitive to the comet rotation period.

The radius of the orbit is selected in the range 10 to 25 comet radii in order to cope with the constraints. The orbits will be retrograde in order to increase stability.

The numerical trajectory obtained is shown in Figure 8-20.

The following list summarises the values of the main parameters along the trajectory for a typical case.

REAL WORLD MANOEUVRES FOR THE GLOBAL MAPPING PHASE
 =====

DATE (MJD2000)	T (DAYS)	MASS (KG)	DIS (KM)	SUND (AU)	VO (M/S)	DV (M/S)	VF (M/S)
5338.9776775	0.000	1138.650	37.1	3.57265	0.283	0.006	0.278
5341.4278355	2.450	1138.646	37.8	3.55887	0.269	0.009	0.277
5343.9291795	4.952	1138.643	37.4	3.54473	0.276	0.006	0.275
5346.3996241	7.422	1138.643	37.4	3.53070	0.278		

TOTAL GLOBAL MAPPING DELTA-V (M/S) : 0.02

Figure 8-21 shows the evolution of other interesting parameters such as distances of the S/C to the comet, Earth or Sun, phase angle, and velocity relative to the comet. The first plot should be a horizontal line in the ideal case. The distance varies by about 500m due to the different perturbations and the picks on the curve represents the correction manoeuvres necessary to keep the S/C on the nominal circular orbit. The sixth plot shows the irregularities on the altitude to the with the navigation during global mapping. A continuous estimation of the navigation parameters is performed as in the previous phase. Figure 8-22, Figure 8-23 and Figure 8-24 show the evolution of the estimation errors in Euler angles and angular rate, landmark position, and gravitational field parameters during this phase. The Figure 8-25 and Figure 8-26 show the intermediate status and final result of the comet mapping with the selected strategy. For this it can be observed that almost the whole comet surface can be mapped with a mapping interval of 0.8 hours between two consecutive images.

At the end of this phase, the values of the main parameters are:

- Duration: 7.5 days.
- Required ΔV : 2 cm/s.
- S/C relative position estimation error: 36 m (1 σ).
- S/C relative velocity estimation error: 0.5 mm/s (1 σ).
- Comet position estimation error: 85 km (1 σ).
- Comet velocity estimation error: 21 mm/s (1 σ).
- Euler angles estimation error: 0.17° (1 σ).
- Comet rotation period estimation error: 0.014 % (1 σ).
- Gravitational cte. estimation error: 0.07 % (1 σ).
- Maximum inertia momentum estimation error: 8.6 % (1 σ).

- Landmark position estimation error: 2.4-7 m (1σ).

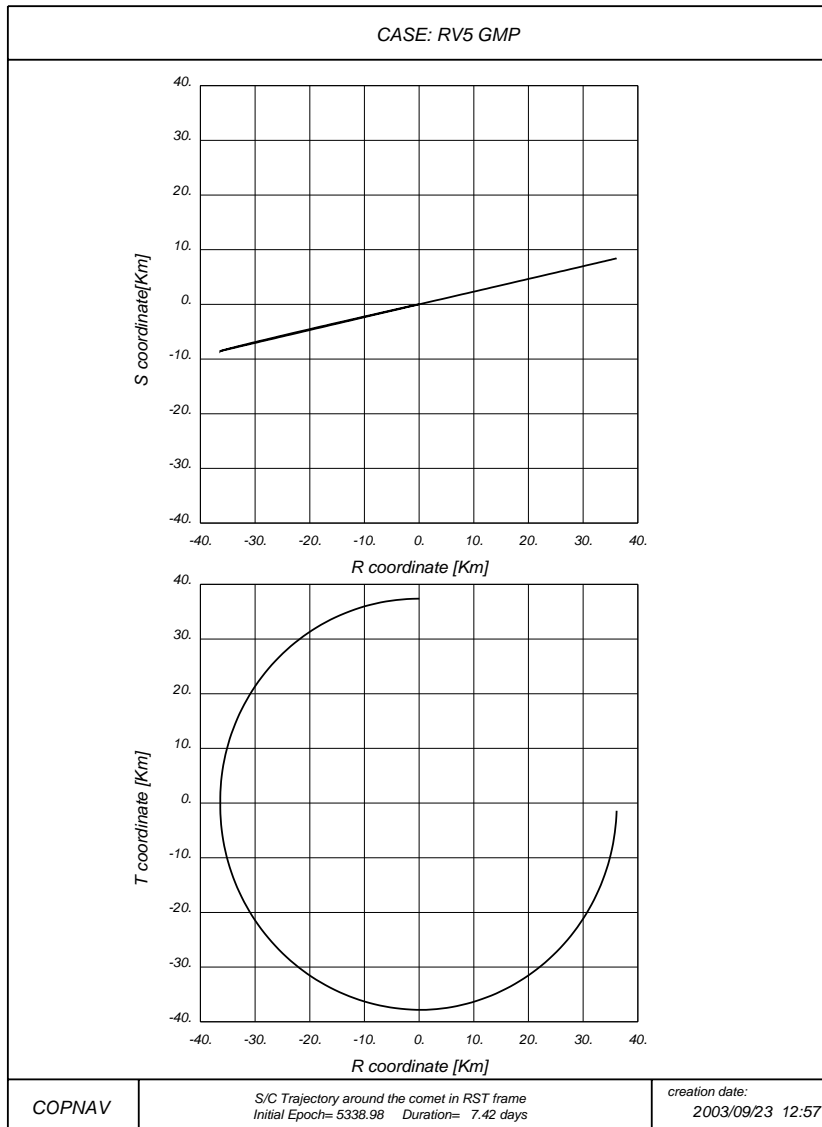


Figure 8-20: GMP Numerical Trajectory (RST Frame)

The R axis has the direction of the position vector of the comet, the S axis is perpendicular to the previous one and contained in the plane of motion of the comet and the T axis makes a right-handed frame with the R and S axis.

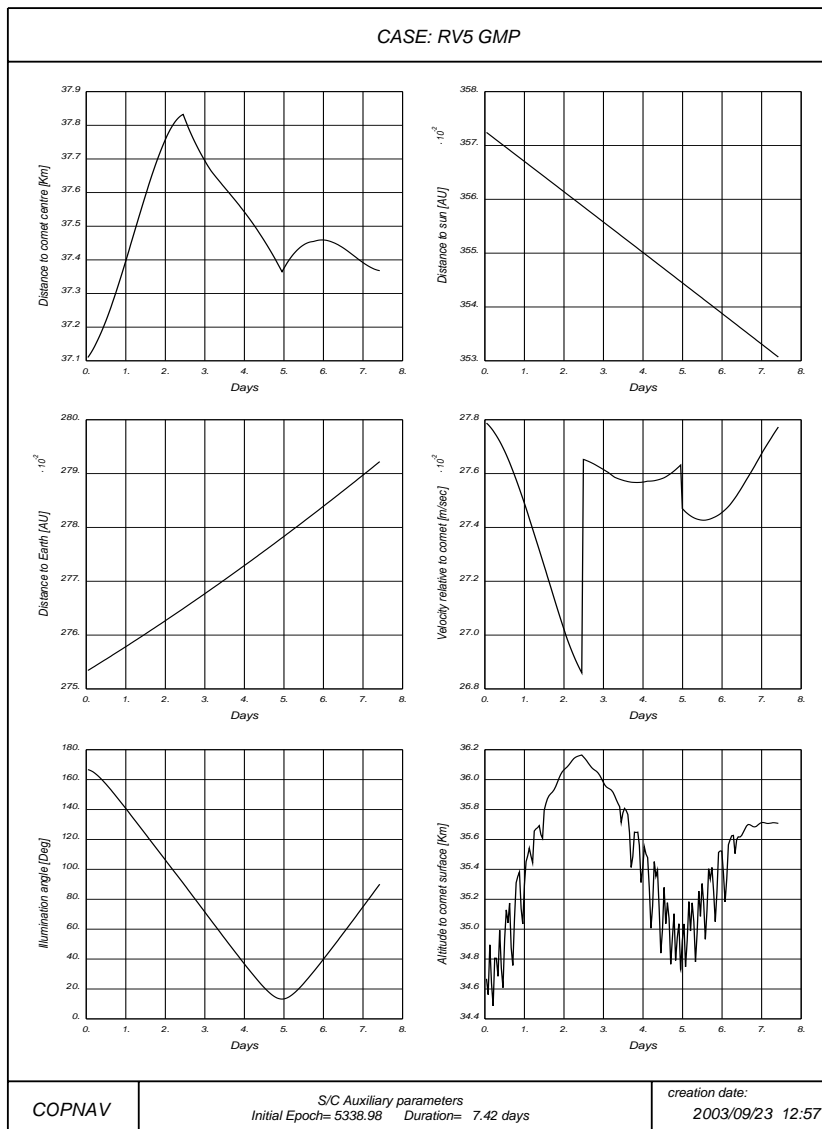


Figure 8-21: S/C Auxiliary Parameters during Global Mapping phase.

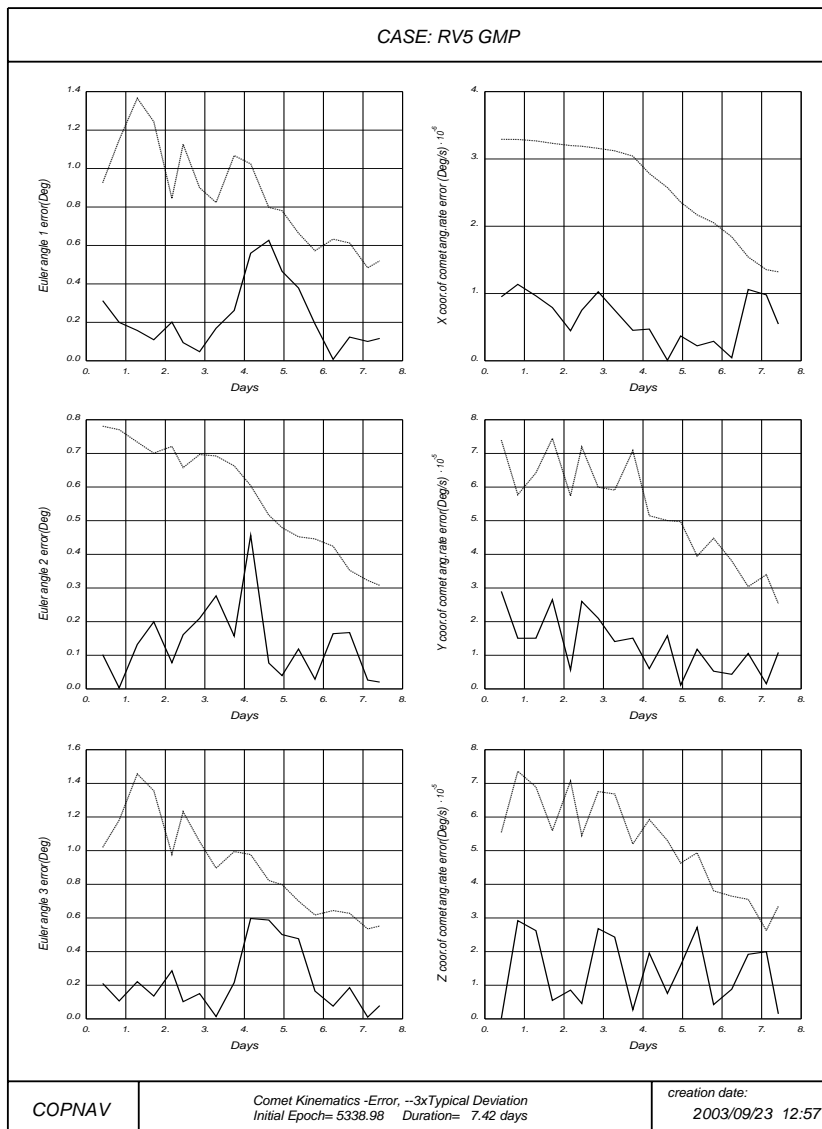


Figure 8-22: Comet Kinematics Estimation Errors during Global Mapping.

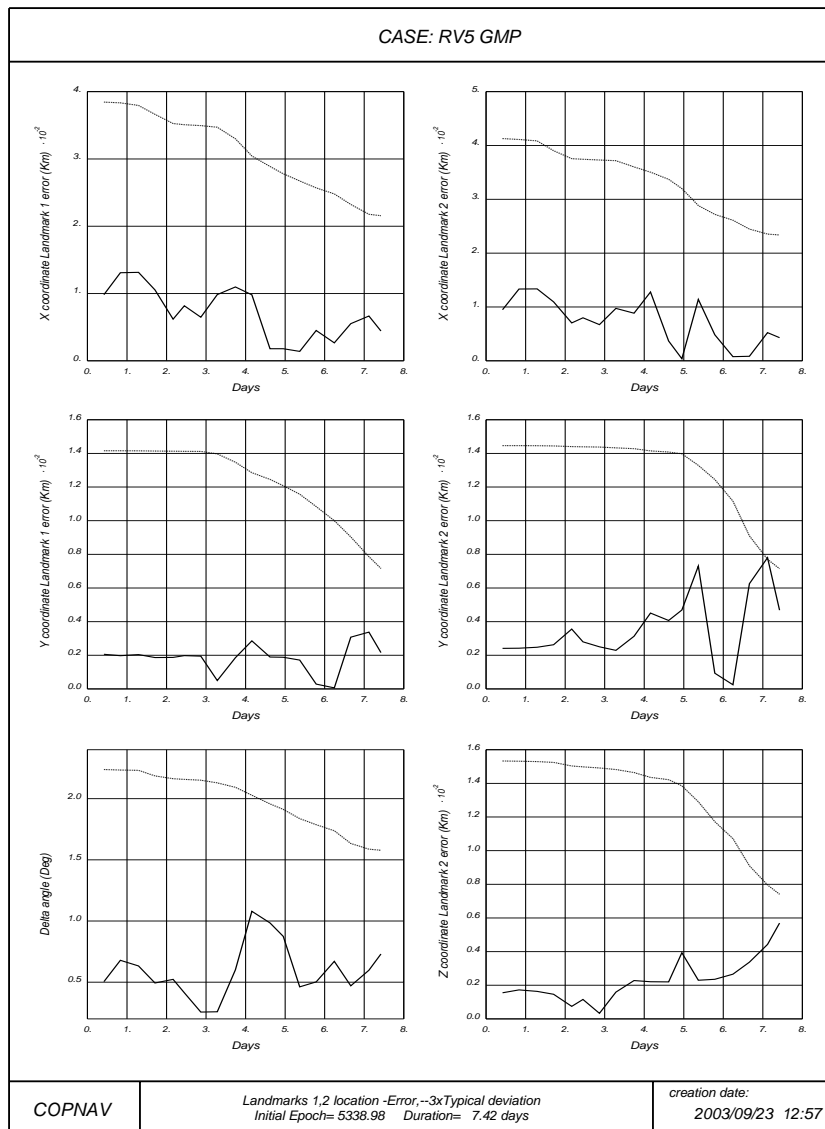


Figure 8-23: Landmark Position Estimation Errors during Global Mapping.

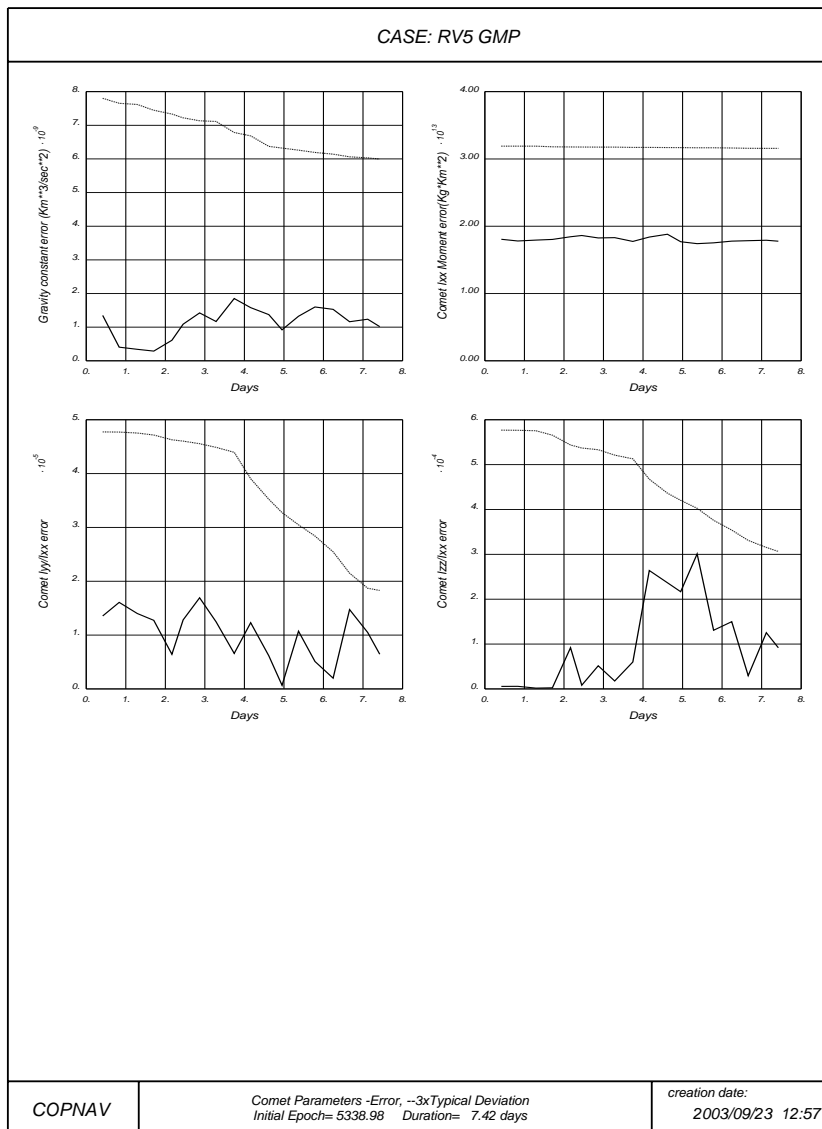


Figure 8-24: Gravitational Field Estimation Errors during Global Mapping.

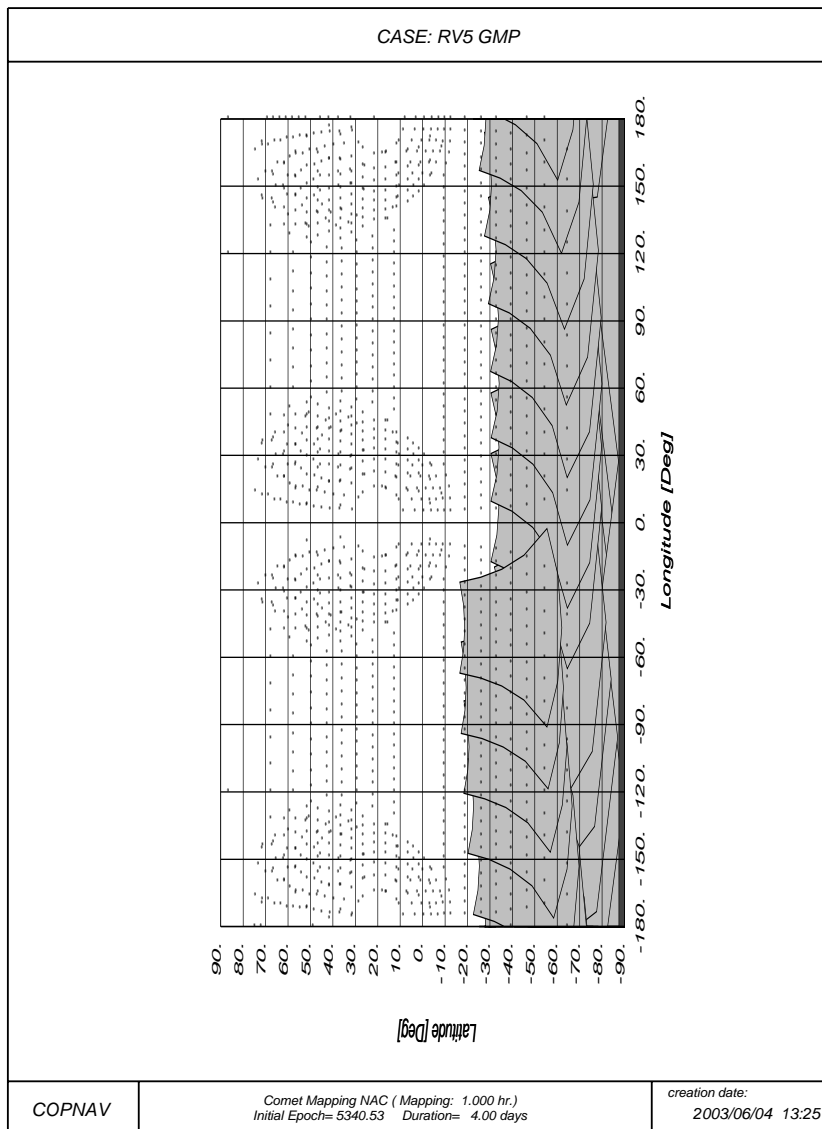


Figure 8-25: Mapped Surface of the Comet after 4 days.

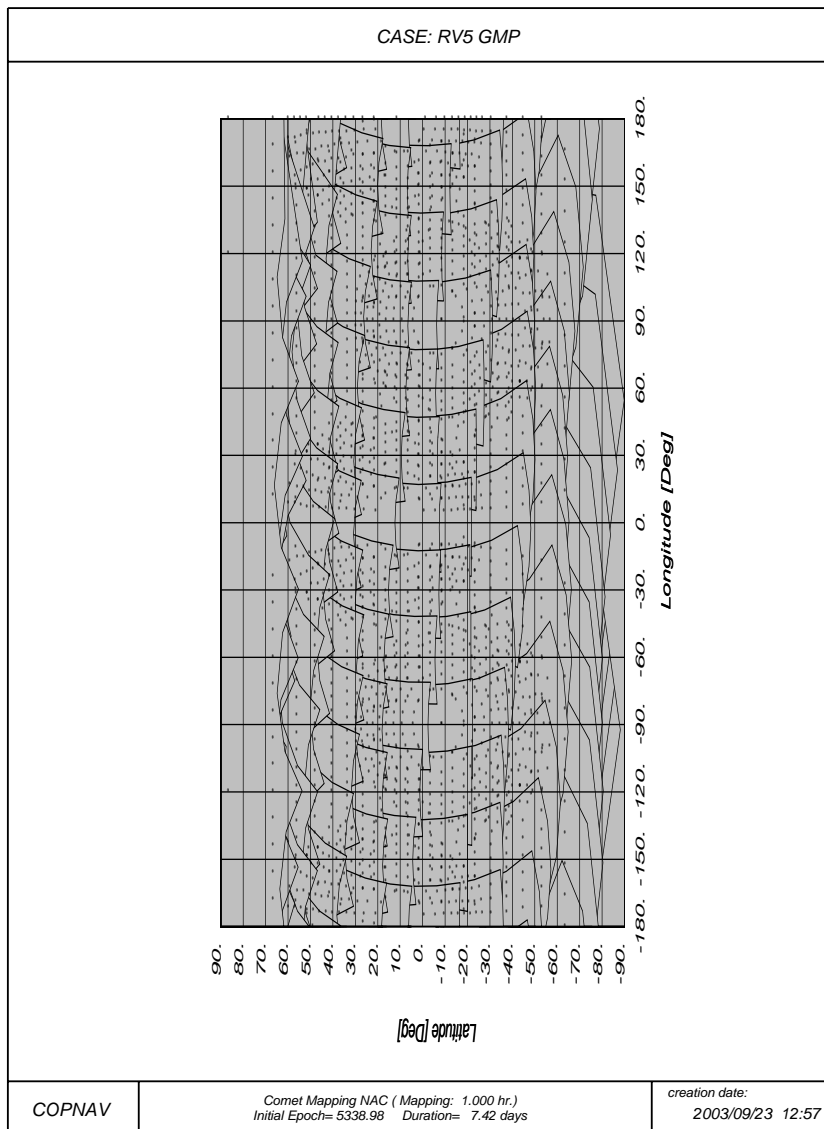


Figure 8-26: Mapped Surface of the Comet at end of GMP.

8.8 Close Observation Phase

The objective of the Close Observation Phase (COP), is to fly-over five different areas on the comet surface at a distance of less than 1 comet radius. Some additional constraints are the following ones:

- The optical resolution shall be 1 m.
- Continuous solar phase and Earth communications are required.
- The orbits shall be safe.
- The observed area shall be illuminated during fly-over with a phase angle below 70°. (Sun direction to local surface normal)
- The surface-viewing angle shall be below 30° . (Local surface normal and orbiter direction)

The orbit strategy has been defined taking into account these constraints. The orbital plane has been chosen to avoid Sun eclipses or Earth occultation and to perform observation close to the terminator. Once the plane has been chosen, the time of fly-over is defined by the crossing of the candidate site with this plane. After performing each fly-over a manoeuvre in the orbit plane is performed such that the S/C will fly-over the next candidate site when it crosses the orbital plane. That means that the crossing time of the orbital plane by the candidate site will be in phase with the fly-over of the observed area by the S/C. In case of long rotation period, it may be necessary to perform several orbits before the next fly-over. This fact makes the strategy duration very sensitive to the angular rate of the comet.

The resolution constraint determines the maximum altitude during this phase. On the other hand the safety constraint sets the minimum distance to the comet surface.

A scheme of the proposed strategy and the numerical trajectory obtained are shown in Figure 8-27 and Figure 8-28.

The following list summarises the values of the main parameters along the trajectory for a typical case.

REAL WORLD MANOEUVRES FOR THE CLOSE OBSERVATION PHASE
 =====

DATE (MJD2000)	T (DAYS)	MASS (KG)	DIS (KM)	SUND (AU)	V0 (M/S)	DV (M/S)	VF (M/S)
5346.3996241	0.000	1138.540	37.4	3.53070	0.278	0.249	0.126
5347.4287795	1.029	1138.538	30.6	3.52483	0.223	0.006	0.222
5348.4520794	2.052	1138.421	4.4	3.51898	1.060	0.282	0.782
5348.5508980	2.151	1138.384	4.4	3.51842	0.810	0.090	0.897
5348.9009967	2.501	1138.347	6.9	3.51641	0.573	0.088	0.587
5349.2573854	2.858	1138.268	5.0	3.51437	0.801	0.191	0.985
5349.4297262	3.030	1138.117	9.9	3.51338	0.647	0.365	0.427
5351.6512718	5.252	1138.051	4.9	3.50062	0.890	0.159	0.888
5352.0881444	5.689	1138.043	10.1	3.49811	0.427	0.019	0.421
5352.5558555	6.156	1137.984	4.9	3.49541	0.886	0.143	0.878
5353.0407952	6.641	1137.950	9.2	3.49261	0.466	0.081	0.443
5353.4583815	7.059	1137.880	4.5	3.49020	0.897	0.169	0.770
5353.7754050	7.376	1137.852	4.6	3.48837	0.786	0.067	0.853
5354.3637075	7.964	1137.852	4.8	3.48496	0.824		

TOTAL CLOSE OBSERVATION DELTA-V (M/S) : 1.91

The Figure 8-29 shows the evolution of other interesting parameters such as distances of the S/C to the comet, Earth or Sun, phase angle, and velocity relative to the comet.

During this phase the navigation system continues providing estimates of all the parameters. The 3rd order terms of the gravitational potential cannot be estimated even with the reduction of the distance to the comet. The errors in the rest of the parameters are reduced slightly or remain on the vicinity of the values obtained on the previous phase. Figure 8-30, Figure 8-31, Figure 8-32 and Figure 8-33 show the evolution of the estimation errors in Euler angles and angular velocity, Landmark position and gravitational field parameters during this phase. The last Figure 8-33 points out that there is no reduction in the typical deviation of the 3rd order coefficients of the gravitational potential.

At the end of this phase, the values of the main parameters are:

- Duration: about 8 days.
- Required ΔV : 2 m/s.
- S/C relative position estimation error: 4 m (1 σ).
- S/C relative velocity estimation error: 0.7 mm/s (1 σ).
- Comet position estimation error: 78 km (1 σ).
- Comet velocity estimation error: 18 mm/s (1 σ).
- Euler angles estimation error: 0.1° (1 σ).
- Comet rotation period estimation error: 0.08 % (1 σ).
- Gravitational cte. estimation error: 0.04 % (1 σ).
- Maximum inertia momentum estimation error: 3.8 % (1 σ).
- Landmark position estimation error: 1.5-3 m (1 σ).

In this study, the five regions selected for close observation are:

(0°,20°), (70°,-20°), (145°,0°), (140°,40°), (-70°,-20°). Each region is defined by the longitude and latitude of its mid point. Figure 8-34 shows the coverage of these areas by the NAC camera.

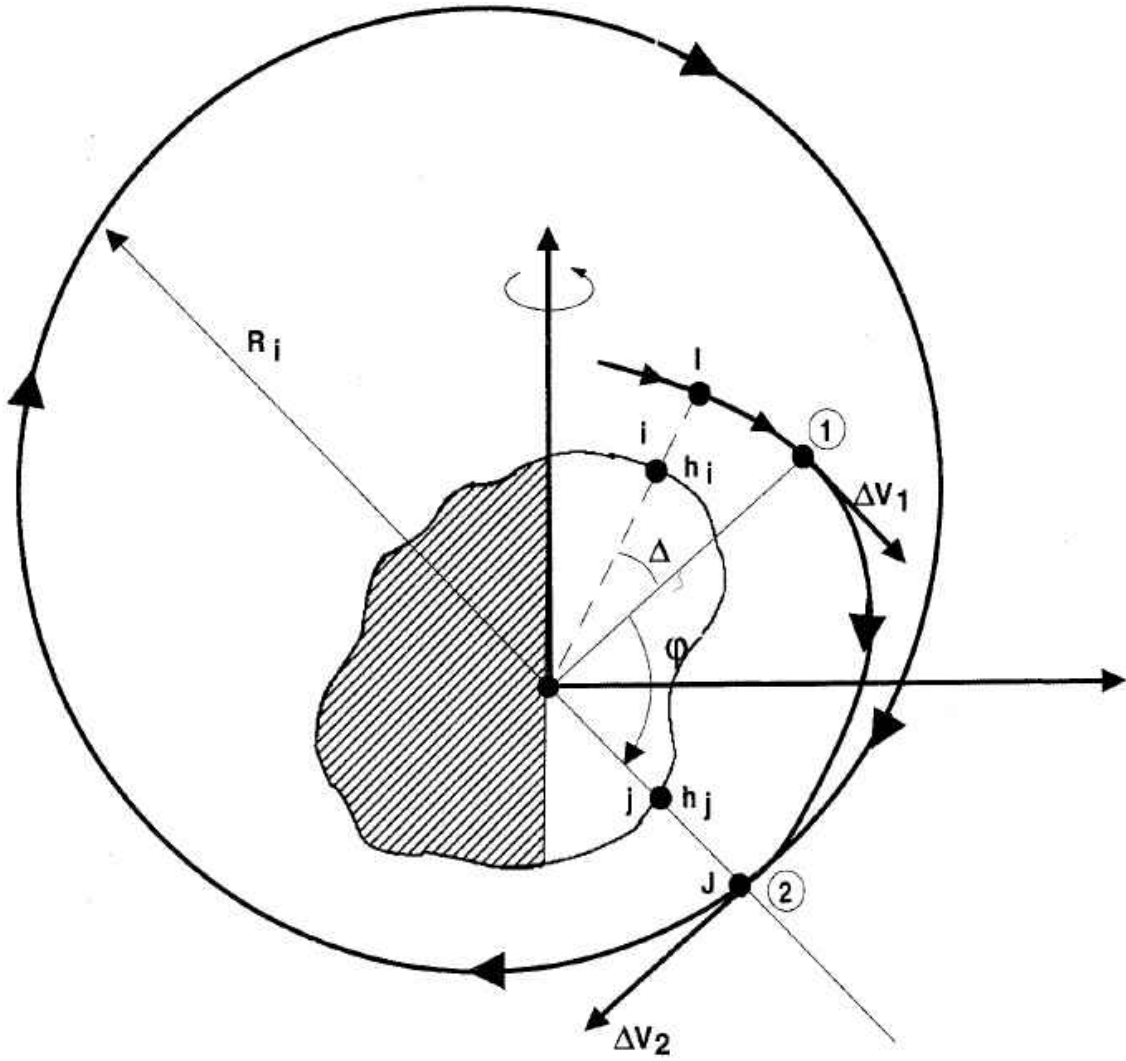


Figure 8-27: COP Strategy

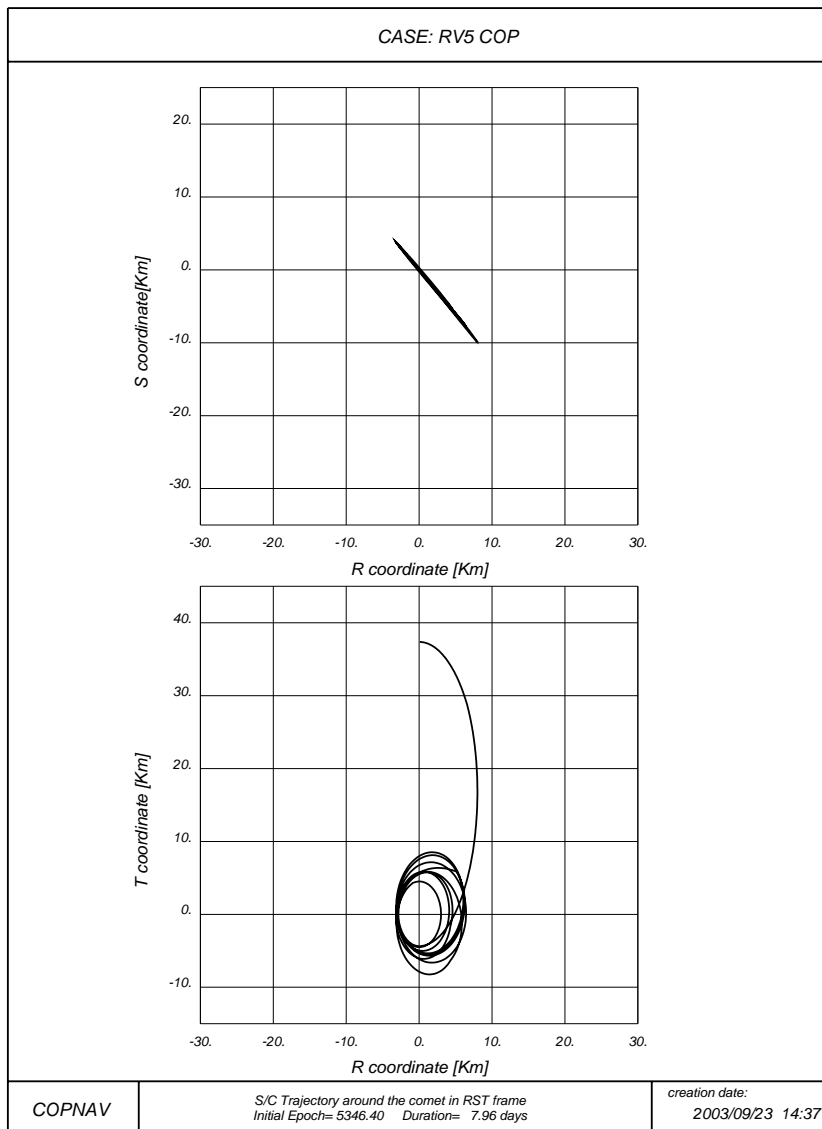


Figure 8-28: COP Numerical Trajectory (RST Frame)

The R axis has the direction of the position vector of the comet, the S axis is perpendicular to the previous one and contained in the plane of motion of the comet and the T axis makes a right-handed frame with the R and S axis.

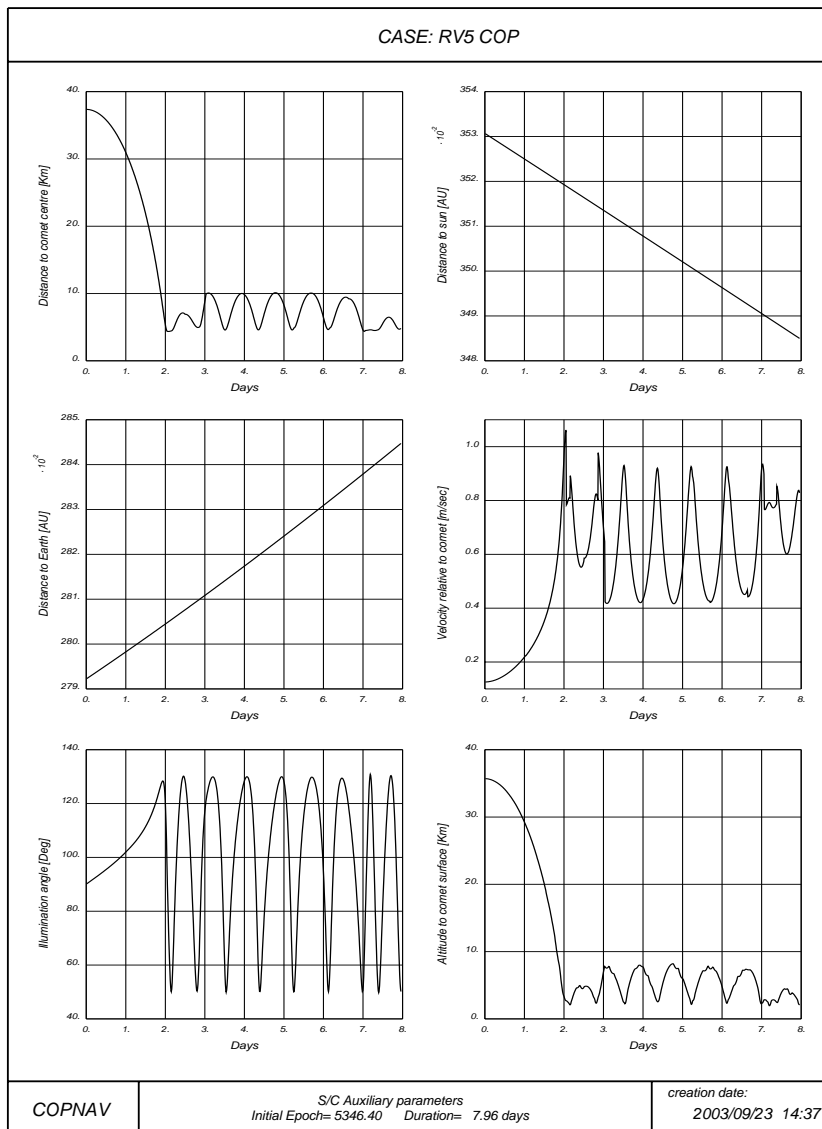


Figure 8-29: S/C Auxiliary Parameters during Close Observation Phase.

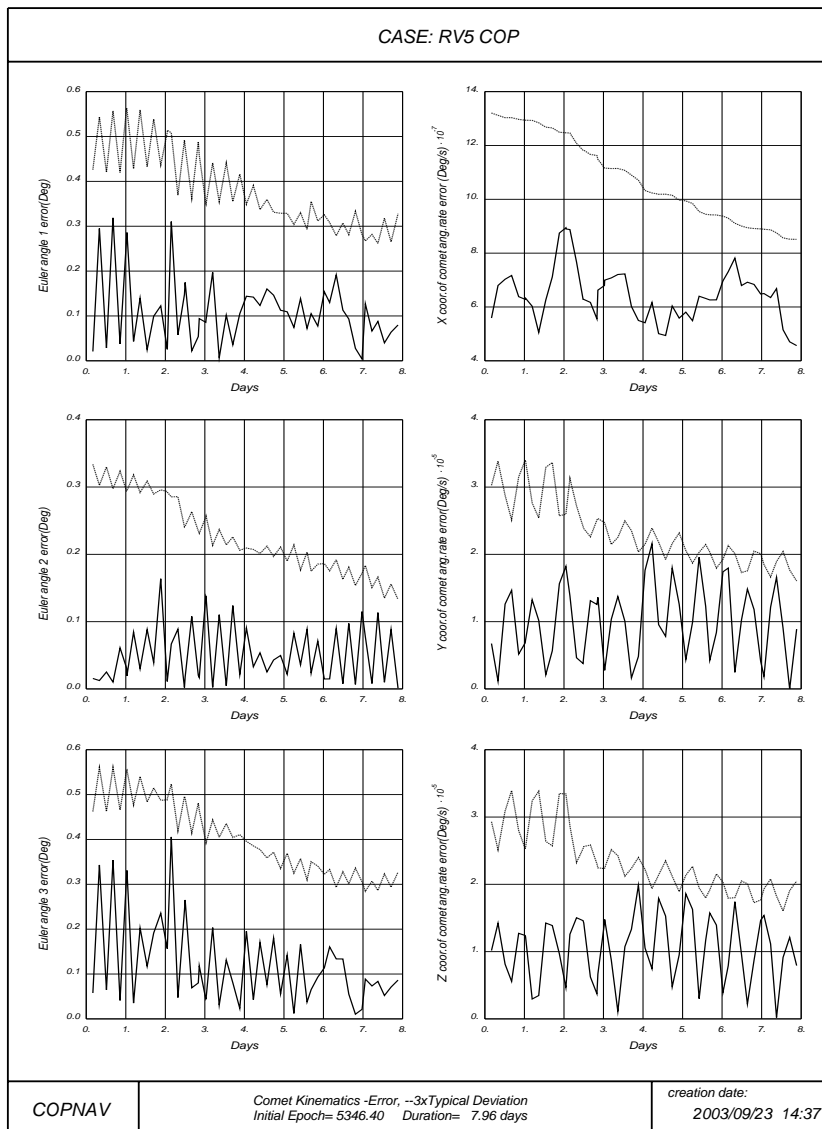


Figure 8-30: Comet Kinematics Estimation Errors during Close Observation Phase.

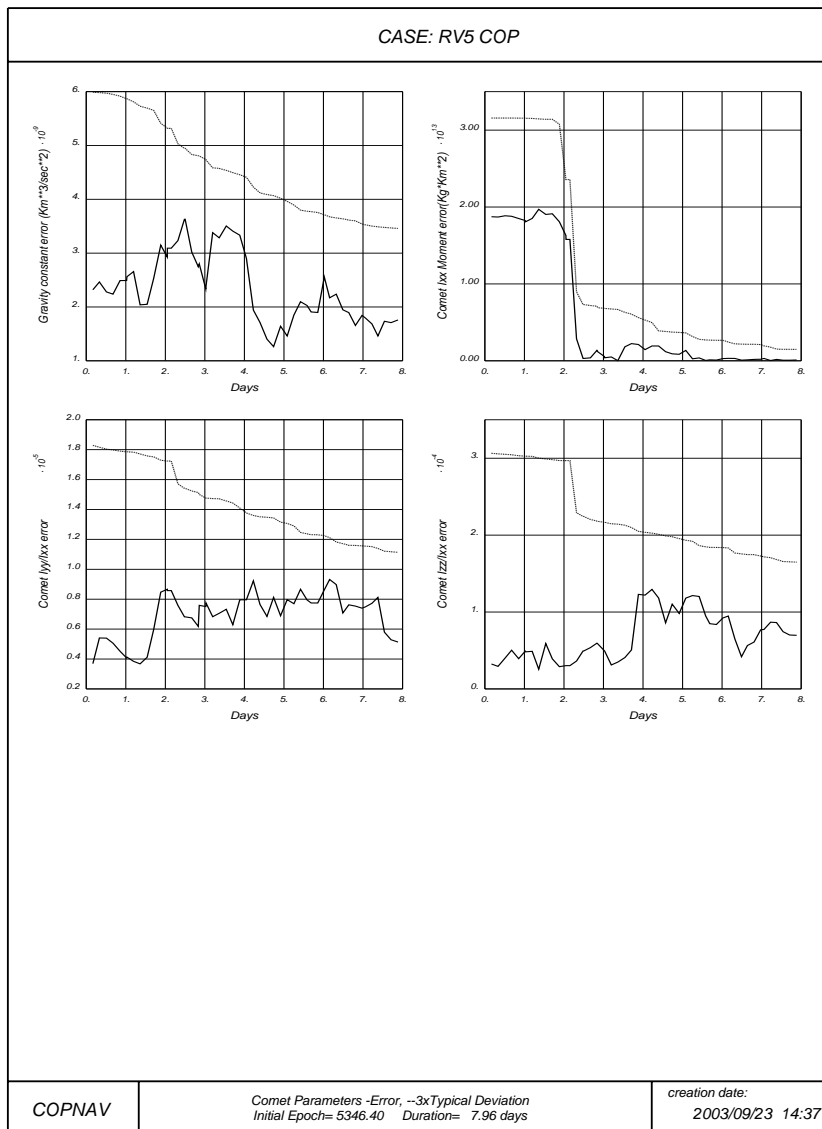


Figure 8-31: Landmark Position Estimation Errors during Close Observation Phase.

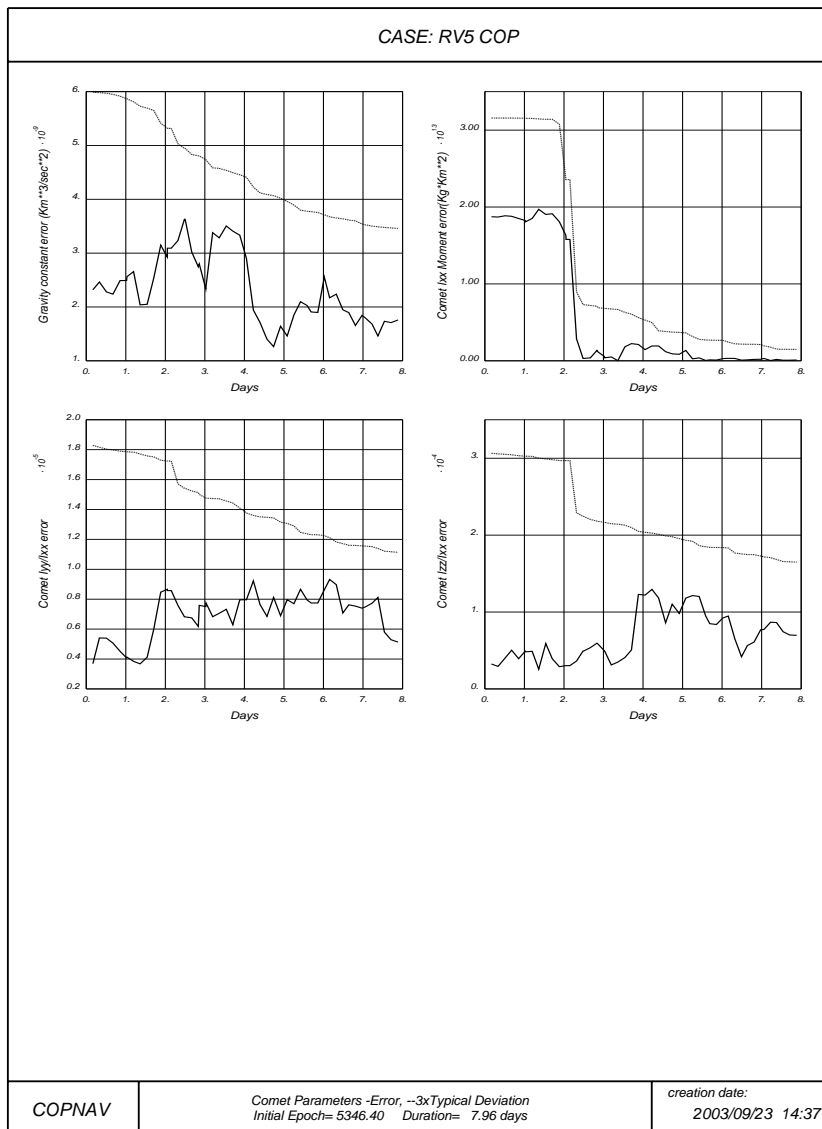


Figure 8-32: Gravitational Field Estimation Errors during Close Observation Phase.

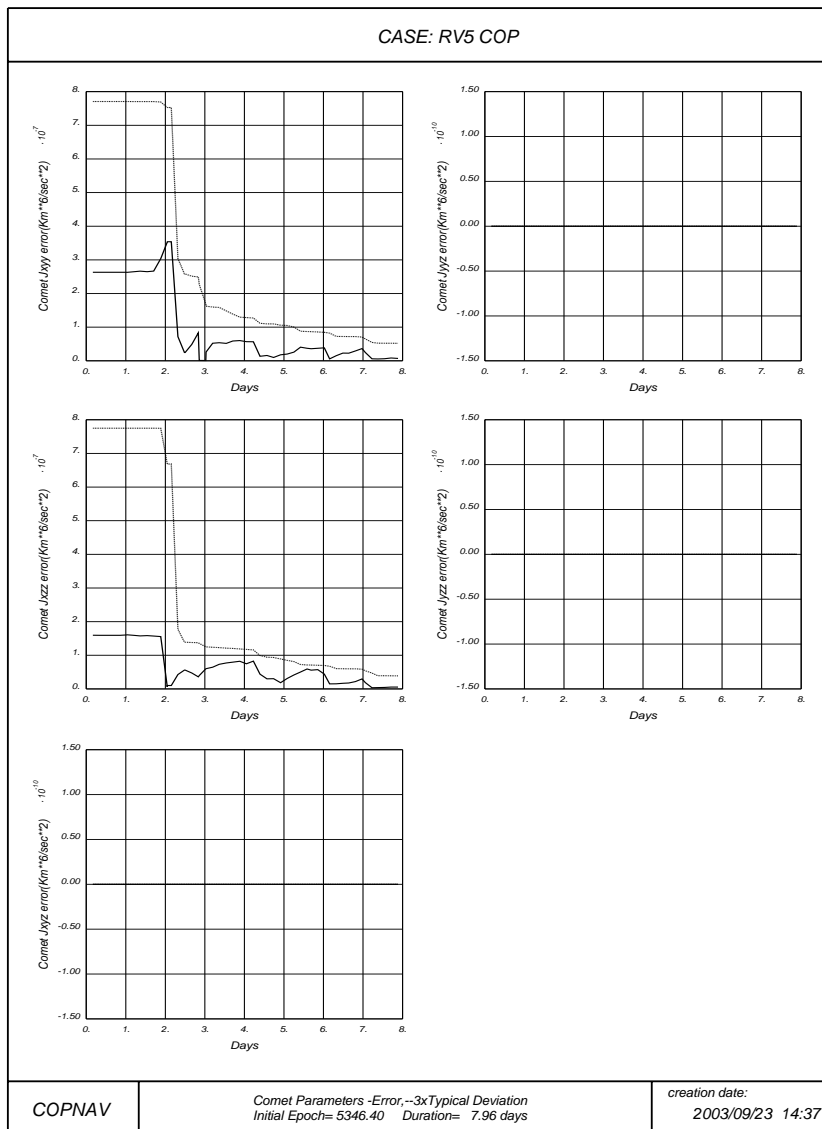


Figure 8-33: Gravitational Field Estimation Errors during Close Observation Phase.

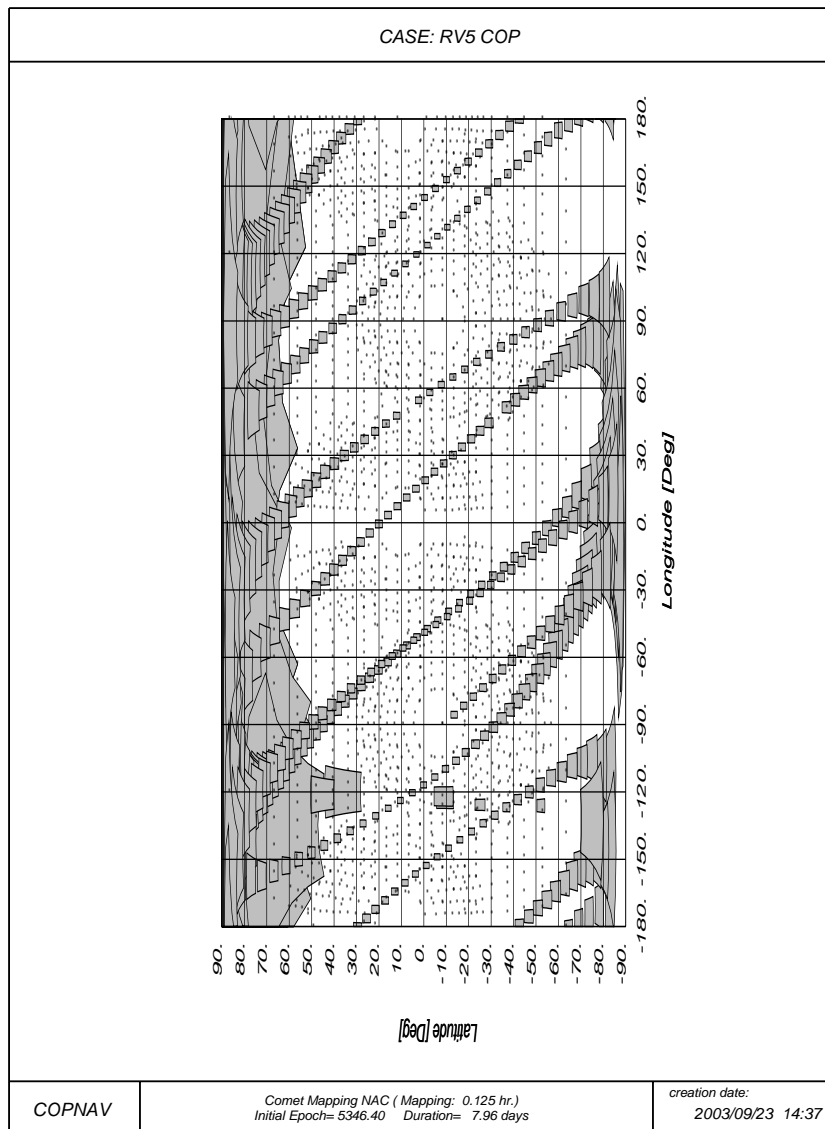


Figure 8-34: Nadir Observation and Field of View of NAC camera

8.9 SSP Delivery

The requirements for the delivery trajectory are:

- The ejection point will be safe (enough altitude over comet surface).
- The orbit shall be safe.
- No eclipse is allowed along the S/C orbit.
- The descent duration will not exceed 6 hours (Batteries performances).
- The minimum time between delivery orbit injection and ejection is 16 hours.
- The maximum ejection ΔV is 50 cm/s.
- The minimum ejection ΔV is 10 cm/s.
- The solar aspect angle at ejection will be in the range 60 - 120° .
- The solar panel articulation mechanism will be limited to 180 degrees rotation.
- The angle of attack, defined as the angle between the SSP spin axis and the normal to the comet surface at the impact point, shall be as close as possible to zero.
- The impact angle, defined as the angle between the probe relative velocity and the normal to the comet surface at the impact point, shall also be as close as possible to zero.
- The SSP relative velocity at impact shall be greater than 5 cm/s.
- The SSP relative velocity at impact shall be less than the comet escape velocity.
- The SSP relative velocity at impact shall be less than 2 m/s (damper performances).
- Maximum phase angle of 60 degrees at impact.

The ejection of the SSP will be performed by means of a Cold Gas System:

The SSP is ejected from the S/C with a tuneable separation velocity. A thruster along the vertical axis will provide a vertical and tuneable ΔV_z . The total ΔV capability of the system is 1 m/s.

Once the conditions at impact (position and velocity) have been fixed, a backwards propagation including intermediate ΔV from the impact until the ejection instant provides the descent orbit of the probe and its velocity just after the ejection. If the ejection conditions (orientation and ΔV) are also defined, the state vector of the Rosetta S/C can be determined and, consequently, the orbit. The plane of this orbit can be rotated around the comet spin axis to avoid Sun eclipses during the delivery operations.

The reach of the delivery orbit is performed in two steps. Firstly, the S/C shall change the plane of motion from the plane of the Close Observation Orbit to the one of the delivery orbit. Secondly, the S/C shall be injected in the delivery orbit to make the ejection.

The change of plane is carried out by means of an intermediate circular orbit with a radius big enough to save ΔV . The radius of this orbit shall be selected in such a way that the total time from the first manoeuvre until the probe reaches the position of the impact point is equal to the time at which the landing site, because of the rotation of the comet, achieves the same position. This situation can occur after a portion or several comet revolutions depending on the constraint of minimum radius imposed on the intermediate circular orbit.

The S/C is injected into this circular orbit by a couple of manoeuvres. The first to leave the close observation orbit, and the second one to circularise. The manoeuvre to change the plane is executed when the S/C crosses the plane of the delivery orbit.

Once the S/C is flying on the delivery plane, a fourth manoeuvre will inject it into the delivery orbit. After the ejection of the probe, additional manoeuvres shall be executed in order to ensure probe visibility (next phase).

This entire trajectory has to be optimised. The optimisation variables are:

- Ejection ΔV
- Ejection Direction ψ
- Impact velocity V_i
- Flight time T_f
- Vertical manoeuvre ΔV_z

The parameter to be minimized is the flight time. The optimisation of the flight time will result in the reduction of the errors at the landing point since the initial errors due to the S/C position, ejection ΔV and comet kinematics will be propagated during a shorter period of time.

Depending on the comet parameters the required delivery orbit will be hyperbolic or elliptic.

The optimisation variables are depicted in Figure 8-35.

A scheme of the proposed strategy is shown in Figure 8-36.

The Figure 8-37 shows the whole trajectory during the SSP ejection operations together with the beginning of the next phase. Figure 8-38 and Figure 8-39 show the last part of the S/C trajectory before ejection and the descent trajectory of the probe after the ejection manoeuvre. On the first figure the projections are provided on the principal frame while in the second they are provided on the usual RST frame. In all figures, the comet nucleus projections have been included to give a better idea of the ejection scenario.

The following list summarises the values of the main parameters along the trajectory for a typical case.

REAL WORLD MANOEUVRES FOR THE SSP DELIVERY PHASE
 =====

DATE (MJD2000)	T (DAYS)	MASS (KG)	DIS (KM)	SUND (AU)	V0 (M/S)	DV (M/S)	VF (M/S)
5354.3637075	0.000	1137.756	4.8	3.48496	0.824	0.232	1.015
5355.9068445	1.543	1137.694	30.5	3.47602	0.156	0.149	0.305
5357.0793329	2.716	1137.469	30.2	3.46920	0.308	0.545	0.304
5360.6059580	6.242	1137.460	29.7	3.44860	0.307	0.022	0.312
5364.1325830	9.769	1137.401	30.3	3.42785	0.308	0.142	0.165
5364.9401670	10.576	1137.383	24.6	3.42308	0.266	0.042	0.264
5365.7595249	11.396	1137.229	5.2	3.41823	0.969	0.374	0.697
5366.0757640	11.712	1137.227	4.7	3.41635	0.760	0.003	0.763
5366.1588782	11.795	1040.227	5.0	3.41586	0.717	0.000	0.762
SSP EJECTION DATE (MJD2000) : 5366.15887819							
S/C POS. AT EJECTION (INE.,KM): 0.32704E+01 0.15776E+01 0.34090E+01							
S/C VEL. AFTER EJ. (INE.,KM/S): -0.37724E-03 0.65957E-03 0.52588E-04							
SSP VEL. AFTER EJ. (INE.,KM/S): -0.87762E-04 0.21044E-03 0.12473E-03							
EJECTION DELTA-V (INE.,KM/S) : 0.26478E-03 -0.41082E-03 0.65988E-04							
EJECTION DELTA-V (MODUL., M/S): 0.49318E+00							
EJECTION ALTITUDE (KM) : 0.29043E+01							
RELAY ORBIT CASE SELECTED : RETROGRADE ELLIPTIC ORBIT							
5366.1627324	11.799	1039.683	5.0	3.41584	0.762	1.437	1.454
SSP LATERAL MAN. DATE (MJD2000): 5366.16273235							
SSP POS. AT LAT. MAN. (INE.,KM): 0.32372E+01 0.16459E+01 0.34461E+01							
SSP VEL. AFTER MAN. (INE.,KM/S): -0.11137E-03 0.19929E-03 0.98329E-04							
LAT. MAN. DELTA-V (INE.,KM/S) : 0.00000E+00 0.00000E+00 0.00000E+00							
LAT. MAN. DELTA-V (MODUL., M/S): 0.00000E+00							
SSP VERTICAL MAN. DATE (MJD2000): 5366.16273235							
SSP POS. AT VER. MAN. (INE.,KM): 0.32372E+01 0.16459E+01 0.34461E+01							
SSP VEL. AFTER MAN. (INE.,KM/S): -0.30739E-03 -0.38168E-06 -0.30690E-03							
VER. MAN. DELTA-V (INE.,KM/S) : -0.19602E-03 -0.19967E-03 -0.40523E-03							
VER. MAN. DELTA-V (MODUL., M/S): 0.49241E+00							
SSP IMPACT DATE (MJD2000) : 5366.20476814							
SSP FLIGHT DURATION (HOURS) : 0.11014E+01							
IMPACT LONGITUDE (DEG) : 0.13098E+02							
IMPACT LATITUDE (DEG) : 0.23649E+02							
IMPACT ALTITUDE (KM) : 0.35135E-03							
SSP IMPACT POINT (PPAL, KM) : 0.10031E+01 0.22330E+01 0.51956E+00							
SSP ABS. IMP. VEL. (PPAL, KM/S): -0.72530E-03 -0.95152E-03 -0.58684E-04							
AB. IMP. POINT VEL. (PPAL, KM/S): 0.16082E-04 -0.83998E-04 0.32996E-03							
SSP REL. IMP. VEL. (PPAL, KM/S): -0.74139E-03 -0.86753E-03 -0.38864E-03							
SSP IMPACT VELOCITY (KM/S) : 0.12055E-02							
IMPACT POINT NORMAL (PPAL) : 0.61512E+00 0.71242E+00 0.33777E+00							
VELOCITY IMPACT ANGLE (DEG) : 0.89026E+02							
SSP AXIS DIRECTION (INERTIAL) : 0.39711E+00 0.39432E+00 0.82874E+00							
SSP ANGLE OF ATTACK (DEG) : 0.49370E+00							
5366.2039243	11.840	1039.683	9.5	3.41559	1.267		
TOTAL SSP DELIVERY DELTA-V (M/S) : 2.95							

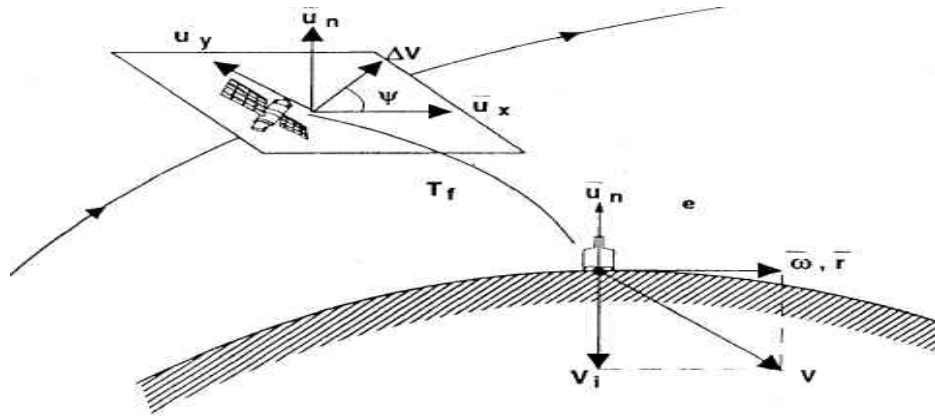
Figure 8-40 shows the evolution of other interesting parameters such as distances of the S/C to the comet, Earth or Sun, phase angle, and velocity relative to the comet.

Figure 8-41 presents plots showing distances and viewing angles to three of the jets (6 have been considered into the comet model) lying on the comet surface. The jets mass flow rate per surface unit and the ejected materials velocity decrease with the distance and angle to the jet axis. The main consequence of over flying one gas jet will be an increase in the errors related to the S/C position. Landing points close to high activity areas (jets) should consequently be avoided during the probe ejection operations.

From the point of view of the navigation, there are no new remarkable features before the Probe ejection. A continuous estimation of all the parameters is performed but no appreciable decrease in the errors is observed during this phase. The ejection of the probe introduces additional errors in the S/C position. The initial error in the probe state vector will propagate until the impact on the comet surface. Figure 8-42 and Figure 8-43 show the evolution of the S/C and Probe state vector errors. The Figure 8-44 show the dispersion ellipse for a typical case. The cross inside represents the real error obtained for that specific simulation case.

The averaged parameters for SSP descent for the whole range of comets after a large simulation campaign are:

- Flight time : 18 -- 76 min.
- Ejection ΔV : 5 -- 50 cm/s
- Impact velocity : 20 -- 160 cm/s
- Position error at landing: 26 m
(largest axis of 1- σ dispersion ellipse)
- Maximum angle between Lander z-axis: 18°
and mean surface normal (attack angle)
at achieved landing point
- Maximum angle between impact velocity: 18°
and mean surface normal (impact angle)
at achieved landing point
- Maximum angle between impact velocity: 7°
and Lander z-axis.
(Important for damping by landing gear)



- Impact velocity V_i
- Flight time T_f
- Ejection ΔV
- Ejection direction angle Ψ

Figure 8-35: SPD optimisation variables.

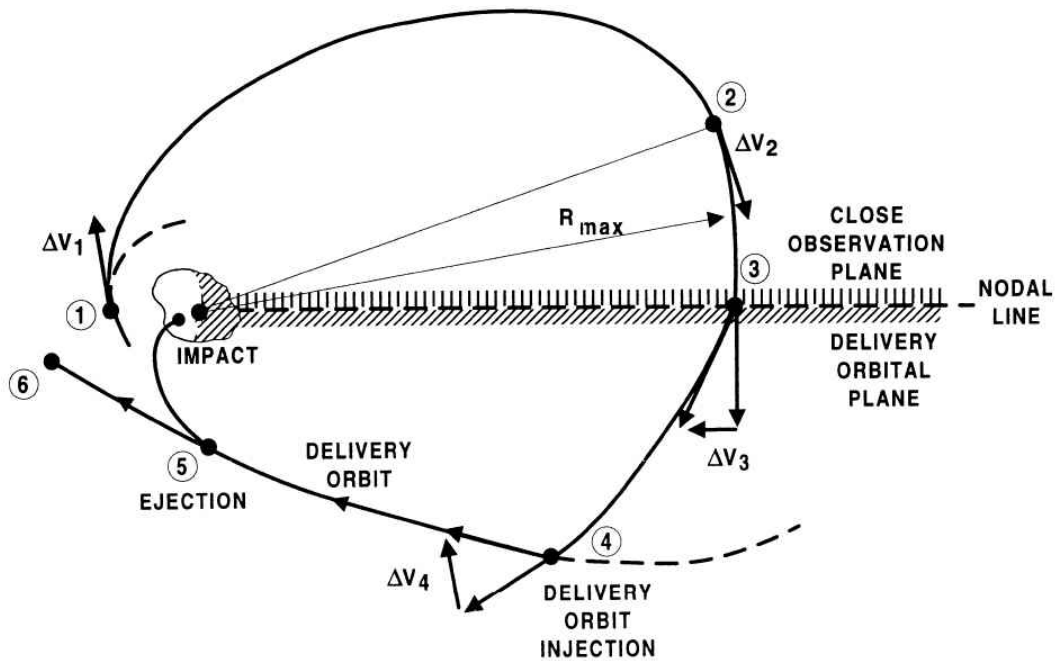


Figure 8-36: SPD Strategy

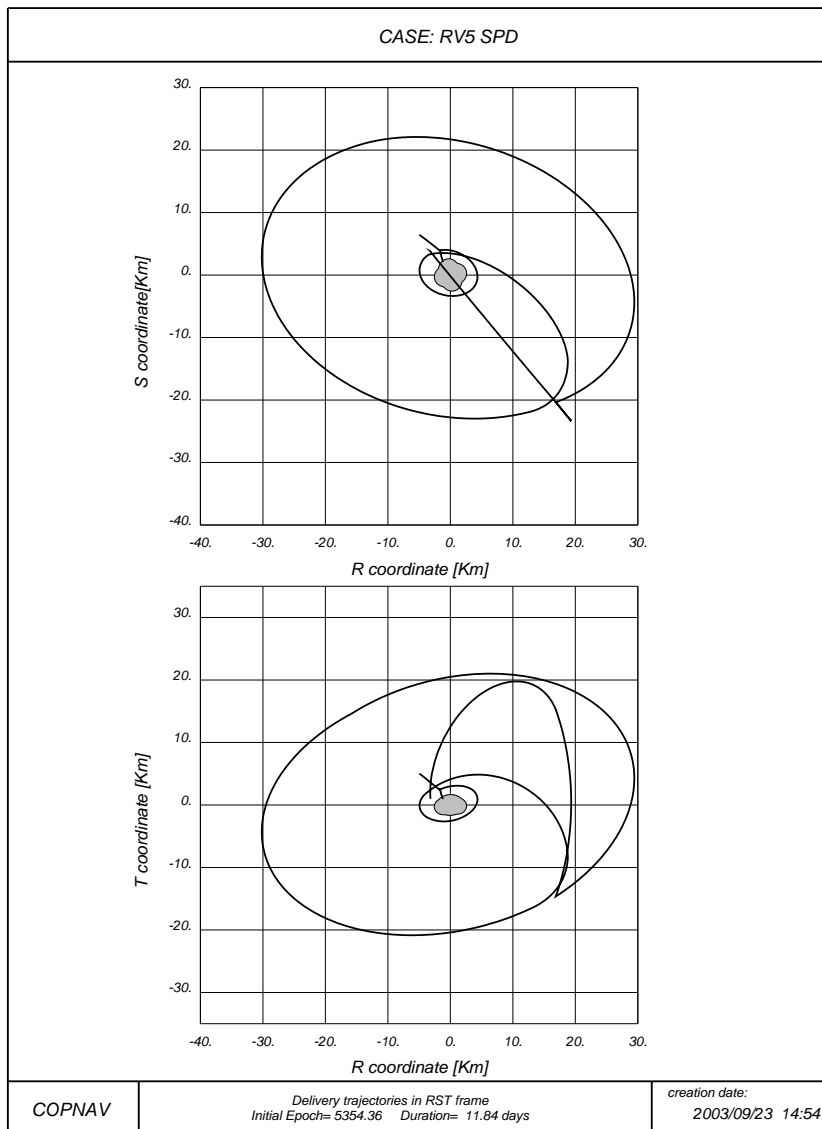


Figure 8-37: S/C Trajectory during SSP Operations. In RST Frame.

The R axis has the direction of the position vector of the comet, the S axis is perpendicular to the previous one and contained in the plane of motion of the comet and the T axis makes a right-handed frame with the R and S axis.

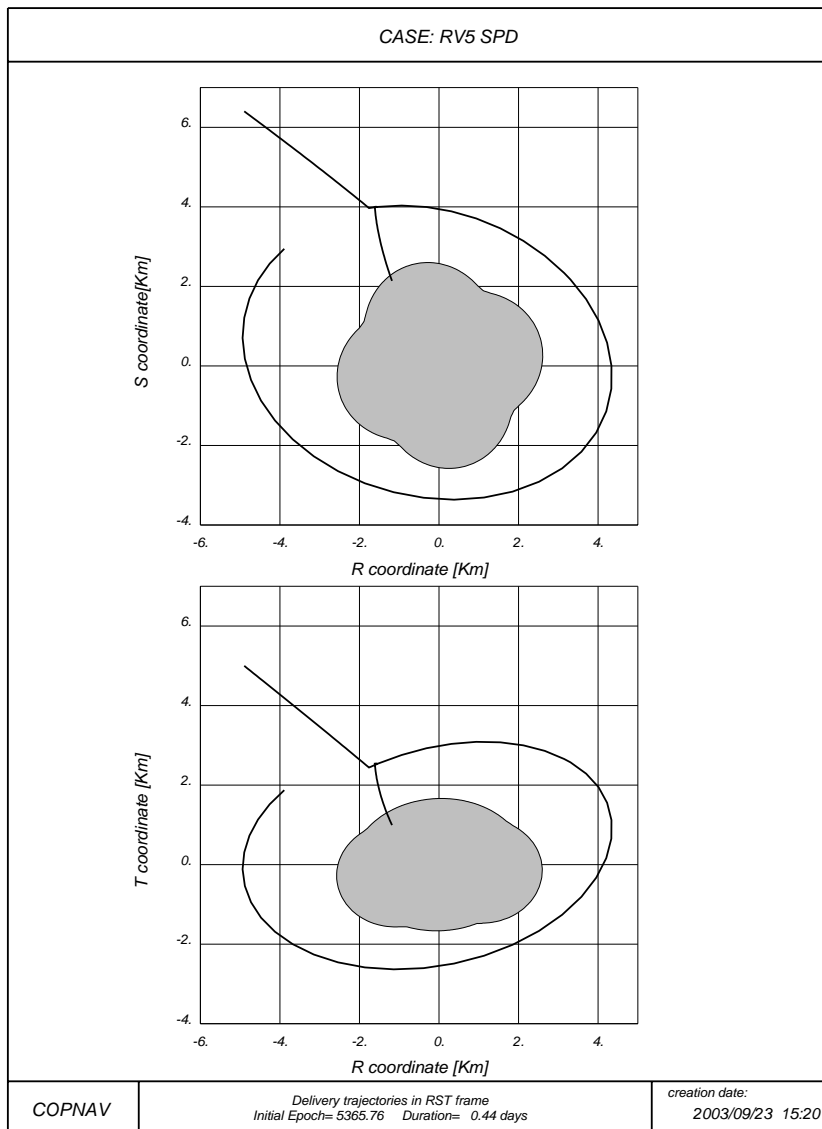


Figure 8-38: Detail of S/C and Probe Trajectories in Principal Frame

This frame is centred in the centre of gravity. The X-axis has the direction of the principal axis with maximum inertia momentum. The Y and Z-axis have the directions of the other two principal axes respectively.

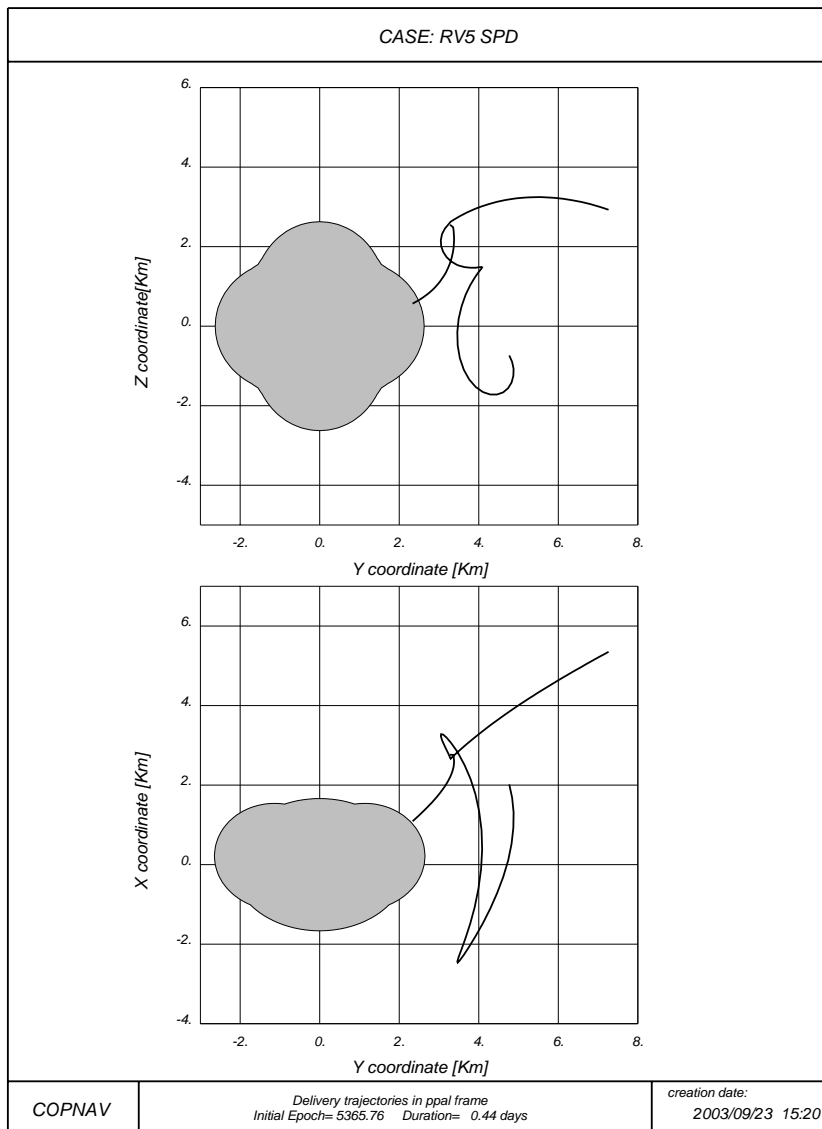


Figure 8-39: Detail of S/C and Probe Trajectories in RST Frame.

The R axis has the direction of the position vector of the comet, the S axis is perpendicular to the previous one and contained in the plane of motion of the comet and the T axis makes a right-handed frame with the R and S axis.

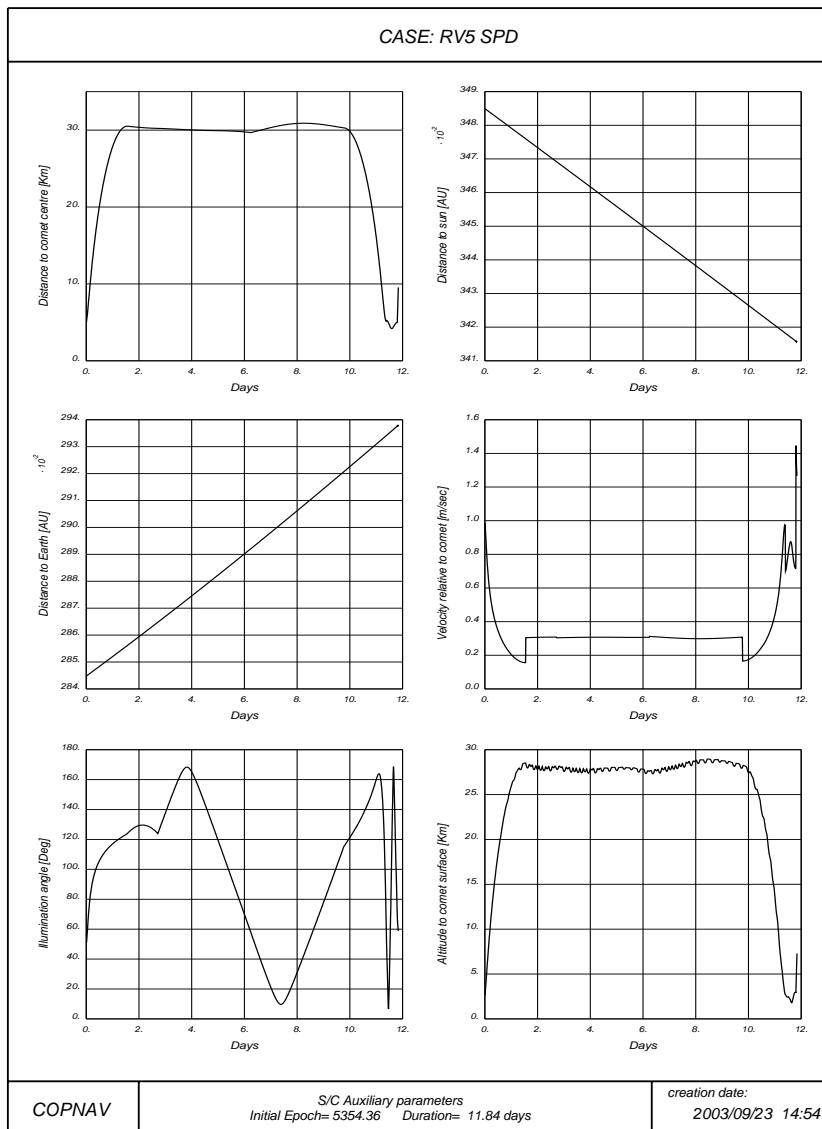


Figure 8-40: S/C Auxiliary Parameters during Surface Probe Delivery Phase.

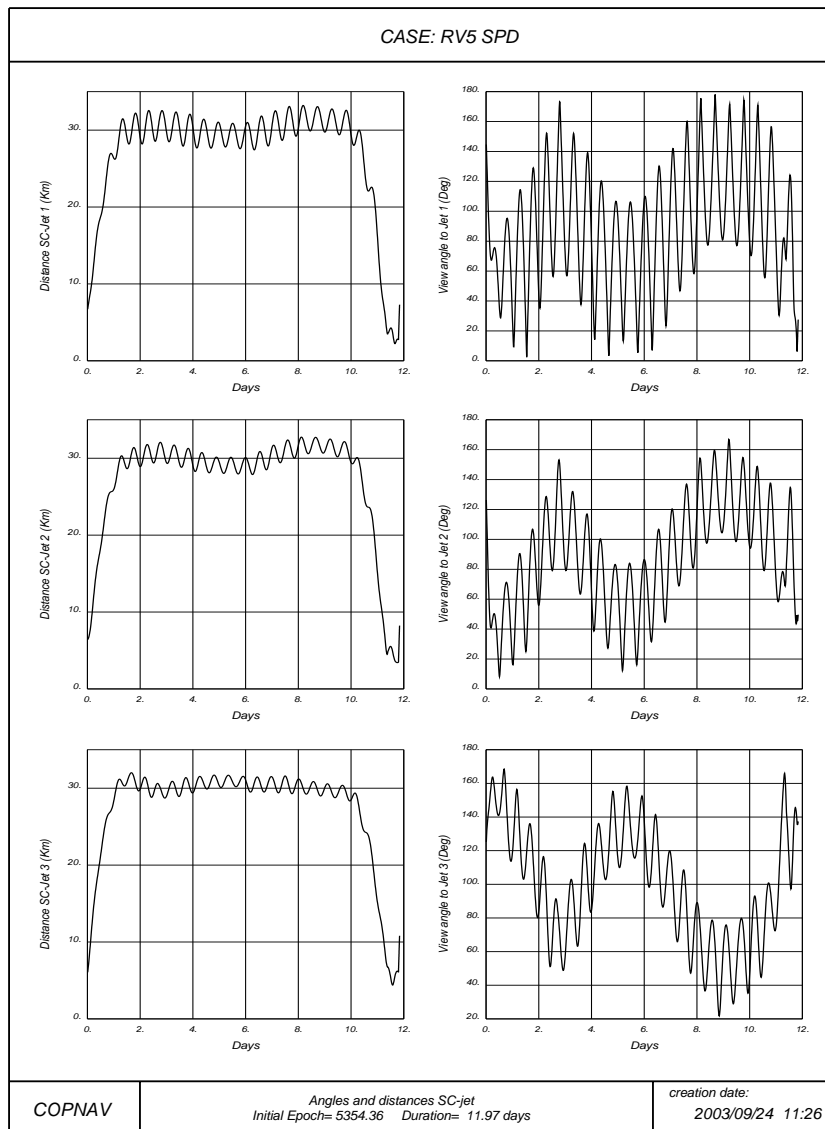


Figure 8-41 Spacecraft position with respect to jets during Surface Probe Delivery Phase.

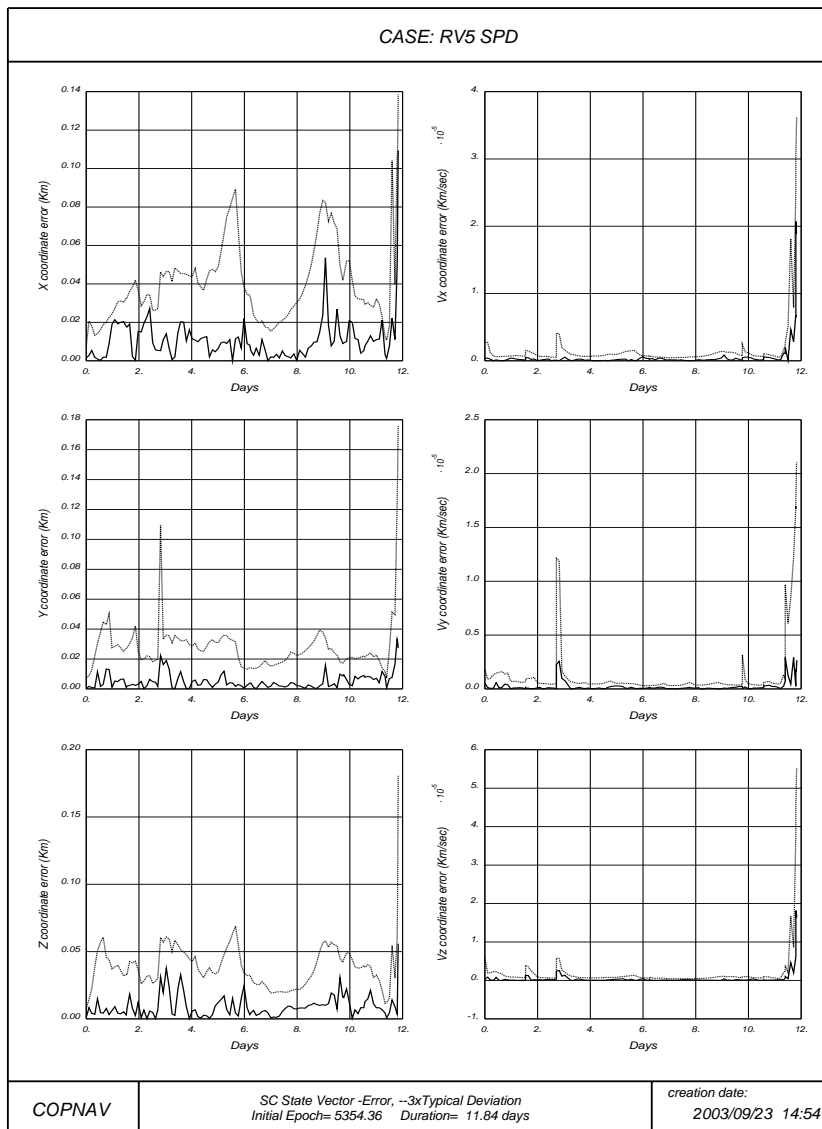


Figure 8-42: S/C Position and Velocity Errors during Surface Probe Delivery Phase.

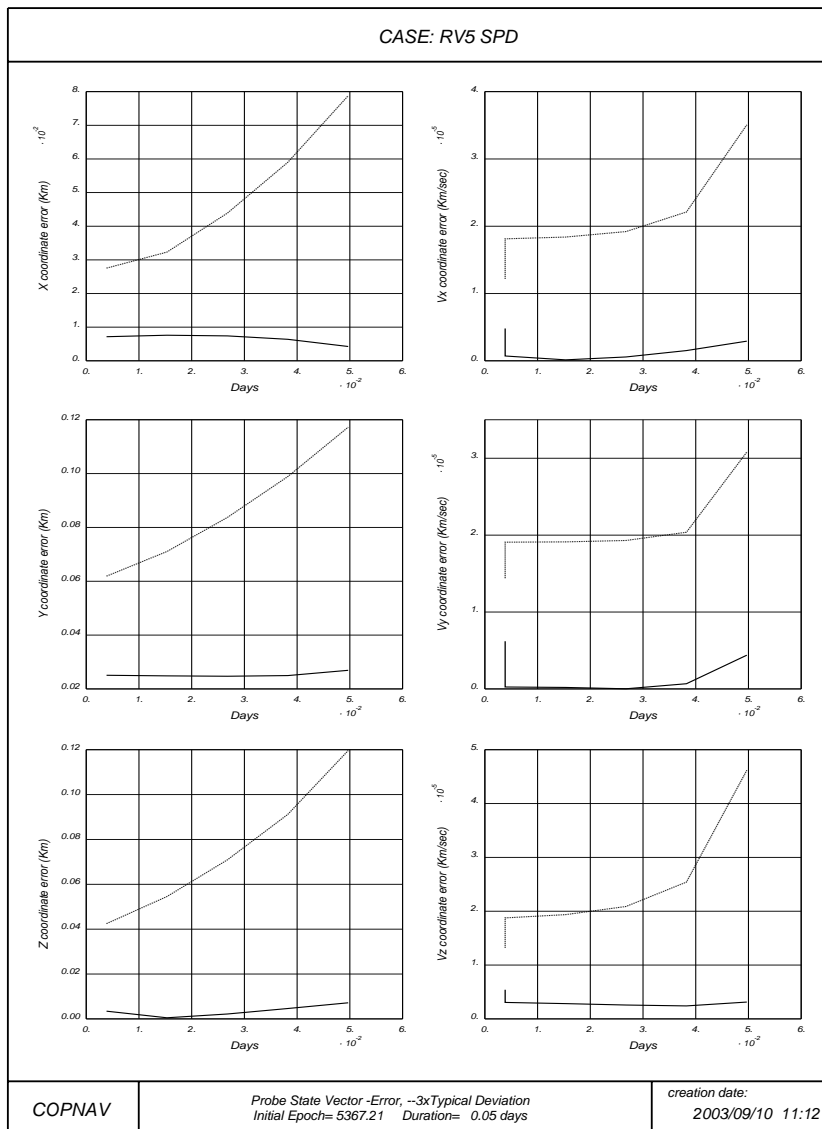


Figure 8-43: Probe Position and Velocity Errors during Surface Probe Delivery Phase.

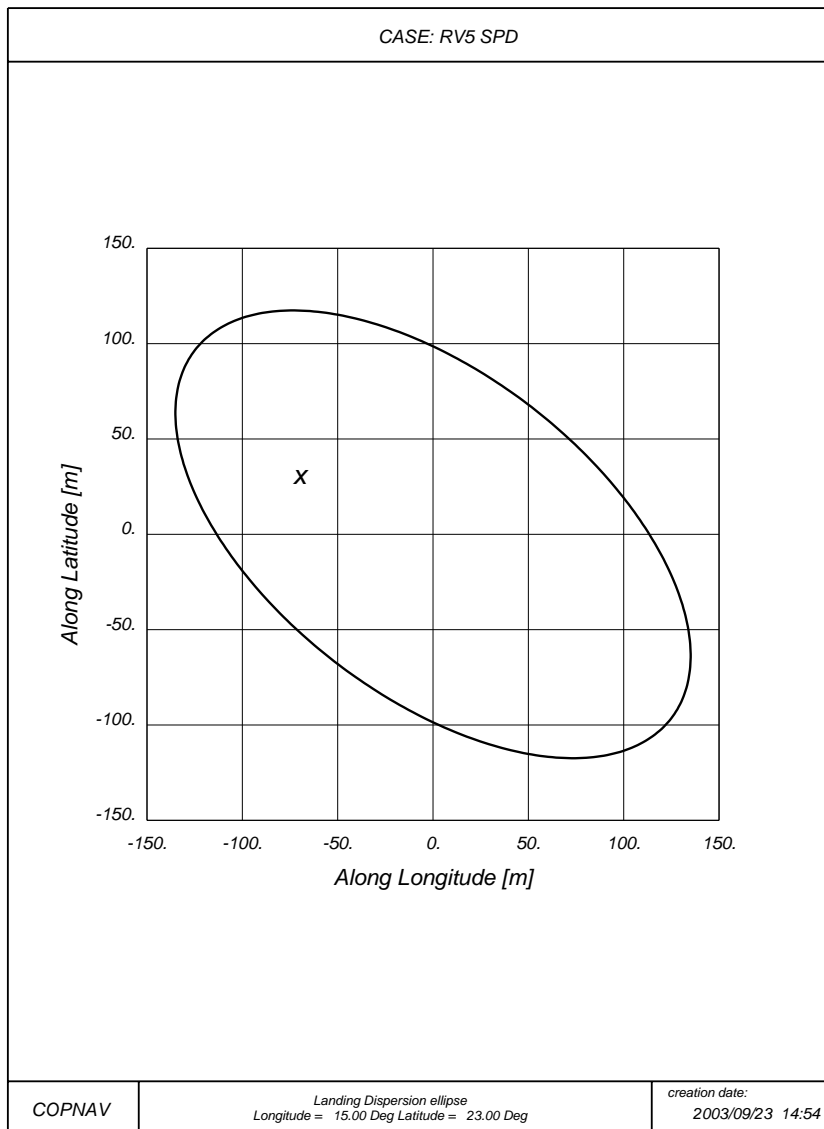


Figure 8-44: Ellipse of Dispersion at the Probe Landing for a Typical Case

8.10 Relay Phase

The relay phase must be defined to maximize the coverage of the SSP. The following requirements have been defined for this phase:

- The SSP must be visible from the spacecraft during a period between 15 minutes before and after nucleus surface impact.
- Communication is needed for three hours or more during the first 24 hours on the surface.
- The minimum elevation of the SSP coverage is 30° .
- The orbit shall be safe.
- Continuous phase of the solar panels and Earth communications are required.

The proposed strategy for this phase depends on the landing latitude and the rotation period. The following cases have been identified:

1. Landing site at high latitude. Polar elliptic orbits.
2. Low latitude and slow rotation period. Equatorial elliptic orbit.
3. Low latitude and fast rotating nucleus. Retrograde elliptic orbit.
4. Low latitude and period from 23 to 60 hours. Retrograde circular equatorial orbit.

Some time after ejection (to avoid effects on the flying probe) a manoeuvre is executed to situate the S/C over the landing site at impact time. This procedure ensures the probe visibility before and after landing. Some time after landing a second manoeuvre shall be performed in order to reach the relay orbit in which the S/C is injected by means of a third manoeuvre.

REAL WORLD MANOEUVRES FOR THE SSP RELAY PHASE
 =====

DATE (MJD2000) T (DAYS) MASS (KG) DIS (KM) SUND (AU) V0 (M/S) DV (M/S) VF (M/S)

RELAY ORBIT CASE SELECTED : RETROGRADE ELLIPTIC ORBIT

5366.2039243	0.000	1039.683	9.5	3.41559	1.267	0.000	1.267
5366.2143410	0.010	1038.884	10.6	3.41553	1.243	2.112	1.917
5366.3289243	0.125	1038.290	23.9	3.41485	1.838	1.573	0.380
5366.8914243	0.688	1038.263	33.5	3.41151	0.277	0.071	0.212
5368.5789243	2.375	1038.262	35.1	3.40148	0.195	0.003	0.195
5369.7039243	3.500	1038.262	18.7	3.39477	0.425		

TOTAL SSP RELAY DELTA-V (M/S) : 3.76

The proposed strategy scheme and the numerical trajectory (equatorial landing) are shown in Figure 8-45 and Figure 8-46.

Figure 8-47 shows the evolution of other interesting parameters such as distances of the S/C to the comet, Earth or Sun, phase angle, and velocity relative to the comet.

The values of the main parameters of this phase are the following ones:

- Duration: 3.5 Days.

- Required ΔV : about 4 m/s.

The visibility conditions of the lander from the orbiter is presented in Figure 8-48.

For the typical comet, the visibility gap with minimum elevation of 30° is about 4.9 hours, so that the orbiter-lander communication requirements are satisfied. The lander occultation with minimum elevation of 0° is at least 3.6 hours, so that the requirements of CONSERT are also satisfied.

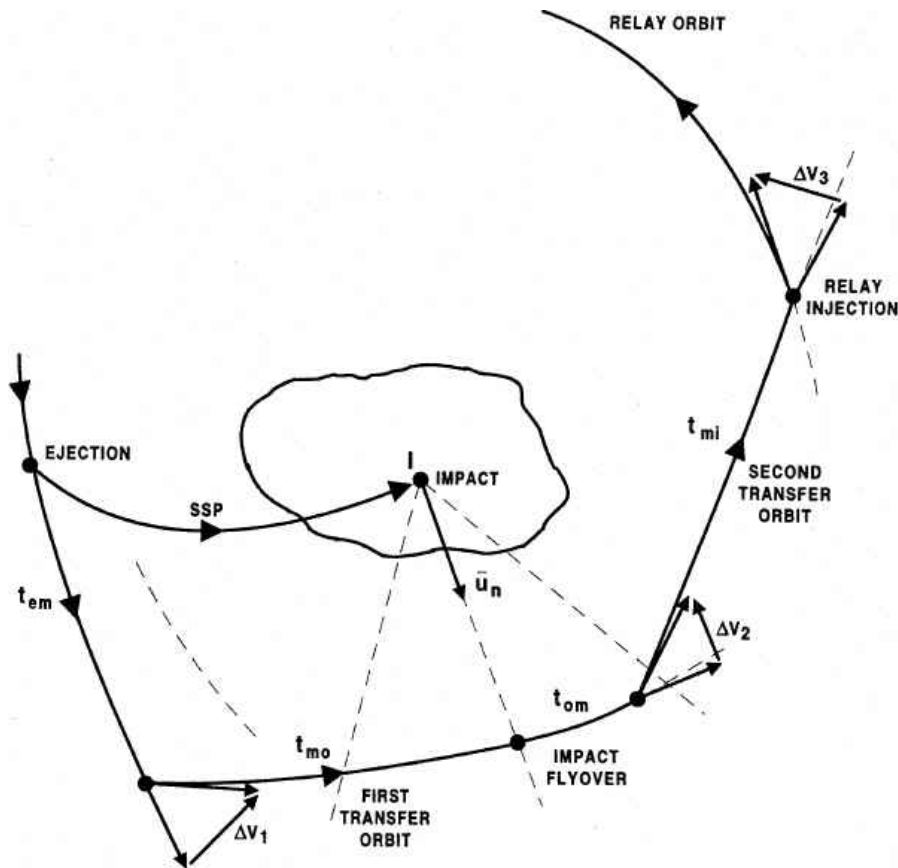


Figure 8-45: SPR Strategy

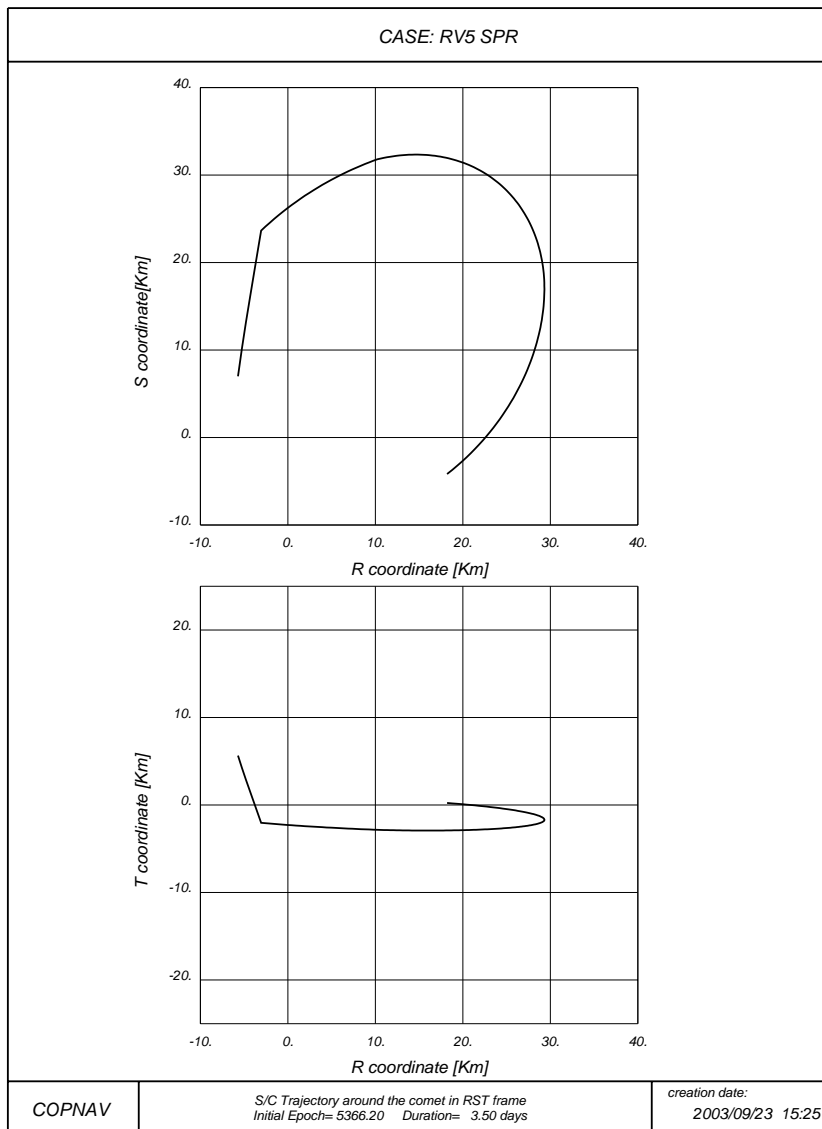


Figure 8-46: SPR Numerical Trajectory (RST Frame)

The R axis has the direction of the position vector of the comet, the S axis is perpendicular to the previous one and contained in the plane of motion of the comet and the T axis makes a right-handed frame with the R and S axis.

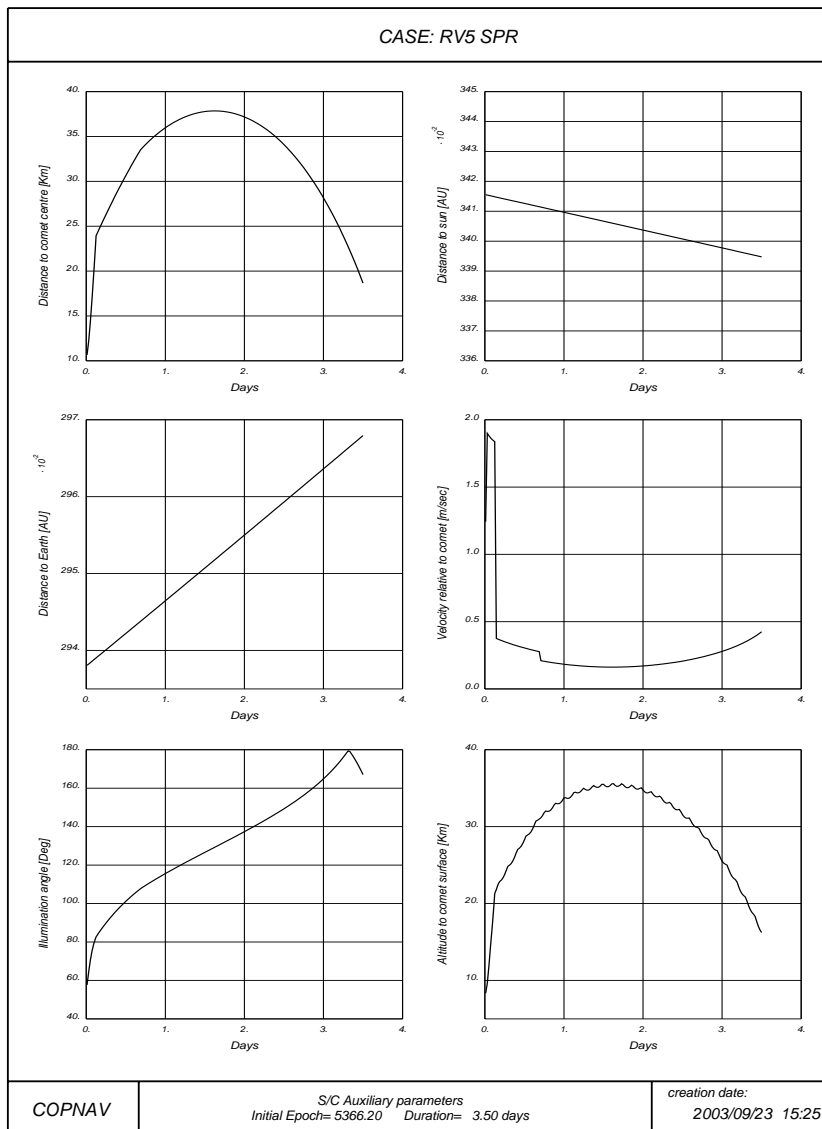


Figure 8-47: S/C Auxiliary Parameters during Relay Phase.

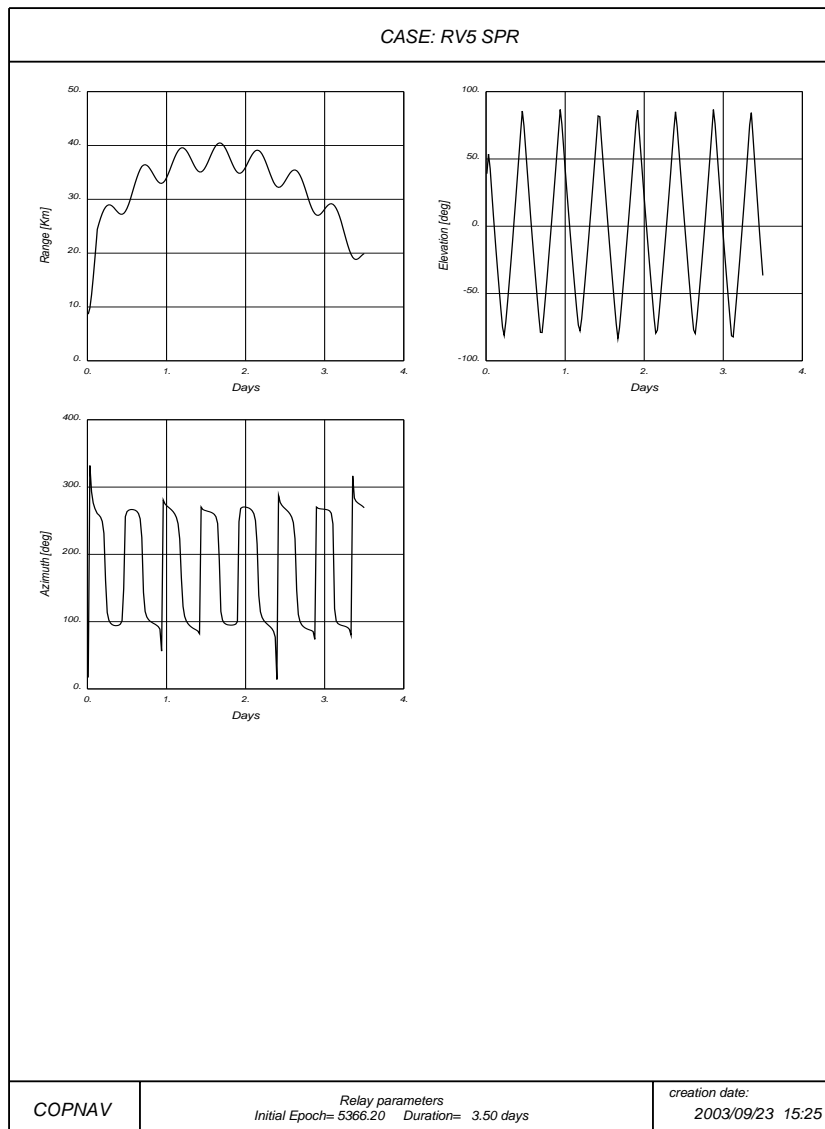


Figure 8-48: Lander – Spacecraft parameters

8.11 Extended Monitoring Phase

The objective of this phase is to monitor the nucleus, dust and gas jets and to analyse gas, dust and plasma in the inner coma from the onset to the peak activity. Orbits design will depend on safety considerations and scientific goals. Mission planning will depend on the result of the previous observations, such as the activity pattern of the comet.

Some scientific experiments, (GIADA, ROSINA, and RPC), may require that the orbiter is injected into trajectories around the comet nucleus with big to very big distances to the nucleus. For GIADA, the requirement is to go up to a few hundred of km away from the nucleus in different directions. For ROSINA the requirements is to travel up to distances of 10000 km, and for RPC is the same distance but several times during the mission. At that distances the orbiter follows linear trajectories with respect to the comet nucleus. Given a distance and a period to be dedicated to that experience, the relative of the orbiter is fixed (1000 km and 10 days will give at least 2.3 m/s). Because it is required to accelerate the spacecraft, and to stop it, the required total ΔV to be applied is 4 times the travelling velocity (in the above example 9.3 m/s). It is clear that the detail planning for that phase of the mission will depend on the resources available at that time.

9. PROPELLANT BUDGET

The ΔV budget is described in the following Table 9-1.

Numerical Interplanetary Trajectory: DSM and RDV	1688 m/s
Asteroid(s) fly-by	7 m/s
Near Comet Operations	120 m/s
Cruise navigation	75 m/s
Launch Window and Flight Tape	10 m/s
First Correction Manoeuvre	160 m/s
Contingencies due to S/C failures	45 m/s
Other Contingencies	30 m/s
TOTAL	2135 m/s

Table 9-1: Propellant Budget.

10. ABBREVIATIONS

AOCMS	Attitude and Orbit Control Monitor System.
AOS	Acquisition Of Signal.
APM	Antenna Pointing Mechanism.
AST1P	Asteroid 1 (Otagawa) Post fly-by.
AST2P	Asteroid 2 (Siwa) Post fly-by.
ATP	Approach Transition Point.
AU	Astronomical Unit (149597870.6 km).
BSM	Bus Support Module.
CAT	Close Approach Trajectory.
CNSR	Comet Nucleus Sample Return.
COP	Close Observation Phase.
CRi	Cruise Phase number "i".
cte.	constant.
CVP	Commissioning and Verification Phase.
ΔDOR	Delta Differential One-way Range.
DEG	Degrees.
DRIF	Near Comet Drift Phase.
DSM	Deep Space Manoeuvre.
DSN	Deep Space Network.
EAP	Solid Propellant Boosters of Ariane-5.
EAR1	Earth Swing-by 1.
EAR2	Earth Swing-by 2.
EMP	Extended Monitoring Phase.
EPC	Cryogenic Propellant Stage with 155 tons. Central stage of Ariane-5.
EPS	Storable Propellant Stage with 9.7 tons. Upper Stage of Ariane-5.
FAT	Far Approach Trajectory.
GMP	Global Mapping Phase.
GTO	Geostationary Transfer Orbit.
H155	Cryogenic Propellant Stage with 155 tons. Central Stage of Ariane-5.
HGA	High Gain Antenna.
HGA-APM	High Gain Antenna. Antenna Pointing Mechanism.
HGA-HRM	High Gain Antenna Hold down and Release Mechanism.
L9.7	Storable Propellant Stage with 9.7 tons. Upper Stage of Ariane-5.
LEOP	Launch and Early Orbit Phase.
LGA	Low Gain Antenna.
LIC	Launcher Injection Errors Correction
LOS	Loss Of Signal.
LSM	Lander Support Module.
LTF	Linearised time of flight.
MAS	Mission Analysis Section.
MC	Mid-Course Correction.
MEEQ2000	Mean Earth Equator 2000.0 reference frame.
MGA	Medium Gain Antenna.
MINC	Comet Activity Moderate Increase.
MJD2000	Modified Julian Day 2000.
MMH	Mono Methyl Hydrazine.

MON	Nitrogen tetroxid.
NCD	Near Comet Drift Phase.
NMCO	Nucleus Mapping. Close Encounter.
OBDH	On Board Data Handling.
OIP	Orbit Insertion Point.
PSM	Payload Support Module.
RAMF	Mission Analysis Final Review
RDV(M)	Rendezvous (Manoeuvre).
RF	Radio Frequency.
SA	Solar Array.
SADM	Solar Array Drive Mechanism.
SA-HRM	Solar Array Hold down and Release Mechanism.
SINC	Comet Activity Sharp Increase.
SMA	Semi-major Axis.
SMI	Semi-minor Axis
SPR	Surface Science Package Relay.
SSP	Surface Science Package.
TBC	To Be Confirmed.
TBD	To Be Determined.
TGM	Transition to Global Mapping.
VEB	Vehicle Equipment Bay.
w.r.t.	with respect to.
ΔVGA	Delta-V Gravity Assist

11. APPENDIX A. DETAILED TRAJECTORY

NOTE: If not explicitly stated, reference system is Mean Earth Equator of 2000.

<p>DEPARTURE FROM: EARTH ----- LAUNCH INJECTION: 2004: 2:26 9:11:50.5 (1517.3832) ----- ARIANE 5 LAUNCH WITH COST ARC DEPARTURE PARAMETERS : MEAN EARTH EQ. 2000 HYP. DEPARTURE VEL. (KM/S): 3.353140 -1.143730 -0.123840 HYPERR. VELOCITY (KM/S): 3.545 EQ.A. DECLINATION (DEG): -2.001959021 ----- MEAN EARTH EQUATOR OF DATE HYP. DEPARTURE VEL. (KM/S): 3.354250 -1.140615 -0.122486 HYPERR. VELOCITY (KM/S): 3.545 EQ.A. DECLINATION (DEG): -1.980071795 ----- LAUNCH INJ. MASS (KG) : 3032.39014780 STATE VECTOR AT INJECTION : X-COORD (KM) : -4544.969 Y-COORD (KM) : -5946.128 Z-COORD (KM) : 764.455 VX-COORD (KM/S) : 5.84226866 VY-COORD (KM/S) : -9.17991944 VZ-COORD (KM/S) : 0.36131775 ----- ORBITAL ELEMENTS AT INJECTION : SEMIMAJOR AXIS (KM) : -31718.023 ECCENTRICITY : 1.211300888 INCLINATION (DEG) : 5.8331364 R. AS. OF A. NODE (DEG) : 141.44025058 ARG. OF PERIC. (DEG) : 54.36320801 TRUE ANOMALY (DEG) : 36.79773372 ----- CORRECTION MAN. : 2004: 2:26 9:11:50.5 (1517.3832) STATE VECTOR BEFORE CORRECTION MANOEUVRE : X-COORD (KM) : -4544.969 Y-COORD (KM) : -5946.128 Z-COORD (KM) : 764.455 VX-COORD (KM/S) : 5.84226866 VY-COORD (KM/S) : -9.17991944 VZ-COORD (KM/S) : 0.36131775 ----- CORRECTION MAN. TO COMPENSATE FOR DLW. : DVX-COORD (M/S) : 0.00000000 DUY-COORD (M/S) : 0.00000000 DVZ-COORD (M/S) : 0.00000000 DV MODULUS (M/S) : 0.00000000 ----- MASS AFTER CORRECTION MAN. (KG) : 3032.39014780 ORBITAL ELEMENTS AFTER CORRECTION MAN. :</p>	<p>SEMIMAJOR AXIS (KM) : -31718.023 ECCENTRICITY : 1.211300888 INCLINATION (DEG) : 5.81893283 R. AS. OF A. NODE (DEG) : 141.67101415 ARG. OF PERIC. (DEG) : 54.18475041 TRUE ANOMALY (DEG) : 36.79773372 ----- STATE VECTOR AFTER CORRECTION MAN. : X-COORD (KM) : -4539.751 Y-COORD (KM) : -5950.348 Z-COORD (KM) : 762.621 VX-COORD (KM/S) : 5.85064795 VY-COORD (KM/S) : -9.17448808 VZ-COORD (KM/S) : 0.36367787 ----- PHASE NUMBER: 1 LEG NUMBER: 1 ----- MISSION TYPE :DEEP SPACE MISSION TYPE OF PROBLEM :BOUNDARY VALUE PROBLEM NAME OF CENTRAL BODY :EARTH COORDINATE SYSTEM :MEAN EARTH EQUATOR OF DATE ----- INITIAL EPOCH: 2004: 2:26 9:11:50.5 (1517.3832) INITIAL MASS (KG) : 3032.390 ----- PERTURBATIONS CONSIDERED: ATMOSPHERIC DRAG: NO SOLAR RADIATION : YES REFLECTIVE COEFF. : 1.200 CROSS SECTIONAL AREA: 70.000 THIRD BODY : YES THIRD BODIES : SUN MOON NON-SPHERICITY : YES - 2 ZONALS & OTESSERALS ----- STOP CONDITION: STOP AT EXIT OF SPHERE OF INFLUENCE OF EARTH ----- INITIAL STATE: X-COORD (KM) : -4539.751 Y-COORD (KM) : -5950.348 Z-COORD (KM) : 762.621 VX-COORD (KM/S) : 5.85064795 VY-COORD (KM/S) : -9.17448808 VZ-COORD (KM/S) : 0.36367787 ----- INITIAL ORBITAL ELEMENTS: SEMIMAJOR AXIS (KM) : -31718.023 ECCENTRICITY : 1.211300888 INCLINATION (DEG) : 5.81893283 R. AS. OF A. NODE (DEG) : 141.67101415 ARG. OF PERIC. (DEG) : 54.18475041 TRUE ANOMALY (DEG) : 36.79773372</p>
--	--

<p>NON-SPHERICITY : NO</p> <p>STOP CONDITION: STOP AFTER A GIVEN TIME</p> <p>INITIAL STATE:</p> <p>X-COORD (KM) : -138201813.486 Y-COORD (KM) : 46668543.401 Z-COORD (KM) : 20338533.113 VX-COORD (KM/S) : -7.29707991 VY-COORD (KM/S) : -26.92372424 VZ-COORD (KM/S) : -11.29625481</p> <p>INITIAL ORBITAL ELEMENTS:</p> <p>SEMIMAJOR AXIS (KM) : 148043691.097 ECCENTRICITY : 0.107910978 INCLINATION (DEG) : 22.82900152 R. AS. OF A. NODE (DEG) : 0.68397776 ARG. OF PERIC. (DEG) : 252.61281625 TRUE ANOMALY (DEG) : 266.53673178</p> <p>FINAL EPOCH: 2004: 5:25 5:51:30.0 (1606.2441)</p> <p>FINAL STATE:</p> <p>X-COORD (KM) : -24667694.126 Y-COORD (KM) : -120026543.128 Z-COORD (KM) : -50449864.477 VX-COORD (KM/S) : 32.60333500 VY-COORD (KM/S) : -5.93421499 VZ-COORD (KM/S) : -2.66092232</p> <p>INITIAL ORBITAL ELEMENTS:</p> <p>SEMIMAJOR AXIS (KM) : 147833315.209 ECCENTRICITY : 0.104061420 INCLINATION (DEG) : 22.84880183 R. AS. OF A. NODE (DEG) : 0.66994273 ARG. OF PERIC. (DEG) : 252.81590301 TRUE ANOMALY (DEG) : 5.83835498</p> <p>PHASE NUMBER: 3 LEG NUMBER: 3</p>	<p>FINAL EPOCH: 2004: 2:29 2:18:24.3 (1520.0961)</p> <p>FINAL STATE:</p> <p>X-COORD (KM) : 869140.376 Y-COORD (KM) : -314097.219 Z-COORD (KM) : -30161.727 VX-COORD (KM/S) : 3.47210637 VY-COORD (KM/S) : -1.16922914 VZ-COORD (KM/S) : -0.12971035</p> <p>INITIAL ORBITAL ELEMENTS:</p> <p>SEMIMAJOR AXIS (KM) : -31692.112 ECCENTRICITY : 1.202125509 INCLINATION (DEG) : 7.43578077 R. AS. OF A. NODE (DEG) : 145.64914364 ARG. OF PERIC. (DEG) : 49.59747459 TRUE ANOMALY (DEG) : 145.00170423</p> <p>CENTRAL BODY STATE VECTOR W.R.T. SUN</p> <p>POSITION (KM) : -136295430.007 53165642.086 23049538.025</p> <p>VELOCITY (KM/S) : -12.133 -25.262 -10.953</p> <p>DEPARTURE HYPERBOLIC VELOCITY (KM/S) : 3.353 -1.144 -0.124</p> <p>MODULE (KM/S) : 3.545</p> <p>PHASE NUMBER: 2 LEG NUMBER: 2</p>
<p>MISSION TYPE : DEEP SPACE MISSION TYPE OF PROBLEM : BOUNDARY VALUE PROBLEM NAME OF CENTRAL BODY : SUN COORDINATE SYSTEM : MEAN EARTH EQUATOR 2000</p> <p>INITIAL EPOCH: 2004: 5:25 5:51:30.0 (1606.2441)</p> <p>INITIAL MASS (KG) : 2852.995</p> <p>PERTURBATIONS CONSIDERED: ATMOSPHERIC DRAG: NO SOLAR RADIATION: YES REFLECTIVE COEFF. : 1.200</p> <p>CROSS SECTIONAL AREA: THIRD BODY : YES</p> <p>THIRD BODIES : EARTH VENUS MARS JUPITER</p> <p>REFLECTIVE COEFF. : 1.200</p>	<p>MISSION TYPE : DEEP SPACE MISSION TYPE OF PROBLEM : BOUNDARY VALUE PROBLEM NAME OF CENTRAL BODY : SUN COORDINATE SYSTEM : MEAN EARTH EQUATOR 2000</p> <p>INITIAL EPOCH: 2004: 2:29 2:18:24.3 (1520.0961)</p> <p>INITIAL MASS (KG) : 3032.390</p> <p>PERTURBATIONS CONSIDERED: ATMOSPHERIC DRAG: NO SOLAR RADIATION: YES REFLECTIVE COEFF. : 1.200</p> <p>CROSS SECTIONAL AREA: THIRD BODY : YES</p> <p>THIRD BODIES : EARTH VENUS MARS JUPITER</p>

<p>CROSS SECTIONAL AREA: 70.000 THIRD BODY : YES THIRD BODIES : EARTH VENUS MARS JUPITER</p> <p>NON-SPHERICITY : NO</p> <p>STOP CONDITION: STOP AT ENTRY OF SPHERE OF INFLUENCE OF EARTH</p> <p>MANOEUVRE APPLIED (M/S) DV X-COORDINATE: 168.55067780 DV Y-COORDINATE: -30.90603021 DV Z-COORDINATE: 27.08100989 DV MODULE : 173.487</p> <p>INITIAL STATE: X-COORD (KM) : -24667718.531 Y-COORD (KM) : -120026586.785 Z-COORD (KM) : -50449878.219 VX-COORD (KM/S) : 32.77188567 VY-COORD (KM/S) : -5.96512102 VZ-COORD (KM/S) : -2.63384131</p> <p>INITIAL ORBITAL ELEMENTS: SEMIMAJOR AXIS (KM) : 149708456.128 ECCENTRICITY : 0.115208051 INCLINATION (DEG) : 22.83615824 R. AS. OF A. NODE (DEG) : 0.50653174 ARG. OF PERIC. (DEG) : 253.73439193 TRUE ANOMALY (DEG) : 5.07045494</p> <p>FINAL EPOCH: 2005: 2:27 20:22: 9.8 (1884.8487)</p> <p>FINAL STATE: X-COORD (KM) : -139479189.826 Y-COORD (KM) : 48379540.751 Z-COORD (KM) : 20895971.767 VX-COORD (KM/S) : -7.16989966 VY-COORD (KM/S) : -26.75254280 VZ-COORD (KM/S) : -11.22953918</p> <p>FINAL ORBITAL ELEMENTS: SEMIMAJOR AXIS (KM) : 149629987.632 ECCENTRICITY : 0.118735344 INCLINATION (DEG) : 22.82174985 R. AS. OF A. NODE (DEG) : 0.52551145 ARG. OF PERIC. (DEG) : 253.94652974 TRUE ANOMALY (DEG) : 264.87201199</p> <p>MISSION TYPE : DEEP SPACE MISSION</p> <p>PHASE NUMBER: 4 LEG NUMBER: 4 -----</p>	<p>TYPE OF PROBLEM : BOUNDARY VALUE PROBLEM NAME OF CENTRAL BODY : EARTH COORDINATE SYSTEM : MEAN EARTH EQUATOR OF DATE</p> <p>INITIAL EPOCH: 2005: 2:27 20:22: 9.8 (1884.8487)</p> <p>INITIAL MASS (KG) : 2852.995</p> <p>PERTURBATIONS CONSIDERED: ATMOSPHERIC DRAG: NO SOLAR RADIATION: YES REFLECTIVE COEFF. : 1.200 CROSS SECTIONAL AREA: 70.000 THIRD BODY : YES THIRD BODIES : SUN MOON</p> <p>NON-SPHERICITY : NO</p> <p>STOP CONDITION: STOP AT NEXT PERICENTRE</p> <p>INITIAL STATE: X-COORD (KM) : -883170.799 Y-COORD (KM) : 271035.603 Z-COORD (KM) : 38997.716 VX-COORD (KM/S) : 3.86115027 VY-COORD (KM/S) : -1.09332216 VZ-COORD (KM/S) : -0.10647002</p> <p>INITIAL ORBITAL ELEMENTS: SEMIMAJOR AXIS (KM) : -26132.589 ECCENTRICITY : 1.397779277 INCLINATION (DEG) : 144.27502695 R. AS. OF A. NODE (DEG) : 166.30405762 ARG. OF PERIC. (DEG) : 138.25995977 TRUE ANOMALY (DEG) : 225.88222484</p> <p>FINAL EPOCH: 2005: 3: 2 8:37:56.7 (1887.3597)</p> <p>FINAL STATE: X-COORD (KM) : 9050.869 Y-COORD (KM) : 3767.494 Z-COORD (KM) : 4191.212 VX-COORD (KM/S) : 4.83881656 VY-COORD (KM/S) : -7.04738388 VZ-COORD (KM/S) : -4.11444644</p> <p>FINAL ORBITAL ELEMENTS: SEMIMAJOR AXIS (KM) : -26157.939 ECCENTRICITY : 1.407601365 INCLINATION (DEG) : 144.17409986 R. AS. OF A. NODE (DEG) : 166.28673746 ARG. OF PERIC. (DEG) : 137.81013165 TRUE ANOMALY (DEG) : 0.00000000</p> <p>BIDIMENSIONAL IMPACT VECTOR (KM) : -21019.193 15154.687</p> <p>TRIDIMENSIONAL IMPACT VECTOR (KM) : 6122.443 20111.752</p>
---	---

<p>15149.394</p> <p>CENTRAL BODY STATE VECTOR W.R.T. SUN POSITION (KM) : -140856183.042 42497030.384 18424430.193</p> <p>VELOCITY (KM/S) : -9.800 -26.059 -11.297</p> <p>ARRIVAL HYPERBOLIC VELOCITY (KM/S) : 3.754 -1.065 -0.103</p> <p>MODULE (KM/S) : 3.904</p> <p>DEPARTURE HYPERBOLIC VELOCITY (KM/S) : -0.958 -3.020 -2.281</p> <p>MODULE (KM/S) : 3.904</p> <p>DEFLECTION ANGLE (DEG) : 90.540</p> <p>PERIC. ALTITUDE (KM) : 4287.169</p> <p>PHASE NUMBER: 4 LEG NUMBER: 5 -----</p> <p>MISSION TYPE : DEEP SPACE MISSION TYPE OF PROBLEM : BOUNDARY VALUE PROBLEM NAME OF CENTRAL BODY : EARTH COORDINATE SYSTEM : MEAN EARTH EQUATOR OF DATE</p> <p>INITIAL EPOCH: 2005. 3: 2 8:37:56.7 (1887.3597) INITIAL MASS (KG) : 2852.995</p> <p>PERTURBATIONS CONSIDERED: ATMOSPHERIC DRAG: NO SOLAR RADIATION: YES REFLECTIVE COEFF. : 1.200 CROSS SECTIONAL AREA: 70.000</p> <p>THIRD BODY : YES MOON NON-SPHERICITY : NO</p> <p>STOP CONDITION: STOP AT EXIT OF SPHERE OF INFLUENCE OF EARTH</p> <p>INITIAL STATE: X-COORD (KM) : 9050.869 Y-COORD (KM) : 3767.494 Z-COORD (KM) : 4191.212 VX-COORD (KM/S) : 4.83881656 VY-COORD (KM/S) : -7.04738388</p>	<p>-4.11444644</p> <p>INITIAL ORBITAL ELEMENTS: SEMIMAJOR AXIS (KM) : -26157.939 ECCENTRICITY : 1.407601365 INCLINATION (DEG) : 144.17409986 R. AS. OF A. NODE (DEG) : 166.28673746 ARG. OF PERIC. (DEG) : 137.81013165 TRUE ANOMALY (DEG) : 0.00000000</p> <p>FINAL EPOCH: 2005. 3: 4 20:59: 5.4 (1889.8744)</p> <p>FINAL STATE: X-COORD (KM) : -203399.150 Y-COORD (KM) : -722900.692 Z-COORD (KM) : -539458.210 VX-COORD (KM/S) : -0.98009435 VY-COORD (KM/S) : -3.09560080 VZ-COORD (KM/S) : -2.32317574</p> <p>FINAL ORBITAL ELEMENTS: SEMIMAJOR AXIS (KM) : -26400.862 ECCENTRICITY : 1.439903542 INCLINATION (DEG) : 144.10716187 R. AS. OF A. NODE (DEG) : 171.25034524 ARG. OF PERIC. (DEG) : 143.33696910 TRUE ANOMALY (DEG) : 132.31511937</p> <p>PHASE NUMBER: 5 LEG NUMBER: 6 -----</p> <p>MISSION TYPE : DEEP SPACE MISSION TYPE OF PROBLEM : BOUNDARY VALUE PROBLEM NAME OF CENTRAL BODY : SUN COORDINATE SYSTEM : MEAN EARTH EQUATOR 2000</p> <p>INITIAL EPOCH: 2005. 3: 4 20:59: 5.4 (1889.8744) INITIAL MASS (KG) : 2852.995</p> <p>PERTURBATIONS CONSIDERED: ATMOSPHERIC DRAG: NO SOLAR RADIATION: YES REFLECTIVE COEFF. : 1.200 CROSS SECTIONAL AREA: 70.000</p> <p>THIRD BODY : YES EARTH VENUS MARS JUPITER NON-SPHERICITY : NO</p> <p>STOP CONDITION: STOP AFTER A GIVEN TIME</p>
--	--

<p>INITIAL STATE: X-COORD (KM) : -143054336.220 Y-COORD (KM) : 36072852.976 Z-COORD (KM) : 15413416.345 VX-COORD (KM/S) : -9.54352918 VY-COORD (KM/S) : -29.51044635 VZ-COORD (KM/S) : -13.77456269</p> <p>INITIAL ORBITAL ELEMENTS: SEMIMAJOR AXIS (KM) : 208119809.006 ECCENTRICITY : 0.287752052 INCLINATION (DEG) : 24.88580166 R. AS. OF A. NODE (DEG) : 358.86292457 ARG. OF PERIC. (DEG) : 161.19911871 TRUE ANOMALY (DEG) : 4.50518481</p> <p>FINAL EPOCH: 2006:10:21 4:31:31.0 (2485.1886)</p> <p>INITIAL STATE: X-COORD (KM) : -14697296.931 Y-COORD (KM) : 21838185.524 Z-COORD (KM) : 8772396.901 VX-COORD (KM/S) : -6.70993312 VY-COORD (KM/S) : -29.98491748 VZ-COORD (KM/S) : -13.94539944</p> <p>INITIAL ORBITAL ELEMENTS: SEMIMAJOR AXIS (KM) : 205896395.465 ECCENTRICITY : 0.279928196 INCLINATION (DEG) : 24.85030006 R. AS. OF A. NODE (DEG) : 358.87239038 ARG. OF PERIC. (DEG) : 161.00133492 TRUE ANOMALY (DEG) : 10.93718213</p> <p>PHASE NUMBER: 6 LEG NUMBER: 7 -----</p> <p>MISSION TYPE : DEEP SPACE MISSION TYPE OF PROBLEM : BOUNDARY VALUE PROBLEM NAME OF CENTRAL BODY : SUN COORDINATE SYSTEM : MEAN EARTH EQUATOR 2000</p> <p>INITIAL EPOCH: 2006:10:21 4:31:31.0 (2485.1886)</p> <p>INITIAL MASS (KG) : 2789.193</p> <p>PERTURBATIONS CONSIDERED: ATMOSPHERIC DRAG: NO SOLAR RADIATION : YES REFLECTIVE COEFF. : 1.200 CROSS SECTIONAL AREA: 70.000 THIRD BODY : YES THIRD BODIES : MARS VENUS</p>	<p>NON-SPHERICITY : NO</p> <p>STOP CONDITION: STOP AT ENTRY OF SPHERE OF INFLUENCE OF MARS</p> <p>MANOEUVRE APPLIED (M/S) DV X-COORDINATE: 14.80981547 DV Y-COORDINATE: 58.95496303 DV Z-COORDINATE: 21.09487237 DV MODULE : 64.343</p> <p>INITIAL STATE: X-COORD (KM) : -146979231.291 Y-COORD (KM) : 21838309.292 Z-COORD (KM) : 8772467.507 VX-COORD (KM/S) : -6.69512330 VY-COORD (KM/S) : -29.92596252 VZ-COORD (KM/S) : -13.92430456</p> <p>INITIAL ORBITAL ELEMENTS: SEMIMAJOR AXIS (KM) : 204525932.223 ECCENTRICITY : 0.275134411 INCLINATION (DEG) : 24.85999767 R. AS. OF A. NODE (DEG) : 358.86913386 ARG. OF PERIC. (DEG) : 160.87079101 TRUE ANOMALY (DEG) : 11.07062295</p> <p>FINAL EPOCH: 2007: 2:27 3: 6:30.3 (2614.1295)</p> <p>INITIAL STATE: X-COORD (KM) : 23078076.290 Y-COORD (KM) : -194323359.131 Z-COORD (KM) : -89807880.837 VX-COORD (KM/S) : 23.82788394 VY-COORD (KM/S) : -3.72534304 VZ-COORD (KM/S) : -1.50691302</p> <p>FINAL ORBITAL ELEMENTS: SEMIMAJOR AXIS (KM) : 204543190.255 ECCENTRICITY : 0.275542042 INCLINATION (DEG) : 24.86011379 R. AS. OF A. NODE (DEG) : 358.86420384 ARG. OF PERIC. (DEG) : 160.86994106 TRUE ANOMALY (DEG) : 116.31385366</p> <p>MISSION TYPE : DEEP SPACE MISSION TYPE OF PROBLEM : BOUNDARY VALUE PROBLEM NAME OF CENTRAL BODY : MARS COORDINATE SYSTEM : NON-ROTAT. EQ. OF MARS</p> <p>PHASE NUMBER: 7 LEG NUMBER: 8 -----</p>
---	--

<p>INITIAL EPOCH: 2007: 2:27 3: 6:30.3 (2614.1295)</p> <p>INITIAL MASS (KG) : 2789.193</p> <p>PERTURBATIONS CONSIDERED: ATMOSPHERIC DRAG: NO SOLAR RADIATION: YES REFLECTIVE COEFF.: 1.200 CROSS SECTIONAL AREA: 70.000</p> <p>THIRD BODY : YES THIRD BODIES : SUN NON-SPHERICITY : NO</p> <p>STOP CONDITION: STOP AT NEXT PERICENTRE</p> <p>INITIAL STATE: X-COORD (KM) : 453134.841 Y-COORD (KM) : 356474.790 Z-COORD (KM) : -30426.600 VX-COORD (KM/S) : -6.86212685 VY-COORD (KM/S) : -5.45463006 VZ-COORD (KM/S) : 0.50700712</p> <p>INITIAL ORBITAL ELEMENTS: SEMIMAJOR AXIS (KM) : -556.570 ECCENTRICITY : 7.474082884 INCLINATION (DEG) : 134.85861066 R. AS. OF A. NODE (DEG) : 35.18140968 ARG. OF PERIC. (DEG) : 93.01638701 TRUE ANOMALY (DEG) : 262.71993029</p> <p>FINAL EPOCH: 2007: 2:27 21:18:33.3 (2614.8879)</p> <p>FINAL STATE: X-COORD (KM) : 1302.492 Y-COORD (KM) : -2177.660 Z-COORD (KM) : 2549.188 VX-COORD (KM/S) : -8.40773928 VY-COORD (KM/S) : -5.47036230 VZ-COORD (KM/S) : -0.37721055</p> <p>FINAL ORBITAL ELEMENTS: SEMIMAJOR AXIS (KM) : -556.626 ECCENTRICITY : 7.461807148 INCLINATION (DEG) : 134.78694956 R. AS. OF A. NODE (DEG) : 35.18857752 ARG. OF PERIC. (DEG) : 93.03513195 TRUE ANOMALY (DEG) : 0.00000000</p> <p>BIDIMENSIONAL IMPACT VECTOR (KM) : -3973.801 1072.434</p> <p>TRIDIMENSIONAL IMPACT VECTOR (KM) : 3883.294 -914.046 1012.795</p> <p>CENTRAL BODY STATE VECTOR W.R.T. SUN POSITION (KM) : 24634526.368 -194562895.415</p>	<p>VELOCITY (KM/S) : -89905736.388 24.986 4.651 1.458</p> <p>ARRIVAL HYPERBOLIC VELOCITY (KM/S) : -1.178 -8.200 -2.884</p> <p>MODULE (KM/S) : 8.772</p> <p>DEPARTURE HYPERBOLIC VELOCITY (KM/S) : -3.334 -7.388 -3.354</p> <p>MODULE (KM/S) : 8.772</p> <p>DEFLECTION ANGLE (DEG) : 15.403</p> <p>PERICE. ALTITUDE (KM) : 199.999</p> <p>PHASE NUMBER: 7 LEG NUMBER: 9 -----</p> <p>MISSION TYPE :DEEP SPACE MISSION TYPE OF PROBLEM :BOUNDARY VALUE PROBLEM NAME OF CENTRAL BODY :MARS COORDINATE SYSTEM :NON-ROTAT. EQ. OF MARS</p> <p>INITIAL EPOCH: 2007: 2:27 21:18:33.3 (2614.8879)</p> <p>INITIAL MASS (KG) : 2789.193</p> <p>PERTURBATIONS CONSIDERED: ATMOSPHERIC DRAG: NO SOLAR RADIATION: YES REFLECTIVE COEFF.: 1.200 CROSS SECTIONAL AREA: 70.000</p> <p>THIRD BODY : YES THIRD BODIES : SUN NON-SPHERICITY : NO</p> <p>STOP CONDITION: STOP AT EXIT OF SPHERE OF INFLUENCE OF MARS</p> <p>INITIAL STATE: X-COORD (KM) : 1302.492 Y-COORD (KM) : -2177.660 Z-COORD (KM) : 2549.188 VX-COORD (KM/S) : -8.40773928 VY-COORD (KM/S) : -5.47036230 VZ-COORD (KM/S) : -0.37721055</p> <p>INITIAL ORBITAL ELEMENTS: SEMIMAJOR AXIS (KM) : -556.626 ECCENTRICITY : 7.461807148 INCLINATION (DEG) : 134.78694956</p>
---	---

<p>R. AS. OF A. NODE (DEG) : 35.18857752 ARG. OF PERIC. (DEG) : 93.03513195 TRUE ANOMALY (DEG) : 0.00000000</p> <p>FINAL EPOCH: 2007: 2:28 15:30:36.5 (2615.6463)</p> <p>FINAL STATE: X-COORD (KM) : -506218.483 Y-COORD (KM) : -267725.702 Z-COORD (KM) : -73464.511 VX-COORD (KM/S) : -7.71425280 VY-COORD (KM/S) : -4.02984059 VZ-COORD (KM/S) : -1.16081748</p> <p>INITIAL ORBITAL ELEMENTS: SEMIMAJOR AXIS (KM) : -556.584 ECCENTRICITY : 7.438831427 INCLINATION (DEG) : 134.72050866 R. AS. OF A. NODE (DEG) : 35.17188236 ARG. OF PERIC. (DEG) : 92.99747823 TRUE ANOMALY (DEG) : 97.31868175</p> <p>MISSION TYPE : DEEP SPACE MISSION TYPE OF PROBLEM : BOUNDARY VALUE PROBLEM NAME OF CENTRAL BODY : SUN COORDINATE SYSTEM : MEAN EARTH EQUATOR 2000</p> <p>INITIAL EPOCH: 2007: 2:28 15:30:36.5 (2615.6463) INITIAL MASS (KG) : 2789.193</p> <p>PERTURBATIONS CONSIDERED: ATMOSPHERIC DRAG: NO SOLAR RADIATION: YES REFLECTIVE COEFF.: 1.200 CROSS SECTIONAL AREA: 70.000</p> <p>THIRD BODY : YES : MARS VENUS EARTH JUPITER</p> <p>NON-SPHERICITY : NO</p> <p>STOP CONDITION: STOP AFTER A GIVEN TIME</p> <p>INITIAL STATE: X-COORD (KM) : 26055169.508 Y-COORD (KM) : -194740769.206 Z-COORD (KM) : -90027775.383 VX-COORD (KM/S) : 21.62736946 VY-COORD (KM/S) : -2.57565560</p>	<p>VZ-COORD (KM/S) : -1.82130812</p> <p>INITIAL ORBITAL ELEMENTS: SEMIMAJOR AXIS (KM) : 176845577.992 ECCENTRICITY : 0.337170955 INCLINATION (DEG) : 24.66874878 R. AS. OF A. NODE (DEG) : 3.69880353 ARG. OF PERIC. (DEG) : 128.99048695 TRUE ANOMALY (DEG) : 144.57434299</p> <p>FINAL EPOCH: 2007: 6:12 5:14:50.0 (2719.2186)</p> <p>FINAL STATE: X-COORD (KM) : 182319755.323 Y-COORD (KM) : -132848244.593 Z-COORD (KM) : -66289962.688 VX-COORD (KM/S) : 11.11391085 VY-COORD (KM/S) : 14.63826521 VZ-COORD (KM/S) : 6.37993286</p> <p>INITIAL ORBITAL ELEMENTS: SEMIMAJOR AXIS (KM) : 176863051.265 ECCENTRICITY : 0.336864156 INCLINATION (DEG) : 24.66878476 R. AS. OF A. NODE (DEG) : 3.69832746 ARG. OF PERIC. (DEG) : 128.98910898 TRUE ANOMALY (DEG) : 188.51774839</p> <p>MISSION TYPE : DEEP SPACE MISSION TYPE OF PROBLEM : BOUNDARY VALUE PROBLEM NAME OF CENTRAL BODY : SUN COORDINATE SYSTEM : MEAN EARTH EQUATOR 2000</p> <p>INITIAL EPOCH: 2007: 6:12 5:14:50.0 (2719.2186) INITIAL MASS (KG) : 2789.186</p> <p>PERTURBATIONS CONSIDERED: ATMOSPHERIC DRAG: NO SOLAR RADIATION: YES REFLECTIVE COEFF.: 1.200 CROSS SECTIONAL AREA: 70.000</p> <p>THIRD BODY : YES : EARTH VENUS MARS JUPITER</p> <p>NON-SPHERICITY : NO</p> <p>STOP CONDITION: STOP AT ENTRY OF SPHERE OF INFLUENCE OF EARTH</p>
<p>PHASE NUMBER: 8 LEG NUMBER: 10 -----</p>	<p>PHASE NUMBER: 9 LEG NUMBER: 11 -----</p>

<p>MANOEUVRE APPLIED (M/S) DV X-COORDINATE: -0.00055634 DV Y-COORDINATE: -0.00605887 DV Z-COORDINATE: -0.00347274 DV MODULE : 0.007</p> <p>INITIAL STATE: X-COORD (KM) : 182319742.837 Y-COORD (KM) : -132848278.472 Z-COORD (KM) : -66289980.093 VX-COORD (KM/S) : 11.11391029 VY-COORD (KM/S) : 14.638825916 VZ-COORD (KM/S) : 6.37992939</p> <p>INITIAL ORBITAL ELEMENTS: SEMIMAJOR AXIS (KM) : 176863012.376 ECCENTRICITY : 0.336864514 INCLINATION (DEG) : 24.66878365 R. AS. OF A. NODE (DEG) : 3.69833150 ARG. OF PERIC. (DEG) : 128.98911270 TRUE ANOMALY (DEG) : 188.51773189</p> <p>FINAL EPOCH: 2007:11:14 6:26: 2.3 (2874.2681)</p> <p>FINAL STATE: X-COORD (KM) : 92998958.199 Y-COORD (KM) : 106772144.168 Z-COORD (KM) : 46183371.904 VX-COORD (KM/S) : -29.98183430 VY-COORD (KM/S) : 10.15087919 VZ-COORD (KM/S) : 5.54581967</p> <p>INITIAL ORBITAL ELEMENTS: SEMIMAJOR AXIS (KM) : 177084290.972 ECCENTRICITY : 0.338411664 INCLINATION (DEG) : 24.67507471 R. AS. OF A. NODE (DEG) : 3.71329213 ARG. OF PERIC. (DEG) : 128.98761756 TRUE ANOMALY (DEG) : 278.98084933</p> <p>MISSION TYPE : DEEP SPACE MISSION TYPE OF PROBLEM : BOUNDARY VALUE PROBLEM NAME OF CENTRAL BODY : EARTH COORDINATE SYSTEM : MEAN EARTH EQUATOR OF DATE</p> <p>INITIAL EPOCH: 2007:11:14 6:26: 2.3 (2874.2681)</p> <p>INITIAL MASS (KG) : 2789.186</p> <p>PERTURBATIONS CONSIDERED: ATMOSPHERIC DRAG: NO</p>	<p>SOLAR RADIATION : YES REFLECTIVE COEFF. : 1.200 CROSS SECTIONAL AREA: 70.000 THIRD BODY : YES THIRD BODIES : SUN MOON</p> <p>NON-SPHERICITY : NO</p> <p>STOP CONDITION: STOP AT NEXT PERICENTRE</p> <p>INITIAL STATE: X-COORD (KM) : 628293.107 Y-COORD (KM) : 654638.894 Z-COORD (KM) : 177953.530 VX-COORD (KM/S) : -6.19399470 VY-COORD (KM/S) : -6.81148734 VZ-COORD (KM/S) : -1.80726673</p> <p>INITIAL ORBITAL ELEMENTS: SEMIMAJOR AXIS (KM) : -4572.890 ECCENTRICITY : 5.457871158 INCLINATION (DEG) : 168.89176861 R. AS. OF A. NODE (DEG) : 138.88504073 ARG. OF PERIC. (DEG) : 191.69860307 TRUE ANOMALY (DEG) : 260.95932723</p> <p>FINAL EPOCH: 2007:11:15 9:29:31.0 (2875.3955)</p> <p>FINAL STATE: X-COORD (KM) : 12273.925 Y-COORD (KM) : -16116.236 Z-COORD (KM) : -724.483 VX-COORD (KM/S) : -8.82910666 VY-COORD (KM/S) : -6.62854718 VZ-COORD (KM/S) : -2.112643185</p> <p>INITIAL ORBITAL ELEMENTS: SEMIMAJOR AXIS (KM) : -4577.142 ECCENTRICITY : 5.428712559 INCLINATION (DEG) : 168.90270508 R. AS. OF A. NODE (DEG) : 137.79802268 ARG. OF PERIC. (DEG) : 190.70117194 TRUE ANOMALY (DEG) : 0.00000000</p> <p>BIDIMENSIONAL IMPACT VECTOR (KM) : -24422.772 -21.288</p> <p>TRIDIMENSIONAL IMPACT VECTOR (KM) : 18038.698 -16464.421 -20.892</p> <p>CENTRAL BODY STATE VECTOR W.R.T. SUN POSITION (KM) : 90035784.349 107748990.096 46712646.012 VELOCITY (KM/S) : -24.137 16.522 7.162</p> <p>PHASE NUMBER: 10 LEG NUMBER: 12 -----</p>
--	--

<p>ARRIVAL HYPERBOLIC VELOCITY (KM/S) : -6.175 -6.763 -1.791 9.332</p> <p>MODULE (KM/S) : 9.332</p> <p>DEPARTURE HYPERBOLIC VELOCITY (KM/S) : -8.252 -4.026 -1.667 9.332</p> <p>MODULE (KM/S) : 9.332</p> <p>DEFLECTION ANGLE (DEG) : 21.230</p> <p>PERICE. ALTITUDE (KM) : 13892.733</p>	<p>FINAL EPOCH: 2007:11:16 12:33: 8.5 (2876.5230)</p> <p>FINAL STATE: X-COORD (KM) : -805544.240 Y-COORD (KM) : -421937.148 Z-COORD (KM) : -167449.364 VX-COORD (KM/S) : -8.28570117 VY-COORD (KM/S) : -4.06250963 VZ-COORD (KM/S) : -1.68209744</p> <p>FINAL ORBITAL ELEMENTS: SEMIMAJOR AXIS (KM) : -4575.088 ECCENTRICITY : 5.426618345 INCLINATION (DEG) : 168.90677993 R. AS. OF A. NODE (DEG) : 137.73446444 ARG. OF PERIC. (DEG) : 190.63275541 TRUE ANOMALY (DEG) : 99.11044602</p> <p>MISSION TYPE : DEEP SPACE MISSION TYPE OF PROBLEM : BOUNDARY VALUE PROBLEM NAME OF CENTRAL BODY : SUN COORDINATE SYSTEM : MEAN EARTH EQUATOR 2000</p> <p>INITIAL EPOCH: 2007:11:16 12:33: 8.5 (2876.5230)</p> <p>INITIAL MASS (KG) : 2789.186</p> <p>PERTURBATIONS CONSIDERED: ATMOSPHERIC DRAG: NO SOLAR RADIATION: YES REFLECTIVE COEFF. : 1.200 CROSS SECTIONAL AREA: 70.000</p> <p>THIRD BODY : SUN NON-SPHERICITY : NO</p> <p>STOP CONDITION: STOP AT EXIT OF SPHERE OF INFLUENCE OF EARTH</p> <p>INITIAL STATE: X-COORD (KM) : 12273.925 Y-COORD (KM) : -16116.236 Z-COORD (KM) : -724.483 VX-COORD (KM/S) : -8.82910666 VY-COORD (KM/S) : -6.62854718 VZ-COORD (KM/S) : -2.112643185</p> <p>FINAL ORBITAL ELEMENTS: SEMIMAJOR AXIS (KM) : -4577.142 ECCENTRICITY : 5.428712559 INCLINATION (DEG) : 168.90270508 R. AS. OF A. NODE (DEG) : 137.79802268 ARG. OF PERIC. (DEG) : 190.70117194 TRUE ANOMALY (DEG) : 0.00000000</p>
<p>PHASE NUMBER: 10 LEG NUMBER: 13 -----</p> <p>MISSION TYPE : DEEP SPACE MISSION TYPE OF PROBLEM : BOUNDARY VALUE PROBLEM NAME OF CENTRAL BODY : EARTH COORDINATE SYSTEM : MEAN EARTH EQUATOR OF DATE</p> <p>INITIAL EPOCH: 2007:11:15 9:29:31.0 (2875.3955)</p> <p>INITIAL MASS (KG) : 2789.186</p> <p>PERTURBATIONS CONSIDERED: ATMOSPHERIC DRAG: NO SOLAR RADIATION: YES REFLECTIVE COEFF. : 1.200 CROSS SECTIONAL AREA: 70.000</p> <p>THIRD BODY : SUN NON-SPHERICITY : NO</p> <p>STOP CONDITION: STOP AT EXIT OF SPHERE OF INFLUENCE OF EARTH</p> <p>INITIAL STATE: X-COORD (KM) : 12273.925 Y-COORD (KM) : -16116.236 Z-COORD (KM) : -724.483 VX-COORD (KM/S) : -8.82910666 VY-COORD (KM/S) : -6.62854718 VZ-COORD (KM/S) : -2.112643185</p> <p>FINAL ORBITAL ELEMENTS: SEMIMAJOR AXIS (KM) : -4577.142 ECCENTRICITY : 5.428712559 INCLINATION (DEG) : 168.90270508 R. AS. OF A. NODE (DEG) : 137.79802268 ARG. OF PERIC. (DEG) : 190.70117194 TRUE ANOMALY (DEG) : 0.00000000</p>	<p>PHASE NUMBER: 11 LEG NUMBER: 14 -----</p> <p>MISSION TYPE : DEEP SPACE MISSION TYPE OF PROBLEM : BOUNDARY VALUE PROBLEM NAME OF CENTRAL BODY : SUN COORDINATE SYSTEM : MEAN EARTH EQUATOR 2000</p> <p>INITIAL EPOCH: 2007:11:16 12:33: 8.5 (2876.5230)</p> <p>INITIAL MASS (KG) : 2789.186</p> <p>PERTURBATIONS CONSIDERED: ATMOSPHERIC DRAG: NO SOLAR RADIATION: YES REFLECTIVE COEFF. : 1.200 CROSS SECTIONAL AREA: 70.000</p> <p>THIRD BODY : EARTH VENUS MARS JUPITER</p> <p>NON-SPHERICITY : NO</p> <p>STOP CONDITION: STOP AFTER A GIVEN TIME</p> <p>INITIAL STATE: X-COORD (KM) : 86860688.205 Y-COORD (KM) : 108916879.904 Z-COORD (KM) : 47234346.155 VX-COORD (KM/S) : -32.78460503 VY-COORD (KM/S) : 12.03889470 VZ-COORD (KM/S) : 5.29736223</p> <p>FINAL ORBITAL ELEMENTS: SEMIMAJOR AXIS (KM) : 238458792.152</p>

<p> ECCENTRICITY : 0.446157458 INCLINATION (DEG) : 23.51457228 R. AS. OF A. NODE (DEG) : 0.23739888 ARG. OF PERIC. (DEG) : 101.61959181 TRUE ANOMALY (DEG) : 311.97139528 FINAL EPOCH: 2009: 3:15 20:11:28.0 (3361.8413) FINAL STATE: X-COORD (KM) : 165041660.821 Y-COORD (KM) : -261748061.698 Z-COORD (KM) : -114183027.611 VX-COORD (KM/S) : 11.38774529 VY-COORD (KM/S) : 9.90341452 VZ-COORD (KM/S) : 4.28853445 FINAL ORBITAL ELEMENTS: SEMIMAJOR AXIS (KM) : 237589051.977 ECCENTRICITY : 0.443380150 INCLINATION (DEG) : 23.51405998 R. AS. OF A. NODE (DEG) : 0.23642846 ARG. OF PERIC. (DEG) : 101.63902582 TRUE ANOMALY (DEG) : 198.16952113 </p>	<p> DV MODULE : 129.394 INITIAL STATE: X-COORD (KM) : 165041731.800 Y-COORD (KM) : -261748054.958 Z-COORD (KM) : -114183024.149 VX-COORD (KM/S) : 11.28136379 VY-COORD (KM/S) : 9.83538005 VZ-COORD (KM/S) : 4.26030336 INITIAL ORBITAL ELEMENTS: SEMIMAJOR AXIS (KM) : 235901545.453 ECCENTRICITY : 0.452169415 INCLINATION (DEG) : 23.51609588 R. AS. OF A. NODE (DEG) : 0.22752019 ARG. OF PERIC. (DEG) : 102.22044752 TRUE ANOMALY (DEG) : 197.59627925 FINAL EPOCH: 2009:11: 9 23:35: 4.7 (3600.9827) </p>
<p> PHASE NUMBER: 12 LEG NUMBER: 15 ----- MISSION TYPE : DEEP SPACE MISSION TYPE OF PROBLEM : BOUNDARY VALUE PROBLEM NAME OF CENTRAL BODY : SUN COORDINATE SYSTEM : MEAN EARTH EQUATOR 2000 INITIAL EPOCH: 2009: 3:15 20:11:28.0 (3361.8413) INITIAL MASS (KG) : 2665.168 PERTURBATIONS CONSIDERED: ATMOSPHERIC DRAG: NO SOLAR RADIATION: YES REFLECTIVE COEFF. : 1.200 CROSS SECTIONAL AREA: 70.000 THIRD BODY : YES EARTH VENUS MARS JUPITER NON-SPHERICITY : NO STOP CONDITION: STOP AT ENTRY OF SPHERE OF INFLUENCE OF EARTH MANOEUVRE APPLIED (M/S) DV X-COORDINATE: -106.38149536 DV Y-COORDINATE: -68.03447144 DV Z-COORDINATE: -28.23108877 </p>	<p> PHASE NUMBER: 13 LEG NUMBER: 16 ----- MISSION TYPE : DEEP SPACE MISSION TYPE OF PROBLEM : BOUNDARY VALUE PROBLEM NAME OF CENTRAL BODY : EARTH COORDINATE SYSTEM : MEAN EARTH EQUATOR OF DATE INITIAL EPOCH: 2009:11: 9 23:35: 4.7 (3600.9827) INITIAL MASS (KG) : 2665.168 PERTURBATIONS CONSIDERED: ATMOSPHERIC DRAG: NO SOLAR RADIATION: YES REFLECTIVE COEFF. : 1.200 CROSS SECTIONAL AREA: 70.000 THIRD BODY : YES </p>

<p>THIRD BODIES : SUN MOON</p> <p>NON-SPHERICITY : NO</p> <p>STOP CONDITION: STOP AT NEXT PERICENTRE</p> <p>INITIAL STATE: X-COORD (KM) : 823466.320 Y-COORD (KM) : 390152.921 Z-COORD (KM) : 157021.293 VX-COORD (KM/S) : -8.89000193 VY-COORD (KM/S) : -4.28884397 VZ-COORD (KM/S) : -1.78310746</p> <p>INITIAL ORBITAL ELEMENTS: SEMIMAJOR AXIS (KM) : -3996.250 ECCENTRICITY : 2.667270252 INCLINATION (DEG) : 129.86534108 R. AS. OF A. NODE (DEG) : 197.07739702 ARG. OF PERIC. (DEG) : 278.62586805 TRUE ANOMALY (DEG) : 248.59193950</p> <p>FINAL EPOCH: 2009:11:11 0:50:37.8 (3602.0352)</p> <p>FINAL STATE: X-COORD (KM) : 286.589 Y-COORD (KM) : -4338.249 Z-COORD (KM) : -5052.826 VX-COORD (KM/S) : -14.41435972 VY-COORD (KM/S) : -2.93269866 VZ-COORD (KM/S) : 1.70039012</p> <p>INITIAL ORBITAL ELEMENTS: SEMIMAJOR AXIS (KM) : -3999.159 ECCENTRICITY : 2.666813462 INCLINATION (DEG) : 129.94464278 R. AS. OF A. NODE (DEG) : 197.05557743 ARG. OF PERIC. (DEG) : 278.61424893 TRUE ANOMALY (DEG) : 0.00000000</p> <p>BIDIMENSIONAL IMPACT VECTOR (KM) : -6447.406 -7495.342</p> <p>TRIDIMENSIONAL IMPACT VECTOR (KM) : 3984.336 -5239.555 -7377.081</p> <p>CENTRAL BODY STATE VECTOR W.R.T. SUN POSITION (KM) : 97903180.541 101978836.863 44210479.677</p> <p>VELOCITY (KM/S) : -22.833 17.972 7.792</p> <p>ARRIVAL HYPERBOLIC VELOCITY (KM/S) : -8.859 -4.250 -1.766</p> <p>MODULE (KM/S) : 9.984</p>	<p>DEPARTURE HYPERBOLIC VELOCITY (KM/S) : -9.165 0.624 3.909 9.984</p> <p>MODULE (KM/S) : 44.046 300.001</p> <p>DEFLECTION ANGLE (DEG) : 44.046</p> <p>PERICE. ALTITUDE (KM) : 300.001</p> <p>PHASE NUMBER: 13 LEG NUMBER: 17 -----</p> <p>MISSION TYPE :DEEP SPACE MISSION TYPE OF PROBLEM :BOUNDARY VALUE PROBLEM NAME OF CENTRAL BODY :EARTH COORDINATE SYSTEM :MEAN EARTH EQUATOR OF DATE</p> <p>INITIAL EPOCH: 2009:11:11 0:50:37.8 (3602.0352)</p> <p>INITIAL MASS (KG) : 2665.168</p> <p>PERTURBATIONS CONSIDERED: ATMOSPHERIC DRAG: NO SOLAR RADIATION : YES REFLECTIVE COEFF. : 1.200 CROSS SECTIONAL AREA: 70.000</p> <p>THIRD BODY : YES : SUN MOON</p> <p>NON-SPHERICITY : NO</p> <p>STOP CONDITION: STOP AT EXIT OF SPHERE OF INFLUENCE OF EARTH</p> <p>INITIAL STATE: X-COORD (KM) : 286.589 Y-COORD (KM) : -4338.249 Z-COORD (KM) : -5052.826 VX-COORD (KM/S) : -14.41435972 VY-COORD (KM/S) : -2.93269866 VZ-COORD (KM/S) : 1.70039012</p> <p>INITIAL ORBITAL ELEMENTS: SEMIMAJOR AXIS (KM) : -3999.159 ECCENTRICITY : 2.666813462 INCLINATION (DEG) : 129.94464278 R. AS. OF A. NODE (DEG) : 197.05557743 ARG. OF PERIC. (DEG) : 278.61424893 TRUE ANOMALY (DEG) : 0.00000000</p> <p>FINAL EPOCH: 2009:11:12 2: 6:33.0 (3603.0879)</p> <p>FINAL STATE: X-COORD (KM) : -852565.224</p>
---	--

<p>Y-COORD (KM) : 49345.086 Z-COORD (KM) : 354498.761 VX-COORD (KM/S) : -9.20768205 VY-COORD (KM/S) : 0.60727367 VZ-COORD (KM/S) : 3.91119198</p> <p>FINAL ORBITAL ELEMENTS: SEMIMAJOR AXIS (KM) : -4002.597 ECCENTRICITY : 2.634191012 INCLINATION (DEG) : 130.63073501 R. AS. OF A. NODE (DEG) : 197.55309761 ARG. OF PERIC. (DEG) : 278.63574442 TRUE ANOMALY (DEG) : 111.70720862</p> <p>PHASE NUMBER: 14 LEG NUMBER: 18 -----</p> <p>MISSION TYPE : DEEP SPACE MISSION TYPE OF PROBLEM : BOUNDARY VALUE PROBLEM NAME OF CENTRAL BODY : SUN COORDINATE SYSTEM : MEAN EARTH EQUATOR 2000</p> <p>INITIAL EPOCH: 2009:11:12 2:6:33.0 (3603.0879) INITIAL MASS (KG) : 2665.168</p> <p>PERTURBATIONS CONSIDERED: ATMOSPHERIC DRAG: NO SOLAR RADIATION: YES REFLECTIVE COEFF. : 1.200 CROSS SECTIONAL AREA: 70.000</p> <p>THIRD BODY : YES THIRD BODIES : EARTH VENUS MARS JUPITER</p> <p>NON-SPHERICITY : NO STOP CONDITION: STOP AFTER A GIVEN TIME</p> <p>INITIAL STATE: X-COORD (KM) : 94957732.300 Y-COORD (KM) : 103647434.571 Z-COORD (KM) : 45267047.560 VX-COORD (KM/S) : -32.39842709 VY-COORD (KM/S) : 18.21853349 VZ-COORD (KM/S) : 11.54689879</p> <p>FINAL ORBITAL ELEMENTS: SEMIMAJOR AXIS (KM) : 469920414.377 ECCENTRICITY : 0.690896183 INCLINATION (DEG) : 26.97721077 R. AS. OF A. NODE (DEG) : 8.26057189 ARG. OF PERIC. (DEG) : 58.80454258</p>	<p>TRUE ANOMALY (DEG) : 343.70448830</p> <p>FINAL EPOCH: 2011:5:10 16:51:11.0 (4147.7022)</p> <p>FINAL STATE: X-COORD (KM) : -487871734.239 Y-COORD (KM) : -407748703.089 Z-COORD (KM) : -169774821.224 VX-COORD (KM/S) : 0.93506265 VY-COORD (KM/S) : -9.63612041 VZ-COORD (KM/S) : -4.92057939</p> <p>FINAL ORBITAL ELEMENTS: SEMIMAJOR AXIS (KM) : 465044052.790 ECCENTRICITY : 0.687820559 INCLINATION (DEG) : 26.96759852 R. AS. OF A. NODE (DEG) : 8.23463950 ARG. OF PERIC. (DEG) : 58.81186862 TRUE ANOMALY (DEG) : 155.85969510</p> <p>PHASE NUMBER: 15 LEG NUMBER: 19 -----</p> <p>MISSION TYPE : DEEP SPACE MISSION TYPE OF PROBLEM : BOUNDARY VALUE PROBLEM NAME OF CENTRAL BODY : SUN COORDINATE SYSTEM : MEAN EARTH EQUATOR 2000</p> <p>INITIAL EPOCH: 2011:5:10 16:51:11.0 (4147.7022) INITIAL MASS (KG) : 2210.142</p> <p>PERTURBATIONS CONSIDERED: ATMOSPHERIC DRAG: NO SOLAR RADIATION: YES REFLECTIVE COEFF. : 1.200 CROSS SECTIONAL AREA: 70.000</p> <p>THIRD BODY : YES THIRD BODIES : VENUS EARTH MARS JUPITER</p> <p>NON-SPHERICITY : NO STOP CONDITION: STOP AFTER A GIVEN TIME</p> <p>MANOEUVRE APPLIED (M/S) DV X-COORDINATE: 232.50035550 DV Y-COORDINATE: -195.58359197 DV Z-COORDINATE: -437.43367901 DV MODULE : 532.595</p> <p>INITIAL STATE: X-COORD (KM) : -487871867.768</p>
---	---

Y-COORD (KM) : -407748671.972	FINAL INJECTED MASS (KG) : 1683.85356092
Z-COORD (KM) : -169774778.545	TOTAL DELTA-V (M/S) : 1673.558
VX-COORD (KM/S) : 1.16756300	
VY-COORD (KM/S) : -9.83170400	
VZ-COORD (KM/S) : -5.35801307	
INITIAL ORBITAL ELEMENTS:	
SEMI-MAJOR AXIS (KM) : 479827984.113	
ECCENTRICITY : 0.659580993	
INCLINATION (DEG) : 28.46875313	
R. AS. OF A. NODE (DEG) : 10.38824286	
ARG. OF PERIC. (DEG) : 59.68854582	
TRUE ANOMALY (DEG) : 153.07632584	
FINAL EPOCH: 2014 : 5:23 0 : 0 : 0.0 (5256.0000)	
FINAL STATE:	
X-COORD (KM) : 132564718.655	
Y-COORD (KM) : -509442671.845	
Z-COORD (KM) : -284654768.051	
VX-COORD (KM/S) : 7.92826972	
VY-COORD (KM/S) : 9.30198440	
VZ-COORD (KM/S) : 4.18694835	
FINAL ORBITAL ELEMENTS:	
SEMI-MAJOR AXIS (KM) : 479779853.126	
ECCENTRICITY : 0.659644029	
INCLINATION (DEG) : 28.46710346	
R. AS. OF A. NODE (DEG) : 10.37576991	
ARG. OF PERIC. (DEG) : 59.74386733	
TRUE ANOMALY (DEG) : 213.95861310	
FLY-BY MANOEUVRE (KM/S) AT Churyumov-G	0.485
	0.581
	0.160
CENTRAL BODY STATE VECTOR W.R.T. SUN	
POSITION (KM) : 132564718.655	
	-509442671.845
	-284654768.051
VELOCITY (KM/S) :	8.413
	9.883
	4.347
ARRIVAL VELOCITY (KM/S) :	7.928
	9.302
	4.187
MODULE (KM/S) :	12.920
RENDEZVOUS MAN. SIZE (M/S) : 773.73234159	
ARRIVAL STATE VECTOR:	
X-COORD (KM) : 132564718.655	
Y-COORD (KM) : -509442671.845	
Z-COORD (KM) : -284654768.051	
VX-COORD (KM/S) : 8.41300177	
VY-COORD (KM/S) : 9.88343224	
VZ-COORD (KM/S) : 4.34699521	